ABSTRACT

ZHU, YUNHUA. Evaluation of Gas Turbine and Gasifier-based Power Generation System (Under the supervision of Dr. H. Christopher Frey).

As a technology in early commercial phase, research work is needed to provide evaluation of the effects of alternative designs and technology advances and provide guidelines for development direction of Integrated Gasification Combined Cycle (IGCC) technology in future. The objective of this study is to evaluate the potential pay-offs as well as risks of technological infeasibility for IGCC systems and to provide insight regarding desired strategies for the future development of advanced IGCC systems.

Texaco gasifier process is widely used in power generation. A process simulation model for a base Texaco gasifier-based IGCC system, including performance (e.g., efficiency), emissions, and cost, was implemented in the ASPEN Plus. The model is calibrated and verified based on other design studies.

To find out the implications of the effects of coal compositions on IGCC plant, the Illinois No.6, Pittsburgh No.8, and West Kentucky coal are selected for comparison. The results indicate that the ash content and sulfur content of coal have effects on performance, SO_2 emissions, and capital cost of IGCC system.

As the main component for power generation, the effects of the most advanced Frame 7H and the current widely used Frame 7F gas turbine combined cycles on IGCC system were evaluated. The results demonstrated the IGCC system based on 7H gas turbine (IGCC-7H) has higher efficiency, lower CO_2 emission, and lower cost of electricity than the 7FA based system (IGCC-7FA).

A simplified spreadsheet model is developed for estimating mass and energy balance of gas turbine combined cycle. It demonstrated that an accurate and sensitive model can be implemented in a spreadsheet. This study implicated the ability to do desktop simulations to support policy analysis.

Uncertainty analysis is implemented to find out the risks associated with the IGCC systems, i.e., there is about 80% probability that the uncertain results of the efficiency of IGCC-7FA system are lower than the deterministic result. The IGCC-7H system is superior to IGCC-7FA despite the uncertainty of inputs. Gasifier carbon conversion and project uncertainty are identified as the key uncertain inputs. The implications of the results provide guidelines for research direction and plant operation.

Integration of air separation unit (ASU) and gas turbine has been used in some IGCC projects. The effects of different integration methods are evaluated. The results indicate that the integration method of nitrogen injection is preferred. The integrated IGCC design has higher efficiency and lower cost than nonintegrated design.

Recommendations are provided based on the simulation and evaluation work, and main conclusions obtained in this study. The Frame 7H gas turbine is a promising technology to enable IGCC to be cost-competitive. Nitrogen injection is preferred for integration design. One or more standard IGCC systems should be developed to provide a consistent basis for benchmarking, verification, and comparison.

EVALUATION OF GAS TURBINE AND GASIFIER-BASED POWER GENERATION SYSTEM

By

YUNHUA ZHU

A dissertation submitted to the Graduate Faculty of
North Carolina State University
in partial fulfillment of the
requirements for the Degree of
Doctor of Philosophy

DEPARTMENT OF CIVIL, CONSTRUCTION, AND ENVIRONMENTAL ENGINEERING

Environmental Engineering and Water Resources

Raleigh

2004

APPROVED BY:

To my father, my mother, and my sister

BIOGRAPHY

Yunhua Zhu was born on January 1st in 1976 in Dayei, Hubei Province, P.R. China. She earned a Bachelor of Engineering degree in Applied Chemistry from Wuhan University, China in 1998. She studied water treatment associated with coal-fired power plants, including water quality and water pollution control. She joined the department of Applied Chemistry in Wuhan University to pursue a M.S. degree under the guidance of Dr. Yunbai Luo. Her area of interest is synthesis of new corrosion inhibitor used in stand-by power plant. She earned a M.S. degree in Applied Chemistry in 2001.

She joined the Department of Civil, Construction, and Environmental Engineering at North Carolina State University to pursue her Ph.D. in Environmental Engineering. She worked on simulation and evaluation of Integrated Gasification Combined Cycle systems under the guidance of Dr. H. Christopher Frey. She also pursued a minor in Statistics along with her major in Environmental Engineering. She completed her thesis research in May 2004.

ACKNOWLEDGEMENT

First, I want to thank my advisor, Dr. Frey, for his guidance and support in my graduate study in North Carolina State University. I also want to thank Dr. Osborne for his help in uncertain analysis area in this project. I would also like to express my thanks to other two committee members, Dr. van der Vaart and Dr. Brill, for their time and helps.

I also want to express my appreciation to other people in Dr. Frey's research group: Jianjun, Kaishan, Allen, Maggie, and Amir. In past three years, they helped me to go through the tough time and we enjoyed the good time together.

I would like to express my deep gratitude to my mother, father, and my older sister. Their love and support to me I will cherish forever. In the end, I would like to thank Luo for his love and support.

TABLE OF CONTENTS

LIST OF TABLES

LIST OF FIGURES

1.0 INTRODUCTION

In 2003, coal-fired plants accounted for 53% of electricity generation in the United States, while nuclear accounted for 21%, natural gas 15%, hydroelectricity 7%, oil 3%, geothermal and "other" 1% (EIA, 2004). With coal likely to remain the primary fuel for the nation's electric power supply for the foreseeable future, there is need for further development of clean coal technology (DOE, 2004). Coal gasification is a promising clean coal technology used in producing coal gas and recently used in Integrated Gasification Combined Cycle (IGCC) for power generation. IGCC is an innovative power generation technology combining with coal gasification and gas turbine combined cycle. At present, conventional coal-fired power generation technology is pulverized coal (PC) power plant.

An IGCC system includes several major components: gasification island, gas cleanup, gas turbine combined cycle, and, in most cases, an air separation unit (ASU). In an IGCC system, coal or other fuels is partially oxidation in a gasifier to produce syngas, which is combusted and expanded in a gas turbine to produce power. The heat from exhaust gas is recovered in a heat recovery steam generator (HRSG) to produced steam, which is expanded in a steam turbine to produce additional power. In a conventional PC plant, pulverized coal is combusted in a boiler and the combustion heat is transferred to produce high pressure steam, which is expanded in a steam turbine to produce power. Advantages of IGCC systems over conventional pulverized coal (PC) power generation include higher thermal efficiency, lower emissions of key pollutants, and greater fuel-flexibility (O’Keefe and Sturm, 2002).

Although there are many environmental and performance benefits associated with application of IGCC technology, the commercialization of IGCC is still in an early phase and actual technical data and experiences are limited. A potential disadvantage of IGCC that impedes more widespread use is cost and also the perception that IGCC plants are more like chemical process plants than the conventional power plants. As a technology in an early phase of development, IGCC plants generally are not cost competitive and typically are subsidized as part of demonstration programs (Mudd, 2003).

As additional development of IGCC systems occur, the capital cost and operation cost are expected to decrease. Therefore, additional research, development, and demonstration (RD&D) is required to identify and evaluate advances in IGCC technology, identify priorities for improvements in IGCC systems over the next decade, provide risk analysis for technology advances, and provide input to decision making regarding selection of technology options in this area. The risks associated with IGCC technology include the technical or cost risks, such as low efficiency, high emissions, and high cost, caused by the uncertainty in process parameters.

In previous work, the advantages of performance and cost of IGCC systems were investigated (Buchanan, *et al*, 1998; O'Keefe and Sturm, 2002; Ratafia-Brown, *et al*., 2002a&b) and alternative designs of IGCC system were evaluated (Falsetti, *et al*., 2001; Holt, 1998, 2003). The performance and cost models were developed for selected IGCC technologies and probabilistic analysis were developed and applied to evaluate the potential risks of IGCC systems (Frey and Rubin, 1991a&b, Frey and Rubin, 1992; Diwekar, *et al.*, 1997, Frey and Akunuri, 2001).

At present, the potential improvements of IGCC technology have taken place in the main components of IGCC systems, including advances in gas turbine combined cycle and integration of different components. The risks associated with advanced in technology need to be evaluated. Therefore, research is required to provide guidelines for improvements in IGCC systems over next decades. Specific areas in which additional progress is needed with regard to IGCC system RD&D include: (a) evaluation of the implications of the use of alternative feedstocks with regard to priorities for system operation; (b) assessment of implications of alternative gas turbine designs on system feasibility; (c) evaluation of the risks associated with performance, emissions, and costs of IGCC technology due to lack of knowledge of technical parameters (d) evaluation the implications of different integration methods between ASU and gas turbine for IGCC system performance. The justification for these specific focus areas is further described in later sections of this chapter.

1.1 Comparison of IGCC to Conventional PC Plant

In this section, the performance, emissions, and costs of IGCC and PC plant are compared. The purpose is to find out the advantage and disadvantages of IGCC technology as an innovative technology. The performance and emissions data for PC plant and IGCC plant are shown in Table 1-1.

For performance comparison, the efficiency of IGCC plant is generally higher than conventional PC plant. The efficiency of an IGCC plant is typically estimated to be 37.8 to 41.5 percent on a higher heating value basis (Holt, 2003). The efficiency of a conventional sub-critical PC plant is typically 35.0 to 37.5 percent (Ratafia-Brown, *et al.*,

Table 1-1 Comparison of IGCC and PC Plant

Description	PC Plant	IGCC Plant
Efficiency, %, HHV [a]	35.0% ~ 37.5% [b]	37.8 ~ 41.5% [c]
Pollution Control Methods [d]		
Sulfur Control	Wet limestone flue gas desulfurization (FGD)	Amine-based scrubber(>98% removal)
Nitrogen Control	Low-NOx burners and selective catalytic reduction (SCR)	Diluents, nitrogen and steam, are used in the gas turbine to control NOx
Particulate Control	Electrostatic precipitator (ESP)	Wet scrubber
Solid Waste	Bottom ash and fly ash	Slag and ash
Environmental Performance [d]		
SO_2 Emissions, lb/10^6Btu	0.2	0.08
NO_x Emissions, lb/10^6Btu	<0.15	0.09
PM_{10}, lb/MWh	<0.03	0.011
CO_2 Emissions, lb/kWh	2.0	1.76
Total Solid Generated, lb/MWh	367	175
Water Usage, gallon/MWh	640 [e]	510~600 [f]

[a] HHV: Higher heating value;
[b] Ratafia-Brown, *et al*., (2002a&b); Buchanan, *et al.* (1998); Smelser, *et al*., (1991).
[c] Holt (2003);
[d] Ratafia-Brown, *et al*., (2002a&b); The emissions and solid generation data of PC plant and IGCC plant are both based on the assumptions: coal with 12,000 Btu/lb HHV and 2.5% sulfur content; pollution control methods listed in the above Table.
[e] The data for water usage comparison of PC plant are from the design study of Smelser, *et al*.(1991), which is also a 35% with similar design as the PC plant in Ratafia-Brown, *et al*., (2002a&b).
[f] The data for water usage of IGCC plant is from the report of Bechtel, *et al.* (2002). Different IGCC designs were investigate in this report, thus a range of the water usage is provided here.

2002a&b; Buchanan, *et al.*, 1998; Smelser, *et al*., 1991). The typical steam condition for sub-critical PC plant is 2400 psia/1000 ^oF/1000 ^oF (Buchanan, *et al.*, 1998).

In Table 1-1, the environmental performance of a conventional PC plant and IGCC plant are listed in terms of environmental emissions and solid generation. For environmental emissions, the SO_2, NO_x, particulates (PM_{10}), and CO_2 emissions from a typical IGCC plant are compared to the emissions of a PC plant. In the PC plant, wet limestone flue gas desulfurization (FGD) is used for SO_2 control, low-NOx burners and selective catalytic reduction (SCR) is used for NO_x control, and an electrostatic

precipitator (ESP) for particulate control. IGCC plant also has related methods for control of these emissions. Based on the data in Table 1-1, the emissions of SO_2, NO_x, PM_{10}, and CO_2 from an IGCC plant, are only 40%, 60%, 36%, and 88% of the corresponding emissions from a PC plant, respectively. It indicated that the IGCC plant has advantages in emissions of criteria pollutants and CO_2 emissions.

In terms of the solid waste generation, the solid generation of IGCC plant is only 48% of the PC plant. The largest solid waste generated by IGCC plant is slag, which is typically a glassy-like material that is a marketable byproduct (Ratafia-Brown, *et al.*, 2002a). The slag is highly non-leachable compared to the waste from PC plant (Wabash River, 2000). Therefore, the slag from IGCC plant need not be treated and is classified as non-hazardous (Ratafia-Brown, *et al.*, 2002a).

In a PC plant with FGD for sulfur removal, the water usage mainly consists of two parts: makeup water for the cooling tower and makeup water for FGD. In cooling tower, fans are equipped that draw air upward through the cooling water to evaporate some of the water and cool the remainder. The water loss from cooling tower mainly consists of the evaporation loss, blow-down loss, and drift loss. Among them, the evaporation loss is biggest one, which contributes approximately 85% of the total water loss of cooling tower in a PC plant (Smelser, *et al.*, 1991). Another part of water consumption is the water used in FGD for sulfur control. Smelser, *et al*. (1991) reported the water usage for a PC plant with 35% efficiency to be 640 gallon/MWh. The water used for make up the loss of the cooling tower in this plant was 549 gallon/MWh. The

water consumption of FGD was 65 gallon/MWh. The sum of the two parts contributes the most of the water use for this PC plant.

In an IGCC plant, the water usage include the water used for gasification as a reactant or temperature moderator, water or steam consumption for NO_x control if water or steam diluents are used, and also the loss of cooling water. However, the cooling water consumption of IGCC is considerably lower than that of a same size PC plant because the power output of steam turbine in an IGCC plant is less than 50% of the total plant power output and more than 50% of the power is generated by the gas turbine, which is air cooled (Buchanna, *et al*. 1998; Ratafia-Brown, *et al*., 2002b). Therefore, the cooling water consumption of IGCC plant is only 40% to 60% of that of a conventional PC plant (Ratafia-Brown, *et al*., 2002a). The water feed for gasification for an entrained gasifier-based IGCC plant with 40% efficiency (HHV) is approximately only 36 gallon/MWh (Buchanan, *et al*., 1998), which is much less than the water loss of cooling tower. The reason for low water consumption in gasification is that coal contains moisture and hydrogen, which are both the hydrogen source in gasification. For the water or steam used for NO_x control, it depends on the moisture fraction of saturated syngas. Bechtel, *et al.* (2002) reported that the total water usage for the IGCC plants is approximately 510 to 600 gallon/MWh, including the water for gasification, water injection to syngas, and cooling water loss. It is 80% to 94% of the total water consumption of the PC plant introduced above.

For the water discharge, the IGCC plant is similar to the PC plant, including two parts. One is the wastewater from the steam cycle, including the blowdowns form boiler

feedwater and the cooling tower; and another is process water blowdown (Ratafia-Brown, *et al.*, 2002b). For the gasification process, a big part of the feed water remained as the moisture in syngas out of the gasifier. Most of the moisture condensates in the followed gas cooling process and is recycled to the gasification process. Thus the water discharge of gasification is only a blowdown stream. Due the smaller share of the steam cycle of IGCC plant compared to the one in PC plant, the wastewater from the steam cycle is generally lower than the PC plant. The process water blowdown for two plants are almost same (Ratafia-Brown, *et al.*, 2002b).

Besides the advantage in environmental performance, IGCC also features fuel flexibility compared to PC plant. Aside from the use of coal as a feedstock in gasification, low or negative value feedstocks, including municipal solid waste (MSW), biomass, industrial waste, and other types of wastes have been used as feedstocks for IGCC systems in the US (Schwager and Whiting, 2003), as well as overseas. For example, the ISAB Energy and Sarlux IGCC plants in Italy use heavy residual oil as feedstock (Collodi, 2000). Thus, IGCC systems offer the potential of improved energy efficiency, lower environmental discharges in most cases, and greater operational flexibility than conventional methods for power generation from coal.

Although IGCC technology is superior to PC plant in performance and environmental emissions, IGCC plant has a higher cost requirement than PC plant at present. For example, the cost requirement of a typical IGCC plant with 40% (HHV) efficiency is 1,400 $/kWh (1998 Dollar), while the capital requirement of a conventional PC plant with efficiency (HHV) of 37.6% is 1,200 $/kWh (1998 Dollar) (Buchanan, *et*

al., 1998). This PC plant has ESP for particulate control and wet limestone FGD for sulfur control with steam condition of 2400psig/1000^{o}F/1000^{o}F. The capital requirement of Tampa IGCC project is approximate 1,900$/kW (2000 Dollars) (Hornick*, et al.*, 2002). Mudd (2003) summarized that the cost investment of IGCC plants at present is from 1,100 to 2,000 $/kW.

Therefore, additional development and research work is required to improve the cost competitiveness of IGCC technology and evaluate the feasibility of potential developments. The motivation of this study is introduced in the following.

1.2 Motivating Questions

In order to estimate and evaluate the benefits and risks of a new technology such as advanced options for IGCC systems, there is a need to develop a systematic approach for technology evaluation. The main components and the interaction of components in an IGCC plant need to be characterized in order to make reasonable estimates of system feasibility in terms of key measures of performance, emissions, and cost. Thus, the key motivating questions for this study are:

1. What are the effects of different fuels on the thermal efficiency, emission, and costs of selected IGCC systems?
2. How do different gas turbine combined cycle designs affect the performance, emissions, and cost of IGCC systems?
3. How does integration of the ASU, both with the gas turbine compressor and the gas turbine combustor, affect the performance, emissions, and cost of IGCC systems?

4. What are the uncertainties in key measures of IGCC feasibility based on uncertainties in inputs?
5. What are the key sources of uncertainties in performance, emissions, and cost of IGCC technologies that could be the target of additional research in order to reduce uncertainty?

1.3 Overview of the Research

The objective of this study is to identify and evaluate key design and operational factors as well as technological alternatives with respect to key measures of the feasibility of IGCC systems. Furthermore, the uncertainty inherent in estimates of system feasibility is evaluated quantitatively in illustrative case studies. Thus, this study provides deterministic estimates and, in some cases, probabilistic estimates of performance, emissions, and costs of alternative IGCC systems. The main tasks of the study are to:

1. Develop a modeling framework for simulation of alternative IGCC systems, including the capability to consider alternative fuels, process integration issues (e.g., with the ASU), and gas turbine combined cycle designs;
2. Develop a simplified model for gas turbine combined cycle systems to facilitate policy analysis and to evaluate the sensitivity of inputs;
3. Compare the effects of different fuels on the performance, emissions, and cost of IGCC systems;
4. Characterize uncertainty in the performance, emissions, and costs of IGCC systems based upon alternative gas turbine designs and compare them based on deterministic and probabilistic analysis; and

5. Evaluate the effects of ASU integration with the gas turbine on the performance, emissions, and cost of IGCC systems.

1.4 Overview of IGCC Technology

The first modern IGCC plant began producing electricity in 1984 (Falsetti, ***et al.***, 1999). Today, several IGCC plants have been constructed for producing power from coal, residual oil, and other low or negative value feedstocks (Preston, 2001). IGCC systems are an advanced power generation technology with fuel flexibility. In addition to power, IGCC system also can produce steam and hydrogen and other coproducts (Preston, 2001). Generally, sulfur is produced as a marketable byproduct in an IGCC system.

A conceptual diagram of an IGCC system is given in Figure 1-1. In a gasification process, coal or other feedstocks are reacted with a high purity oxidant and steam to produce a syngas rich in carbon monoxide (CO) and hydrogen (H_2). The high purity oxidant is produced in an ASU. The syngas flows through cooling and cleaning steps prior to combustion in a gas turbine combined cycle system. In the combined cycle, the syngas reacts with the compressed air from the compressor. The combustion product is expanded in the turbine and shaft work is produced. The heat from the gas turbine exhaust is used to make steam in a HRSG. The steam is expanded in a steam turbine. Electricity is generated both by the gas turbine and a steam turbine.

In the following sections, the details of the technologies used in three main components if an IGCC are introduced, including gasification, gas turbine combined cycle, and air separation unit.

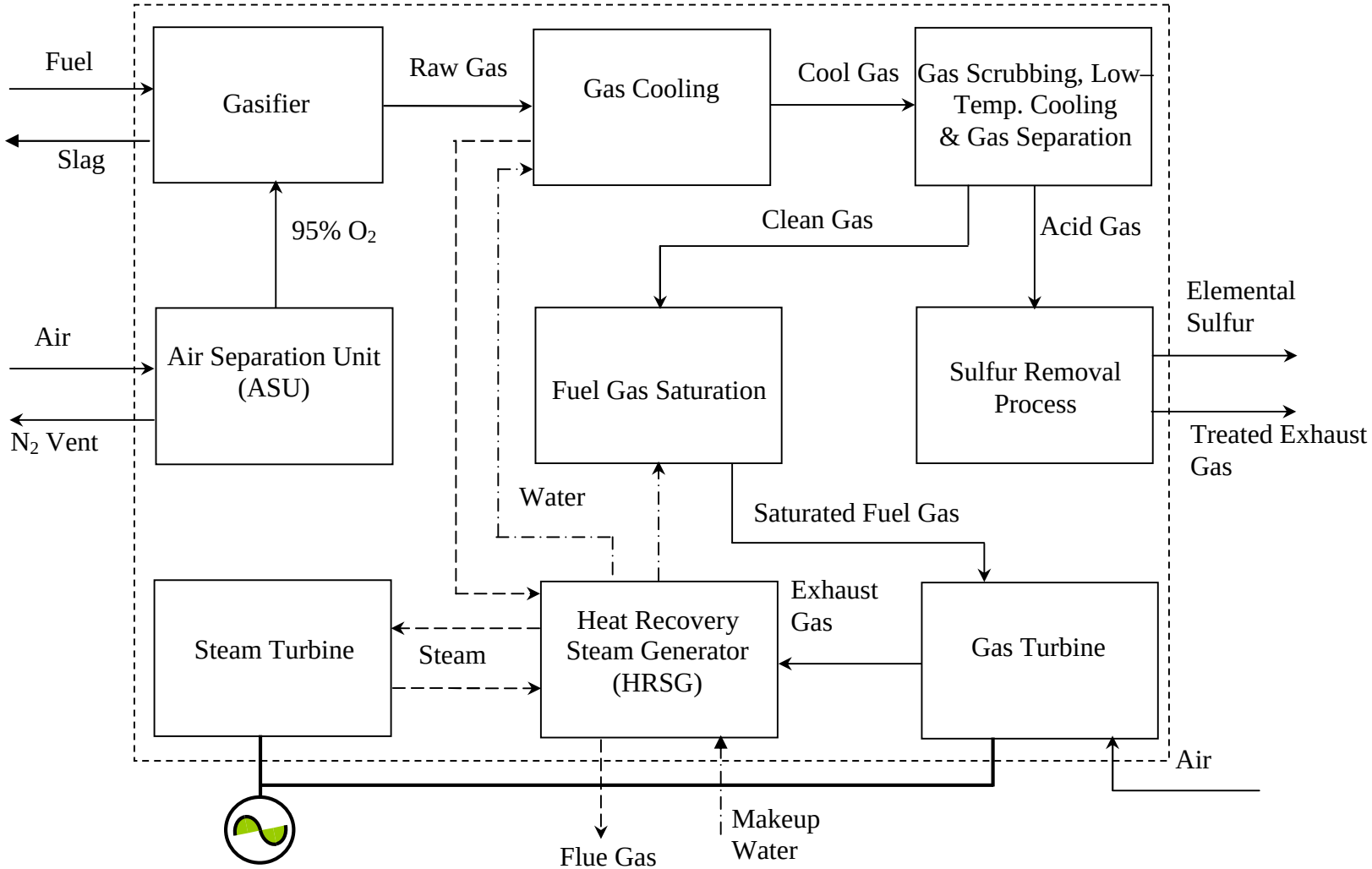

Figure 1-1 Conceptual Diagram of IGCC System

1.4.1 Gasification Technology

Gasification is a process that produces syngas containing hydrogen and carbon monoxide from coal or other carbonaceous feedstocks. High purity oxidant is fed into gasifier to partially oxidize fuels. Water or steam is used as a source of hydrolysis in the reactions. Three kinds of gasification technology are generally applied in IGCC systems, including moving-bed, fluidized-bed, and entrained-flow gasifiers. The three gasifiers are briefly discussed and that the reasons for focusing on the entrained flow gasifiers as the basis of the case studies in this work are described.

1.4.1.1 Countercurrent Gasifier

In a countercurrent gasifier, the oxygen and steam are introduced in the lower part of the gasifier and flow vertically upward, while fuel is introduced at the top of the gasifier and flows downward. The fuel is heated as it descends, which drives off the lower molecular weight and more volatile compounds in the fuel. The portions of fuel that reach the bottom of the gasifier are combusted to heat the sygnas that are flowing upward through the gasifier. The heat from the combustion zone provides thermal energy to the endothermic gasification reactions that occur in the middle portion of the gasifier.

The generated syngas ascends in a counter-current flow to the fuel. As the hot gas moves upward and contacts the cooler fuel, a relatively large amount of gaseous methane is produced at the low temperature at the top of the gasifier. The outlet temperature of this kind of gasifier is lower than other two kinds of gasifiers. Because of the efficient heat transfer in a counter-current flow method, the oxygen requirement for efficient utilization of fuel is lower than alternative gasifiers (delaMora, ***et al.***, 1985).

This gasifier is suitable for gasification of large particles of approximately 4 mm to 30 mm due to the feature of countercurrent flow (Simbeck *et al.*, 1983). A typical outlet temperature of the gasifier is about 1,100 ^{o}F (delaMora, *et al.*, 1985). At this temperature, heavy hydrocarbon compounds, such as tars and oils, will not be cracked. These compounds can condense in the syngas cooling process. Thus, these types of gasifiers typically are associated with the need for a downstream process condensate treatment process.

An important measure of gasifier performance is the cold gas efficiency. The cold gas efficiency is the ratio of the heating value of the syngas at standard temperature to the total heat input of the required fuel. This kind of gasifier cannot be used to handle fine particles because the syngas flows upward in a countercurrent flow to the fuel flow and would tend to entrain fine particles and carry them to downstream equipment. For fine particles, an entrained gasifier should be used. A typical example of this kind of gasifier is the British Gas/Lurgi (BGL) slagging gasifier. The BGL gasifier is suitable for handling of large particles, such as solid wastes (delaMora, *et al.*, 1985).

1.4.1.2 Fluidized-Bed Gasifier

In a fluidized-bed gasifier, the fuel, oxidant or air, and steam are mixed and introduced into the bottom of the gasifier. The reaction bed is fluidized as the fuel gas flow rate increases, in which particles are suspended in a stream of flowing gases. The fuel particles are gasified in the central zone of the gasifier. The ash and char particles flow with the raw gas out of the gasifier and are captured by a cyclone and recycled. The fluidized bed is operated at a nearly constant temperature of 1800 ^{o}F. This is higher than

the operation temperature of BGL gasifier and thus the formation of tars is avoided (Cargill, *et al*., 2001). Once heated, ash particles in the bed tend to stick together and agglomerate. The agglomerated ash falls to the bottom of the gasifier where it is cooled by recycled syngas and removed from the reactor.

The fluidized bed is suitable for fuel particles in a size range of 0.1 mm to 10 mm. It is restricted to reactive, non-caking fuels for uniform backmixing of fuel and syngas and gasification of the char entering the ash zone. A typical example for fluidized bed gasifier is Kellogg Rust Westinghouse (KRW) gasifier. An air-blown KRW gasifier is used in Pinon Pine IGCC project (Cargill, *et al*., 2001).

1.4.1.3 Entrained-Flow Gasifier

The entrained-flow gasifier features a plug type reactor and is suitable for gasification of fine fuel particles less than 0.1 mm in diameter. Entrained-flow gasifiers use oxygen as the oxidant and operate at high temperatures well above ash slagging conditions in order to assure reasonable carbon conversion and to provide a mechanism for ash removal (Simbeck *et al.,* 1983). The gasification temperature is above 2300 ^{o}F. At such a high temperature, low amount of methane is produced and no other hydrocarbon is found in the syngas. The product is a syngas rich in CO and H_2.

The entrained-flow gasifier has advantages over other alternative gasifiers in that almost all types of coals can be gasified regardless of coal rank, caking characteristics, and amount of coal fines. The high gasification temperature makes it easy to gasify less reactive fuels that are not efficiently gasified in lower temperature counter-current or

fluidized-bed gasifers. Due to the high temperature, the consumption of oxygen during partial combustion in this kind of gasifier is higher than for other gasifiers.

A typical example of an entrained-flow gasifier is the Texaco Gasification Process (TGP). The TGP uses coal in a water slurry as the feedstock, in which the water acts as a heat moderator. The TGP gasifier has higher operation pressure than other types of entrained flow gasifiers, which leads to higher syngas production capacity of a gasifier of a given size (Simbeck, ***et al.***, 1983). The TGP is more widely used than other types of gasifiers for gasification of various fuels, including less reactive feedstocks due to high temperature and high pressure (Preston, 2001). The TGP is used for conversion of heavy oils, petroleum coke, biomass, and even hazardous wastes, to products including power, steam, hydrogen, ammonia or other chemicals (EPA, 1995; Richter, 2002).

1.4.2 Gas Turbine Combined Cycle

Gas turbines have been widely used for power generation. A typical simple cycle natural gas-fired gas turbine has an efficiency of 35% or greater (Brooks, 2000). Most new power plants also use a heat recovery steam generator (HRSG) and steam turbine in addition to a gas turbine, which is a combined cycle system (DOE, 2003). In a combined cycle system, the waste heat in the exhaust gas is recovered to generate high temperature steam for a steam turbine.

In Figure 1-2, a conceptual diagram of a simple cycle is illustrated. In a simple cycle gas turbine, air enters a compressor. The syngas produced from the gasifier or natural gas is sent to the combustor of a gas turbine. The syngas is combusted with the compressed air. The high pressure hot product gases from the combustor enters the

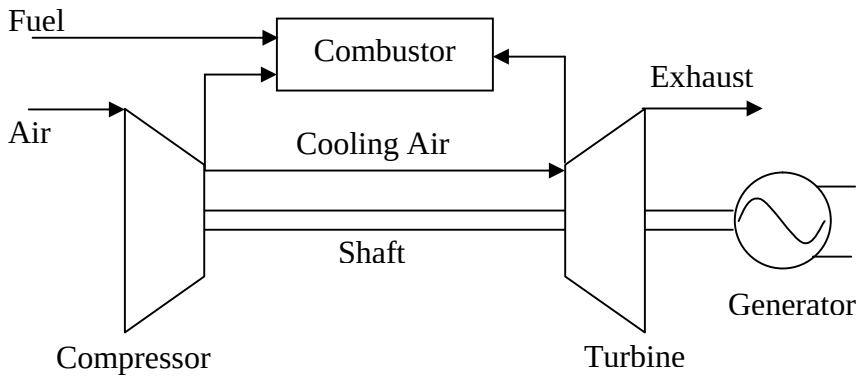

Figure 1-2 Simplified Schematic Diagram of a Simple Cycle Gas Turbine

turbine, or expander. In the turbine, the gases are expanded and reduced in pressure, resulting in a corresponding reduction in temperature. The expansion and cooling of the hot gases in the turbine results in an energy conversion from the heat of the hot product gases to shaft work and electricity is produced.

In most IGCC systems, a HRSG and a steam cycle are combined with a simple cycle gas turbine to form a gas turbine combined cycle (CC). In a combined cycle, the hot exhaust gas is further cooled in the HRSG. The heat is recovered by producing high temperature and high pressure steam. The steam is expanded in a steam turbine to produce shaft work, which is converted into electricity in a generator. Typically, the steam cycle will have several different pressure levels and the steam turbine will have several corresponding stages. A portion of steam may be diverted to the gasifier. Furthermore, some steam may be generated by heat recovered from cooling of hot syngas that exits the gasifier. Thus, there is typically some degree of integration between the steam cycle and other components of an IGCC plant.

Technological advances in gas turbines provide the potential to further improve the efficiency of the overall IGCC system and decrease the cost of electricity. The heavy duty "Frame 7F" design represents current state-of-practice, which has been used in the Tampa IGCC plant and Wabash river IGCC project (Bechtel, 2002; Hornick and McDaniel, 2002). The newest steam-cooled "7H" gas turbine is the most advanced recently introduced commercial gas turbine (Matta *et al.*, 2000). The details of the two gas turbine technologies are discussed in Chapter 2.

1.4.3 Air Separation Unit (ASU)

There are three methods used for air separation at present, which are cryogenic separation, pressure swing absorption (PSA) and polymeric membranes (Bolland and Mathieu, 1998). The cryogenic separation technology is the most mature and widely used for medium and very large oxygen production requirements with high purity. It is capable of producing oxygen of purity higher than 99.5% and production ranging from 600 tons per day to over 8000 tons per day (Thomas, 2001). Thus cryogenic separation technology is typically the basis for air separation in IGCC systems.

The PSA is suitable for oxygen production less than 40 tons per day of high purity (about 90%) oxygen in the product gas (Bolland and Mathieu, 1998). The polymeric membrane is not applicable for supplying oxygen to power plants for low oxygen purity, which is less than 50% (Prasad, *et al.*, 2002). Thus, the two technologies are not suitable for used in large IGCC systems.

An emerging breakthrough air separation technology is Oxygen Transport Membrane (OTM). OTM features high operation temperature and thus could enable

efficient integration with IGCC. The results of a design study indicate that an IGCC system with OTM would have lower cost and higher efficiency than one with cryogenic air separation. However, commercialization of OTM is not yet realized. A pre-commercial demonstration is expected to be finished in 2007 (Prasad, *et al.*, 2002) Therefore, the cryogenic ASU is still the predominant technology option for air separation applications in IGCC systems.

A cryogenic ASU mainly consists of an air compression system, cryogenic separation units, and an oxygen compression system. Cryogenic ASU designs can be classified into low pressure (LP) and elevated pressure (EP). The LP ASU has a lower cryogenic unit pressure than the EP ASU (Foster Wheeler, 1999; Smith, *et al.*,1997). The pressure level affects the power consumption of the air compressor, oxygen compressor, and nitrogen compressor. In turn, power consumption of the ASU affects the performance of IGCC system since the ASU is the IGCC process area that typically has the largest auxiliary power consumption (Buchanan, *et al.*, 1998). Therefore, selecting a suitable ASU design is important for optimal operation of IGCC systems.

1.4.4 Current Status of Texaco Gasifier-based IGCC Technology

Since this study will focus on entrained flow gasifiers as the basis for case studies, the review of IGCC technology status is primarily with respect to Texaco gasifier-based systems. A summary of Texaco gasifier-based IGCC plants is given in Table 1-2. In 2000 and 2001, there were thirteen Texaco gasification plants that were started up in six countries, including five plants in Asia, four in Europe, three in the U.S., and one in Australia. Three of these plants produce power and other products. In total, there are 60

Table 1-2 Texaco Gasifier-Based IGCC Projects Under Operation or Construction

Project	**Location**	**Start-up Date**	**Plant Size (MW)**	**Products**	**Fuel**	**Status**
Cool Water IGCC	Barstow, California	1984	120	Power	Coal	Full Commercial Operation
Tempa Electric	Polk, Florida	1996	250	Power	Coal	Full Commercial operation
Texaco El Dorado	El Dorado, Kansas	1996	40	Power, steam and H_2	Pet Coke	Full Commercial Operation
ISAB Energy	Priolo Gargallo, Italy	1999	510	Power	Oil	Full Commercial Operation
Sarlux	Sarroch, Italy	2000	550	Power, Steam and H_2	Oil	Full Commercial Operation
API Energia	Falconara Marittima, Italy	2000	242	Power and Steam	Oil	Full Commercial Operation
Motiva Delaware City	Delaware City, Delaware	2000	120	Power and Steam	Pet Coke	Delayed in Operation
CITGO Lake Charles[a]	Lake Charles, Louisiana	2005	670	Power, Steam, H_2	Pet Coke	Under Construction

[a] Teco Power Services (2001), "CITGO Lake Charles IGCC Project Update", 2001 Gasification Technologies Conference. Others projects are described in Preston (2001), "Texaco Gasification 2001 Status and Path Forward," 2001 *Gasification Technologies Conference.*

Texaco gasification facilities that generate 3.5 billion standard cubic feet per day (scfd) of syngas. By mid-decade, over it is expected that over 5.0 billion scfd syngas will be produced at more than 70 facilities (Preston, 2001).

1.5 Overview of Methodology

Based on the objective of this study in the above sections, the performance and cost models need to be developed for evaluation of alternative IGCC technologies. In this section, the general methodology used for developing IGCC systems models and evaluating alternative designs of IGCC system is described.

Several performance simulation models of IGCC systems have been developed in ASPEN by the U.S. Department of Energy and a number of the models have been refined and extended by Frey and others (Frey and Rubin, 1990, Frey and Rubin, 1991a&b, 1992; Frey, *et al*., 1994, Frey and Akunuri, 2001). The refinements included additional technology options, more detailed modeling of the gas turbine process area, more detail regarding environmental discharges, and improved accuracy with respect to auxiliary power consumption. In addition, a detailed cost model for estimating the capital, annual, and levelized costs has been developed by Frey and Rubin (1990). Probabilistic simulation has been implemented to evaluate the risks associated with IGCC technology (Frey and Rubin, 1991a; Diwekar, *et al*., 1997; Frey and Akunuri, 2001). The studies introduced in the above provide methodology basis for this study.

1.5.1 Process Modeling in ASPEN Plus

Process simulation enables estimation of the behavior of a process by using basic mass and energy balances, suitable thermodynamic models, and chemical equilibrium. In this study, process simulation of a Texaco gasifier-based IGCC was conducted using ASPEN Plus (Advanced System for Process Engineering Plus). ASPEN Plus is an upgraded simulator based on ASPEN, a deterministic steady-state chemical process simulator. The main difference between ASPEN and ASPEN Plus is that the latter has a graphical user interface and is regularly updated and maintained by a commercial vendor (Aspen Technology, Inc., 1994).

In order to simulate a process technology in ASPEN Plus, the technology must be described in terms of a flowsheet. In a flowsheet, unit operations are connected via

material, heat, or work streams. Unit operations are represented by “blocks”, which essentially are computer subroutines in the simulator library that perform mass and energy balance calculations for specific unit operations such as heat exchangers, compressors, pumps, reactors, and others. ASPEN Plus includes an extensive thermodynamic data base to support energy balance and chemical equilibrium calculations.

ASPEN Plus uses a sequential-modular approach to simulation. In this approach, the simulator progresses from one unit operation block to another in a calculation sequence that can be specified by the user or selected by the simulator. In a large flowsheet such as that for an IGCC system, the simulation results for the input streams to some blocks often depend on results for output streams of other blocks that are calculated later in the sequence. Such streams are often referred to as recycle or tear streams. In such cases, the simulator starts with initial values for such streams and iterates on the flowsheet solution until the simulation values for the inlet of an upstream block and outlet of a downstream block converge.

Another type of iterative solution occurs when the user wishes to specify that the value of a stream or block variable should be varied to achieve a particular design target. This type of iterative calculation is performed using a “design specification” block.

Other useful capabilities in ASPEN Plus include “calculator” blocks and “transfer” blocks. A calculator block enables a user to specify their own computer code, in FORTRAN, such as for a unit operation not available in the ASPEN Plus library or for other calculations. For example, a CALCULATOR block is used in this study to

calculate costs of IGCC systems by calling external FORTAN subroutine. A transfer block enables the values of a block or a stream variable to be transferred to other variables. This can be useful to facilitate feed-forward calculations.

1.5.2 Methodology of Cost Estimation

There are several kinds of cost estimation methods that vary with respect to level of detail and complexity. For example, there are four types of cost estimates defined by the Electric Power Research Institute. They include simplified, preliminary, detailed, and finalized (EPRI, 1986). A preliminary cost estimate provides a more detailed consideration of the costs of specific process areas and specific equipments than the simplified cost estimate. It also includes the use of scaling relationships to adjust costs for various operation conditions. The detailed and finalized cost estimates methods often are used for site-specific projects intended for construction (Frey and Rubin, 1990). Since the purpose of this study is to evaluate technology advances and provide guidelines for research planning, the preliminary type of cost estimate is appropriate for cost evaluation of IGCC systems in this study.

The cost model used as a basis for this study was developed by Frey and Rubin (1990) and modified by Frey and Akunuri (2001). The cost model uses key performance outputs from the ASPEN simulation, such as mass flow rates for specific streams, as inputs. The cost models for specific process areas were developed by using regression analysis of published cost and corresponding performance data. For example, the oxidant feed model was a function of oxidant flow rate. The cost model can be used to evaluate the capital, annual, and levelized costs of an IGCC plant. Besides the performance and

design variables from the process flowsheet, important cost parameters are used in the cost model, such as engineering and home office fees, process contingency factors, and project contingency factors. In this study, key process variables from the performance model were input to the cost model. The cost model is simulated in an external FORTRAN subroutine, which is complied in ASPEN Plus simulation engine. The compiled file is put in the same folder with the process model file. When the model is running, the compiled file is called by the process model through the call command in CALCULATOR block, COST. The inputs for the subroutine are from the results of the process model.

1.5.3 Methodology of Uncertainty Analysis

Uncertainty is mainly due to lack of knowledge regarding the true value of a variable or parameter (Cullen and Frey, 1999, Henrion and Morgan, 1990). There can be various reasons as to why uncertainty exists when attempting to predict the future performance, emissions, and cost of a particular design at a commercial scale. For example, the design may not previously have been fully implemented or tested at a commercial scale. Some data upon which predictions are based may be only for pilot or demonstration scale plants, analogies with similar systems, or based solely upon simulation models. Available measurements may be subject to measurement errors or might be for conditions that differ from the anticipated future implementation of the technology. In some cases, data may be unavailable. This is often the case with proprietary data. In such cases, judgments must be made regarding some model parameters, such as internal mass flows within a gas turbine. Uncertainty in inputs and

parameters results in uncertainty in the predictions of performance, emissions, and cost of IGCC technology.

Estimates of process feasibility that are based only on point values can be misleading. For example, Frey and Rubin (1991a) demonstrated that when uncertainties were quantified in model inputs, several factors contributed to identification of biases in the deterministic point estimates. In particular, for models that are nonlinear, or for cases in which probability distributions for some model inputs are skewed, the mean of a probabilistic estimate could differ from the point estimate of a deterministic estimate. Because many inputs may be simultaneously uncertain, it is important to account for the interactions among uncertainty inputs.

Probabilistic analysis provides an indication of both the range and relative likelihood of possible values and therefore can provide insight regarding the probability that a deterministic estimate might underestimate cost or emissions or overestimate efficiency. Thus, probabilistic estimates, when implemented correctly, are expected to provide a degree of realism to cost estimates not readily obtainable with a deterministic approach. Implications are that probabilistic estimates can provide insight into the potential pay-offs that the technology will do better than expected, as well as to the downside risk that the technology will do worse than expected. The pay-offs and risks can be weighed by a decision maker to ascertain whether the technology is sufficiently attractive to continue to pursue, whether the uncertainty is sufficiently large that more data or information should be obtained to reduce it, or whether the downside risks outweigh potential benefits and thus other options should be pursued instead.

Uncertainty analysis has been applied to evaluate the risks associated with performance, emissions, and cost of many process technologies, including combined SO_2/NO_x control technologies (Frey and Rubin, 1991), IGCC technology (Frey and Rubin, 1991a&b; Diwekar, *et al.*, 1997), toxicity assessment of chemical process designs (Chen, *et al.*, 2002), and cost of process technology (Frey and Rubin, 1997). In the probabilistic analysis approach, the uncertainty of inputs can be specified using probability distributions representing the likelihood of different values (Frey and Rubin, 1991a). The development of probability distributions of parameters was based on literature review, data analysis, or expert judgments. The uncertainty of inputs can be propagated to the outputs through the process model using simulation techniques, such as Latin Hypercube Sampling. The uncertainty in outputs can be quantified using a cumulative distribution function (CDF). The key uncertain inputs can be identified using sensitivity analysis.

Incorporating uncertainties in the development of new technology model helps in identifying key factors affecting process designs, comparing competing technology to determine the risks associated new advances in technology, and providing information for research planning.

1.6 Overview of the Report

The organization of thesis is as follows:

Chapter 2 introduces the technical background for the main components in a Texaco gasifier-based IGCC systen with radiant and convective cooling design. For the gas turbine process, two different technologies, Frame 7F and 7H, are introduced.

Chapter 3 describes the development of an ASPEN Plus model of an entrained-flow gasifier-based IGCC system featuring a Frame 7F gas turbine. The calibration and verification of the model are described.

Chapter 4 describes the development of a new gas turbine combined cycle ASPEN Plus model for Frame 7H gas turbine combined cycle technology based upon steam, rather than air, cooling of the hot gas path in the turbine. The gas turbine model is calibrated based on natural gas and syngas. The model results for the IGCC system based on the Frame 7H gas turbine is verified.

Chapter 5 describes several case studies based on deterministic models. The effects of fuel composition on IGCC system performance, emissions, and cost are evaluated. Also, the comparison of Frame 7F and 7H gas turbines with respect to IGCC system performance, emissions, and cost are discussed.

Chapter 6 describes the development of a spreadsheet model of a Frame 7F gas turbine combined cycle system. The calibration of the Frame 7F gas turbine model is discussed. Sensitivity analysis was performed to identify the sensitive inputs of the model.

Chapter 7 documents the uncertainty analysis for the IGCC systems based on the Frame 7F and 7H gas turbine combined cycles. The uncertainty in main outputs of performance, emissions, and costs are discussed. Key sources of uncertainty are identified and prioritized based upon sensitivity analysis.

Chapter 8 evaluates the effects of different integration methods for the ASU and gas turbine on IGCC system performance, emissions, and cost. An ASPEN Plus model for the ASU process is developed and combined with IGCC process simulation model model. Different integration methods are evaluated based on case studies.

Chapter 9 presents the findings and conclusions of this study. The recommendations based on the findings and the recommendations for future studies are presented.

2.0 TECHNICAL BACKGROUND FOR TEXACO GASIFIER-BASED IGCC SYSTEMS

IGCC systems were briefly introduced in Section 1.3. The purpose of this chapter is to describe the technical background as the basis for simulation of the main processes in an IGCC system. In this study, the base design is a Texaco gasifier-based IGCC system with radiant and convective cooling design. The conceptual diagram of IGCC system has been shown in Figure 1-1. The main processes in an IGCC system include Texaco gasification process, gas cooling, gas scrubbing, gas saturation, gas cleaning, sulfur removal, and gas turbine combined cycle.

In a Texaco gasifier-based IGCC system, the coal is crushed and slurried with water. The coal slurry and oxidant are reacted in the Texaco gasifier to produce syngas. The crude raw gas leaving the gasifier contains a small portion of unburned carbon and the molten ash. The gas is cooled in the radiant and convective cooling system for sensible heat recovery via generating high-pressure saturated steam. The cooled gas flows through a particulate matter scrubber. After water scrubbing, the syngas is fed to the low temperature gas cooling section, in which the sysgas is further cooled. The cold syngas enters the Selexol units, in which most of H_2S and a portion of COS are removed from the syngas. The H_2S is recovered to elemental sulfur in Claus plant and the Beavon-Streford plant. The clean syngas is combusted in the gas turbine. The heat of exhausted gas is recovered in the HRSG to produce high pressure steam. In the combined cycle, the gas turbine and the bottoming steam cycle provide shaft energy to a generator to produce electricity.

In the following sections, the technical background for the main processes areas is described in details. These include the Texaco gasification island, high temperature gas cooling and gas scrubbing, low temperature gas cooling, sulfur removal, gas saturation, and gas turbine combined cycle. For the technical background for ASU, it is introduced in Chapter 8 about simulation of integration design of ASU in IGCC system.

2.1 Texaco Gasifier Process

The Texaco gasification process (TGP) is a commercial gasification process that converts organic materials into syngas, a mixture of hydrogen and carbon monoxide. The advantage of adopting TGP over other reactors has been introduced in section 1.3.1.1. In this study, the Texaco gasifier used in the IGCC system with radiant and convective cooling design includes two parts: a reaction chamber and a radiant cooling chamber. The conceptual diagram for gasification and high-temperature gas cooling and gas scrubbing is shown in Figure 2-1.

The feed coal slurry is pumped in the gasifier together with oxidant (normally 95% oxygen). The coal slurry reacts with oxygen in TGP at temperatures between 2400^{o}F ~ 2600^{o}F and at pressures of 600 psig (Flour, 1984). The coal is converted primarily to H_2, CO, CO_2, and a little CH_4 with no liquid hydrocarbon being found in the gas (Simbeck, *et al*., 1983). The exothermic reactions provide heat for endothermic reactions in gasification process. The water in the coal slurry can moderate the gasifier temperature to avoid excessively high temperatures.

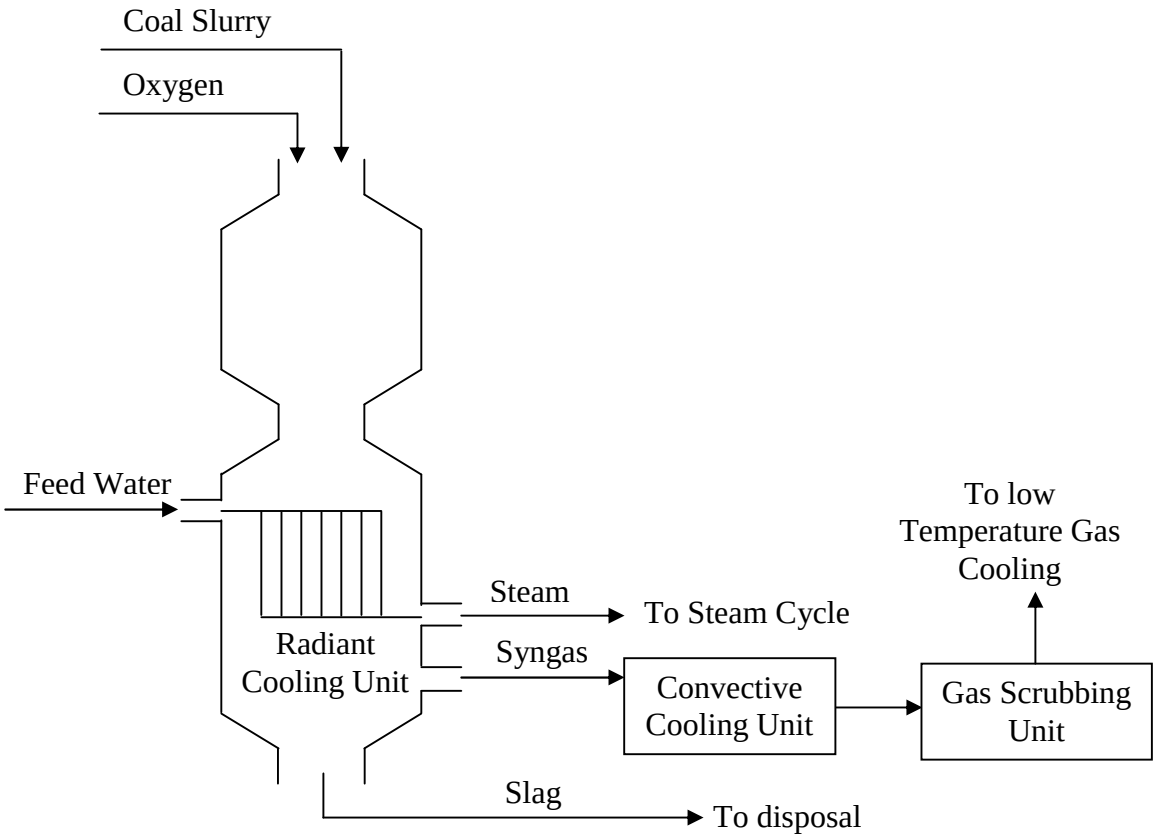

Figure 2-1 Simplified Schematic of Texaco Gasification Process

2.2 High-Temperature Gas Cooling and Gas Scrubbing

There are three high-temperature cooling methods used in IGCC system, including radiant and convective cooling design, radiant only design, and total quench design. The IGCC system with radiant and convective cooling design generally has higher efficiency than the IGCC plants with total quench design (Frey and Akunuri, 2001) and radiant only design (Flour, 1984). Therefore, in this study, the radiant and convective cooling design is selected and simulated.

From the reaction chamber of Texaco gasifier, the raw syngas and molten slag

flow into the radiant cooling chamber, where the gas is cooled to 1500 ^{o}F. The high temperature steam is generated by the heat recovery from sygnas cooling. The molten ash drops into the water quench pool at the bottom of the radiant cooler. It is cooled and removed. The raw gas is further cooled in the convective cooling unit. The syngas leaves the convective cooler at about 650 ^{o}F. The raw gas is scrubbed of particulates with recycled process condensate and makeup water and routed to the ammonia separation unit. All ammonia in the syngas is transferred into the process water. The scrubbed gas flows to the low-temperature gas cooling unit (Flour, 1984).

2.3 Low-Temperature Gas Cooling

The scrubbed syngas flows through various heat exchanger in the low temperature gas cooling process. The syngas is first cooled by heating the circulating saturator water. The syngas is further cooled by exchanging heat to condensate and makeup water. The raw gas is cooled to 105 ^{o}F in a trim cooled against cooling water. The heat removed from the syngas is recovered to produce low pressure steam by heating condensate and makeup water heat feed water or as a source of heat for fuel gas saturation (Flour, 1984). The cooled syngas is sent to the acid gas removal unit.

2.4 Acid Removal and Sulfur Recovery Processes

The sulfur components in syngas are removed in a Selexol process. In this process, the syngas from the low temperature gas cooling unit flows through an acid gas absorber and is contacted with the Selexol solvent. Most of the hydrogen sulfide (H_2S) is absorbed by the Selexol solvent, typically with 95 to 98 percent removal efficiency. About one third of carbonyl sulfide and some of carbon dioxide are absorbed producing a

low sulfur fuel gas. This solvent has a high molecular weight, high boiling point and can be used at ambient temperatures. The absorbed H_2S, COS, and CO_2 are stripped from the Selexol solvent to form the acid gas. The acid gas is sent to the Claus sulfur plant for element sulfur recovery (Simbeck, *et al*., 1983).

In the Claus unit, the acid gas is combusted in a sulfur furnace. The combustion product is sent to a converter to produce elemental sulfur. The tail gas from the Claus process is further treated in a Beavon-Stretford plant. The H_2S is converted to elemental sulfur in the Stretford process. The sulfur is separated, washed, and melted to form a molten sulfur product (Flour, 1984).

2.5 Fuel Gas Saturation

The fuel gas from the Selexol unit is saturated by hot water before it enters the gas turbine. The introduction of water is to control the formation of thermal NO_x because the water vapor lowers the peak flame temperatures. The formation of NO_x from nitrogen and oxygen in the inlet air is highly temperature sensitive. Lowering the peak temperature can decrease the formation of the thermal NO_x and hence, lower the NO_x emissions (Fluor, 1984).

The fuel gas is saturated in an adiabatic saturator vessel. The hot water at a temperature higher than the syngas is sprayed from the top of the vessel. The saturated gas is heated to a temperature of about 350 ^oF and exits from the saturator from the top of the vessel while the hot water exits from the bottom of the vessel. The heat needed for heating the water is transferred from low temperature gas cooling units and the heat

recovery steam generators to the fuel gas saturation unit. The saturated gas is heated by the hot water from HRSG and then fed into the gas turbine combustor (Flour, 1984).

2.6 Gas Turbine Combined Cycle

A combined cycle consists of a gas turbine and a bottoming steam cycle. The gas turbine is composed of a compressor, a combustor, and an expander. A steam cycle includes a heat recovery steam generator (HRSG) and a steam turbine. The gas turbine combined cycle is the main part for power generation in IGCC technology. In this study, two gas turbine combined cycles are selected for evaluation and comparison, which are Frame 7F and 7H gas turbine combined cycles. The 7FA represents current state-of-practice whereas the Frame 7H gas turbine is the most advanced recently introduced commercial gas turbine. The Frame 7H gas turbine uses steam rather than air cooling for the hot gas path, thereby enabling higher firing temperatures and efficiency. The details of two gas turbine technologies are introduced in the following.

2.6.1 Frame 7F Gas Turbine Combined Cycle

In this study, a Frame 7F gas turbine combined cycle is simulated and combined with other processes in an IGCC system. The Frame 7F gas turbine, such as the General Electric MS7001FA, has typically been the basis of the gas turbine design used in IGCC system studies (Buchannan, *et al.*, 1998). The Frame 7F gas turbine uses air cooling technology.

2.6.1.1 Gas Turbine

In an F class gas turbine, the air flows through the compressor to the combustor. Combustion of the fuel gas takes place in the combustor. The high pressure hot product

gases from the combustor enter the turbine, or expander of the gas turbine system. In the turbine, the gases are reduced in pressure, resulting in a corresponding reduction in temperature. The heat-removal process associated with expansion and cooling of the hot gases in the turbine results in an energy transfer from the gases to shaft work, leading to rotation of a shaft. The net difference between the work output of the turbine and the work input to the compressor is available for producing electricity in the generator. The ratio of compressor work to turbine work is referred to as the back work ratio (Eric, 2000).

As noted by Frey and Rubin (1991), the mass flow through a gas turbine is limited by the critical area of the turbine inlet nozzle. The critical area of the turbine inlet nozzle is a constant for a given make and model of gas turbine. Gas turbine operation on natural gas typically involves a relatively small fuel mass flow rate compared to the compressor mass flow rate. However, when operating on syngas, which may have a heating value substantially smaller than that of natural gas, a larger fuel mass flow rate is needed in order to supply approximately the same amount of energy to the gas turbine. The mass fuel-to-air ratio will be larger for a low BTU fuel than for a high BTU fuel. However, the total mass flow at the turbine inlet remains approximately the same. Therefore, the mass flow at the compressor inlet must be reduced to compensate for the higher fuel-to-air ratios needed for low BTU syngases.

2.6.1.2 Steam Cycle

The hot gas turbine exhaust gases enter the heat recovery steam generator (HRSG) units. The sensible heat from the hot exhaust gases is recovered to produce high

pressure saturated steam. The heat from the radiant and convective cooling process is also used in this unit to superheats the high pressure saturated steam. The exhaust gases out of HRSG is at the range of 250 ^{o}F to 300 ^{o}F (Buchanan, *et al.*, 1998). Most of the steam generated in the HRSG is sent to the steam turbines. The steam is expanded in a steam turbine to provide shaft energy to a generator to produce power. A diagram of a Frame 7F gas turbine combined cycle is shown in Figure 2-2(a).

2.6.2 Frame 7H Gas Turbine Combined Cycle

In this study, a Frame 7H is chosen as the basis for evaluating the effects of advanced gas turbine technology on IGCC systems. In contrast to the 7FA design, the 7H gas turbine uses steam rather than air cooling for the hot gas path of the first and second stage of the turbine, thereby enabling higher firing temperatures. For the third stage, air cooling is still used. A conceptual diagram of a Frame 7H gas turbine is shown in Figure 2-2(b). The steam from the outlet of high pressure turbine is sent to the first nozzle and stage 1 and 2 of the turbine for cooling. Because only one stage of the turbine of the Frame 7H system is cooled by air while the entire turbine of the Frame 7F system is cooled by air, the cooling air requirement in the Frame 7H gas turbine is much less than that of the Frame 7F gas turbine. Part of the high pressure steam from the steam turbine is sent to the gas turbine for cooling the hot gas path and then the heated steam is sent back to the reheater of the steam cycle. The heat recovered from the hot gas path in the turbine is used to generate high temperature steam in the steam cycle (Carcasci and Facchini, 2000).

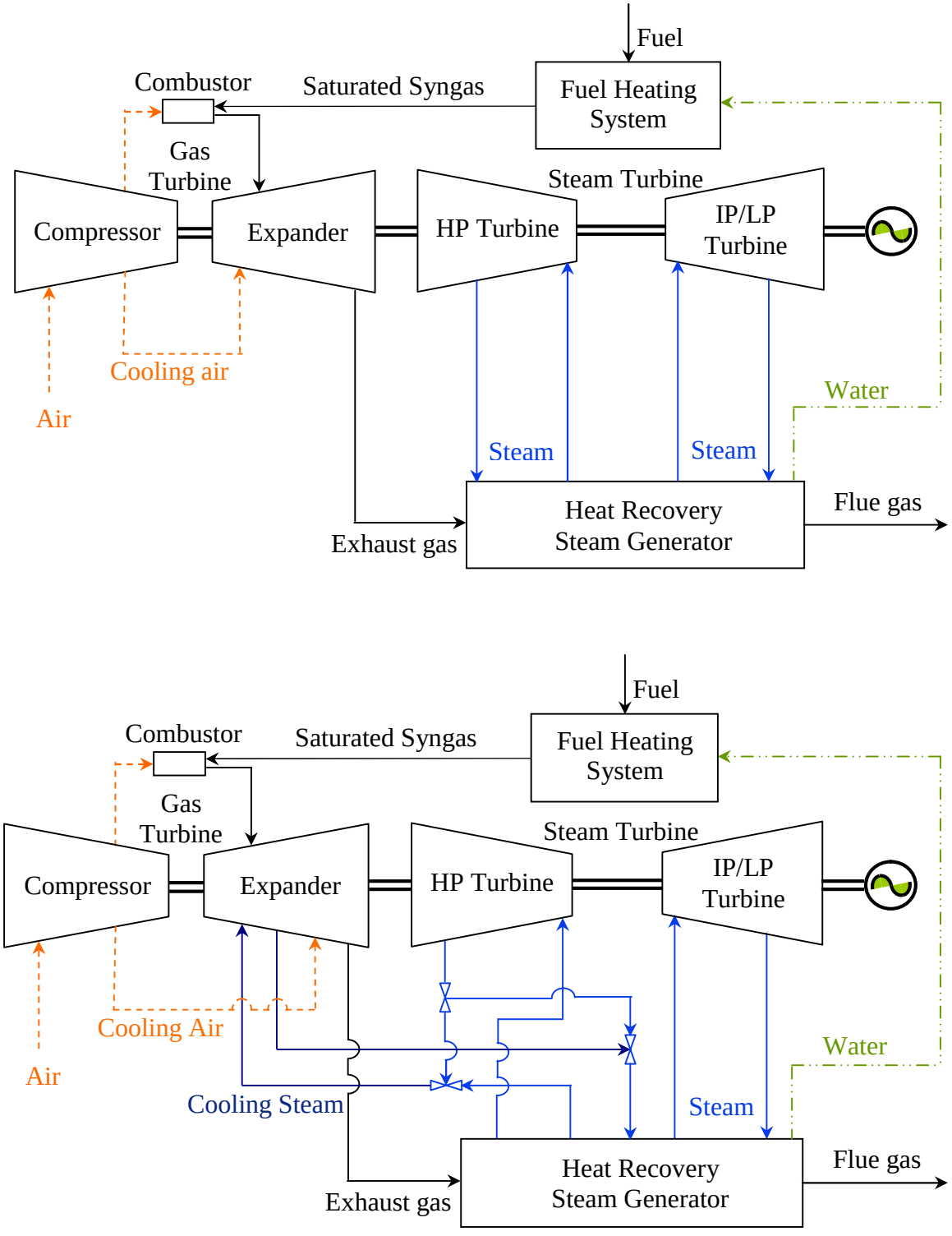

Figure 2-2 (a) Conceptual Diagram of Frame 7F Combined Cycle; (b) Conceptual Diagram of Frame 7H Combined Cycle.

Table 2-1 Frame F and H Technology Performance Characteristics (Eric, 2000; Matta, *et al.*, 2000)

	Frame 7F Gas Turbine	Frame 7H Gas Turbine
Firing Temperature, ^{o}F	2,350	2600
Air Flow, lb/s	940	1230
Pressure Ratio	15.5	23
	Frame 7F Combined Cycle	Frame 7H Combined Cycle
Net Output, MW	263	400
Thermal Efficiency (% at LHV)	56	60
NO_x emissions, ppm@15%O_2	9	9
Steam Condition, psia/^{o}F/^{o}F	1454/997/997	2400/1050/1050

[a] Fuel = Natural Gas.

The main specifications and performance of a Frame 7F and 7H gas turbine combined cycle based on natural gas are listed in Table 2-1. The Frame 7H gas turbine has higher air flow rate, higher firing temperature, and higher pressure ratio compared to Frame 7F gas turbine. Higher firing temperature and less power consumption leads to higher power output and efficiency of a Frame 7H gas turbine than a Frame 7F (Matta, *et al.*, 2000).

In the above sections, the technical background for the main processes o fan IGCC system is described. Specially, the different gas turbine technologies are discussed. Based on the technical background, the simulation of a Texaco gasifier-based IGCC system is implemented in ASPEN Plus, which is described in the next chapter.

3.0 SIMULATION OF TEXACO GASIFIER-BASED IGCC SYSTEM WITH FRAME 7F GAS TURBINE

In this chapter, the methodology for simulation of a Texaco gasifier-based IGCC system with a Frame 7F gas turbine is introduced. The details of the process modeling of the major process sections are described. The simulation model is developed in ASPEN Plus. Therefore, the specifications of the unit operation blocks are described and the flowsheets implemented in ASPEN Plus are shown. The simulation convergence sequence is described. The power balance model and the cost model are discussed.

3.1 Overall Process Description

The Texaco gasifier-based IGCC model developed in ASPEN Plus in this work is based on an ASPEN model by DOE (1985) and a cost model developed by Frey and Akunuri (2001). The system model can simulate the interaction among various process areas within the IGCC system and evaluate the performance and cost of the system. Each main process in IGCC system is modeled by various unit operations blocks in ASPEN Plus. By specifying configurations of unit operations and the flow rate of materials, heat, and work streams into a unit, the mass and energy balance are computed for each unit operation block under the user-defined sequence. The detailed modeling processes of each main parts of IGCC plant are introduced in the following sections. For the base model of the IGCC system, the ASU is represented by a simple unit operation block. For purposes of some of the case studies developed later in this thesis, a more detailed ASU model was developed. The detailed model for ASU process is described in Chapter 6.

3.2 Major Process Sections in Texaco Gasifier-based IGCC Model

The base design of the IGCC system is a Texaco gasifier-based system with radiant and convective cooling and a Frame 7F gas turbine combined cycle. The model consists of the following parts: coal slurry and oxidant feed, Texaco gasification, high-temperature gas cooling and particulate removal, low-temperature gas cooling and fuel gas saturation, sulfur recovery, gas turbine, and steam cycle. The detailed description of each process is given in the following sections. The convergence and computation order, inputs and outputs are introduced.

3.2.1 Gasification Process

The main modeling process of gasification described in this section includes the processes of coal slurry feed, gasification, radiant and convective cooling, and gas scrubbing. The flowsheet of Texaco gasifier island is shown in Figure 3-1. The base fuel selected in the modeling process is Illinois No.6 coal. The compositions of it are listed in Table 3-1. The specifications of the unit operation blocks the overall gasification process are described in Table 3-2.

The coal slurry flows through a pump, modeled by the block SLURPUMP. The pressure of the slurry is raised to 650 psia. The water/coal ratio in the slurry is specified in a CALCULATOR block, SETFEED. The slurry is sent to the block BREAKDON, which serves to decompose the coal into its elements. The yields of the carbon, sulfur, hydrogen, nitrogen, oxygen, ash and water from the decomposition are set by a CALCULATOR block, MASSFLOW. The portions of the coal for the formation of soot

Table 3-1 Proximate and Ultimate of Illinois No.6 Coal

Description	Illinois No.6 Coal [a]
Proximate Analysis, wt%, As Received Basis	
Moisture	10.00
Fixed Carbon	48.87
Volatile Matter	32.22
Ash	8.91
Ultimate Analysis, wt%, Dry Basis	
Carbon	69.62
Hydrogen	5.33
Nitrogen	1.25
Chlorine	0.0
Sulfur	3.87
Oxygen	10.03
Ash	9.90
Higher Heating Value (HHV), Btu/lb, Dry Basis	12,774

[a] Flour Engineer (1984).

and slag are modeled by the blocks MAKESLAG and MAKESOOT. The block MAKESLAG is used to calculate the heat required converting a portion of the coal to slag and the MAKESOOT is to calculate the heat required by the formation of soot. Both the heat streams are sent to the gasifier main reactor modeled by the block GASIFIER. The equations used in MAKESOOT and MAKESLAG are:

$$0.012\ C + 0.852\ ASH \rightarrow SOOT \qquad (3\text{-}1)$$

$$0.0007\ C + 0.992\ ASH \rightarrow SLAG \qquad (3\text{-}2)$$

The oxidant feed is modeled to consist of 95% pure oxygen at 250 ^{o}F and 734 psia. The mass flow rate of oxidant is modeled by a design specification SETO2, which get the heat stream, QLOST, to be 1 % of the total energy input, by varying the feed rate of stream OXIDANT.

The coal slurry and oxygen are injected into the gasifier where partial oxidation of the coal takes place. The coal is converted into syngas, which consists of hydrogen, carbon monoxide, carbon dioxide, water vapor, small amount of hydrogen sulfide, carbonyl sulfide, methane, argon, and nitrogen. The operation condition of the gasifier is 615 psia and 2400 ^{o}F (DOE, 1985). The unit operation block GASIFXR simulates the gasification process. GASIFXR is an RGIBBS reactor. In an RGIBBS reactor, the approach temperatures of specified reactions can be adjusted to calculate equilibrium for each reaction at a specific temperature. Approach temperature is a measure of the difference between the equilibrium temperature of a specific reaction and the outlet temperature of the reactor. The purpose of adjusting the approach temperatures of the reactions represented by Equations (3-3) to (3-9) is to match the typical syngas compositions from a Texaco gasifier. The adjustment results of approach temperatures are a little different from that of Akunuri (1999). The approach temperature for Equation (3-6) is adjusted from –500 ^{o}F to –490 ^{o}F in order to match the published syngas compositions. The details of adjustment of approach temperatures are listed in Appendix B. The reactions in the gasifier and their approach temperatures are:

$$C + 2\,H_2 \leftrightarrow CH_4 \qquad -300\ ^{o}F \qquad (3\text{-}3)$$

$$C + 1.5O_2 \leftrightarrow CO + CO_2 \qquad -500\ ^{o}F \qquad (3\text{-}4)$$

$$C + H_2O \leftrightarrow CO + H_2 \qquad -500\ ^{o}F \qquad (3\text{-}5)$$

$$CO + O_2 \leftrightarrow 2CO_2 \qquad -490\ ^{o}F \qquad (3\text{-}6)$$

$$S + H_2 \leftrightarrow H_2S \qquad -500\ ^{o}F \qquad (3\text{-}7)$$

$$0.5\,N_2 + 1.5\,H_2 \leftrightarrow NH_3 \qquad -500\ ^{o}F \qquad (3\text{-}8)$$

$$CO + H_2S \leftrightarrow COS + H_2 \qquad -500\ ^{o}F \qquad (3\text{-}9)$$

The hot gas from the gasifier is initially cooled in a radiant heat exchanger. High pressure steam is generated in tubes built into the heat transfer surface. Molten slag entrained in the raw gas dropped into a water quench pool at the bottom of the radiant gas cooler. The gas leaves the radiant cooler at a temperature of approximately 1500 ^{o}F and enters a convective heat exchanger. In the convective gas cooler, the gas flows across boiler tube banks and generate the high pressure steam. The cooled syngas at 650 °F flows to the gas scrubbing unit, where it is washed with water to remove fine particles. The particle-laden water is sent to a water treatment plant and soot is separated out. The scrubbed gas is cooled through various heat exchangers in the low temperature gas cooling section. The heat is used to generate low-pressure steam to heat feed water or used for gas saturation.

The crude gas leaving the GASIFXR enters the radiant syngas coolers, simulated by RADCOOL. It is cooled by generating high pressure (1545 psia) saturated steam through recovery of high sensible heat. RADCOOL simulates cooling of the syngas to 1500 ^{o}F. The cooled syngas flowed to the SLAGOUT block, which simulated the separation of slag from the syngas. Block QRCSPLIT is used to model sensible heat lost due to radiation. A default assumption is 6% of the total heat is lost to the surroundings due to radiant heat transfer from the hot walls of the heat exchanger (Akunuri, 1999).

The cooled raw gas is further cooled to 650 ^{o}F in the vertical convective syngas coolers, simulated by block CONCOOL. The heat stream QCONCOOL is obtained by transferring heat for the cooled syngas. QCONCOOL is used to generate the additional high pressure (1545 psia) saturated steam to be used in the steam cycle. The cooled

syngas from the convective cooler, CONGAS, is further cooled to 403 ^{o}F by a gas-gas heat exchanger, simulated by the GASCOOL block. The heat stream QGASCOOL leaving the GASCOOL block is used to reheat the saturated fuel gas entering the gas turbine combustor. The cooled gas is sent to the particulate scrubbing sections of the model, simulated by PARTSCRB. The solids in the raw gas are removed by contacting with recycled condensate from the low-temperature gas cooling section and makeup water. The scrubbed gas, NH3FREE, entered the low-temperature gas cooling section.

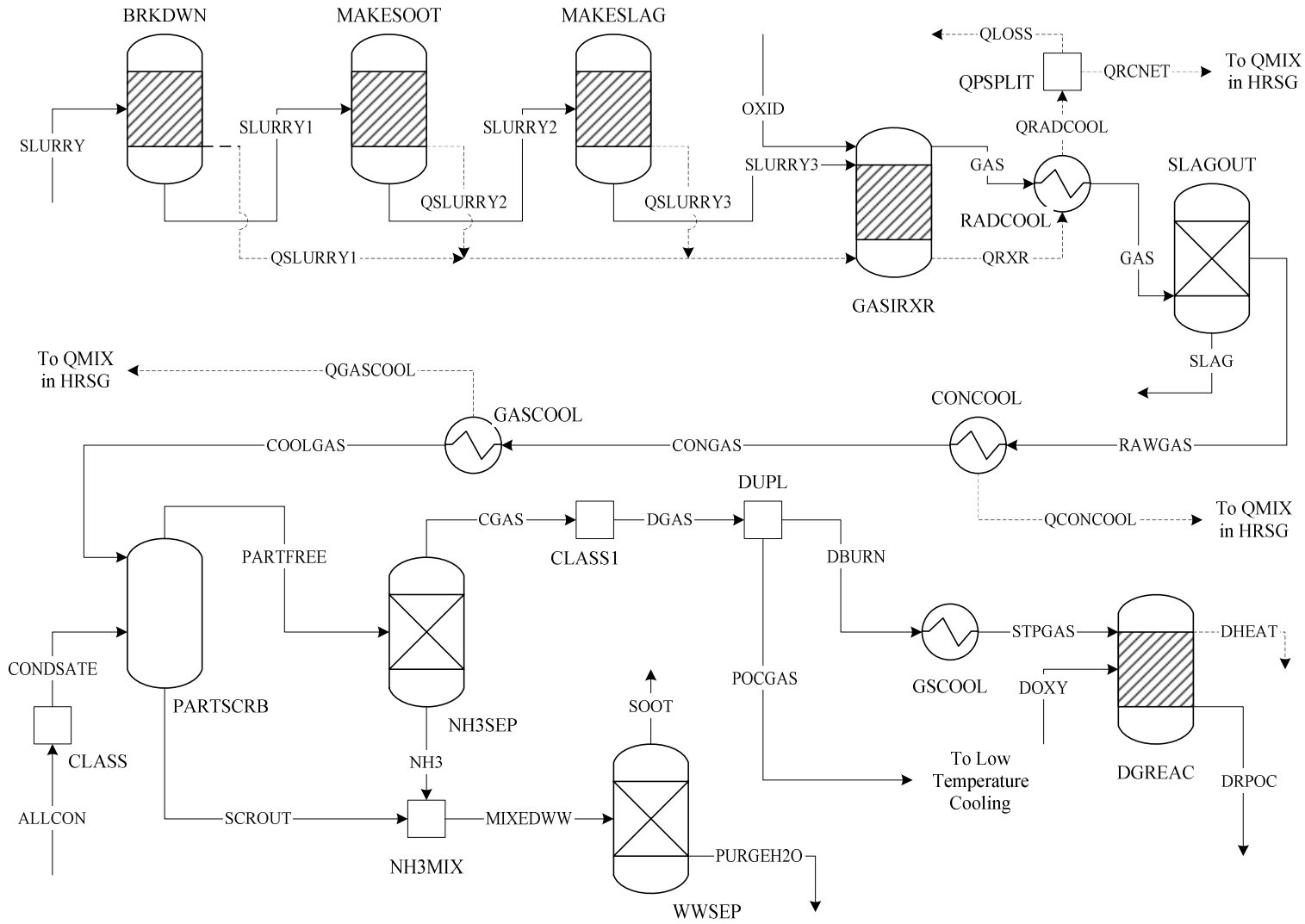

Figure 3-1 Flowsheet of Gasification Process in ASPEN Plus

Table 3-2 Gasification Section Unit Operation Block Description

No	BLOCK ID	BLOCK PARAMETERS	DESCRIPTION
1	SLURPUMP	Pressure = 650 °F Efficiency = 0.65	Simulates the pumping of the slurry to the gasifer
2	BREAKDON (RYIELD)	Temperature = 90 °F P drop = 0 psia	Yields of carbon, sulfur, hydrogen, nitrogen, oxygen, ash and water set by CALCULATOR block MASSFLOW.
3	MAKESOOT (RSTOIC)	CISOLID CARBON –0.0123 NC ASH –0.852 SOOT 1.00 T = 90 °F; P drop = 0	Simulates the stoichiometric reaction which produces soot based on the coal's ultimate analysis.
4	MAKESLAG (RSROIC)	CISOLID CARBON -0.000685 NC ASH –0.992 SOOT 1.00 T = 90 F; P drop = 0	Simulates the stoichiometric reaction which produces slag based on the coal's ultimate analysis.
5	GASIFMIX (MIXER)		Simulates a mixer which mixes the coal slurry and the oxidant feed.
6	GASIFRXR (RGIBBS)	Temperature = 2400 °F Pressure = 615 psia Temperature Approach for each reaction: 1. –300 °F; 2. –500 °F 3. –500 °F; 4. –490 °F 5. –500 °F; 6. –500 °F 7. –500 °F	Simulates the stoichiometric reactions associated with the gasifer reactor.
7	RADCOOL (HEATER)	Temp. = 1500 °F Pressure = 613 psia	Simulates a Radiant cooler which lowers the temperature of the syngas from 2500 oFto 1500 F
8	SLAGOUT (SEP2)	MIXED RAWGAS 0.99 CISOLID SLAG 1 FRAC SUBS=NC STRM=SLAG COMP= COAL 1.0 ASH 1.0 SLAG 1.0 SOOT 0.0	Separates the slag out from the warmgas and put it into the gasifier bottoms stream.
9	QRCSPLIT (FSPLIT)	FRAC QRCLOST =0.08 RFRAC QRCNET =1.0	Simulates some amount of heat is lost from the Radiant cooler.
10	CONCOOL (HEATER)	Temp. = 650 °F Pressure = 603 psia.	Simulates a convective Syngas cooler
11	GASCOOL	Temp. = 403 °F Pressure = 598 psia	Simulates a fuel gas reheater-hot side.

(Continued)

Table 3-2 (Continued)

12	PARTSCRB (FLASH2)	Temperature = 326 °F Pressure = 572 psia	Simulates a particulate scrubber to remove soot from gas stream
13	NH3MIX (MIXER)		The block takes the scrubbed bottoms of the particulate scrubber and mixes it
14	WWSEP (SEP2)		The block separates soot and water from the mixed water from the NH3MIX block
15	NH3SEP (SEP2)		Simulates the absorption of ammonia in the syngas into scrubbed water
16	CLCHNG1 (CLCHNG)		Changes stream class from conventional to mixing.
17	DUPL (DUPL)		The block duplicates the syngas so that a heating value can be calculated
18	HEATER (HEATX)	Pressure = 14.7 psia Temperature = 59 °F	The block drops the gas stream to STP.
19	BURN (RSTOIC)	Pressure = 14.7 psia Temperature = 59 °F	The block completely combusts the fuel using stoichiometric oxygen

3.2.2 Low-Temperature Gas Cooling and Fuel Gas Saturation Processes

This section describes the modeling of the low-temperature gas cooling and fuel gas saturation processes. The flowsheet of low-temperature gas cooling and gas saturation is shown in Figure 3-2. The details of unit blocks is this process are described in Table 3-3. In this model, the input stream POCGAS is the cooled syngas from the gasifer. The scrubbed gas, POCGAS, is cooled by circulation saturator water in a heat exchanger, simulated by block COOL1. The gas is further cooled to 130 ^{o}F by a vacuum condensate (Frey and Akunuri, 2001), which is simulated by the heater block COOL2. The raw gas is cooled from 130 ^{o}F to 101 ^{o}F in the trim cooler, COOL3. The mixer block simulates the collection of the condensate from the heat exchangers in the condensate collection drum. The COLDGAS is sent to the Selexol acid gas removal unit.

The Selexol unit separates the stream COLDGAS into streams CLEANGAS, ACIDGAS, and FLASHGAAS. ACIDGAS is sent to the mixer, CLAUSMIX, and the FLASHGAS is sent to the mixer, BSMIX, in the Beavon-Stretford tail gas treatment plant. For this block, the split fractions of each component in each stream are specified.

The clean gas enters the saturation unit. The required amount of water to be added to clean gas from moisturization is set by a CALCULATOR block SATURH2O, which calculates the required water to be used to saturate the clean gas, simulated by stream SATCOM, which is split from the block FAKESPLT.

The equation used to specify the mass flow of saturated water is:

$$y_{H_2O,wt} = \frac{m_{H_2O}}{m_{syngas} + m_{H_2O}}$$

When rearranged, the following is obtained:

$$m_{H_2O} = \frac{y_{H_2O,wt} \times m_{syngas}}{1 - y_{H_2O,wt}} \quad (3\text{-}10)$$

Where,

m_{H2O} is the massflow of injected hot water;

m_{syngas} is the massflow of clean syngas;

$y_{H2O,wt}$ is the weight percent of moisture in the saturated syngas.

A design specification SETSATR is used to set the heat stream, QEXCES, to be 0 by varying the required amount of hot water entering the heater FAKECOOL through the block FAKESPLIT. The saturated fuel gas from FAKEMIX, SATGAS1, is heated to the required temperature of 347 ^{o}F in the block FAKEHEAT. The fuel gas exits the saturator as 347 ^{o}F with a certain moisture content and is reheated to 570 ^{o}F in the block RHEAT with the heat stream QGASCOOL from the high temperature gas cooling section. The reheated steam, GTFUEL, is fed into the gas turbine combustor.

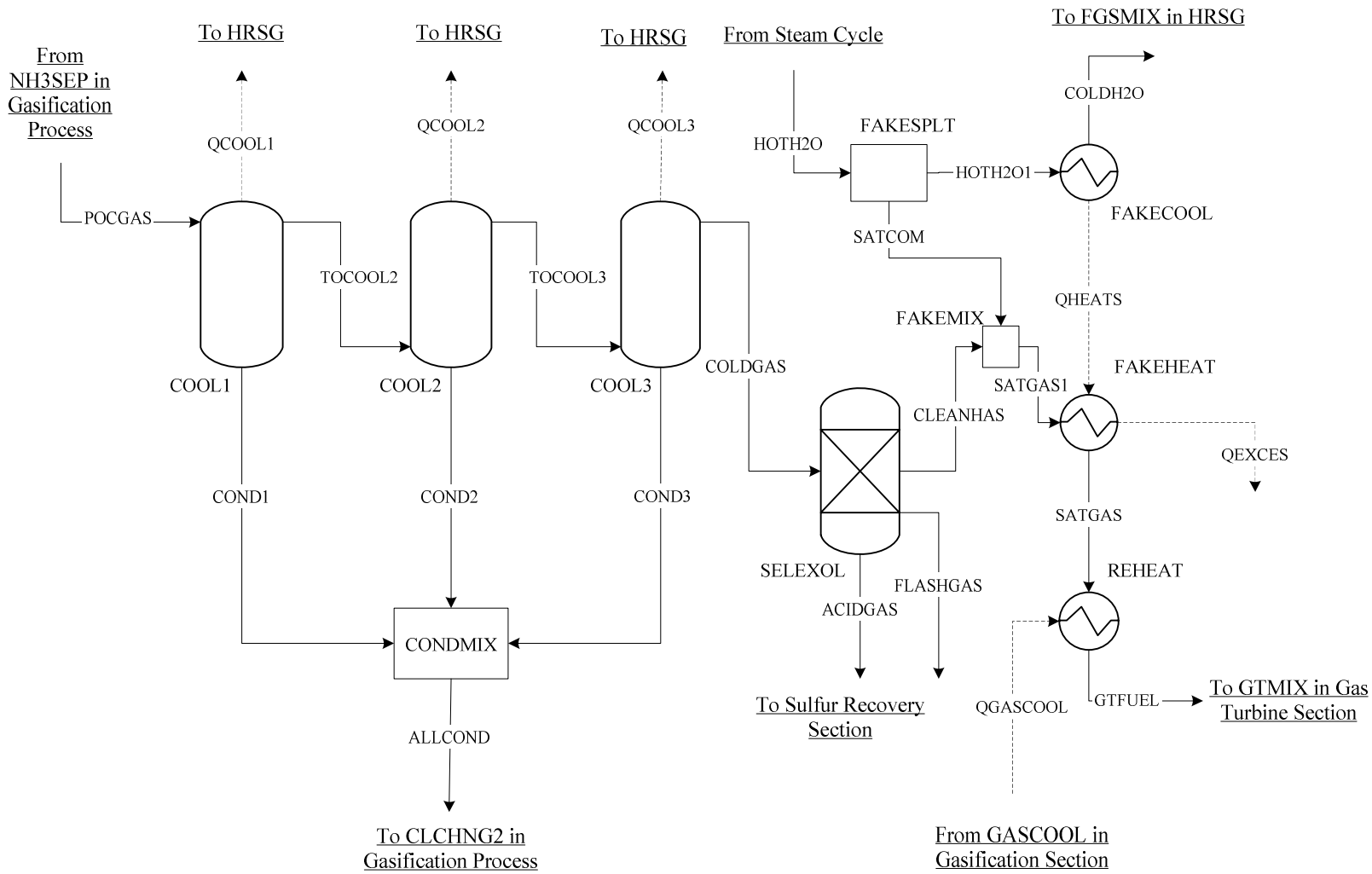

Figure 3-2 Flowsheet of Low Temperature Gas Cooling and Saturation Process in ASPEN Plus

Table 3-3 Low-Temperature Gas Cooling and Saturation Section Units Blocks Description

No	BLOCK ID	BLOCK PARAMETERS	DESCRIPTION
1	COOL1 (FLASH2)	Temp. =262 ^{o}F Pressure = 567 psia	This block simulates a heat exchanger which reduces the temperature of the syngas to 262 ^{o}F from 323 across a pressure drop of 5 psia
2	COOL2 (FLASH2)	Temp. =130 ^{o}F Pressure = 562 psia	This block simulates a heat exchanger which reduces the temperature of the syngas to 130 ^{o}F from 562 across a pressure drop of 5 psia
3	COOL3 (FLASH2)	Temp. =101 ^{o}F Pressure = 557 psia	This block simulates a heat exchanger which reduces the temperature of the syngas to 101 ^{o}F from 130 across a pressure drop of 5 psia
4	CONDMIX (MIXER)		This block simulates the mxing of al condensates.
5	SELEXOL (SEP)	CLEANGAS T=85 ^{o}F, P= 429 psia ACIDGAS T= 120 ^{o}F, P = 22 psia FLASHGAS T= 58 ^{o}F, P= 115 psia	This block separates the syngas into the acid gas, flash gas, and clean gas
6	FAKESPLIT (SPLIT)		This block splits the HOTH2O to get he required water for the saturation of cold gas to 28.2 wt% moisture, which is set by CALCULATOR block SATURH2O.
7	FAKECOOL (HEATER)	Temp.= 235 ^{o}F Pressure = 429 psia	It simulates the cooling os the hot BFW
8	FAKEMIX (MIXER)		It simulates the mixture of the CLEANGAS and SATCOM
9	FAKEHEAT	Temp. = 347 ^{o}F Pressure = 419 psia	It simulates the heating of the saturated gas to 347 ^{o}F before entering REHEAT
10	REHEAT (HEATER)	P = 414 psia	Simulate a Fuel Gas Reheater

3.2.3 Acid Removal and Sulfur Recovery Process

The sulfur recovery section consists of a Claus plant and a Beavon-Stretford plant for tail gas treatment. The process model for sulfur recovery is developed in ASPEN Plus based on the model developed by Stone in ASPEN (US DOE, 1991). The flowsheet of sulfur recovery process is shown in Figure 3-3 and the specifications of operation blocks are listed in Table 3-4.

The acid gas, ACIDGAS, from the separation block, SELEXOL, is sent to the Claus plant. The air is compressed in a compressor, CAIRCOMP, to 23 psia. The compressed air is mixed with the acid gas in a mixer, simulated by CLAUSMIX. The mixed stream, FURIN, is sent to a reactor, simulated by FURNACE. In this reactor, about one third of the H_2S is oxidized to SO_2. The product stream, CLRXRIN, is sent to another reactor, CLAUSRXR. Half of SO_2 is converted to elemental sulfur. The element sulfur is separated from the mixed stream in CLAUSSEP. The left stream, TAILGAS, is sent to Beavon-Stretford for further recovery, as shown in Figure 3-3. The reactions for H_2S oxidation and element sulfur production in Claus plant are:

$$H_2S + O_2 \rightarrow SO_2 + H_2O \qquad (3\text{-}11)$$

$$H_2S + SO_2 \rightarrow H_2O + S \qquad (3\text{-}12)$$

The tail gas stream is sent to a compressor, BSCOMP2. It is compressed to 30 psia. The air from the atmosphere is compressed in BSCOMP1 to 30 psia. The compressed air is mixed with the compressed tail gas stream and a fraction of clean

syngas from SELEXOL block. The mixture, BSCOMBIN, is sent to a combustor block, BSCOMBST. The combustible components, CO and H_2, in the mixture is combusted in the BSCOMBIN block. The combustion product is sent to a reactor, STRETFRD, simulating Stretford process. The left-over H_2S is converted to elemental sulfur. In this process, the following reactions are modeled:

$$SO_2 + 3H_2 \rightarrow H_2S + 2H_2O \quad (3\text{-}13)$$

$$H_2S + \tfrac{1}{2}O_2 \rightarrow H_2O + S \quad (3\text{-}14)$$

$$H_2 + \tfrac{1}{2}O_2 \rightarrow H_2O \quad (3\text{-}15)$$

The elemental sulfur is separated from the gaseous stream in the SSPLIT block BSSEP.

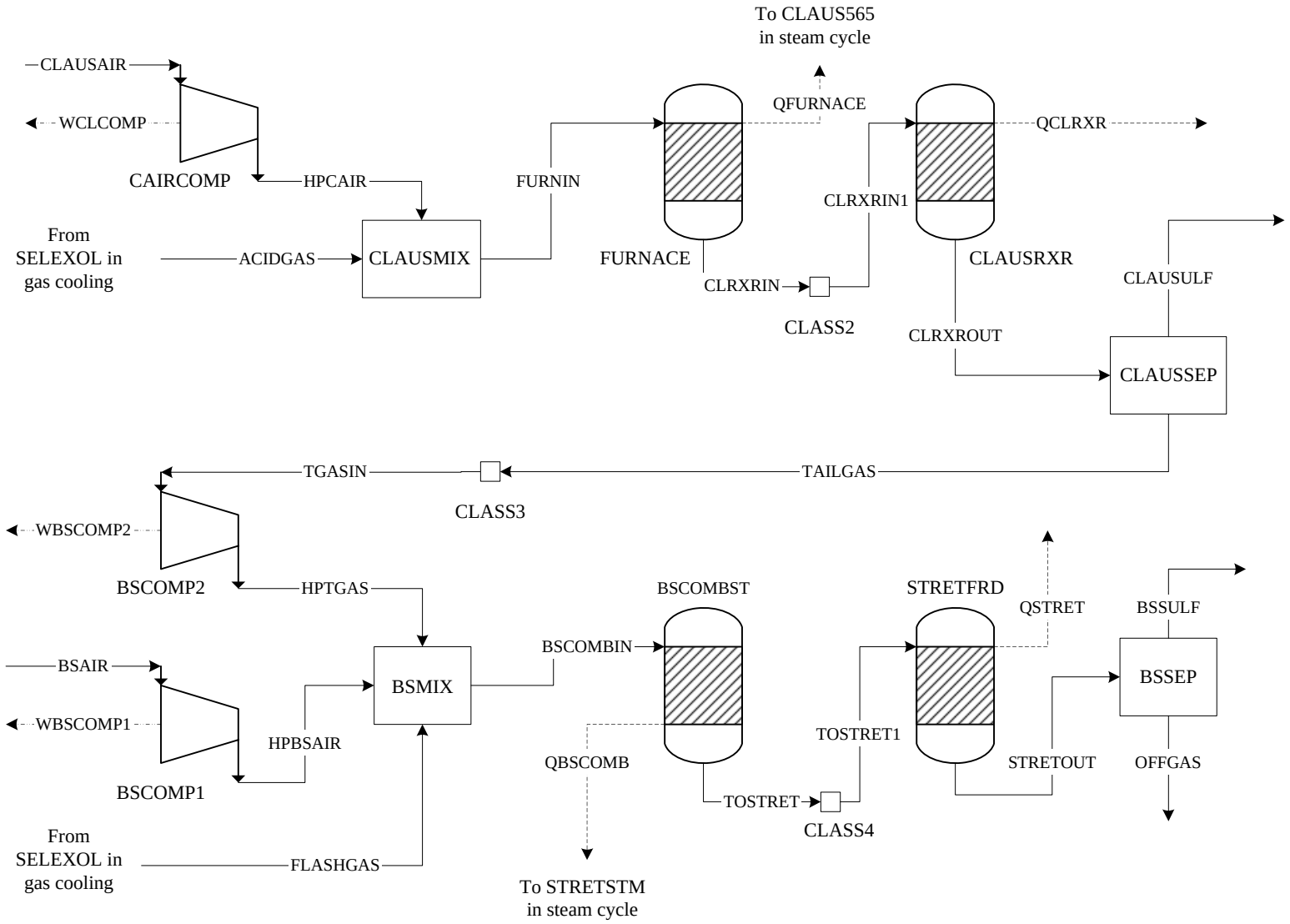

Figure 3-3 Flowsheet of the Sulfur Recovery Process in ASPEN Plus

Table 3-4 Sulfur Recovery Section Unit Operation Block Description

No	BLOCK ID	BLOCK PARAMETERS	DESCRIPTION
1	CAIRCOMP (COMP)	TYPE = ISENTROPIC Pressure = 23 psia Isentropic Efficiency = 0.89	The process air from the atmosphere is compressed in this block
2	CLAUSMIX (MIXER)		It simulates the mixing of air and acid gas from the Selexol process
3	FURNACE (RSTOIC)	Temperature = 1722 °F Pressure drop = 0 psia	The 1/3 of the H_2S is converted into SO_2
4	CLASS2 (CLCHNG)		The class of stream is changed from conventional to mixed class
5	CLAUSRXR (RSTOIC)	Temperature = 270 °F Pressure drop = 0 psia	The 94 percent of remaining H_2S is converted to elemental sulfur
6	CLAUSEP (SSPLIT)	TAILGAS FRAC MIXED = 1.0 CLAUSULF FRAC CISOLID = 1.0	The solid sulfur product is separated from the gaseous stream of the Claus plant
7	CLASS3 (CLCHNG)		The class of stream is converted from mixed to conventional class
8	BSCOMP1 (COMP)	TYPE = ISENTROPIC Pressure = 30 psia Isentropic Efficiency = 0.89	The air from the atmosphere is compressed to the required pressure
9	BSCOMP2 (COMP)	TYPE = ISENTROPIC Pressure = 30 psia Isentropic Efficiency = 0.89	The tail gas from the Claus plant is compressed
10	BSMIX (MIXER)		Mixes process air, gaseous emissions from Claus plant, expansion gas from liquor separation and fuel gas
11	BSCOMPST (RSTOIC)	Temperature = 600 °F Pressure drop = 0 psia	Combusts the carbon compounds in the gas
12	CLASS4 (CLCHNG)		The class of stream is converted from conventional class to mixed class
13	STRETFRD (RSTOIC)	Temperature = 100 °F Pressure drop = 0 psia	Converts the H_2S to solid Sulfur and water
14	BSSEP (SSPLIT)	OFFGAS FRAC MIXED = 1.0 BSSULF FRAC CISOLID = 1.0	Separates the solid sulfur product from the gaseous tail gas.

3.2.4 Gas Turbine

The gas turbine simulated in this study is assumed to be a heavy duty Frame 7F gas turbine. The model developed in ASPEN Plus is based on the model of Akunuri (1999) developed in ASPEN. The gas turbine consists of a multi-staged compressor, which compresses the air required for combustion. From the compressors, some amount of compressed air is extracted and injected to the hot turbine stages to cool the blades and vanes. The syngas and compressed air is mixed and combusted in the combustor. The hot product gas is expanded in the expander turbine in several stages. The exhaust gas is sent to steam cycle. The flowsheet of gas turbine is shown in Figure 3-4. The details of unit blocks is this process are described in Table 3-5

3.2.4.1 Modeling Process of Gas Turbine

The ambient condition is assumed to be 59 ^{o}F, 14.7 psia, and 60 percent relative humidity. The default compressor ratio of a Frame 7F class gas turbine is 15.5 and the firing temperature is 2350 ^{o}F (Gebhardt, 2000). The compressors are simulated by three unit operation blocks, GT-COMP1, GT-COMP2, and GT-COMP3. The outlet pressure for each stage is estimated in the CALCULATOR block GTRP. The pressure ratio for each stage of the compressor is assumed to be same.

$$PR_{C,i} = PR^{1/3} \tag{3-16}$$

The pressure of the compressor outlet is:

$$P_{C,3} = P_{ambient} \times PR \tag{3-17}$$

Where,

PR = Pressure ratio = 15.5; i = 1, 2, and 3

The isentropic efficiencies for each stage of the compressor were specified in GTPR. From each stage, a fraction of air was extracted for cooling of the turbine. The cooling air streams are simulated by GT-COOL1, GT-COOL2, GT-COOL3, and GT-COOL4. The extraction fractions are specified in CALCULATOR block, AIRCOOL.

The fuel gas, GTFUEL and the compressed air, AIR7, are mixed in a mixer, simulated by GT-MIXER. The mixed stream is then sent to the combustor, simulated by the stoichiometric reactor block, GT-BURN. The chemical reactions in the combustor mainly include the combustion of CO, H_2, and CH_4. The formation of thermal NO_x is simulated by the reaction of N_2 and O_2. The details are described in Akunuri (1999). The typical combustor pressure drop is 4% based on the inlet pressure (McDougald, 2003). Therefore, the outlet pressure of the combustor was specified as the following:

$$P_{combustor} = P_{ambient} \times PR \times (1 - 4\%) \tag{3-18}$$

The outlet pressure of the combustor is 218.74 psia.

The combustion product gas out of the combustor is sent to the turbine or expander. The turbine is divided into three stages, simulated by three expander blocks, GT-TURB1, GT-TURB2, and GT-TURB3. The outlet pressure and the isentropic efficiency for each stage of the turbine are specified in the block, GTPR. Similar to the compressor, the pressure ratio of each stage of the turbine is assumed to be same. Before each stage of turbine, there is a mixer block, simulated by GT-MIX1, GT-MIX2, and GT-MIX3. In the mixter blocks, the cooling air from the compressor is mixed with the product gas for cooling. The exhaust gas, GTPOC, enter the heat recovery steam generator (HRSG) in the steam cycle process.

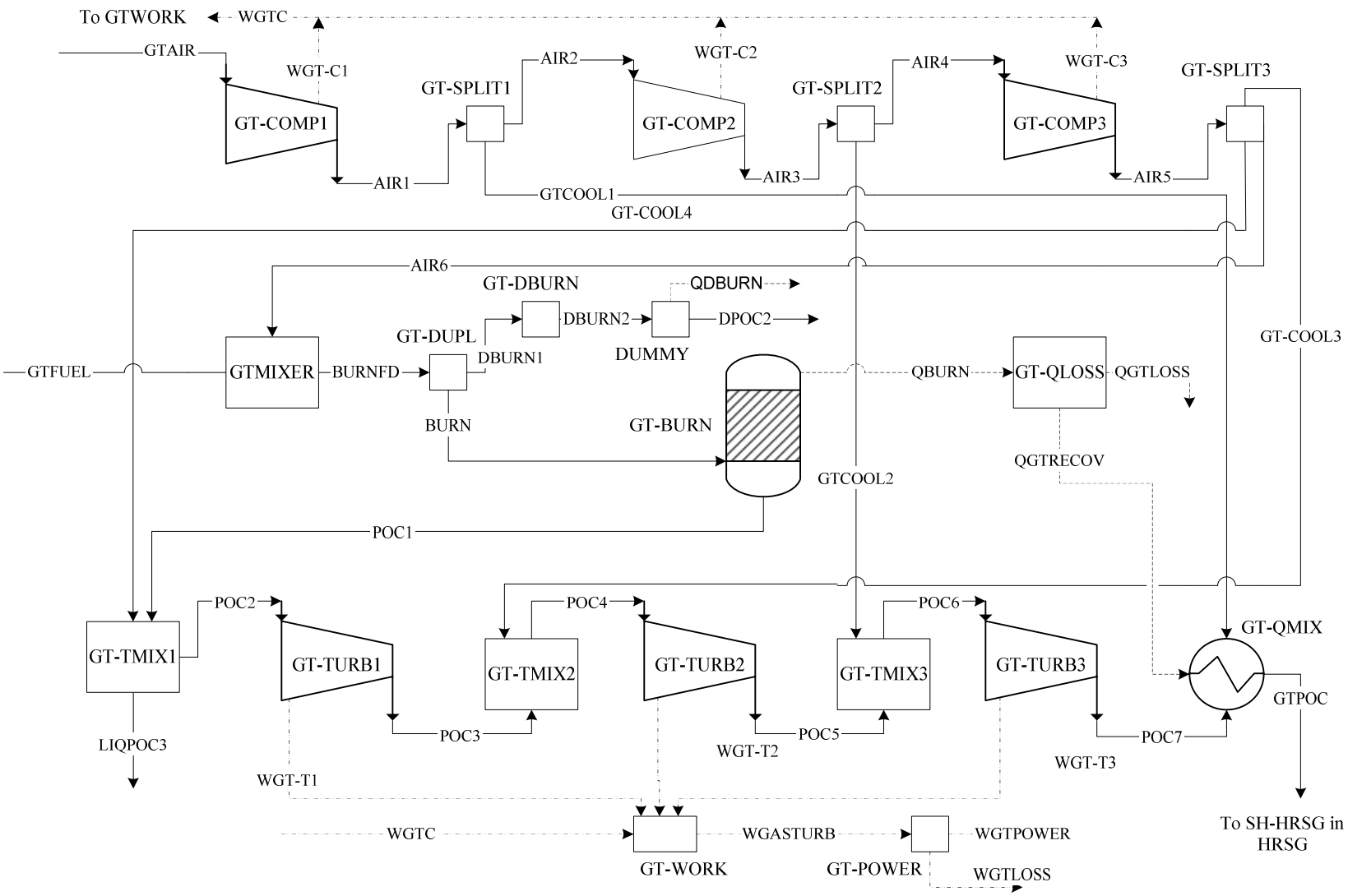

Figure 3-4 Flowsheet of Gas Turbine Process in ASPEN plus

Table 3-5 Gas Turbine Section Unit Operation Block Description

No	BLOCK ID (Block Type)	BLOCK PARAMETERS	DESCRIPTION
1	GT-COMP1 (COMP)	TYPE = ISENTROPIC Pressure = 36.65 psia Isentropic Efficiency = 0.809	Compresses the air entering the gas turbine.
2	GT-SPLT1 (FSPLIT)	FRAC GTCOOL1 = 0.03	Block splits the compressed air coming out of the block GT-COMP1 and directs one stream to cool the products of combustion of the gas turbine.
3	GT-COMP2 (COMP)	TYPE = ISENTROPIC Pressure = 91.38 psia Isentropic Efficiency = 0.809	Similar to GT-COMP1.
4	GT-SPLT2 (FSPLIT)	FRAC GTCOOL2 = 0.03	Similar to GT-SPLT1. This corresponds to 1st stage rotor and 2nd stage vane cooling.
5	GT-COMP3 (COMP)	TYPE = ISENTROPIC Pressure = 227.85 psia Isentropic Efficiency = 0.809	Similar to GT-COMP1.
6	GT-SPLT3 (FSPLIT)	FRAC GTCOOL3 = 0.06 GTCOOL4 = 0.06	Similar to GT-SPLT1. This corresponds to 1st stage vane cooling.
7	GT-MIXER (MIXER)		The block mixes the compressed air and fuel gas.
8	GT-DUPL (DUPL)		Duplicates the mixed fuel and air stream for heating value calculation purposes.
9	GT-BURN (RSTOIC)	Temperature = 2,350 °F Pressure = 218.74 psia	Simulates the stoichiometric reactions that take place in the gas turbine combustor.
10	GT-DBURN (RSTOIC)	Temperature = 2,350 °F Pressure = 218.74 psia	Simulates the stoichiometric reactions that take place in a dummy gas turbine combustor.
11	GT-QLOSS (FSPLIT)	FRAC QGTLOSS = 0.5 FRAC QGTRECOV = 0.5	Simulates the loss of heat from the gas turbine combustor.
12	GT-MIX1 (FLASH2)	Temperature = 2350 °F Pressure drop = 0	Simulates the mixing of cool air with the hot products of combustion.
13	GT-TURB1 (COMPR)	TYPE = ISENTROPIC Pressure = 87.73 psia Isentropic Efficiency = 0.922	Simulates a compressor for the expansion and subsequent cooling of the mixing of products of combustion and cool air.

(Continued)

Table 3-5 (Continued)

No	BLOCK ID	BLOCK PARAMETERS	DESCRIPTION
14	GT-MIX2 (MIXER)	Pressure = 87.73 psia	Simulates the mixing of cool air with the hot products of combustion.
15	GT-TURB2 (COMPR)	TYPE = ISENTROPIC Pressure = 35.19 psia Isentropic Efficiency = 0.922	Simulates a compressor for the expansion and subsequent cooling of the mixing of products of combustion and cool air.
16	GT-MIX3 (MIXER)	Pressure = 35.19 psia	Simulates the mixing of cool air with the hot products of combustion.
17	GT-TURB3 (COMPR)	TYPE = ISENTROPIC Pressure = 15.2 psia Isentropic Efficiency = 0.921	Simulates a compressor for the expansion and subsequent cooling of the mixing of products of combustion and cool air.
18	GT-MIX4 (HEATER)	Pressure Drop= 0	Simulates the mixing of cool air with the hot products of combustion.
19	GT-WORK (MIXER)		Sums the work from all compressor and expander stages.
20	GT-POWER (FSPLIT)	FRAC WGTPOWER = 0.985	Accounts for power loss in the gas turbine.

3.2.4.2 Design Specification and CLACULATOR Blocks

The main unit blocks and streams used in the gas turbine model have been introduced above. Some design-spec blocks and the CALCULATOR blocks were used in the gas turbine model for control of flowsheet variables. The design-spec blocks include TCHOKE and GTHEAT. The CALCULATOR blocks include GTPR and AIRCOOL. These blocks are used to specify gas turbine parameters, i.e. outlet pressure of each stage of compressor, control air flow to satisfy the turbine inlet constraint, specify air cooling fraction, and control syngas flow rate,

In the design-spec TCHOKE, the air flow is varied to satisfy a choked flow constraint at the turbine first nozzle inlet. The overall mass flow in a gas turbine is typically limited by the turbine first nozzle as noted by Frey and Rubin (1991). The critical area of the turbine inlet nozzle is a constant for a given model of gas turbine. Therefore, the mass flow though for a given gas turbine is constrained. The choked mass flow at the first nozzle is calculated in TCHOKE based on a reference mass flow, adjusted for differences in pressure, temperature, and molecular weight. The air flow to the compressor is varied to make the flow rate at the first nozzle to ba same as the computed choke flow rate. The design-spec GTHEAT determines the fuel flow rate to gasfier in order to keep the mixture heat of air and fuel gas to be zero.

The CALCULATOR block, GTPR, has been introduced in section 3.2.4.1. It is mainly used to specify the pressure levels and the isentropic efficiencies of compressor and turbine. The CALCULATOR block AIRCOOL specifies the split fractions to each turbine stage.

3.2.4.3 Calibration

In this section, the calibration of the Frame 7F simple cycle was implemented based on the reference data of General Electric MS7001FA gas turbine fueled with natural gas and syngas. In order to calibrate the model, selected parameters were varied in order to closely match published values for key outputs of system performance. Specifically, the isentropic efficiency for the turbine and compressor were varied in order to match the published gas turbine exhaust temperature and simple cycle efficiency respectively. The reference mass flow at the turbine inlet was varied in order to match the

published power output of gas turbine. The exhaust temperature affects the heat recovery in HRSG. Thus, three unknown parameters, the isentropic efficiency of the compressor, the isentropic efficiency of turbine, and the turbine inlet reference mass, were varied to match three outputs, including simple cycle power output, simple cycle efficiency, and gas turbine exhaust temperature, to reported values exactly.

The curves showed in Figure 3-6 represent the calibration process for selecting the isentropic compressor efficiency and turbine efficiency of a simple cycle gas turbine model fueled with natural gas. For a commercial Frame 7F gas turbine, the exhaust temperature is 1120 ^{o}F (Holt, 1998). The simple cycle efficiency is 36.38% and the power output is 167.8 MW for the GE MS7001FA gas turbine (Gebhardt, 2000). First, the isentropic efficiency of turbine is varied. With increasing of isentropic efficiency of turbine, the exhaust temperature decrease due to more efficient expansion. Thus, the isentropic turbine efficiency of 0.887 is selected to match the published exhaust temperature. After the turbine isentropic efficiency is selected, the isentropic compressor efficiency is varied to match the simple cycle efficiency. The result is 0.918 and the corresponding efficiency is 36.37%, which is varied close to the published value, 36.38%. The reference mass flow is varied to obtain the published power output of simple cycle. The published values and corresponding inputs values are shown in the figure.

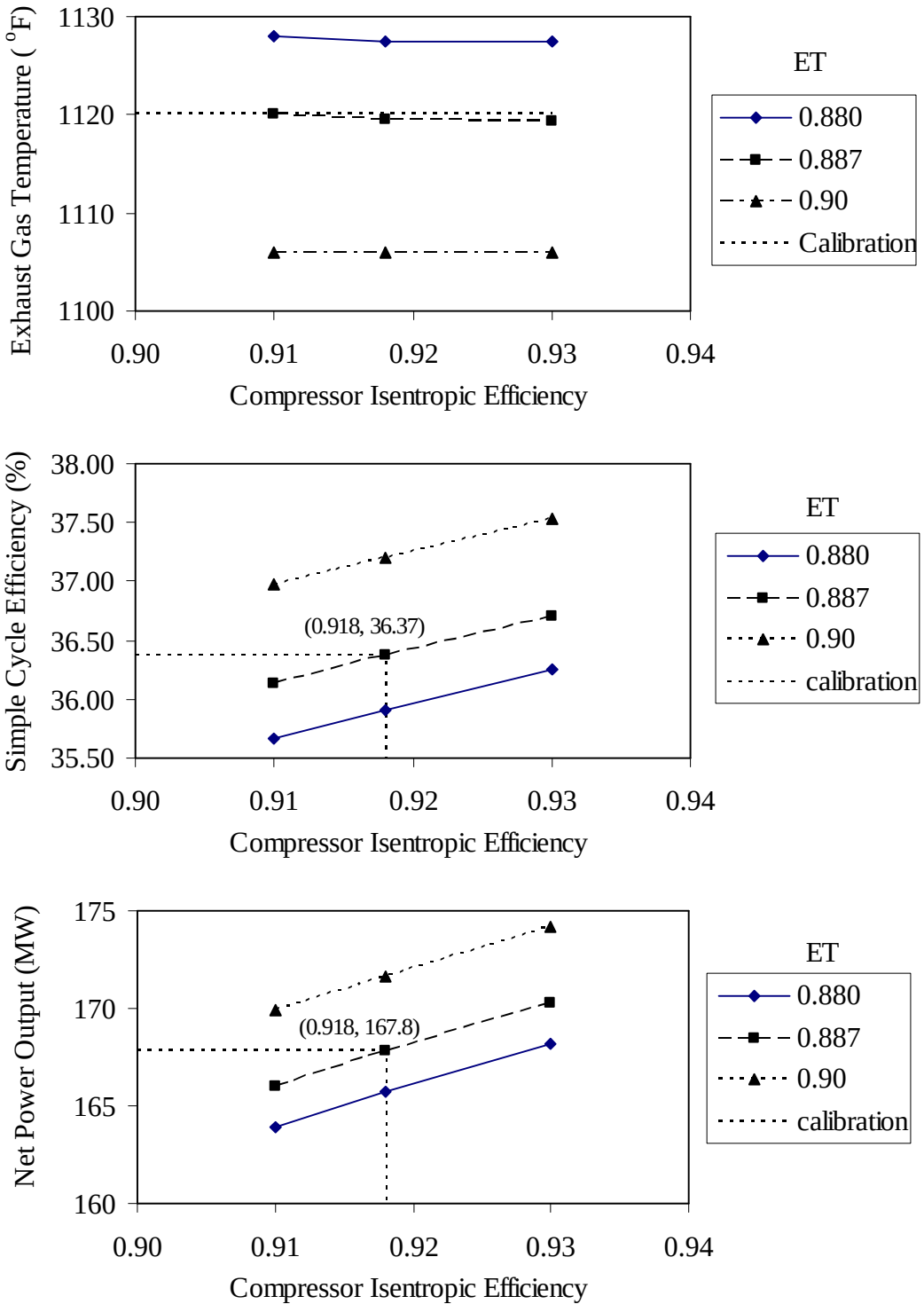

Figure 3-5 Calibration of Frame 7F Gas Turbine Combined Cycle Model – plot s of (a) Exhaust Temperature, (b) Combined Cycle Efficiency (LHV), and (c) Combined Cycle Output versus Isentropic Compressor Efficiency of Gas Turbine.

Note: ET = Isentropic Turbine Efficiency of Gas Turbine

A similar procedure was used to calibrate the model to proprietary values provided by General Electric for a gas turbine firing syngas. The turbine isentropic efficiency of 0.808 and the compressor isentropic of 0.912 are selected. The difference of calibration results for the natural gas and syngas is due to the difference in fuel type. The more detailed discussion can refer to the section 6.4.

3.2.5 Steam Cycle

The steam cycle model consists of three parts: heat recovery steam generator (HRSG), steam turbine, and auxiliaries. The details are given in the following sections.

3.2.5.1 Heat Recovery Steam Generator (HRSG)

The HRSG consists of gas-gas heat exchangers, reheaters, evaporators and super-heaters that recover the sensible heat from the gas turbine exhaust and produce steam (Buchanan, *et al*., 1998). The HRSG in this model is used to preheat boiler feed water, reheat intermediate pressure steam, supplement high pressure and 100 psia steam generation, and to superheat to produce high pressure steam. The flowsheet of HRSG process is shown in Figure 3-6 and the main unit operation blocks are described in Table 3-6.

The HRSG consists of a superheater at a pressure of 1465 psia and a reheater at 997 ^{o}F, two economizers, a high-pressure boiler, and a low-pressure boiler. The low pressure boiler is used to produce steam for the deaerator for the flue gas leaving the economizer at 366 ^{o}F. The heat loss in the HRSG process is set through block QSPLIT. GTPOC, simulating the hot exhaust gases from the gas turbine section, are cooled by a series of heat exchangers, modeled by blocks SH-HRSG, HP-HRSG, E2-HRSG, LP-

HRSG, and E1-HRSG in that order. The heat obtained from the heat exchangers, E1-HRSG, E2-HRSG, and HP-HRSG is collected in a mixer, simulated by QMIX. The heat stream from SH-HRSG, QSH-HRSG is split into three heat streams by the block QSPLIT. One represented the heat loss. QRHEAT is sent to the block TURBHEAT in steam turbine section. And the remaining heat stream, QSUPER, is sent to the block QMIX.

The total heat from QMIX block, QTOTHRSG, is sent to the block ECONOMZR simulating a heat exchanger. ECONOMZR heat water to 553 ^{o}F. The remaining amount heat available is sent to block HPBOILER which simulates a high pressure steam boiler in HRSG. The steam generated by HPBOILER is sent to the superheater, SUPERHTR and generates superheated steam at 997 ^{o}F, which is sent high pressure steam turbine.

Steams TOECON and TOB100, which are from block H2OSPLIT, are sent to blocks ECONMZR and BOIL100 respectively. BOIL100 simulates a low pressure boiler to generate 100 psia steam. The steam from BOIL100 is split by the block SPLIT100 into stream SLXSTM and STM100. Both are sent to the auxiliaries section.

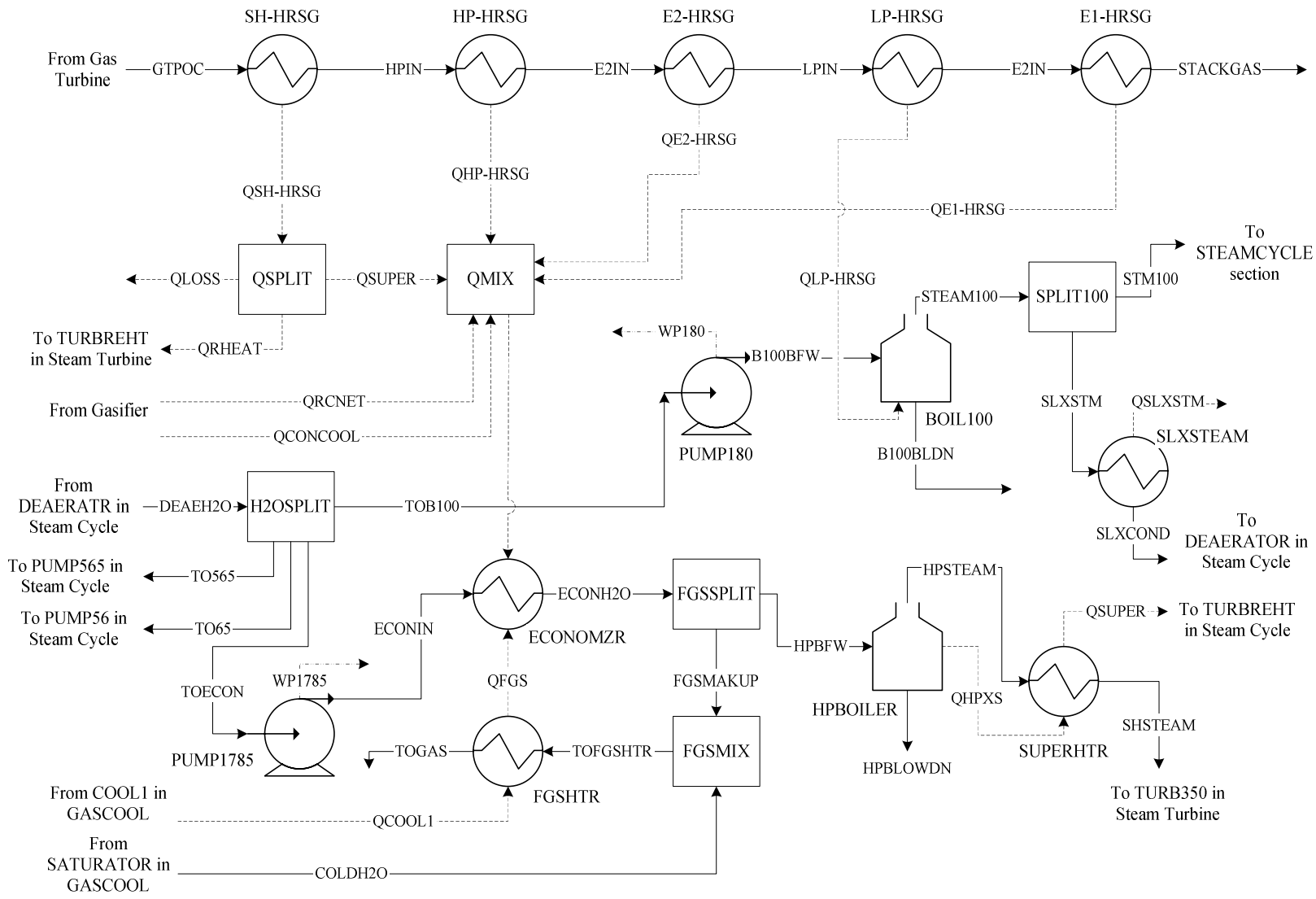

Figure 3-6 Flowsheet of HRSG Section in ASPEN Plus

Table 3-6 HRSG Section Units Blocks Description

No	BLOCK ID	PARAMETERS	DESCRIPTION
1	SH-HRSG (HEATER)	Temp. = 743 ^{o}F Pressure drop = 0 psia	This block is part of the HRSG and simulates to remove heat form the products of gas turbine.
2	HP-HRSG (HEATER)	Temp. = 641 ^{o}F Pressure drop = 0 psia	This block is part of the HRSG and simulates to remove heat form the products of the gas turbine.
3	E2-HRSG (HEATER)	Temp. = 401 ^{o}F Pressure drop = 0 psia	This block is part of the HRSG and simulates to remove heat form the products of combustion of the gas turbine.
4	LP-HRSG (HEATER)	Temp. = 366 ^{o}F Pressure drop = 0 psia	This block is part of the HRSG and simulates to remove heat form the products of combustion of the gas turbine.
5	E1-HRSG (HEATER)	Temp. = 271 ^{o}F Pressure drop = 0 psia	This block is part of the HRSG and simulates to remove heat form the products of combustion of the gas turbine.
6	QSPLIT (FSPLIT)	Frac QPADPOSS 0.03 QREHEAT 0.1	This block simulates the radiation losses in HRSG and diverts QREHEAT to REHEAT in HRSG section
7	QMIX (MIXER)		This block simulates the mixing of the various heat stream in HRSG.
8	PUMP1785 (PUMP)	P = 1785 psia	This block simulates a pump which delivers the condensates to the HRSG economizer
9	ECONOMZR (HEATER)	Temp.= 553 ^{o}F Pressure = 1625 psia	It simulates the economizers 1 and 2 of HRSG
10	FGSSPLIT (FSPLIT)	Mole Flow FGSMAKUP 1.0	Provides hot water for gas saturation
11	FGSMIX (MIXER)		Mixes makeup water and cold water form SATURATR
12	FGSHTR (HEATER)	T = 366 ^{o}F Pressure drop = 0	Simulates a heater which heats the makeup water
13	HPBOILER (FLASH2)	Pressure = 1545 psia, Vfrac = 0.995	Simulates a high pressure boiler in HRSG.
14	SUPERHTR (HEATER)	Pressure = 1465 psia	Simulates the steam superheater in HRSG.
15	PUMP 180 (PUMP)	P= 180 psia	Simulates a pump which delivers the water to 100 psia boiler

(Continued)

Table 3-6 (Continued)

No	BLOCK ID	PARAMETERS	DESCRIPTION
16	BOIL100 (FLASH2)	Pressure = 100 psia Vfrac = 0.995	It simulates a low pressure steam boiler
17	SPLLIT100 (FSPLIT)	Mole-Flow SLXSTM 0.1	This block splits the steam from BOIL100. The splits are set by the CALCULATOR block SETSTEAM

3.2.5.2 Steam Turbine and Auxiliary Section

Four steam turbines are modeled in this section: TURB350, TURB115, TURB70, and TURB1. The steam from the HRSG is expanded through three stages, consisting of a high pressure turbine (350 psia), an intermediate pressure (115 psia) turbine, followed by two parallel low pressure turbines (70 psia and 1 psia). The flowsheet of the steam cycle is shown in Figure 3-7 and the main unit operation blocks of steam cycle and auxiliary sections are listed in Table 3-7.

The superheated steam, stream SHSTEAM, from the HRSG section enters the block TURB350 which simulates a 350 psia exhaust steam turbine. The outlet stream, STEAM350 is mixed with STEAM 565 from the auxiliary section in the block TURBHEAT simulating a mixer and is heated by heat stream QREHEAT to a temperature, which is specified in the design specification SETTEMP. The outlet stream, HOTSTEAM at a pressure of 350 psia enters the block TURB115. The steam at 115 psia is split by the block SPLIT115 into streams TURB70IN and TURB1IN. The split ratio is decided by the design specification DEAERHT. The outlet stream modeled by TURB70IN enters the low pressure (70 psia) exhaust turbine, simulated by TURB70. The resulting stream from TURB70, STEAM70, enters the DEAERATOR block. The ouput stream from TURB1, STEAM1, enters the block CONDENSR.

The low-pressure (1 psia) steam generated by ultra low pressure steam turbine, simulated by TURB1, is cooled by a heater block, CONDENSR. A heater block in ASPEN Plus can be used to simulate either a heater or a cooler and is a method for representing a generic heat exchanger. The condensate from CONDENSR is pumped to 25 psia and delivered to a dearator, simulated by DEAERTOR. In the deaerator, the various condensates from the auxiliaries section, steam WATER25 and the makeup water, which is used to makeup the water sent to the fuel saturation unit from the steam cycle section. The mixed condensate, represented by DEAERH2O is sent to the block H2OSPLIT which simulates the splitting of the total condensate to streams TOECON, TOB100, and TO65. The mole flows of the splits are calculated by the CALCULATOR block SETSTEAM.

Streams TOECON and TOB100 are sent to the blocks ECONMZR and BOIL100 respectively in HRSG section. The steam from BOIL100 is split by the block SPLIT100 into streams SLXSTM and STM100, both of which are sent to the auxiliaries section.

A water stream, TO565, split from the stream out of the deaerator is pumped to 565 psia. The boiler, CLAUS565, simulates the heat recovery of the heat from the claus process. The water is heated to become steam, STEAM565, and is sent to the reheater, simulated by a heater block, TURBREHT.

In the auxiliaries section, stream TO65 from the block H2OSPLIT are sent to PUMP65 respectively. TO65 is pumped to be 65 psia, which is simulated by WATER65. The stream is further heated in the block STRETSTM. The resulting stream, STRFDSTM, is mixed with STM100 from SPLIT100 in DESUPER. The resulting

stream, LIQ55, is sent to the DEAERATOR. Another stream, STEAM55 is split into three streams, MISCSTM, WWSTEAM and STM55. STEAM55 is sent to the deaerator. The stream MISCSTM is heated in the block MISCUSE. And the stream WWSTEAM is heated in the block WWTREAT, which simulates the 55 psia steam condensation in Texaco waste water treatment. The two resulting streams are sent to the block DEAERATOR.

3.2.5.3 Design Specifications and CALCULATOR blocks in Steam Cycle

The design specifications used in the steam cycle section of the model are DEAERTHT and STMTEMP. DEAERTHT is used to model that the deaerator operates at approximately adiabatic condition. The heat stream out of DEAERHT should be less than 100.0 BTU/hr, which is a neglible heat loss and thus approximates adiabatic operation. The design specification is achieved by varying the ratio of splitting of the stream, SPLIT115. STMTEMP sets the temperature of stream leaving the HRSG block, which is HOTSTREAM, to be equal to that of the superheated stream, which is modeled by SHSTEAM.

The CALCULATOR blocks used in the steam cycle section of the model are SETSTEAM, SETTEMP and SETMAKEUP. SETSTEAM specified the mass flow of various water streams, including TOECON, TOB100, TO565, and TO65.

In the CALCULATOR block SETTEMP, the temperature of superheated stream, modeled by SHSTEAM, is specified based on the temperature of GTPOC and the change of the HRSG entrance temperature. The desired superheated steam temperature is 997 ^{o}F.

The CALCULATOR block SETMAKEUP is used to calculate the mass flow of the stream MAKEUP to the deaerator. The mass flow of MAKEUP is set to equal to the sum of various boiler blowdown steams and makeup water to FGSMIX, which are HPBLOWDN, B100BLDN, CLBLOWDN, and FGSMAKUP.

$$M_{MAKUP} = M_{BD100} + M_{BDHP} + M_{CLBLOWDN} + M_{FGSH2O} \quad (3\text{-}19)$$

Where,

M_{MAKUP} = Flow rate of stream MAKEUP;

M_{BD100} = Flow rate of stream B100BLDN;

M_{BDHP} = Flow rate of stream HPBLOWDN;

$M_{CLBLOWDN}$ = Flow rate of stream CLBLOWNDN;

M_{FGSH2O} = Flow rate of stream FGSMAKUP.

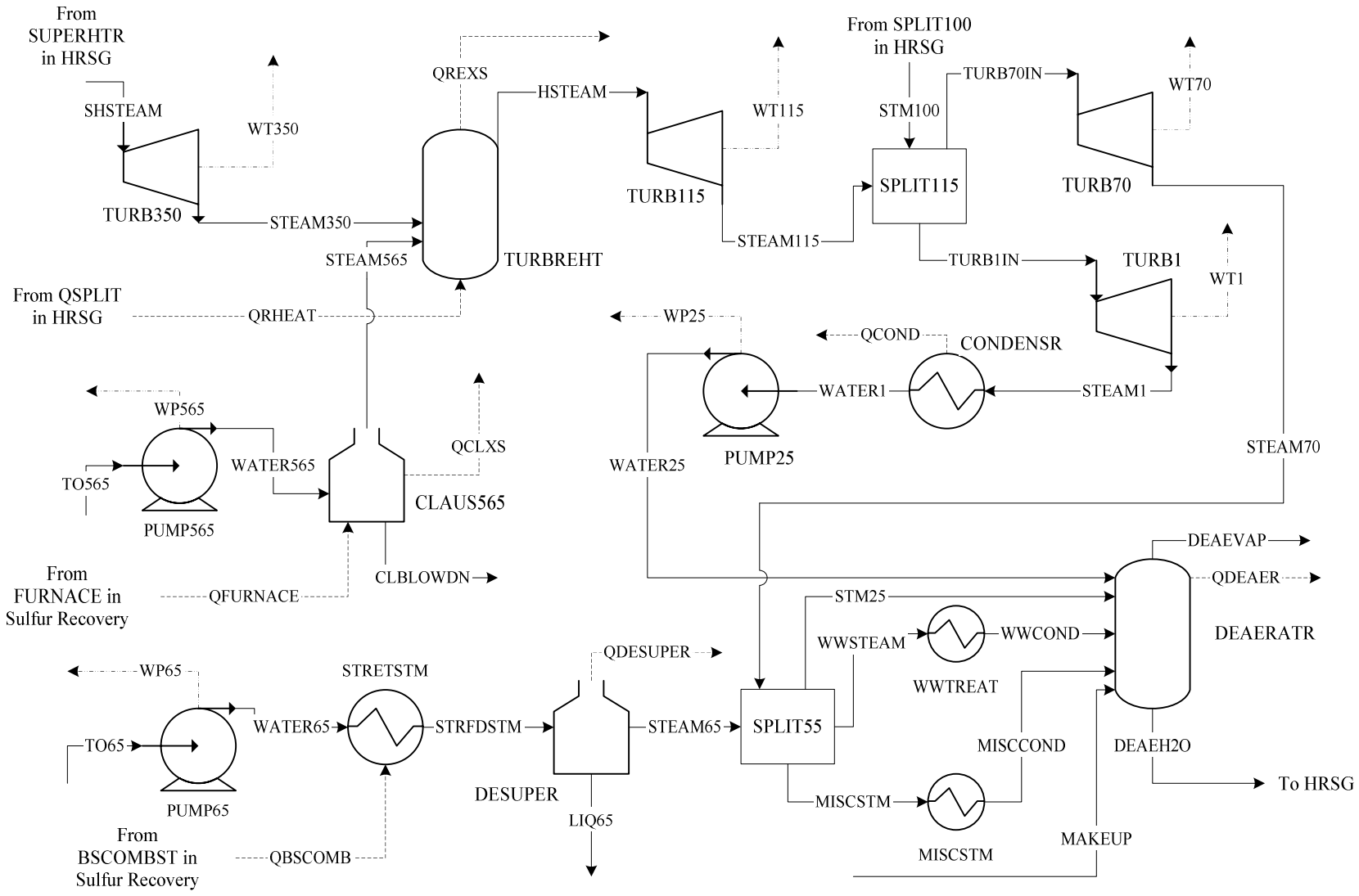

Figure 3-7 Flowsheet of Steam Cycle and Auxiliary Section in ASPEN Plus

Table 3-7 Units Blocks Description of Steam Cycle and Auxiliary Section

No	BLOCK ID	PARAMETERS	DESCRIPTION
1	TURB350 (COMPR)	Pressure = 350 psia Efficiency = 0.859	Simulates a high pressure steam turbine
2	TURBREHT (MIXER)		Simulates the mixing of steams at 350 psia and 565 psia
3	TURB115 (COMPR)	Pressure = 115 psia Efficiency = 0.901	Simulates an intermediate pressure steam turbine
4	SPLIT115 (FSPLIT)	Frac TURB70IN 0.015	Splits the steam from TURB115. The split fractions are set by the design-spec DEAERHT
5	TURB70 (COMPR)	Pressure = 70 psia Efficiency = 0.849	This block simulates a low pressure (70 psia) steam turbine.
6	TURB1 (COMPR)	Pressure = 1 psia Efficiency = 0.847	This block simulates a low pressure (1 psia) steam turbine.
7	H2OSPLIT (FSPLIT)	MOLE-FLOW TOECON 1.0 TOB100 1.0 TO565 1.0	Simulates the split of the total condensate in to the required ratios in which the condensate will be sent to various blocks.
8	CONDENSR (HEATER)	Pressure = 1 psia Vfrac = 0	Simulates the heating of the steam out of Steam Turbine section
9	PUMP25 (PUMP)	Pressure = 25 psia	Simulates a pump which delivers the condensate to the deaerator.
10	DEAERATOR (FLASH2)	Pressure = 25 psia Vfrac = 0	Simulates the mixing of the condensates and steam.
11	PUMP65 (PUMP)	Pressure = 65 psia	Simulates a pump which delivers water to the BS plant steam generator
12	STRETSTM (HEATER)	Pressure = 65 psia	Simulates the BS plant steam generator
13	SLXSTEAM (HEATER)	Pressure = 115 psia Vfrac = 0	Simulates the 115 psia steam condensation in Selexol process
14	DESUPER (FLASH2)	Pressure = 55 psia Vfrac =1	Simulates 55 psia steam desuperheater
15	SPLIT55 (FSPLIT)	MOLE-FLOW WWSTEAM 1.0 MISCSTM 1.0	Simulates the split of the steam from DESUPER. The splits are set by CALCULATOR block SETSTEAM
16	WWTREAT (HEATER)	Pressure = 55 psia Vfrac = 0	Simulates the condensation of 55 psia steam condensation in Texaco Waste Water Treatment
17	MISC-USE (HEATER)	Pressure = 55 psia Vfrac = 0	Simulates the miscellaneous user of 55 psia steam.
18	MIXWM (MIXER)	Pressure= 25 psia	Simulates a mixer

3.3 Convergence Sequence

The convergence sequence for the model simulation is based on nine design specifications and eleven CALCULATOR blocks. The CALCULATOR blocks have been described in the previous sections for each process area.

The convergence sequence of the overall model is shown in Figure 3-8. The convergence sequence starts with the initialization of key input variables of gas turbine in the CALCULATOR block GTPR. The gas turbine compressors process is operated in the sequence of GT–SEQ1. The gasification, radiant and convective cooling, and gas scrubbing process are simulated in the sequence named GS-SEQ1. Consistent with the flow path of syngas stream, other processes are simulated in the following sequence: the low temperature gas cooling process; the fuel gas saturation process, and then the gas turbine combustion and expansion. The design-spec block, GTFUEL is used to vary the coal flow rate and thus control the syngas flow rate to the combustor. The above sequence is iterated until target variable match the specified value. The design-spec TCHOKE is used to control the air flow rate to the compressor. After the targets of two design-spec blocks are satisfied, the processes of the sulfur recovery and steam cycle are simulated. Finally, the CALCULATOR block, COST, computes the outputs for performance, costs, and emissions of the system via an external FORTRAN subroutine.

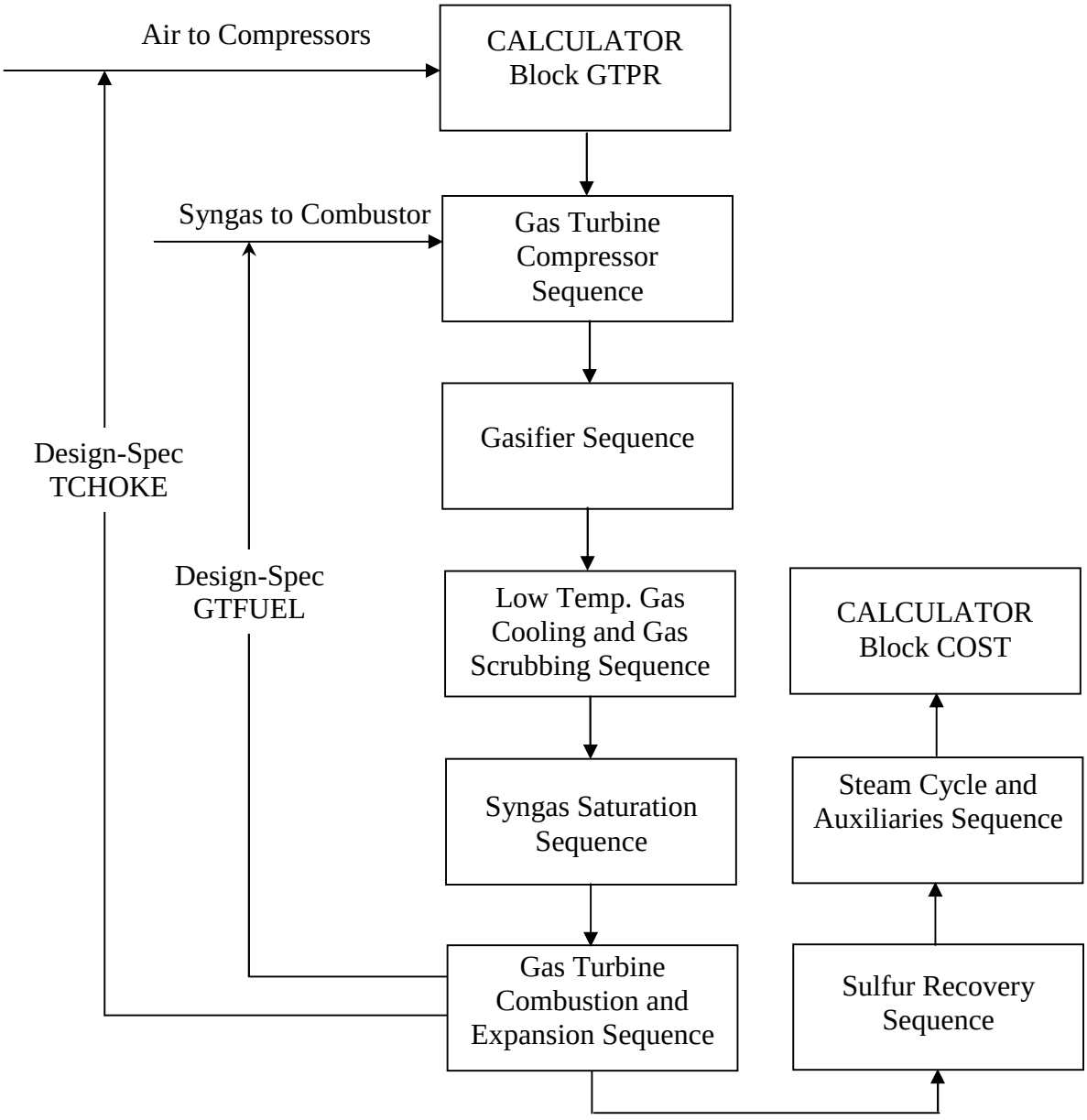

Figure 3-8 Convergence Sequence of the Overall IGCC System

3.4 Plant Energy Balance Model

The plant energy balance is comprised of three parts, including:

(1) The net power output of gas turbine;

(2) The net power output of steam turbine;

(3) The auxiliary power consumption.

The gas turbine power output is calculated by the sum of the shaft work produced by the gas turbine expanders and work required by the gas turbine compressors. The generator efficiency is assumed to be 98.5% (Frey and Akunuri, 2001). Thus, the net power output from the gas turbine is the product of the total shaft word and the generator efficiency.

The power output of the steam turbine is the sum of the total shaft work produced by the four steam turbines. The generator efficiency is also considered. The net power output of the gas turbine and steam turbine is 98.5% of the total shaft work.

The auxiliary power consumption is estimated based on the model of Frey and Akunuri (2001). It mainly consists of:

(1) The power consumption of the compressors in the Claus and Beavon-Stretford plant.

(2) The power consumption by all the pumps in the model delievering slurry or water;

(3) The power consumption by the air separation unit.

The auxiliary parts of a power plant, including pumps, conveyors, and compressors, consume a significant amount of power known as auxiliary power load, which lowers the net power output of the power system and the overall plant efficiency. The details of

auxiliary power model are described in the thesis of Akunuri (1999). In the model developed in ASPEN Plus, the auxiliary loads were computed in an external FORTRAN subroutine file. Some results from the performance model are used as inputs for the FORTRAN subroutine.

3.5 Environmental Emissions

Three emissions are estimated in this study, including SO_2, NO_x, and CO_2. The pollution control and estimation methods used for three pollutants in this IGCC system are discussed in the following.

3.5.1 Emissions of SO_2

The SO_2 emissions of IGCC systems are controlled by sulfur removal processes, including the Selexol process, and Claus and Beavon-Stretford plants. Thus, the sulfur species in syngas is removed and recovered before the syngas enters the combustor. No post-combustion control is used in this system. Thus, the SO_2 emissions of IGCC system are mainly from the oxidation of H_2S and COS in the gas turbine combustion process. The SO_2 emission in unit of $lb/10^6Btu$ is estimated based on the SO_2 concentration in the exhaust of gas turbine and the total energy input of IGCC system.

3.5.2 Emissions of NO_x

The NO_x emissions mainly include the emissions of NO and NO_2 in the exhaust of the gas turbine. The NO_x emissions are low for this IGCC system because water injection is injected into the syngas prior to combustion. The NO_x emissions of IGCC systems are mainly from thermal NO_x formation. The formation of thermal NO_x is temperature-sensitive, as described by the Zeldovich mechanism (Zeldovich, 1946).

Water injection, or syngas moisturization, helps to lower the adiabatic flame temperature (Smith, *et al.*, 2001). The NO_x emissions are estimated based on NO_x in gas turbine exhaust in unit of lb/10^6 Btu.

3.5.3 Emissions of CO_2

The CO_2 emissions are mainly from three sources: gasification, conversion of CO into CO_2 in gas turbine process, and Beavon-Stretford tailgas treatment. The emissions of CO_2 are estimated based on the amount of CO_2 in gas turbine exhaust and the power output of IGCC system, in unit of lb/kWh.

3.6 Cost Model of Texaco Gasifier-based IGCC System

The cost model is developed for the coal-fueled Texaco gasifier-based IGCC plant with radiant and convective high temperature gas cooling. The direct capital costs model for the main process areas of oxidant feed section, coal handling and slurry preparation, gasification, low temperature cooling, Selexol section, Claus sulfur recovery, Beavon-Stretford tail gas removal section, boiler feedwater system, process condensate system, gas turbine section, heat recovery steam generator section, steam turbine section, and general facilities are included in the cost model. The details of the cost model can be found in Frey and Akunuri (2001).

The original direct costs models were developed based on January 1989 dollars. To compare to the reference data in recent years, the direct cost of a process section can be adjusted for other years based on the year they were developed using the appropriate Chemical Engineering Plant Cost Index (PCI) (Chemical Engineering Editorial Staff, 1984 -2003), which are listed in Table 3-8.

Table 3-8 Plant Cost Indexes Values (Chemical Engineering, 1984 – 2003)

Year	Plant Cost Index
1984	320.3
1985	324.7
1986	323.5
1987	318.3
1988	336.3
1989	354.7
1990	357.6
1991	360.0
1992	359.5
1993	357.2
1994	361.4
1995	376.1
1996	380.9
1997	383.3
1998	388.0
1999	389.0
2000	391.1
2001	395.4
2002	390.3
2003	398.3

Since the PCI in 1989 January is 351.5, the direct cost in year i is:

$$\mathrm{DC}_i = DC_{1989} \times (\frac{PCI_i}{351.5}) \tag{3-20}$$

For example, if a direct cost model was developed based on January 1989 dollar, the direct cost capital cost in January 1998 dollars, is given by:

$$\mathrm{DC}_{1998} = DC_{1989} \times (\frac{388.0}{351.5})$$

3.7 Running the Model

There are total 92 unit operation blocks in the IGCC model. The running sequence of blocks has been introduced in section 3.6. The IGCC model was run on a Pentium 4 PC with Windows XP operating system. For calibration, verification, and case studies, the ASPEN Plus version 11.1 and Visual FORTRAN were used. A deterministic analysis takes approximately 1 minute to run, including execution of external FORTRAN subroutine.

3.8 Verification of IGCC Model

A complete performance, emissions, and cost model for a Texaco gasifier-based IGCC with radiant and convective cooling with a Frame 7F gas turbine has been developed based on the study of Akunuri (1999). In this work, the model is implemented in ASPEN Plus whereas in the previous work the model was implemented in the U.S. DOE version of ASPEN. The gasifer and gas turbine processes are recalibrated in this work. In order to verify the accuracy of the estimates of this model developed in ASPEN Plus, the results of this study are compared to the results of the model developed in ASPEN, which has been verified by Akunuri (1999). In addition, the results of this model were compared to the results from another reference report about a Texaco IGCC system.

3.8.1 Input Assumptions

The main inputs of the performance model are listed in Table 3-9. Two assumptions noted as initial values may be modified in the simulation. The coal mass flow is varied by the design-spec block, GTFUEL, to satisfy the combustor heat loss. The

Table 3-9 Summary of the Selected Model Inputs of the IGCC based on Frame 7F gas turbine

Description	Value [a]
Gasification process Area	
Coal Feed Rate, lb/hr (Initial)	585,000
Slurry Water/Coal Ratio, lb H_2O/lb Coal	0.504
Oxygen/Coal Ratio, lb O_2/lb Coal (Initial)	0.915
Gasifier Pressure, psia	615
Gasifier Outlet Temperature, ^oF	2,400
Radiant Cooler Outlet Temperature, ^oF	1,500
Convective Cooler Outlet Temperature, ^oF	650
Gas Turbine Process Area	
Inlet Syngas Temperature, ^oF	570
Moisture in Fuel Gas, wt-%	28.2
Pressure Ratio [b]	15.5
Turbine Inlet Temperature, ^oF [b]	2,350
Compressor Isentropic Efficiency, %	80.8
Expander Isentropic Efficiency, %	92.2
Generator Efficiency, %	98.5
HRSG and Steam Cycle Area	
Steam Condition, psia/^oF/^oF	1450/997/997
HRSG Stack Temperature, ^oF	271

[a] Main of the values are from Flour (1984) except the specifications of Frame 7F gas turbine.
[b] The data are the parameters of a Frame 7F gas turbine (Eric, 2000).

Oxygen/Coal ratio in the gasifier is varied by a design-spec SETOXID in order to overcome the heat loss from the gasifier. Illinois No. 6 coal is used, which compositions are listed in Table 5-1.

3.8.2 Comparison to Model Results in ASPEN

The model developed in ASPEN Plus in this study is compared to the case study implemented in ASPEN (Frey and Akuniri, 2001). The modeling results of ASPEN Plus model and ASPEN model are listed in Table 3-10. The purpose of this comparison is to find out if the model developed in ASPEN Plus will produce obviously different results compared to the model in ASPEN based on the same input assumptions. This comparison can also indicate if the model results are reasonable since the results of Akunuri have

been verified. Compared to ASPEN, the model runtime in ASPEN Plus is much shorter than that of ASPEN model. The runtime in ASPEN Plus is about 1 minute, while the runtime in ASPEN is about 5 minutes (Frey and Akunuri, 2001). In addition, ASPEN Plus has amore friendly user interface.

The comparison results indicate that the results of the ASPEN Plus model are very close to the model results in ASPEN. The relative differences are all 1 or 2 percent. These small differences indicate that the model developed in this study can produce predictions of the performance of the IGCC system comparable to those of the ASPEN model.

The cost results of the model developed in ASPEN Plus are compared to the results of the model in ASPEN. The cost results include the capital, annual, and levelized cost of electricity. The comparison results were given in Table 3-11. The relative difference between the cost results of two models are all less than one percent, which means that the results of the model in this study are very close to the results of ASPEN model.

The comparison of the results between two models indicates that the model developed in ASPEN Plus can estimate the performance and costs of the IGCC system reasonably well.

Table 3-10 Comparison of Models Results in ASPEN Plus and ASPEN

Description	Model in ASPEN Plus	Model in ASPEN [a]	Relative Difference
Coal Feed Rate, lb/hr, dry basis	578,000	585,000	-1.2%
Gas Turbine Net Power (3 trains), MW	576.5	579.5	-0.5%
Steam Turbine Net Power, MW	396.6	400.8	-1.0%
Auxiliary Power Demand [a]			
Coal Handling, MW	7.2	7.3	
Oxidant Feed, MW	81.7	83.5	
Gasification, MW	1.1	1.2	
Low T. Cool. , MW	2.4	2.4	
Selexol, MW	4.9	4.8	
Claus, MW	0.4	0.4	
Beavon-Streford, MW	1.0	1.3	
Process Condensate, MW	0.6	0.6	
Steam Cycle, MW	6.9	5.3	
General Facilities, MW	10.6	10.7	
Total Auxiliary Load, MW	116.8	117.4	-0.5%
Net Plant Power Output, MW	856.2	863	-0.8%
Heat Rate, Btu/kWh (HHV)	8,624	8,664	-0.5%
Plant Efficiency, %	39.60	39.41	0.5%
SO_2 Emissions, lb/10^6Btu	0.22	0.22	0
NO_x emissions, lb/10^6Btu	0.13	0.13	0
CO_2 Emissions, lb/kWh	1.69	1.70	-0.6%

[a] Akunuri (1999).

Table 3-11 Comparison of Cost Model Results in ASPEN Plus and ASPEN

Description	Model in ASPEN Plus	Model in ASPEN	Relative Difference
Capital Cost Summery ($/kW)			
Total Direct Cost	819	815	0.5%
Total Indirect Costs	300	299	0.3%
Process Contingencies	94	94	0
Project Contingency	212	211	0.5%
Total Plant Cost	1,424	1,419	0.4%
AFDC [a]	228	227	0.4%
Total Plant Investment	1,652	1,647	0.3%
Startup Costs and Land	43	43	0
Total Capital Requirement [b]	1,737	1,732	0.3%
Fixed operation Cost, $/(kW-yr)	50.5	50.4	0.2%
Incremental Variable Costs, mills/kWh	1.2	1.2	0
Byproduct Credit, mills/kWh	-1.5	-1.5	0
Fuel Cost, mills/kWh	10.9	10.9	0
Variable operating Cost, mills/kWh	10.5	10.6	-0.9%
Cost of Electricity, mills/kWh [c]	50.9	50.9	0

[a] AFDC = Allowances for Funds used During Construction;

[b] Total Capital Requirement includes Total Plant Investments, Startup costs and Land, Inventory Capital, Initial Catalysts and Chemicals. Cost year is 1998 Jan.

[c] Fuel Cost, $/MMBT = 1.26 (Jan 1998 Dollars) (Buchanan *et al.*, 1998)
Capital Recovery Factor = 0.1034

Table 3-12 Comparison of Results of ASPEN Plus Model and Reference Data

Description	Model in ASPEN Plus	Reference Data [a]	Relative Difference
Net Plant Power Output, MW	856	847	1.1%
Heat Rate, Btu/kWh (HHV)	8,624	8,741	-1.3%
Plant Efficiency, %	39.6	39.0	1.5%

[a] Sturm, *et al.* (2003)

3.8.3 Comparison to Reference Data

In this section, the modeling results in this study are compared to a reference report for verification the results of the model. Flour (1984) reported a detailed design study for a Texaco gasifier-based IGCC system. However, the gas turbine used in that system is out of date and has big difference with the Frame 7F gas turbine. Thus, it can not be used for verification. Another study by Sturm, *et al.* (2003) is selected for comparison. A nominal 850MW coal-fueled IGCC plant based on Texaco gasification technology was studied in the report. The system included low temperature gas cooling, acid gas removal process, and three 7FA gas turbines. This design is very similar to the configuration of the model in this study, which provides a reasonable comparison basis. However, the coal compositions data or coal type and the steam cycle specifications were also not given in that report. Therefore, the Illinois No.6 coal is used as a default coal.

The comparison results are listed in Table 3-12 for power output, heat rate, and efficiency. Cost estimates were not provided in the reference report; thus, cost results cannot be compared. The differences of the net power output, heat rate, and plant efficiency are all about one or two percent. The comparison of the main performance results indicates that the model developed in ASPEN Plus can provide reasonable estimates for main outputs of IGCC plant.

4.0 SIMULATION OF TEXACO GASIFIER-BASED IGCC SYSTEM BASED ON FRAME 7H GAS TURBINE

As an advanced technology in early commercial phase, there is great potential for advances of IGCC in future. The potential progresses include advances in gas turbine, optimization of the design, and integration among the various components of the system (Holt, 2003; Carcasci and Facchini, 2000). The development of gas turbine provides the potential to further improve the efficiency of the overall IGCC system and decrease the cost of electricity. The 7FA represents current state-of-practice whereas the 7H gas turbine is the most advanced recently introduced commercial gas turbine. The 7H gas turbine uses steam rather than air cooling for the hot gas path, thereby enabling higher firing temperatures and efficiency (Matta, *et al*., 2000).

Although some investigation of the performance, emissions, and cost of 7H-based IGCC system has been reported (Falsetti, *et al*., 2000), advanced concepts for IGCC that incorporate state-of-the-art gas turbine systems are not commercially demonstrated. The objective of this study is to evaluate the effects of advances in gas turbine technology on the performance, emissions, and cost of IGCC systems. Therefore, a model for IGCC system based on the advanced 7H gas turbine is developed in this study.

4.1 Overall Process Description

Since the purpose of this study is to compare the effects of different gas turbine on IGCC system outputs, the processes of gasification, gas cooling, gas cleaning, and gas saturation of IGCC with 7H gas turbine system are same as that of the IGCC with 7FA

gas turbine system. It is to provide a consistent comparison basis for two systems. The processes mentioned above have been described in section 3.0. In this section, the emphasis is to describe the process of 7H gas turbine combined cycle model. In the following sections, the gas turbine combined cycle model is described in detail.

4.2 Main Process Sections in Frame 7H Gas Turbine Combined Cycle Model

The H gas turbine combined cycle consists of H gas turbine and a steam cycle, which include HRSG and a steam turbine. In the following sections, the modeling process of gas turbine and steam cycle are described.

4.2.1 Gas Turbine

The gas turbine consists of a multi-staged compressor, the combustor, and a multi-stage expander. The model of Frame 7H gas turbine developed in this study was designed to include the details regarding air cooling, steam cooling, the size of gas turbine, and other main features of H gas turbine. The air from atmosphere is compressed by the compressor. Part of compressed air is extracted from the last stage and sent to the expander for cooling. The natural gas or syngas is combusted with air in the combustor. The exhaust from the combustor is expanded in the turbine. A part of high pressure steam from the steam cycle is sent to the turbine for cooling of combustion product. The syngas is expanded and the shaft work is produced, which is converted into power by the generator. Hot exhaust is sent to the steam cycle.

4.2.1.1 Main Process Modeling

The air at 14.7 psia and 59 ^{o}F is compressed in a three-stage compressor. Part of the compressed air from the last stage of compressor is sent to the third stage of the turbine for cooling. The extraction of air is simulated by a split unit block, SPLITAIR. The split fraction is 0.1 of the total compressed air (Buchanan, ***et al.***, 1998). The rest of air is sent to the combustor.

The outlet pressures of each compressor stage and expander stage are estimated in the CALCULATOR block GTRP. There are three stages in a compressor. The pressure ratio for each stage is assumed to be same. Thus, the pressure ratio for a stage is estimated as:

$$r_{c,i} = PR^{1/3} \tag{4-1}$$

Where,

$r_{C,i}$ = pressure ratio of a stage of a compressor;

PR = pressure ratio of a compressor, which is 23 for 7H gas turbine;

i = stage number, 1, 2, or 3.

The natural gas is mixed with the compressed air in a mixer, GT-MIXER and combusted in the combustor, GT-BURN. The pressure drop due to combustion is assumed to be 4% of the inlet pressure of combustor or the outlet pressure of compressor. The hot product gas is expanded in the expander turbine of four stages. The pressure ratio of the turbine is 23. The pressure ratio for each stage of the turbine is assumed to be same. Thus, the pressure ratio of a stage in a turbine is estimated as:

$$r_{T,i} = PR^{1/4} \tag{4-2}$$

Where,

$r_{T,i}$ = pressure ratio of a stage of a turbine;

PR = pressure ratio of a compressor, which is 23 for 7H gas turbine;

i = stage number, 1, 2, 3, or 4.

The pressure of the outlet of each stage can be estimated based on the pressure ratio and the inlet pressure of each stage.

The first two stages of the expander are cooled by the steam from part of the HP turbine exhaust steam. The heater block, STMC1, simulates the steam cooling of the first nozzle of the stage 1. In STMC1, the exhaust gas is cooled to 2,600 ^{o}F, which is the typical firing temperature of H gas turbine. The heater block, STMC2, simulates the steam cooling of stage 2. The heat from two blocks is sent a heater block, STMCOOL. This block simulates the heat from the exhaust gas is transferred to the cooling steam and the steam temperature increases. The exhaust gas from the last stage of the expander is sent to the HRSG to generate high temperature and high pressure steam. The details of steam cooling simulation are introduced in section 4.2.2.2 of steam cycle.

The flowsheet of gas turbine simulation is shown in Figure 4-1. The unit operation blocks of gas turbine in the simulation are described in Table 4-1

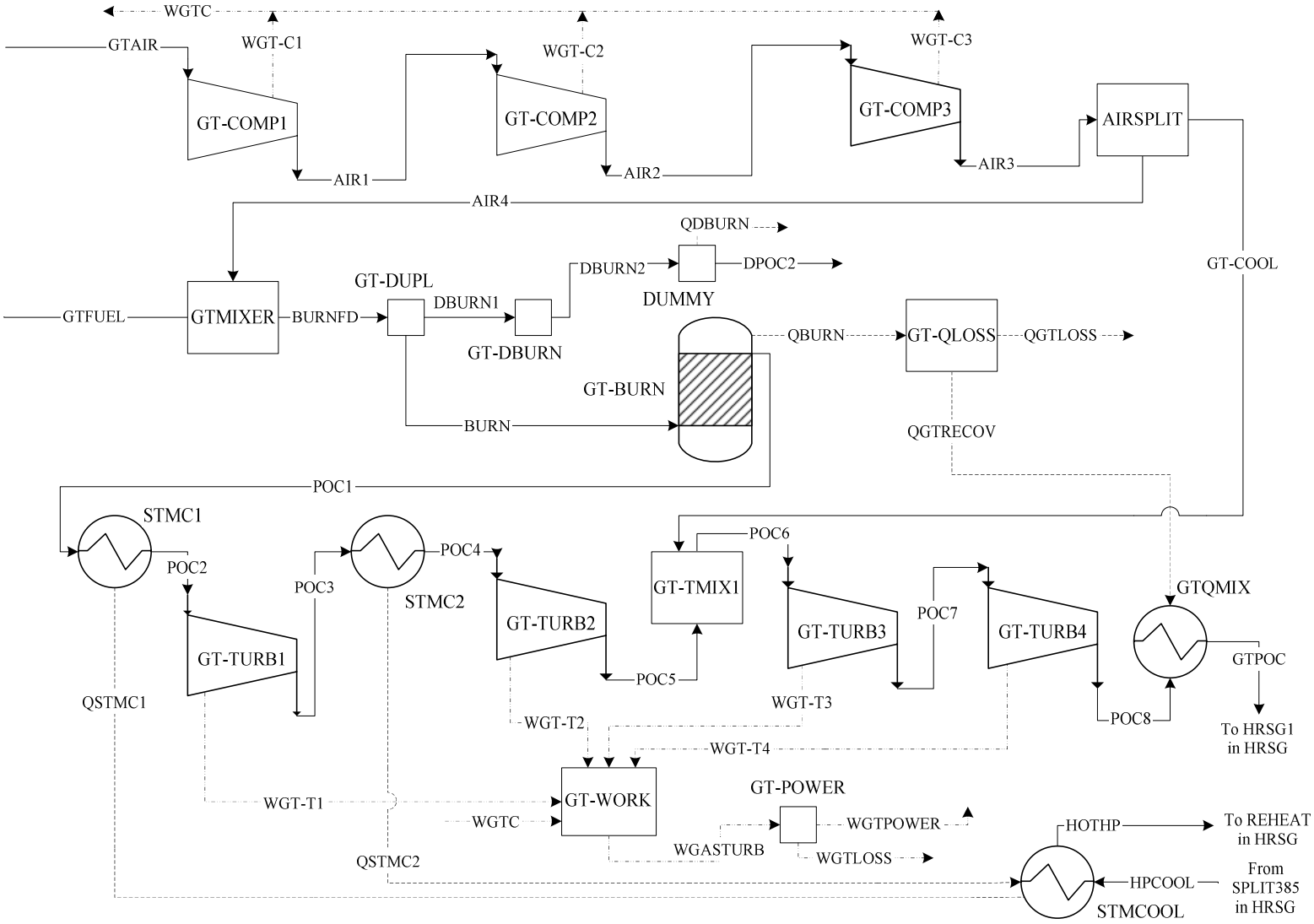

Figure 4-1 Flowsheet of H-class Gas Turbine in ASPEN Plus

Table 4-1 Gas Turbine Section Unit Operation Block Description

No	BLOCK ID	BLOCK PARAMETERS	DESCRIPTION
1	GT-COMP1 (COMP)	TYPE = ISENTROPIC	Compresses the air entering the gas turbine. The outlet pressure and isentropic efficiency are specified in the CALCULATOR GTPR
2	GT-COMP2 (COMP)	TYPE = ISENTROPIC	Similar to GT-COMP1.
3	GT-COMP3 (COMP)	TYPE = ISENTROPIC	Similar to GT-COMP1.
5	AIRSPLIT (FSPLIT)	FRAC AIRCOOL1 = 0.11	Simulates the split of the cold compressed air. AIRCOOL1 is sent to the third stage of the expander for cooling.
6	GT-MIXER (MIXER)		The block mixes the compressed air and fuel gas.
7	GT-DUPL (DUPL)		Duplicates the mixed fuel and air stream for heating value calculation purposes.
8	GT-BURN (RSTOIC)	Temperature = 2,680 °F Pressure = 334.58 psia	Simulates the stoichiometric reactions that take place in the gas turbine combustor.
9	GT-DBURN (RSTOIC)	Temperature = 59 °F Pressure = 14.7 psia	Simulates the stoichiometric reactions that take place in a dummy gas turbine combustor.
10	GT-QLOSS (FSPLIT)	FRAC QGTLOSS = 0.5 FRAC QGTRECOV = 0.5	Simulates the loss of heat from the gas turbine combustor.
11	STMC1 (HEATER)	T change = 2600 F P drop = 0	Simulates the steam cooling of the first nozzle and stage 1 of the expander.
12	GT-TURB1 (COMPR)	TYPE = ISENTROPIC	Simulates a compressor for the expansion. The outlet pressure and isotropic efficiency is specified in CALCULATOR block GTPR
13	STMC2 (HEATER)	Heat duty = 1 P drop = 0	Simulates the steam cooling of stator and rotor of stage 2 of the expander
14	GT-TURB2 (COMPR)	TYPE = ISENTROPIC	Simulates a compressor for the expansion
16	GT-MIX1 (MIXER)	Pressure drop = 0	Simulates the mixing of cool air with the hot products of combustion.
17	GT-TURB3 (COMPR)	TYPE = ISENTROPIC	Simulates stage 3 of the expander

(Continued)

Table 4-1 (Concluded)

No	BLOCK ID	BLOCK PARAMETERS	DESCRIPTION
18	GT-MIX2 (HEATER)	Pressure Drop= 0	Simulates the recovery of the heat loss of combustion.
19	GT-WORK (MIXER)		Sums the work from all compressor and expander stages.
20	GT-POWER (FSPLIT)	FRAC WGTPOWER = 0.985	Accounts for power loss in the gas turbine.
21	STMCOOL (HEATER)	P drop = 0	Simulates the heating of the cooling steam by the heat transferred from the hot gas in gas turbine

4.2.1.2 Design Specifications and CALCULATOR Blocks

The design-spec TCHOKE controls the mass flow at the turbine inlet nozzle by varying the mass flow of air flowing to the compressors. The design-spec GTHEAT determines the fuel flow rate to the gasifier in order to keep the mixture heat of air and fuel gas to be zero.

In the CALCULATOR block, GTPR, the pressure ratio, firing temperature, and the efficiencies of the compressor and the expander are specified. The pressure level of each stage of compressor and expander is calculated.

In the CALCULATOR block, TCHOKE, the mass flow requirement of first nozzle of the turbine is calculated based on the reference pressure, reference temperature, and the molecular weigh of the exhaust gas at the first nozzle. The reference mass flow is assumed to be same as the combustor outlet pressure, 324.56 psia. The reference temperature is the firing temperature or the turbine let temperature (TIT), 2600 ^{o}F. The reference mass flow is varied to make the combined cycle output match the computed

chocked mass flow at first nozzle. The computation method was introduced in Frey and Akunuri (2001).

4.2.2 Steam Cycle

The steam cycle consists of HRSG, steam turbine and other auxiliary parts. The hot exhaust gas from gas turbine is sent to heat recovery steam generator (HRSG). The heat of exhaust gas is recovered by generating high temperature steam. The steam is expended in steam turbine to produce shaft work and it is converted into energy.

The model of steam cycle used in H combined cycle is different from the steam cycle model used in 7F gas turbine combined cycle. There are no steam cooling parts in the previous steam cycle. In addition, the steam conditions used that model is different from that of the steam cycle in an H gas turbine combined cycle. Based on the design basis of H gas turbine combined cycle described in section 2.6.2, the steam cycle is developed with some modifications of the previous model, including:

- Part of high pressure steam is extracted for cooling;
- The specifications of main blocks, including the turbines outlet pressure and boilers pressures are modified to be the reference specifications of a steam cycle in H combined cycle;

The details of the modeling process for steam cycle are introduced in the following.

4.2.2.1 Heat Recovery Steam Generator

The flowsheet of HRSG is shown in Figure 4-2 and the description of the unit blocks in the model is given in Table 4-2. The exhaust gas exits the gas turbine around 1,133 °F (Carcacci and Falsetti, 2000). The HRSG cools the gas to approximately 271

°F, recovering the sensible heat in steam production. Four HEATER blocks, HRSG1, HRSG2, HRSG3 and HRSG4 simulated the heat recovery of hot exhaust. The exhaust gas of the gas turbine is cooled in the four blocks.

The four HEATER blocks provide heat to four "trains" of heat requirements, high-pressure steam generation, intermediate-pressure steam generation, low-pressure steam generation and deaeration. The heat from the block, HRSG1, is sent to HPBOILER and SUPERHTR to produce high-pressure steam. The HRSG2 provides heat for intermediate-pressure (IP) level steam generation. The blocks used for producing IP steam include IPECON, IPBOILER and IPSPRHTR. The HRSG3 provides heats for low-pressure (LP) steam generation, which involves the blocks HPECON and LPBOILER. Finally, HRSG4 provides heat streams for deaeration and condensate heating in the blocks DEAERATR and CONDHEAT.

Liquid water, DEAERH2O, enters the steam cycle process area at 30 psia. The design-spec, ***SETBFW***, determines water requirements of the steam cycle. LPPUMP pumps the water to 200 psia before splitting it to the three pressure levels by BFWSPLT. The design-specs, ***SETLPSTM*** and ***SETIPSTM***, determine the amount of water to the low- and intermediate-pressure levels, respectively. The low-pressure level consists of a boiler, LPBOILER, generating saturated steam at 250 °F. The steam, used in the steam turbine, supplies heat to the deaerator.

The water is heated to 461 °F in IPECON, before being heat to 479 °F saturated steam in IPBOILER. IPSPRHTR super-heats the steam to 716 °F and 508 psia before mixing with high-pressure steam in STMMIX.

The block, HPPUMP, first pumps high-pressure BFW to 2,720 psia before the block, HPSPLIT, splits it for use in the plant. The CALCULATOR block, SETHPSTM, calculates all high-pressure steam and BFW requirements. Although not used in this design, the block, HPSPLIT, is used for integration with an air separation plant. High-pressure BFW used for heating in the fuel gas saturation area, mixes with the high-pressure BFW in HPMIX. The block, HPECON, heats the mixture to 597 °F. The heating water, used in the fuel gas saturation area, splits out in block HOTSP. HPBOILER creates 2,480 psia saturated steam, which is then super-heated by SUPERHTR to 1,050 °F and 2,400 psia. This super-heated steam feeds the first stage of the steam turbine, HPTURB.

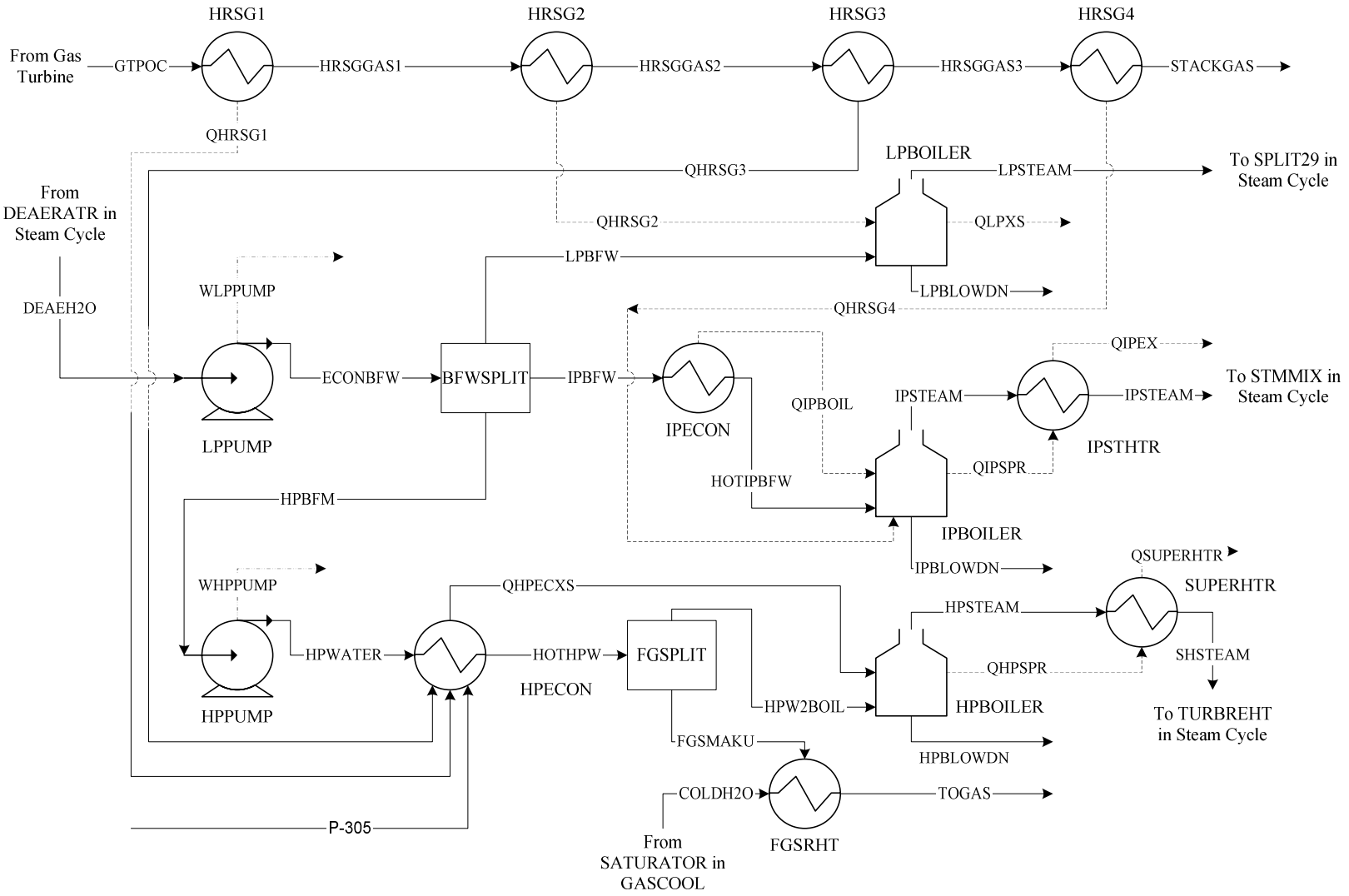

Figure 4-2 Flowsheet of Heat Recovery Steam Generator (HRSG) in ASPEN Plus

Table 4-2 HRSG Unit Operation Block Description

No	BLOCK ID	BLOCK PARAMETERS	DESCRIPTION
1	HRSG1 (HEATER)	Temperature = 674 °F Pressure Drop = 0 psia	Cools the gas turbine exhaust gas temperature providing heat for generating high-pressure steam.
2	HRSG2 (HEATER)	Temperature = 595 °F Pressure Drop = 0 psia	Cools the Gas turbine exhaust gas temperature providing heat for generating intermediate-pressure steam.
3	HRSG3 (HEATER)	Temperature = 278 °F Pressure Drop = 0 psia	Cools the gas turbine exhaust gas temperature providing heat for generating low-pressure steam.
4	HRSG4 (HEATER)	Temperature = 271 °F Pressure Drop = 0 psia	Cools the gas turbine exhaust gas temperature providing heat for generating high-pressure deaeration.
5	LPPUMP (PUMP)	Pressure = 600 psia	Increases pressure of BFW to steam cycle.
6	BFWSPLIT (FSPLIT)	FRAC LPBFW = 0.1618 IPBFW = 0.1744	Splits inlet BFW to low, intermediate and high-pressure steam drums.
7	LPBOILER (FLASH2)	Temperature = 250 °F VFRAC = 0.995	Simulates a boiler, producing low-pressure steam.
8	IPECON (HEATER)	Temperature = 461 °F VFRAC = 0	Using heat from the HRSG, the block preheats the BFW.
9	IPBOILER (FLASH2)	Temperature = 479 °F VFRAC = 0.9901	Simulates a boiler, producing intermediate-pressure steam.
10	IPSPRHTR (HEATER)	Temperature = 716 °F Pressure = 350 psia	Superheats the steam from the intermediate-pressure boiler.
11	HPPUMP (PUMP)	Pressure = 2720 psia	Increases pressure of BFW for high-pressure steam drum.
12	HPECON (HEATER)	Temperature = 597°F Pressure Drop = -5.0 psia	Using heat from the HRSG, the block preheats the high-pressure BFW.
13	FGSPLIT (FSPLIT)		Splits high-pressure BFW for use in the fuel gas saturation section.
14	FGSRHT (MIXER)		Mixes returned, high-pressure BFW from the fuel gas saturation section.
15	HPBOILER (FLASH2)	Temperature = 616 °F VFRAC = 0.9901	Simulates a boiler, producing high-pressure steam.
16	SUPERHTR (HEATER)	Temperature = 1,050°F Pressure = 2,400 psia	Superheats the steam from the high-pressure boiler.

4.2.2.2 Steam Turbine

The flowsheet of steam cycle is shown in Figure 4-3 and the description of the unit blocks in the model is given in Table 4-3. From block SUPERHTR, the super-heated, high-pressure steam enters the high pressure steam turbine, HPTURB. The design-spec, STMQUAL, determines the isentropic efficiency of HPTURB based on a specified outlet vapor fraction in the steam turbine exhaust. The transfer block, SETSTEFF, sets the isentropic efficiencies of the remaining turbine stages equal to HPTURB. The steam is expanded in the block, HPTURB, and the outlet pressure is 385 psia. The steam is split into two parts in a split block, SPLIT508. One part of the steam is sent to the gas turbine for cooling, which is simulated by the block STMCOOL.

The mass flow rate of the steam required for gas turbine cooling is specified in a CALCULATOR block, SETSTMC. In this block, the mass flow rate of the cooling steam is set to be proportional to the combustion product mass flow rate, which is 8% of the mass flow rate of the combustion product (Buchanan, ***et al.***, 1998). The heat streams from the blocks in gas turbine process, STMC1 and STMC2 are sent to STMCOOL. The steam used for cooling the combustion product of the gas turbine is heated to 1050 ^{o}F, which is the same as the reheat temperature. After cooling, the heated syngas is sent back to the steam cycle.

The heated steam mixes with intermediate-pressure steam from IPSPRHTR in STMMIX. The mixed steam is sent to a reheater, REHEAT. After being reheated to 1,050 °F, the steam proceeds to the second stage of the steam turbine, IPTURB, expanding the steam to 116 psia. After the steam from the low-pressure boiler splits to

feed the deaerator, the remaining steam mixes with the steam from LPTURB, in the block, MIX29. LPTURB further expands the steam to 31 psia. The steam expands in VLPTURB to 0.591 psia.

The block, CONDENSR, condenses the steam to 86 °F, while the block, CONDPUMP, increases the pressure to 30 psia. Make-up water is also added at CONDPUMP. The block, CONDSPLT, diverts a portion of the water for cooling water in the Gas Cooling Section. The block, CONDMIX, combines plant condensate, and hot water from the Gas Cooling Section, with the steam cycle water. The block, CDHTSP, splits a portion of the condensate to be heated, in the block, CONDHEAT, before entering the deaerator, modeled by the block DEAERTR. The deaerated water is sent back to LPPUMP.

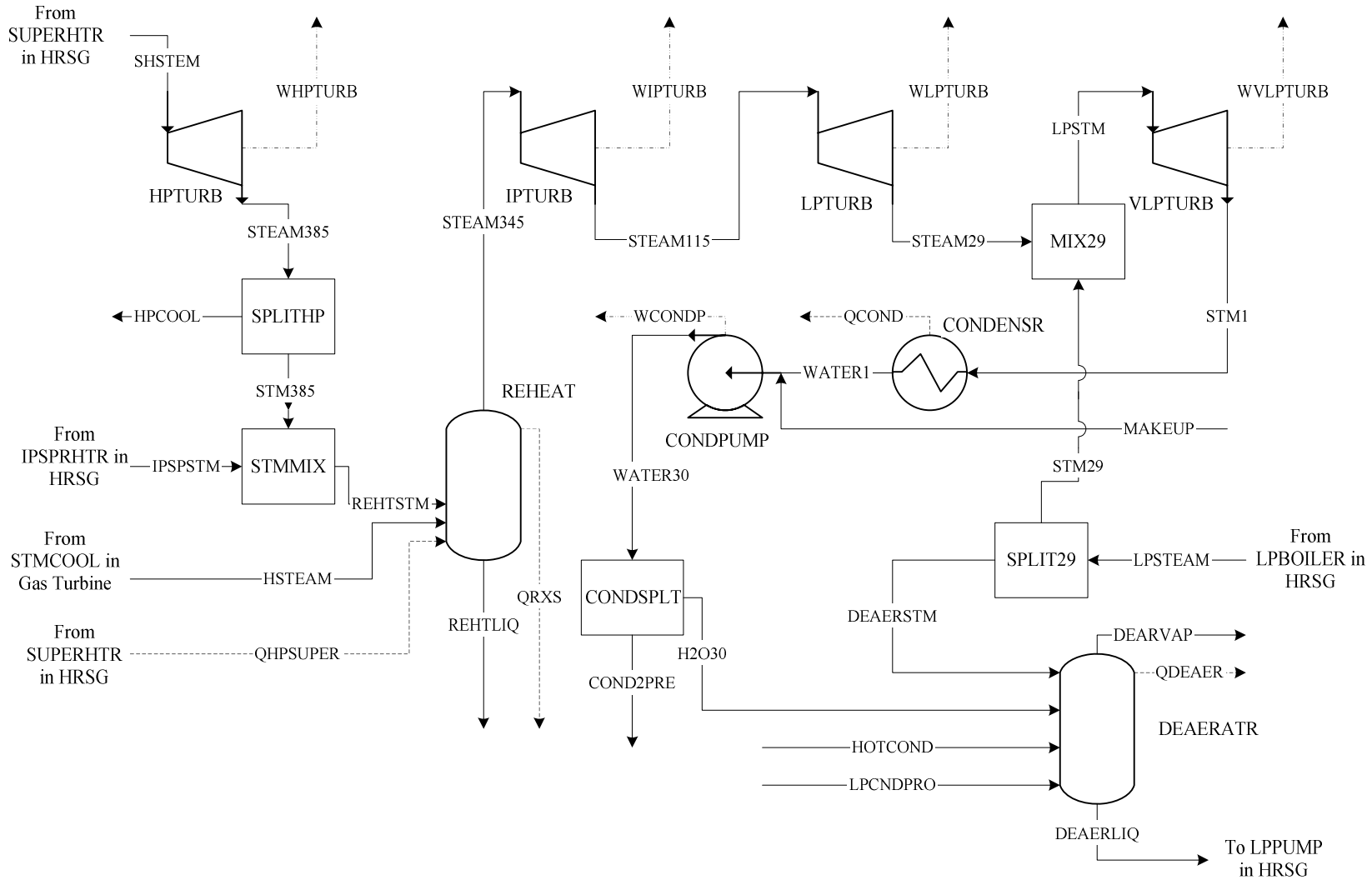

Figure 4-3 Flowsheet of Steam Turbine and Auxiliary Process in ASPEN Plus

Table 4-3 Steam Cycle Unit Operation Block Description

No	BLOCK ID	BLOCK PARAMETERS	DESCRIPTION
1	HPTURB (COMPR)	TYPE = ISENTROPIC Pressure = 385 psia Isentropic Efficiency = 0.85	Simulates the high-pressure stage of the steam cycle turbine.
2	SPLITHP (FSPLIT)	Frac HPCOOL = 0.3	Splits HP steam for steam cooling in gas turbine
3	STMMIX (MIXER)		Mixes the superheated intermediate-pressure steam with high-pressure steam.
4	REHEAT (FLASH2)	Temperature = 1,050 °F Pressure = 345 psia	Steam from the high-pressure turbine and intermediate-pressure boiler is superheated.
5	IPTURB (COMPR)	TYPE = ISENTROPIC Pressure = 116 psia	Simulates the first-intermediate stage of the steam turbine.
6	LPTURB (COMPR)	TYPE = ISENTROPIC Pressure = 31 psia Isentropic Efficiency = 0.85	Simulates the second-intermediate stage of the steam turbine.
7	VLPTURB (COMPR)	TYPE = ISENTROPIC Pressure = 0.591 psia Isentropic Efficiency = 0.921	Simulates the last stage of the steam turbine.
8	MIX29 (MIXER)		Mixes steam from the low pressure boiler and LPTURB.
9	SPLIT29 (FSPLIT)	FRAC DEAERSTM = 0.3737	Splits the steam produced in LPBOILER between the deaerator and the steam turbine.
10	CONDENSR (HEATER)	Temperature = 86 °F VFRAC = 0	Condenses steam from the steam turbine.
11	CONDPUMP (PUMP)	Pressure = 200 psia	Increases the pressure of the condensate from the steam turbine.
12	CONDSPLT (FSPLIT)	MASS-FLOW COND2PRE = 716,492	Splits steam turbine condensate to be heated in the Gas Cooling section.
13	DEAERATR (FLASH2)	Pressure = 30 psia VFRAC = 0 NPHASE = 2	Simulates a dearation vessel that removes any entrained gases from the steam turbine condensate.
14	ST-MISC (MIXER)		Totals work done by pumps for calculating auxiliary power demands of the steam cycle.
15	ST-WORK (MIXER)		Totals work produced by all stages of the steam turbine.
16	ST-POWER (MIXER)		Simulating the total power produced by steam turbine

4.3 Calibration of Frame 7H Gas Turbine Combined Cycle

In this section, the calibration of Frame 7H combined cycle model was implemented based on the reference data of Frame 7H fueled with natural gas and syngas.

4.3.1 Natural Gas

The natural gas is assumed to be 100% CH_4. Three inputs of the gas turbine model are selected for calibration of this model. They are the turbine isentropic efficiency, the compressor isentropic efficiency, and the reference mass flow at the inlet of the turbine. Since the 7H gas turbine must be connected with the steam cycle for steam cooling, there is no simple cycle for Frame 7H gas turbine. Thus different from the calibration of 7FA gas turbine, the combined cycle efficiency and power output were selected not the simple cycle specifications. The gas turbine exhaust temperature is also selected for it affects the heat recovery of exhaust gas in HRSG. The isentropic efficiencies of compressor and turbine will affect the performance of the combined cycle. Therefore, the isentropic efficiency of the turbine is varied to match the reference data for the exhaust temperature. The compressor isentropic efficiency is varied to match the combined cycle efficiency. After the exhaust temperature and the combined cycle efficiency match the reference values, the reference mass flow is varied to match the power output of 7H combined cycle.

In Figure 4-4, the curves were obtained from the sensitivity analysis of the 7H combined cycle model. The published data are an exhaust temperature of 1133 ^{o}F (Carcasci and Facchini, 2000), a combined cycle efficiency of 60% on LHV basis, and a

combined cycle net power output of 400 MW (Matta, *et al.*, 2000). The calibrated parameters and the corresponding outputs were shown in the figure by using the "calibration" line. The isentropic turbine efficiency of 0.889 was selected to match the published exhaust temperature. To obtain the combined cycle efficiency of 60%, the isentropic compressor efficiency of 0.918 was selected. With these two parameters were set, the reference mass flow in the design specification for choked flow is set to 4,200,000 lb/hr in order to match the reference combined cycle power output.

After all the specifications are set, the model results are compared to the published value, which are listed in Table 4-4. Results based on natural gas match the published data very well. The model results for the exhaust temperature, combined cycle power output, and combined cycle efficiency are exactly the same as the published values. The relative differences between predicted and reported gas turbine air flow are less than one percent. The comparison results indicate the 7H combined cycle model can predict the performance of the actual gas turbine well.

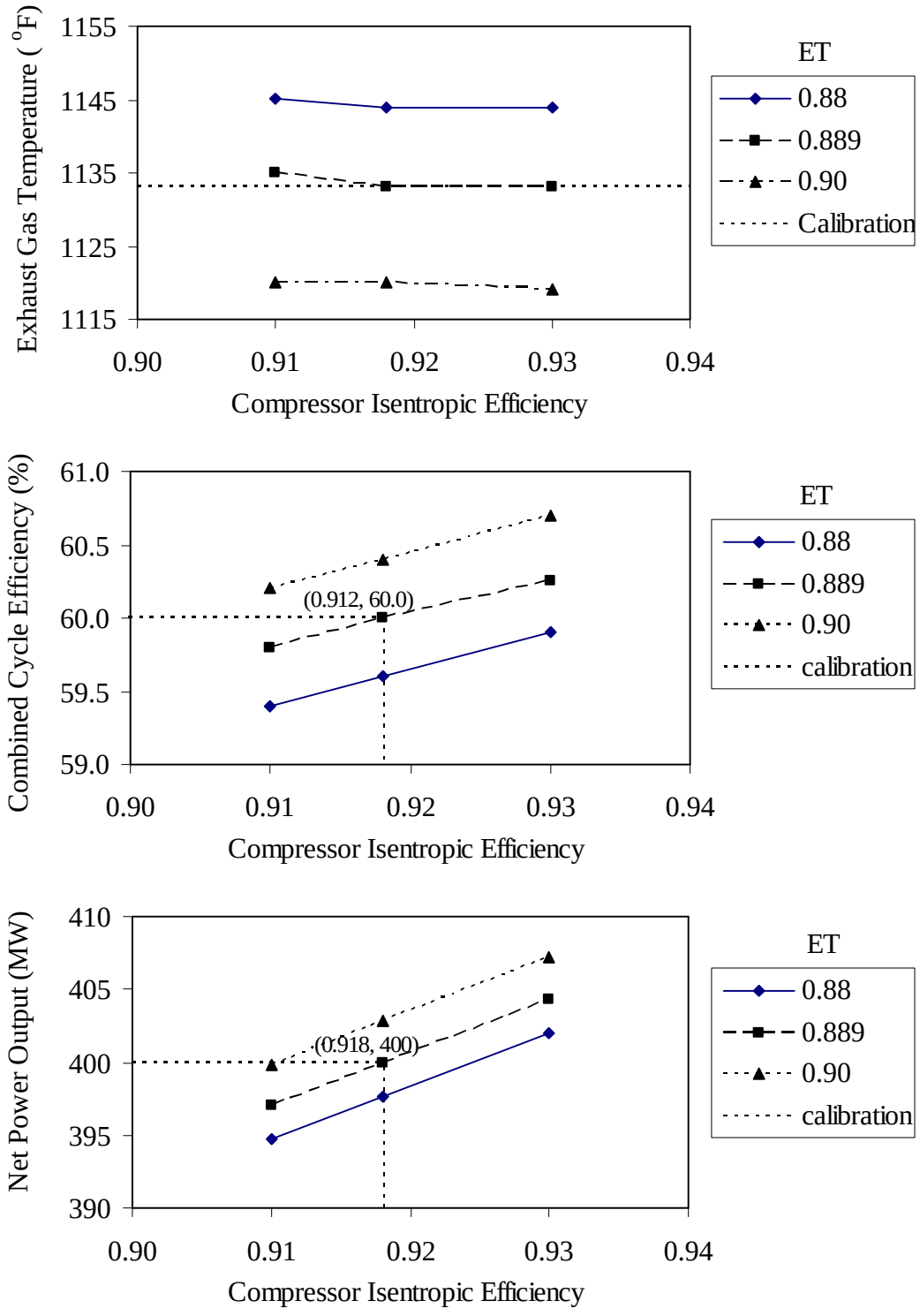

Figure 4-4 Calibration of Frame 7H Gas Turbine Combined Cycle Model – plot s of (a) Exhaust Temperature, (b) Combined Cycle Efficiency (LHV), and (c) Combined Cycle Output versus Isentropic Compressor Efficiency of Gas Turbine.

Note: ET = Isentropic Turbine Efficiency of Gas Turbine

Table 4-4 Main Results and Comparison to Reference Values of Frame 7H Gas Turbine Combined Cycle fired with Natural Gas

Variables	Model Results	Reference Value [a]	Difference (%)
Mass flow of Natural Gas, lb/hr	105,300	--	--
Massflow of Air, 10^6lb/hr	4.410	4.428	-0.4%
Exhaust Temperature, ^oF	1133	1133[b]	0
Combined Cycle Power Output, MW	400	400	0
Combined Cycle Efficiency, % LHV	60.0	60	0

[a] The reference values are from the GE Power System report (Matta, *et. al*., 2001).
[b] The published exhaust temperature is from Carcasci and Facchini (2000).

4.3.2 Syngas

For calibration of 7H combined cycle fired with syngas, the reference data that can be used for calibration is very limited. The possible reason is that the IGCC plant based on 7H gas turbine has not commercialized yet. A design study of IGCC with 7H gas turbine by Bechtel *et al.* (2002) is selected as calibration basis. From the results of the design study, the syngas heat input to gas turbine is 2,427 $\times 10^6$ Btu/hr (LHV). The total power output of the combined cycle is 464.2 MW. Therefore, the combined cycle efficiency is 65.28% (LHV) based on the syngas heat input. The composition data of syngas at the inlet of gas turbine combustor are not available in Bechtel, *et al.* (2002). Therefore, the syngas composition from Illinois No.6 coal gasification in this study is used and these two values are taken as typical performance data for a 7H gas turbine combined cycle fired with syngas. The exhaust temperature of syngas fired gas turbine is not available in Bechtel *et al.* (2002). Therefore, the same exhaust temperature of the natural gas is selected for this case of syngas. A similar calibration process as natural gas case is used for the gas turbine combined cycle fired with syngas. The isentropic turbine efficiency of 0.914 is selected to match the exhaust temperature of 1133 ^oF. The isentropic compressor

Table 4-5 Main Results and Comparison to Reference Values of Frame 7H Gas Turbine Combined Cycle fired with Syngas

Description	Model Results	Reference Value [a]	Relative Difference (%)
Mass flow of Natural Gas, lb/hr	637,680	--	--
Massflow of Air, 10^6lb/hr	4.291	--	--
Exhaust Temperature, ^{o}F	1133	1133[b]	0
Combined Cycle Power Output, MW	464.4	464.2	0.0
Combined Cycle Efficiency, % LHV	65.26	65.28	0.0

[a] The reference values are from DOE report (Bechtel, *et al*., 2001).
[b] The published exhaust temperature is from Carcasci and Facchini (2000).

of 0.820 is used to obtain the combined cycle efficiency of 65.26%. The reference mass flow is set to 4,610,000 lb/hr.

The main results of the calibrated model and the reference values are compared to each other in Table 4-5. The air flow rate 7H gas turbine is not available in Bechtel, *et al*., (2001). The comparison results indicate that the gas turbine combined cycle model can give reasonable estimates of the gas turbine performance based on syngas.

4.4 Cost Model of Frame 7H Gas Turbine

The cost model for IGCC-7FA system was developed by Frey and Akunuri [8]. Since the cost of a gas turbine is influenced by the design factors, such as pressure ratio and firing temperature, the direct cost model for 7H gas turbine should be developed. The direct cost model for 7H gas turbine is based on the number of gas turbine and the cost for a single 7H gas turbine. The direct cost of a single 7H gas turbine is $47,303 (1998 Dollar) (Buchanan, *et al*., 1998). Although there is no simple cycle for the H class gas turbine due to steam cooling feature, the gas turbine power output is estimated to be about 300 MW in a combined cycle (Bechetl, *et al*., 2001). The number of gas turbine is

estimated based on the power output for a single Frame 7H gas turbine. The cost model is:

$$DC_{GT} = 47{,}303\ N_{T,GT} \quad (4\text{-}3)$$

Where,

DC_{GT} is the direct cost of gas turbine, $;

N_{GT} is the number of gas turbine in operation.

The cost model of 7H gas turbine is combined with other processes cost model to form the cost model of IGCC-7H system.

4.5 Verification of Model for IGCC System based on 7H Gas Turbine

In order to verify the accuracy of the estimation of IGCC-7H system model, a case study by DeLallo *et al.* (2000) is selected for comparison basis. In this project, an entrained-bed gasifier and Illinois No. 6 coal is used. Considering the Texaco gasifier is also an entrained gasifier, the modeling results are compared to the published data for IGCC-7H system.

The modeling results and the reference data are listed in Table 4-6. The predicted efficiency by the model is close to the reference data. The difference may be caused by different cooling methods in the model and the report, which is not provided in the reference report. Falsetti, *et al*. (2000) mentioned the efficiency of an IGCC with 9H gas turbine with radiant only cooling is 43.7%. This value is same as the result of this study. It indicates that the estimates based on the modeling for IGCC system with H gas turbine are accurate. For the cost of electricity, the available information is capacity of 65 percent

Table 4-6 Comparison of Modeling Results and Reference Date for IGCC based Frame 7H Gas Turbine System

Description	Modeling Results	Reference Data [a]	Relative Difference
Coal Feed Rate, lb/hr	253,400	--	--
Gross Plant Power Output, MW	464.5	474.0	-2.0%
Total Auxiliary Load, MW	49.9	49.5	-0.8%
Net Plant Power Output, MW	414.6	424.5	-2.3%
Heat Rate, Btu/kWh (HHV)	7,812	7,915	-1.3%
Net Plant Efficiency, %	43.7	43.1	1.4%
Cost of Electricity, mills/kWh [b]	50.0	52.4	-4.6%

[a] DeLallo, et al. (2000);
[b] COE are in constant 2000 Dollars.

and 2000 dollars basis, which are the same as the cost factors used in this study. Other detailed information of cost is not available. Therefore, the difference of COE may be decreased or the reason for the difference can be further discussed if more details of the design study are available. The relative differences for all the performance and cost outputs are all less than 5%. That indicates the modeling results can estimate the actual IGCC-7H project well.

5.0 CASE STUDY BASED ON DETERMINISTIC MODEL OF IGCC SYSTEM

In this chapter, the deterministic models based on 7FA and 7H Gas Turbine were applied to two case studies. The first case study is to evaluate the effects of fuel compositions on the performance of IGCC system. The second case study is to compare the effects of different gas turbines, 7FA and 7H, on the performance, emissions, and costs of IGCC systems.

5.1 Comparison of IGCC Performance and Cost for Different Coals

A wide variety coals have been used in IGCC systems. Coal compositions vary with coal rank and geographical region. In this case study, three coals are selected, including Illinois No.6 coal, Pittsburgh No. 8 coal, and West Kentucky coal. Some designs studies have used these three kinds of coals as fuel for Texaco gaisfier-based IGCC plants (Fluor Engineers, 1984; Pichetl, *et al.*, 1992; Condorelli, *et al.*, 1991). The effects of different coal compositions on performance and cost of same IGCC design are evaluated.

5.1.1 Input Assumptions

The compositions of three kinds of coals are listed in the Table 5-1. The composition analyses of coals include proximate analysis and ultimate analysis. Except the coal compositions, other inputs keep same for IGCC systems fired with three coals. The main inputs assumptions of IGCC system have been listed in Table 3-9.

Table 5-1 Proximate and Ultimate Analysis of Illinois No. 6, Pittsburgh No.8, and West Kentucky Coal

Proximate Analysis, wt%, As Received Basis	Illinois No.6 [a]	Pittsburgh No.8 [b]	West Kentucky [c]
Moisture	10.00	6.0	9.46
Fixed Carbon	48.87	46.0	43.62
Volatile Matter	32.22	36.5	29.99
Ash	8.91	11.5	16.93
Ultimate Analysis, wt%, Dry Basis			
Carbon	69.62	73.21	65.78
Hydrogen	5.33	4.94	4.62
Nitrogen	1.25	1.38	1.26
Chlorine	0.0	0.09	0.04
Sulfur	3.87	3.30	4.74
Oxygen	10.03	4.85	4.86
Ash	9.90	12.23	18.70
Higher Heating Value (HHV), Btu/lb, Dry Basis	12,774	13,138	11,969

[a] Fluor Engineers(1984);
[b] Pichetl, *et al.* (1992);
[c] Condorelli, *et al.* (1991).

Base on Table 5-1, the coal compositions are compared each other. For carbon content as the primary source of energy, the Pittsburgh No.8 coal has the highest carbon content among three. For the HHV of coals, they are consistent with the carbon contents of coals. For example, Pittsburgh No.8 coal with highest carbon content has highest HHV. For sulfur content, the West Kentucky coal has highest sulfur content among three. For ash content, the West Kentucky coal has the highest ash fraction.

Table 5-2 Comparison of results of Illinois No. 6, Pittsburgh No.8, and West Kentucky Coal

Description	Illinois No.6	Pittsburgh No.8	West Kentucky
Saturated Syngas Composition, Fraction			
H_2	0.263	0.250	0.255
CO	0.327	0.336	0.320
CO_2	0.087	0.085	0.095
N_2	0.006	0.007	0.007
Ar	0.008	0.008	0.009
CH_4	0.003	0.003	0.002
H_2O	0.306	0.311	0.311
LHV, Btu/scf	181.4	180.2	176.0
Saturated Syngas flow rate, lb/hr	491,710	503,220	517,000
Performance			
Coal Feed Rate, lb/hr	192,370	188,160	216,000
Gas Turbine Net Power (1 trains), MW	192.1	192.5	193.7
Steam Turbine Net Power, MW	132.1	131.0	136.8
Total Auxiliary Load, MW	39.5	41.6	43.9
Net Plant Power Output, MW	284.6	281.9	286.6
Heat Rate, Btu/kWh (HHV)	8639	8775	9027
Plant Efficiency, % (HHV)	39.53	38.92	37.83
Emissions			
SO_2 Emissions, lb/10^6Btu	0.223	0.199	0.294
NO_x emissions, lb/10^6Btu	0.127	0.126	0.124
CO_2 Emissions, lb/kWh	1.69	1.75	1.75
Cost [a]			
Total Capital Cost ($/kW)	1,882	1,901	1,993

[a] Cost Year = January 2000;

5.1.2 Results

The model results for three kinds of coals are listed in Table 5-2. For three kinds of coals, the saturated syngas compositions for three coals are listed. As combustible components, the sum of molar fractions of hydrogen (H_2) and carbon monoxide (CO) is related with the heating value of syngas. As shown in Table 5-2, the sum of molar fraction of H_2 and CO of West Kentucky coal is lowest in three, which is 0.555. Thus, the LHV of saturated syngas produced from West Kentucky coal is also the lowest one in

three syngas. Considering the composition of coals, West Kentucky coal has highest ash content. Low ash content leads to high energy content in coal and thus high energy content of syngas.

Based on the same IGCC design, the West Kentucky coal has the highest coal feed rate. Considering the LHV values of syngas into gas turbine, the sygnas produced from West Kentucky coal has lowest LHV. In order to keep same firing temperature, the gas turbine fired with low heating value syngas required higher flow rate of syngas than the syngas with high heating value. Thus, the syngas produced from West Kentucky coal has highest flow rate compared other two coals. Therefore, it has highest coal feed rate to produce syngas with highest flow rate.

For the results of efficiency, the Illinois No.6 coal based system has the highest efficiency. The reason is that the syngas produced from Illinois No.6 coal has highest compositions of CO and H_2, which is the combustible part of syngas. The high content of two represent more energy content per unit fuel that can be converted into power. Therefore, IGCC fueled with Illinois No. 6 has highest efficiency. From the results in Table 5-2 and the ash contents of coals, the plant efficiency with Pittsburgh No.8 coal is 0.6 percent lower than that of Illinois No. 6 coal and the ash content in Pittsburgh is 30% higher than that of Illinois No.6 coal. The ash content of West Kentucky coal is approximately 90% higher than that of Illinois No.6 and the plant efficiency of it is 1.7 percents lower than that of Illinois No. 6 coal.

Another finding is that the sulfur content in fuel compositions has important effect on the emissions of SO_2. The sulfur content in West Kentucky coal is the highest one in

three and the IGCC system fueled with it has the highest SO_2 emissions. The SO_2 emissions of IGCC fueled with West Kentucky coal is 32% higher than that of Illinois No.6 coal. For high sulfur content coal, a sulfur control system with higher removal efficiency would be considered. For example, a 99.5+% removal level would require a Rectisol system compared to the Selexol process with approximately 99% removal efficiency (Trapp, *et al*., 2004).

The difference in capital cost mainly is caused by the difference in the direct capital cost of coal handling, oxidant feed, and gasification for three coals. The three capital costs are associated with the coal feed rates and thus the oxygen flow rates. The capital cost of Illinois No.6 coal based system has lowest capital cost. Since the West Kentucky coal has the highest coal flow rate and the highest oxygen consumption, the capital cost of the IGCC based on this coal is highest in three, which is 6% higher than that of Illinois No.6 coal fueled system. It is also consistent with the ash contents of coals.

In a summary, the coal parameters have important effects on performance, emission, and costs of IGCC systems. Since there is wide variety in coals or other fuels compositions, the design of IGCC systems should consider the features of fuels parameters, such as an acid gas removal unit with high efficiency is required for high sulfur content fuel.

Table 5-3 Summary of Inputs of IGCC system based on Frame 7F and 7H Gas Turbines

Description	IGCC-7FA	IGCC -7H
Gasification process Area		
Gasifier Pressure, psia	2400	2400
Gasifier Outlet Temperature, °F	615	615
Slurry Water/Coal Ratio, lb H_2O/lb Coal	0.504	0.504
Radiant Cooler Outlet Temperature, °F	1500	1500
Convective Cooler Outlet Temperature, °F	650	650
Gas Turbine Process Area		
Inlet Syngas Temperature, °F	570	570
Moisture in Fuel Gas, wt-%	28.2	28.2
Pressure Ratio	15.5	23
Turbine Inlet Temperature, °F	2,350	2,600
Compressor Isentropic Efficiency, %	80.8	82.0
Expander Isentropic Efficiency, %	92.2	91.4
Generator Efficiency, %	98.5	98.5
HRSG and Steam Cycle Area		
Steam Condition, psia/°F /°F	1450/997/997	2400/1050/1050
HRSG Stack Temperature, °F	271	271

5.2 Effects of Different Gas Turbine Combined Cycles on IGCC System

The IGCC systems with Frame 7F gas turbine combined cycle were compared to the IGCC with Frame 7H gas turbine combined cycle. The objective of this study is to find out the effects of gas turbine technology advances on IGCC system based on deterministic simulation results.

5.2.1 Input Assumptions

The input assumptions for two systems, IGCC-7FA and IGCC-7H, are summarized in Table 5-3. The Illinois No.6 coal is used in two systems. The four inputs of gas turbine process, pressure ratio, turbine inlet temperature, compressor and expander isentropic efficiency, are specified based on the corresponding specifications of 7FA and 7H combined cycles. For 7H combined cycle, the parameters for steam cycle are different from that of 7FA.

5.2.2 Results

The main outputs of the 7FA and 7H systems are compared and the results are listed in Table 5-4. The performance, emissions, and costs results for IGCC-7FA and IGCC-7H systems are compared to each other. For performance, the power output and efficiency of two systems are compared to each other. It is found that the net plant power output of IGCC-7H is 45.7% higher than the power output of IGCC-7FA system. The efficiency of IGCC-7H is also higher than that of IGCC-7FA.

For emissions, the two systems have close emissions of SO_2 and NO_x. However, the emissions of CO_2 of IGCC-7H system is about 10% lower than that of IGCC-7FA system.

For the cost comparison, the cost of electricity of IGCC-7H system is also lower than the IGCC-7FA system. The comparison of two IGCC systems based on deterministic modeling indicates that the advances in gas turbine technology can improve the efficiency of IGCC system, lower the CO_2 emissions, and lower that cost of electricity. Therefore, Frame 7H gas turbine is a promising choice for future IGCC technology improvement.

Table 5-4 Comparison of IGCC systems based on Frame 7F and 7H Gas Turbine

Description	IGCC-7H	IGCC-7FA	Relative Difference
Performance			
Coal Feed Rate, lb/hr	253,400	192,370	
Gas Turbine Net Power (1 trains), MW	291.1	192.1	
Steam Turbine Net Power, MW	173.4	132.1	
Total Auxiliary Load, MW	49.9	39.5	
Net Plant Power Output, MW	414.6	284.6	45.7%
Plant Efficiency, %	43.71	39.53	9.6%
Emissions			
SO_2 Emissions, lb/10^6Btu	0.218	0.223	-2.2%
NO_x emissions, lb/10^6Btu	0.132	0.127	3.9%
CO_2 Emissions, lb/kWh	1.53	1.69	-9.5%
Cost			
Total Direct Cost ($/kW)	805	886	
Total Indirect Costs	296	327	
Process Contingencies	91	103	
Project Contingency	209	230	
Total Plant Cost	1,402	1,545	
AFDC [b]	224	248	
Total Plant Investment	1,626	1,793	
Startup Costs and Land	42	46	
Total Capital Requirement	1,710	1,882	-9.1%
Fixed Operation Cost, $/(kW-yr)	54	66	
Incremental Variable Costs, mills/kWh	1.1	1.2	
Byproduct Credit, mills/kWh	-1.4	-1.5	
Fuel Cost, mills/kWh	9.8	10.8	
Variable operating Cost, mills/kWh	9.5	10.4	
Cost of Electricity, mills/kWh	50.0	56.1	-10.9%

[a] Fuel = Illinois No.6 Coal, Cost Year = January 2000;
[b] AFDC = Allowances for Funds used During Construction;
Fuel Cost, $/MMBT = 1.26 (Jan 1998 Dollars) (Buchanan et al., 1998)
Capital Recovery Factor = 0.1034.

6.0 SPREADSHEET MODEL OF GAS TURBINE COMBINED CYCLE

In previous chapters, the development of gas turbine model has been descried. In this chapter, a simplified spreadsheet performance model for a gas turbine combined cycle system was developed. The model is intended for incorporation into the Integrated Environmental Control Model (IECM), which has been developed by Carnegie Mellon University (CMU) under sponsorship of the U.S. Department of Energy (e.g., Rubin *et al.*, 1986, 1988, 1991, 1997; Berkenpas, *et al.*, 1999). Under subcontract to CMU, North Carolina State University has developed the performance model for the gas turbine combined cycle system. The performance model for the IECM builds upon experience from development of process simulation models of gas turbine systems in ASPEN and ASPEN Plus (Frey and Rubin, 1990a; Frey and Akunuri, 2001).

The objective of this study is to develop a performance model of simple and combined cycle gas turbine power plants. The mass and energy balance models for the simple cycle and combined cycle were implemented in an Excel spreadsheet. The method for calibrating the models is discussed and illustrated with examples based on natural gas and syngas. The sensitivity analysis of gas turbine performance based on different syngas compositions were implemented and discussed. The sensitivity of inputs of model was evaluated. The results suggested careful attention to the key sensitive inputs needed to obtain accurate estimation of gas turbine performance.

6.1 Technology Basis

A simple cycle gas turbine (SCGT) is comprised of three major components, including the compressor, combustor, and turbine. Air at ambient conditions enters the compressor. Compression takes place approximately adiabatically. Therefore, the temperature of the compressed air is higher than the ambient temperature of the inlet air. The performance of an ideal adiabatic and isentropic compressor can be calculated using straight-forward thermodynamic principles. The compressed air enters a combustor, where it is mixed with high pressure gaseous fuel. The fuel and air are burned at essentially constant pressure. The conventional fuel for SCGT systems is natural gas, which is comprised mostly of methane. However, other fuels may be burned in a gas turbine, including syngas obtained from a gasification process. Syngas typically contains carbon monoxide (CO), hydrogen (H_2), methane (CH_4), carbon dioxide (CO_2), nitrogen (N_2), and water vapor (H_2O) as the primary constituents. Syngases also may contain relatively small amounts of hydrogen sulfide (H_2S), carbonyl sulfide (COS), and ammonia (NH_3). These latter three components are significant in terms of the formation of SO_2 and NO_x emissions, but are less important in terms of calculating the mass and energy balance of the system because they comprise only a small portion of the total fuel flow rate and the total fuel heating value. The combustor typically has a small pressure drop. Therefore, the exit pressure from the combustor is slightly less than that compared to the compressor outlet.

The high pressure hot product gases from the combustor enter the turbine, or expander, portion of the SCGT system. In the turbine, the gases are reduced in pressure,

resulting in a corresponding reduction in temperature. The heat-removal process associated with expansion and cooling of the hot gases in the turbine results in an energy transfer from the gases to shaft work, leading to rotation of a shaft. In many heavy duty SCGT designs, the compressor, turbine, and a generator turn on the same shaft. The turbine must supply enough rotational shaft energy to power the compressor. The net difference between the work output of the turbine and the work input to the compressor is available for producing electricity in the generator. The ratio of compressor work to turbine work is referred to as the back work ratio.

As noted by Frey and Rubin (1991), the mass flow through a gas turbine is limited by the critical area of the turbine inlet nozzle. The critical area of the turbine inlet nozzle is a constant for a given make and model of gas turbine. The mass flow at the turbine inlet nozzle is estimated, assuming choked flow conditions, based upon the following relationship (Frey and Rubin, 1991):

$$m_{act} = m_{ref}\left(\frac{P_{act}}{P_{ref}}\right)\sqrt{\left(\frac{MW_{act}}{MW_{ref}}\right)\left(\frac{T_{ref}}{T_{act}}\right)} \qquad (6\text{-}1)$$

The reference values are determined based upon calibration to published data for gas turbine operation on natural gas. The actual values are determined based upon the desired simulated conditions.

A combined cycle gas turbine (CCGT) is comprised of a gas turbine and a steam cycle. The steam cycle consists of a heat recovery steam generator, a steam turbine, and other auxiliary parts. The exhaust gas from gas turbine flows through a series of heat exchangers in HRSG. The high temperature exhaust gas from the gas turbine is cooled

through the heat exchangers to heat superheated steam, saturated steam, and boiler feedwater via a series of heat exchangers. The cooled flue gas is exhausted from the stack. A substantial portion of the steam is sent to the steam turbine and expanded through several stages. The shaft work is converted into electricity by the generator. The combined cycle system overall performance model is presented in this section.

6.2 Simple Cycle Gas Turbine Mass and Energy Balance Model

The SCGT mass and energy balance model is based upon the air-standard Brayton cycle, as described in Wark (1983). The mass and energy balance for each of the following components are presented in the following sections: (1) compressor; (2) combustor; (3) turbine; and (4) net power output. The calculation of overall SCGT performance is also discussed. Part of the equations used in the model is listed here. The complete model and the symbols used in the model are described in Appendix D.

6.2.1 Compressor

The compressor consists of three stages. From each stage, a fraction of air is extracted for use in cooling various stages of the turbine. The conceptual for compressor is shown in Figure 6-1. The outlet pressure of a compressor is specified by multiplying the pressure ratio and the inlet pressure.

The pressure ratio for each stage (i=1 to 3) is estimated as:

$$r_{p,i} = (r_p)^{0.33} \tag{6-2}$$

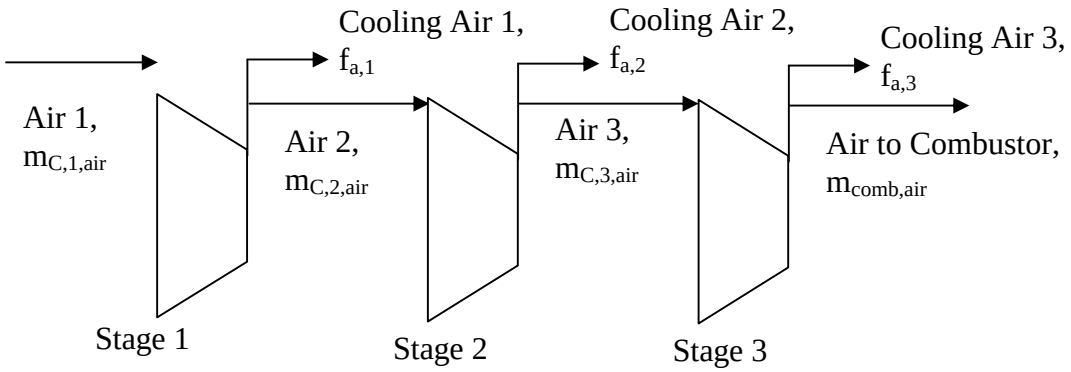

Figure 6-1 Simplified Diagram of a Three-Stage Compressor

The cooling air fractions split from three stages are specified as $f_{a,1}$, $f_{a,2}$, and $f_{a,3}$ of the total air flow rate respectively. Therefore, the air flow rates through three stages and the combustor are:

$$m_{C,1,air} = m_{air} \tag{6-3}$$

$$m_{C,2,air} = (1- f_{a,1})\, m_{air} \tag{6-4}$$

$$m_{C,3,air} = (1- f_{a,1}- f_{a,2})\, mair \tag{6-5}$$

$$m_{comb,air} = (1- f_{a,1}- f_{a,2} - f_{a,3})m_{air} \tag{6-6}$$

For each stage, the outlet temperature is estimated. To take into account the irreversibilities in an actual compressor, based upon the estimated enthalpy for the actual compressor outlet air, the actual outlet temperature is estimated based upon a regression model:

$$T_{C,i,out} = -9\times10^{-5}h_{C,i,out} + 1.0563h_{C,i,out} - 9.0996 \tag{6-7}$$

6.2.2 Combustor

In general, the syngas into the combustor contains carbon monoxide (CO), hydrogen (H_2), methane (CH_4), carbon dioxide (CO_2), nitrogen (N_2), and water vapor (H_2O). The mole fraction of each of the six major components is known and the syngas heating value can be estimated based upon data reported by Flagan and Seinfeld (1988). Air is a mixture primarily of oxygen and nitrogen. The major products of combustion are carbon dioxide, water vapor, nitrogen, and excess oxygen. Gas turbine combustors operate with a significant amount of excess air. The mass balance for the case with excess air can be developed based upon the stoichiometric mass balance by introducing a new variable for the fraction of excess air, e_a. The fraction of excess air is given by:

$$e_a = \frac{\textit{(Total air - stoichiometric air)}}{\textit{(Stoichiometric air)}} \tag{6-8}$$

The mass balance for excess air is:

$$[y_{CO}CO + y_{H_2}H_2 + y_{CH_4}CH_4 + y_{CO_2}CO_2 + y_{N_2}N_2 + y_{H_2O}H_2O] + a(1+e_a)O_2 + 3.76a(1+e_a)N_2 \rightarrow bCO_2 + cH_2O + d'N_2 + (a)(e_a)O_2$$

The enthalpy for syngas, air, and combustion product are estimated and the solution for the excess air fraction is given by:

$$e_a = \frac{H_{fuel} + H_{air,stoich} + \Delta h_{r,fuel} - H_{products,stoich}}{a\,[3.76\{H_{N_2}(T_{T,in}) - H_{N_2}(T_{C,out})\} + \{H_{O_2}(T_{T,in}) - H_{O_2}(T_{C,out})\}]} \tag{6-9}$$

After the computation of excess air, the molar fraction per mole fuel gas of exhaust gas of combustor can be estimated. Based Equation (6-1), the mass flow of exhaust gas out of the combustor or at the turbine inlet can be estimated.

6.2.3 Turbine

The energy balance for the turbine is estimated in a manner similar to that for the compressor. However, a key difference is that the exhaust gas is not air, and therefore the thermodynamic data for air are not strictly applicable for use with the turbine. In addition, pressure losses in the combustor and the turbine back pressure must be accounted for when estimating the work capability of the turbine. The turbine consists of three stages. The cooling air from the compressor is injected into the outlet flow from each stare. The conceptual diagram is shown in Figure 6-2.

The pressure at the turbine outlet is given by:

$$P_{T,out} = P_a + \Delta p_{back} \tag{6-10}$$

Therefore, the pressure ratio for the turbine is given by:

$$r_{p,turb} = \frac{P_{T,in}}{P_{T,out}} = \frac{(P_a r_P - \Delta p_{comb})}{(P_a + \Delta p_{back})} \tag{6-11}$$

The turbine consists of three stages. The pressure ratio for each stage is same and estimated as:

$$r_{p,turb,i} = (r_{p,turb})^{0.33} \tag{6-12}$$

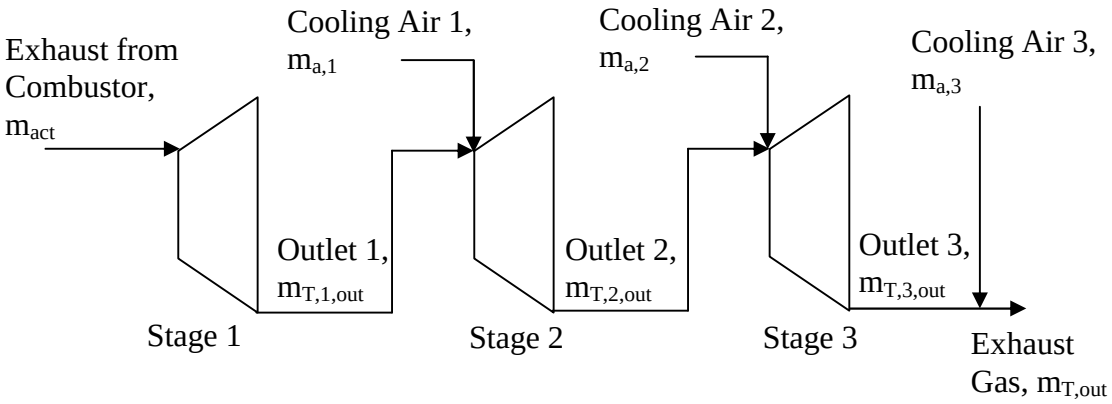

Figure 6-2 Simplified Diagram of a Three-Stage Turbine

For each stage of the turbine, the cooling air is injected and mixed with the exhaust from the previous stage. Therefore, the mass flow rate through each stages and at the turbine outlet are:

$$m_{T,1,out} = m_{act} \tag{6-13}$$

$$m_{T,2,out} = m_{act} + m_{air}\, f_{a,1} \tag{6-14}$$

$$m_{T,3,out} = m_{act} + m_{air}\, (f_{a,1} + f_{a,2}) \tag{6-15}$$

$$m_{T,out} = m_{act} + m_{air}\, (f_{a,1} + f_{a,2} + f_{a,3}) \tag{6-16}$$

For each stage, the turbine outlet temperature is calculated. The isentropic turbine work output is given by the difference between the enthalpies of the inlet and outlet under isentropic conditions. For each stage, the outlet temperature is estimated based on the enthalpy of exhaust gas at the outlet of a stage:

$$T_{T,i,out} = -3.2769 \times 10^{-5}\, h_{T,i,out}{}^{2} + 0.9347\, h_{T,i,out} + 17.3221 \tag{6-17}$$

After each stage, the cooling air is mixed with the exhaust flow. The mixture temperature is estimated based on the specific heat and the mass flow of the streams in the mixture.

6.2.4 Net Power Output

The net shaft work per mole fuel is estimated based on the differences in work between compressor and turbine. Furthermore, the generator is subject to inefficiencies. The generator efficiency η_s can be calibrated to calculate to the actual generator output. Therefore, the actual shaft work is estimated as:

$$Q_S = (\Delta h_T - \Delta h_C)\eta_s \, M_{fuel} \tag{6-18}$$

where the shaft work is in units of BTU/hr.

The total energy input of the system is estimated based on the heating value and the mass flow of fuel:

$$Q_{fuel} = m_{fuel} \, LHV \tag{6-19}$$

The simple cycle efficiency is computed as:

$$\eta_{SC} = \frac{Q_S}{Q_{fuel}} \tag{6-20}$$

The net electricity produced in the simply cycle is estimated to be:

$$W_{SC} = 2.93\times10^{-7}\,(\text{MWh/Btu})Q_s\,(\text{Btu/hr}) \tag{6-21}$$

where the net electricity is in units of MW.

6.3 Combined Cycle Gas Turbine Mass and Energy Balance Mode

A combined cycle consists of a gas turbine, HRSG, and a steam cycle. The mass and energy model has been introduced in previous section. In a combined cycle, the exhaust from the gas turbine is sent to HRSG for heat recovery. For natural gas and syngas fired gas turbine combined cycle, the energy input to HRSG is estimated by different equations. For a natural gas fueled combined cycle, the total energy input to HRSG or the steam cycle is:

$$Q_{H,NGCC} = \Delta h_H M_{fuel} \tag{6-22}$$

Where the energy input is in units of BTU/hr.

For a combined cycle used in IGCC plant, the total heat input to HRSG should take into account heat obtained from high temperature and low temperature cooling of syngas between the gasifier outlet and the gas turbine inlet. In addition, the thermal energy due to steam or water injection, for purposes of syngas humidification, should be deducted. A significant fraction of the thermal energy from the gas cooling is recovered to generate steam and hot water for the steam cycle. Buchanan *et al.* (1998) mentioned that the high pressure saturated steam is generated in the gas cooler and is joined with the main steam supply. A similar process for syngas cooling is also described by Bechtel *et al.* (2002). Since there is some heat loss in the process of syngas cooling and part of heat is used in other process, it is assumed that 90% of the heat from syngas cooling is recovered in the steam cycle. This assumption is discussed in Section 6.4.

$$Q_{H,IGCC} = \Delta h_H M_{fuel} + f_{cooling} \Delta h_{cooling} M_{fuel} - h_{moisture} \tag{6-23}$$

The heat from gas cooling is computed based on the clean dry syngas composition and the temperature drop during cooling.

The power generated from the steam turbine in the combined cycle is dependent on the heat rate of the steam cycle, HR:

$$W_{ST} = \frac{1000\,Q_H}{HR} \tag{6-24}$$

where the power is in units of MW. Therefore, the total energy output from the combined cycle is the sum of the electricity generated from the simple cycle gas turbine and that of the steam turbine in the combined cycle.

$$W_{CC} = W_{SC} + W_{ST} \tag{6-25}$$

The total system energy input is computed based on the simple cycle output and simple cycle efficiency. Therefore, the combined cycle efficiency is computed as:

$$\eta_{CC} = \frac{W_{CC}\,\eta_{SC}}{W_{SC}} \tag{6-26}$$

6.4 Calibration of Gas Turbine Performance Model

The calibration of the gas turbine model of 7FA+e heavy duty gas turbines fueled with natural gas and syngas is implemented in this study. The air extraction from the compressor is assumed to be 12%. The compressor is divided into three stages. The air extraction fractions from three stages are 3%, 3%, and 6% respectively (Frey and Rubin,

1991). The ambient condition is 288 K (59 ^{o}F) and 14.7 psia, which is the International Standard Organization (ISO) conditions for the gas turbine industry (Brooks, 2000).

6.4.1 Natural Gas

The natural gas is assumed to be 100% CH_4. In Table 6-1, the main specifications for the gas turbine and steam cycle are listed. The reference mass flow at the inlet of turbine, adiabatic compressor efficiency, adiabatic turbine efficiency, and the heat rate of steam cycle are selected during calibration of the model. In order to calibrate the model, selected parameters were varied in order to closely match published values for key outputs of system performance. Specifically, the adiabatic efficiency for the turbine and compressor were varied in order to match the published gas turbine exhaust temperature and simple cycle efficiency respectively. The reference mass flow at the turbine inlet was varied in order to match the published power output of gas turbine. The exhaust temperature affects the heat recovery in HRSG. The heat rate of the combined cycle was varied to match the published value for combined cycle efficiency because the heat rate of the steam cycle affects the power output of steam turbine. Thus, theses four unknown parameters were varied to match the reference values of four outputs, including simple cycle power output, simple cycle efficiency, exhaust temperature, and combined cycle efficiency, exactly. Therefore, there may not be an exact match for other outputs, such as the exhaust mass flow and the combined cycle power output.

Table 6-1 Main Input Specifications of the Combined Cycle Model based on Natural Gas

Description	Value
Ambient Pressure, psia	14.7
Ambient Temperature, K	288
Compressor Pressure Ratio	15.7[a]
Combustor Pressure Drop, psia	4
Turbine Back Pressure, psia	2
Turbine Inlet Temperature, K	1600[a]
Turbine Inlet Reference Mass Flow, lb/hr	3,159,000 [b]
Cooling Air Extraction Fraction, %	12
Adiabatic Compressor Efficiency	0.9285[b]
Adiabatic Turbine Efficiency	0.8485[b]
Shaft/Generator Efficiency	0.98
Steam Cycle Heat Rate, BTU/kWh	8960[b]
HRSG Outlet Temperature, ^{o}F	238[c]
Fuel Composition, vol%	**Value**
CH_4	100

[a] Brooks, F.J. (2000), GER-3567H, GE Power Systems
[b] Values selected based on a calibration process
[c] Bechtel *et al.* (2002). The flue gas temperature is 238 ^{o}F in a 7FA+e gas turbine combined cycle

The curves showed in Figure 6-3 represent the calibration process for selecting the adiabatic compressor efficiency and turbine efficiency of a simple cycle gas turbine model. For a GE 7FA+e gas turbine, the published values are an exhaust temperature of 1,119 ^{o}F, a simple cycle LHV efficiency of 36.47%, and a power output of 171.7 MW (Brooks, 2000). From Figure 10(a), the adiabatic turbine efficiency of 0.8485 was selected to obtain the desired exhaust temperature. To obtain the simple cycle efficiency of 36.47%, the adiabatic compressor efficiency of 0.9285 was selected. After selecting the adiabatic efficiencies for the turbine and compressor, the reference mass flow at the turbine inlet was adjusted to obtain the desired power output. The estimated power output for simple cycle is 171.7 MW.

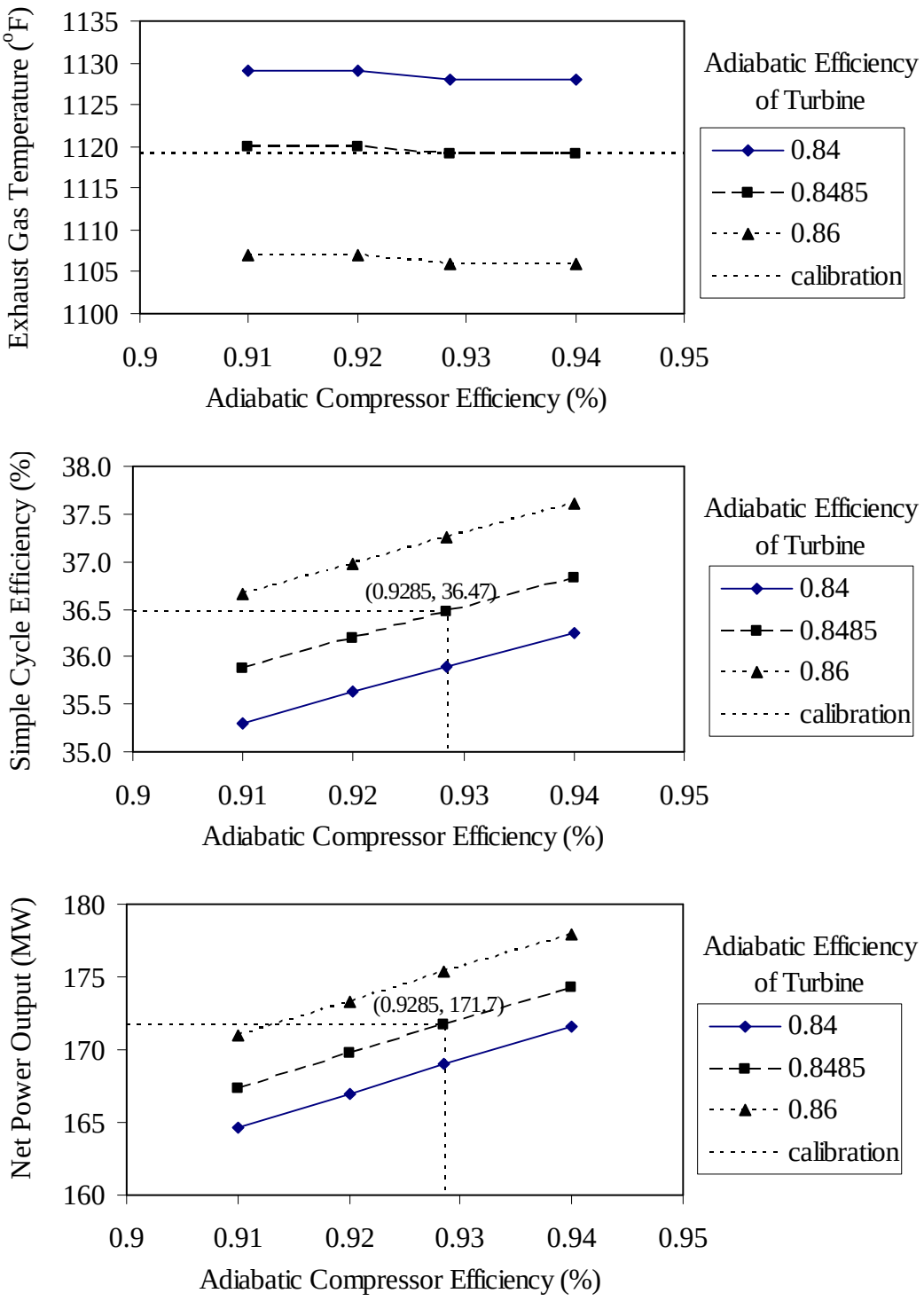

Figure 6-3 Calibration of Simplified Gas Turbine Model based on Natural Gas – plot s of (a) Exhaust Temperature, (b) Simple Cycle Efficiency, and (c) Simple Cycle Output versus Adiabatic Compressor Efficiency of Gas Turbine.

Table 6-2 Main Results and Comparison to Published Value based on Natural Gas

Variables	Predicted	Published Value [a]	Relative Difference
Simple cycle heat rate, BTU/kWh	9,360	9,360	0
Gas Turbine Power Output, MW	171.7	171.7	0
Air Flow, lb/hr	3,499,800	3,431,000 [b]	2.0%
Exhaust Flow, lb/hr	3,574,000	3,543,000	0.9%
Exhaust Temperature, ^{o}F	1,119	1,119	0
Combined Cycle Power Output, MW	266.0	262.6	1.3%
Combined cycle efficiency, %LHV	56.5	56.5	0

[a] Brooks, F.J. (2000), GER-3567H, GE Power Systems.
[b] Matta, *et al.* (2000), GER-3935B, GE Power Systems

Results based on natural gas match the published data reasonably well, as shown in Table 6-2. The predicted values for the simple cycle heat rate, simple cycle power output, exhaust temperature, and combined cycle efficiency are exactly the same as the published values because of the calibration process. The relative differences between predicted and reported gas turbine exhaust flow and combined cycle power output are only approximately one to two percent. The results indicate the gas turbine model can predict the performance of the actual gas turbine well.

6.4.2 Syngas

For the case study of syngas, a design study for a nominal 1,100 MW coal IGCC power plant was selected as the basis for calibration (Bechtel *et al.*, 2002). Four GE 7FA+e combustion turbines are used in this plant. The gas turbines produce 840 MW and the steam turbines produce 465.2 MW. Based on this report, he heat rate for a 7FA+e gas turbine simple cycle fired with syngas is 8552 Btu/kWh. The exhaust flow for a single gas turbine of a single 7FA+e gas turbine unit is 3,982,200 lb/hr. The stack exhaust

Table 6-3 Main Input Specifications of the Combined Cycle Model based on Syngas

Description	**Value**
Ambient Pressure, psia	14.7
Ambient Temperature, K	288
Compressor Pressure Ratio	15.7[a]
Combustor Pressure Drop, psia	4
Turbine Back Pressure, psia	2
Turbine Inlet Temperature, K	1600[a]
Turbine Inlet Reference Mass Flow, lb/hr	3,612,000 [b]
Cooling Air Extraction Fraction, %	12
Adiabatic Compressor Efficiency	0.774[b]
Adiabatic Turbine Efficiency	0.872[b]
Shaft/Generator Efficiency	0.98
Steam Cycle Heat Rate, BTU/kWh	9,150
HRSG Outlet Temperature, ^{o}F	238 [c]
Fuel Composition, vol%	**Value** [c]
CH_4	0.53
CO	27.75
H_2	19.98
CO_2	8.59
N_2 + Ar	1.58
H_2O	41.57
LHV, Btu/lb	2,831
Temperature, ^{o}F	530

[a] Brooks, F.J. (2000), GER-3567H, GE Power Systems
[b] Values selected based on a calibration process
[c] Bechtel, et. al, (2002).

temperature is 238 ^{o}F. The power outputs for a single gas turbine combined cycle is 326.3MW, including 210.0MW from gas turbine and 116.3 MW from steam turbine. The efficiency of 7FA gas turbine combined cycle is computed based on the heat input of fuel is 62%. The main inputs in the spreadsheet model are listed in Table 6-3.

The same calibration method used in the case of natural gas is applied to the case of syngas. For GE 7FA+e gas turbine based on syngas, the estimated key measures of performance are a simple cycle LHV efficiency of 39.93%, and a power output of 210 MW. The constraint for exhaust temperature is less than 1,120 ^{o}F (Holt, 1998). For

convenience, the exhaust temperature is assumed to the same as that of natural gas, which is 1,119^{o}F. An adiabatic turbine efficiency of 0.872 and an adiabatic compressor efficiency of 0.774 were selected to obtain the reference values for the exhaust temperature and the simple cycle efficiency, respectively. The reference mass flow at the turbine inlet was adjusted to obtain the desired power output.

To calibrate the heat rate of steam cycle for a gas turbine combined cycle fires with syngas, the heat input to the steam cycle need to be estimated first. As described in Section 6.2, the heat content of the steam used for syngas moisturization should be deducted from the total heat input to HRSG since it is not available for purpose of power production from the steam turbine. The pressure of steam used for injection in a 7FA+e gas turbine combined cycle is 400 psi (Amick *et al.*, 2002). The enthalpy of saturated steam at 400 psia is 1205.5 Btu/lb (Wark, 1983).

Another part of heat need to be estimated is the heat recovered from high temperature and low temperature gas cooling processes in an IGCC system. In the design study used as the calibration basis, an E-Gas (Destec) gasifier is used (Bechtel *et al.*, 2002), which is also an entrained-flow gasifier. The typical temperature of syngas out of the gasifier is 1950 ^{o}F (Buchanan, *et al.*, 1998). After gas cooling, the syngas is sent to the gas turbine at a temperature of 530 ^{o}F (Bechtel *et al.*, 2002). A significant faction of the sensible heat in the hot gas is recovered by producing high temperature saturated steam, which is sent to the steam cycle. Thus, it can be assumed that a fraction of the sensible heat of cooling syngas from 1,950 ^{o}F to 530 ^{o}F is recovered by the steam cycle. However, the value of the fraction of heat recovery is not reported in the design study.

Table 6-4 Main Results and Comparison to Published Value based on Syngas

Variables	Predicted	Published Value [a]	Relative Difference
Simple cycle heat rate, Btu/kWh	8,550	8,552	0
Gas Turbine Power Output, MW	210	210	0
Air Flow Rate, lb/hr	3,381,000	N/A	--
Exhaust Flow, lb/hr	4,014,700	3,982,200	0.8%
Exhaust Temperature, ^{o}F	1,119	<1,120 [b]	--
Steam Turbine Power Output, MW	116.5	116.3	-0.1%
Combined Cycle Power Output, MW	326.4	326.3	0.0%
Combined cycle efficiency, %LHV	62.0	62.0	0

[a] Bechtel, *et al.* (2002)
[b] Holt, N. (1998), 1998 Gasification Technologies Conference

Therefore, the selection of the fraction value is based on the model results of a similar Texaco gasifier-based IGCC system in ASPEN Plus and the result of the steam cycle heat rate after calibration. The fraction of heat recovered from syngas cooling in the ASPEN model is about 0.9. The reference value of the steam cycle heat rate is generally 9,000 Btu/kWh (Buchanan *et al.*, 1998). Thus, the initial value of the heat recovery fraction is assumed to be 0.9. The total heat input into the steam cycle is estimated. To match the published combined cycle efficiency, a steam cycle heat rate of 9,150 Btu/hr is selected, which is close to 9,000 Btu/kWh. Therefore, the fraction of 0.9 is considered to be a reasonable value for estimating heat recovery from gas cooling in steam cycle.

In Table 6-4, the model results after calibration are listed. The predicted values match the reference values well. The result of the combined cycle power output is very close to the published values. It also indicates the values for the heat recovery fraction and the steam cycle heat rate are reasonable.

6.5 Discussion of Calibration Results

In this section, the calibration results of the gas turbine model based on natural gas and syngas are compared and discussed. In the natural gas-fired gas turbine combined cycle, the turbine inlet reference mass flow is 3,159,000 lb/hr. In the syngas-fired gas turbine combined cycle, the turbine inlet reference mass flow is 3,612,000 lb/hr. The difference of turbine inlet mass flows for the two cases is due to the difference in fuel type. According to Brdar and Jones (2000), gas turbines fired on syngas have significantly larger flow rate compared to those fired on natural gas. This is due to the low heating value of syngas compared to natural gas and of the composition of the the combustion product passing through the turbine. To obtain same turbine inlet temperature as natural gas, the flow rate of syngas is much higher than that of natural gas. Therefore, the estimated difference between the turbine inlet reference flow rate of natural gas and syngas is reasonable. The exhaust gas flow rate is mainly decided by the calibration result of the turbine reference mass flow. The results for the exhaust gas flow of two case studies both match the related published values well. This indicates that the calibration results for turbine inlet mass flow for the two fuels are reasonable.

For natural gas, the adiabatic efficiencies for the compressor and turbine are 0.9286 and 0.8485 respectively. The heat rate of the steam cycle is 8,960 Btu/kWh. For syngas, the adiabatic efficiencies for the compressor and turbine are 0.774 and 0.872 respectively and the calibration result for the steam cycle heat rate is 9,150 Btu/kWh. Compared to the case of natural gas, there is a significant increase of the flow rate of syngas. However, the air flow to the compressor for the syngas case is 3,381,000 lb/hr,

which is lower than that of the natural gas case, 3,499,800 lb/hr. Since there is less air flowing through the compressor of the syngas case, the efficiency of the compressor for the syngas case is lower than that of natural gas. Conversely, for the syngas case, there is a larger mass flow through the turbine than for the natural gas case, which is associated with the slightly higher adiabatic efficiency for the turbine. The results of the steam cycle for two cases are very close and thus are approximately the same.

When using the gas turbine combined cycle model as part of the IECM model, the user should pay attention to the heating value of the syngas. For example, steam injection has a significant effect on the heating value of syngas. This in turn influences the power output of the gas turbine. Steam injection will increase the power output of the gas turbine (Mathuousakis, 2002; Brdar and Jones, 2000). Therefore, if there are substantial differences in moisture fraction and the heating value of syngas, the model may need to be recalibrated to obtain reasonable power output.

Future gas turbine development mainly includes higher firing temperature, higher pressure ratio, and greater capacity. Therefore, the specifications for firing temperature, pressure ratio, and the turbine inlet mass flow should be updated and the model recalibrated for these data changes.

6.6 Sensitivity Analysis of Different Syngas Compositions and Inputs

In this section, sensitivity analysis is conducted to evaluate the effects of different sygnas compositions. The effects of different syngas compositions based on difference moisture fraction and CO_2 removal percentages on gas turbine performance are investigated. The syngas in the calibration case was selected as a basis. Other four syngas

compositions were obtained by changing moisture fraction and removed CO_2. Another part is about the effects of different published syngas compositions without CO_2 removal on the performance of gas turbine. The syngas compositions were input to the gas turbine model and the main performance outputs of gas turbine combined cycle were compared and analyzed. Therefore, the purpose of this study is to find out how the syngas compositions changes affect the gas turbine performance and what is the general rule of the change of gas turbine performance due to different syngas composition. It can be used to evaluate the feasibility of the gas turbine model for different syngas composition.

In IGCC systems with CO_2 removal, a water-gas shift process is used to convert carbon monoxide in the syngas to carbon dioxide. The CO_2 is then removed using a separation process. After CO_2 is separated, sygnas rich in hydrogen is sent to the gas turbine combustor. In the base, the saturated syngas composition without CO_2 removal used in the calibration case (Bechtel, ***et. al***, 2002) is used as the basis for syngas composition prior to saturation or any additional treatment. For case 1, the same dry clean syngas composition as the base case is used, while the moisture fraction is 30% and it is 41.2% in the base case. For case 2 to case 4, it is assumed that 95% CO in the same cleaned syngas is converted into CO_2 in the shift reaction. Then three removal percentages of CO_2, 85%, 90%, and 95%, are considered in three cases respectively. In case 2 to 4, the saturated moisture fraction is also 30%. The main outputs for base case and other cases are listed in Table 6-5. The effects of different moisture fraction and different CO_2 removal on the gas turbine performance are discussed respectively.

Table 6-5 Effects of Different Syngas Compositions on Performance of Gas Turbine Combined Cycle

Saturated Syngas Composition, vol%	Base Case [a]	Case 1: No CO_2 Removal	Case 2: 85% of CO_2 Removal	Case 3: 90% of CO_2 Removal	Case 4: 95% CO_2 Removal
CH_4	0.53	0.63	0.67	0.69	0.71
CO	27.75	33.25	1.76	1.82	1.88
H_2	19.98	23.94	58.90	60.83	62.89
CO_2	8.59	10.29	6.66	4.59	2.37
N_2+Ar	1.58	1.89	2.00	2.07	2.14
H_2O	41.57	30	30	30	30
Total	100	100	100	100	100
Fuel LHV	2831 Btu/lb (144 Btu/scf)	3327 Btu/lb (173 Btu/scf)	6168 Btu/lb (168 Btu/scf)	6910 Btu/lb (174 Btu/scf)	7856 Btu/lb (180 Btu/scf)
Air Flow Rate, lb/hr	3,381,000	3,539,000	3,677,000	3,710,000	3,743,000
Fuel Flow Rate, lb/hr	634,000	523,100	282,400	250,800	219,600
Heat Input to Gas Turbine, 10^6Btu/hr	1,795	1,740	1,742	1,733	1,725
Exhaust Flow, lb/hr	4,015,000	4,062,000	3,959,000	3,961,000	3,962,700
Steam Injection for Moisturization, lb/hr	237,700	138,900	142,800	137,600	132,500
Exhaust Temp., ^oF	1,119	1,114	1,112	1,111	1,111
Gas Turbine Power Output, MW	210.0	193.1	189.5	186.5	183.6
Simple Cycle Efficiency, %LHV	39.93	37.88	37.14	36.74	36.34
Heat Input to HRSG, 10^6Btu/hr	983	967	977	975	973
Steam Turbine Power Output, MW	116.5	126.5	127.1	127.6	128.0
Combined Cycle Power Output, MW	326.4	319.6	316.6	314.1	311.7
Combined Cycle Efficiency, % LHV	62.08	62.69	62.06	61.87	61.68

[a] Bechtel et al. (2002).

6.6.1 Effects of Moisture Fraction

The effects of moisture fraction can be evaluated by comparing the base case and case 1 since the only difference of the two syngas compositions is the moisture fraction. More moisture fraction in the base case leads lower heating value of syngas compared to that of case 1. The heating value of syngas has influence in the power output of gas turbine. In Anand *et al.* (1996), the effects of two syngas with different heating values on

IGCC performance were evaluated. The two syngas are based on the same clean syngas compositions, while the lower heating value has more moisture than the higher heating value sygnas. This situation is similar to the two syngas in base case and case 1. Therefore, the relative difference of syngas heating values and the gas turbine power outputs for base case and Case 1 are compared to that of Anand *et al.* (1996), which is listed in Table 6-6. The smaller related decrease in heating value for the base case and case 1 produced a smaller relative change in power output when compared to the results of Anand *et al.* (1996), which appears to be reasonable and consistent. When the moisture fraction decreases, the heating value of syngas increases. To reach certain firing temperature, the requirement for syngas decreases when the energy content of syngas increases. Under the same flow rate constraint of the turbine first nozzle, the air requirement increases with the flow rate of syngas decreasing. That leads to the power consumption of the compressor increasing. Therefore, the power outputs of gas turbine decrease with syngas heating value increasing. In a summary, a gas turbine fired with higher heating value fuel will have lower power output than that fired lower heating value fuel. This conclusion was verified by the results of the simulation. It is also consistent with the studies by others (Brdar and Jones, 2000; Anand, *et al.*, 1996; and Doctor *et al.*, 1996).

Difference in moisture fraction also caused the difference in the steam turbine performance. The steam turbine power output of case 1 is higher than that of base case. Less moisture fraction means the less steam injection into the cleaned syngas and less heat deduction from the steam cycle. From the base case to Case 1, the decrease in the heat deduction is 119×10^6 Btu/hr, while the decrease in the heat input is only to HRSG,

Table 6-6 Effects of Fuel Heating Values on Gas Turbine Power Output

	Base Case and Case 1		Anand et al. (2000)	
	LHV, Btu/scf	Gas Turbine Power Output, MW	LHV, Btu/scf	Gas Turbine Power Output, MW [a]
Syngas 1	144	210	120	112%
Syngas 2	173	193.1	150	100%
Relative Difference	20%	-8%	25%	-11%

[a] The gas turbine power outputs are represented as fraction with the power output of syngas 2 as basis. The relative difference is based on values of syngas 1.

16×10^6 Btu/hr. Therefore, the net energy used for power production by the steam turbine in case 1 is 103×10^6 Btu/hr higher than the base case, which leads to more power output of the steam turbine in case 1. The combined cycle efficiency of case 1 is higher than that of base case. The combined cycle efficiency is decided by the total heat input to the gas turbine and the total combined cycle power output. The difference of the heat input to the gas turbine in case 1 is –3.1% compared to the base case, while the difference of the combined cycle power output is –2.1%. Therefore, the efficiency of the combined cycle increase. The reason related is too complicated to explain because it is related to not only the heating value of the syngas, but also the different composition of combustion products, which is related to the steam cycle power output.

In a summary, the effects of moisture change caused the change of syngas heating value. Actually, the different heating value is the direct reason of different gas turbine performance. Another effect of moisture change is on the steam turbine performance because different moisture fraction means different steam injection from the steam cycle, which affects the net energy used for producing power in the steam cycle.

6.6.2 Effects of CO_2 Removal

Comparing Case 1 and Case 4, the difference is that the syngas without CO_2 removal is used in Case 1 and the syngas with 95% CO_2 removal in Case 4. The case 4 in this study is similar to the glycol case in Doctor *et al.* (1996), which is also 95% CO_2 removal. The system in the report was a KRW Oxygen-Blown IGCC plant with two GE 7F gas turbines. The power output of two gas turbines is 298.8 MW in the case without CO_2 removal and it is 284.1 MW in the glycol case. The gas turbine output of the glycol case is 4.7% less than that of the case without CO_2 removal. The relative difference of the gas turbine power outputs of Case 1 and Case 4 is – 4.9%. The two difference values are very close. It indicates that the results of this study are reasonable and consistent with the result of Doctor *et al.* (1996).

For case 1 and case 4, it was found that the heating values in volume basis (Btu/scf) for two syngas are almost same, while the heating value in mass basis of syngas in case 1 is much lower than that in case 4, which is due to the unique thermodynamic features of hydrogen. In Anand *et al.* (1996), the decrease in syngas heating value is obtained by adding moisture. Since moisture is not combustible matter, the heating value on mass basis have the same change trend as the heating value on volume basis. However, hydrogen is combustible and hydrogen has a low heating value of 273 Btu/scf on a volume basis but a very high heating value of 51,872 Btu/lb on a mass basis (Moliere, 2002). Therefore, increase in hydrogen composition increases the heating value of syngas in mass basis, while the heating value in volume basis of syngas has no big change. The heating value in mass basis has predominant effects on the energy performance of gas turbine (Moliere, 2002). Therefore, the conclusion is gas turbine

fueled with syngas with lower heating value on mass basis has higher power output than that fueled with higher heating value on mass basis syngas. The comparison results of case 1 and case 4 are consistent with the comparison results of base case and case 1. The simple cycle efficiency of the case 4 is lower than the case 1 is due to the lower power output of gas turbine of case 4. The steam turbine power output of case 4 is higher than that of case 1, because the steam injection of case 4 is lower than that of case 1 and the energy input to HRSG of case 4 is 7×10^6 Btu/hr higher than that of case 1. The combined cycle efficiency of case 4 is lower than that of base case due to the big decrease of gas turbine power outputs in case 4.

Comparing case 2 to 4 with different CO_2 removal percentages, the exhaust flows are almost same for three cases. The hydrogen content in syngas increases with the removal percentages, which leads to the heating values of fuel increasing both on mass basis and volume basis. The simple cycle efficiency is related to the gas turbine power output and the heat input, which also decreases with the CO_2 removal fraction increasing due to the power output of gas turbine decrease. For the steam turbine, the power output increase with the CO_2 removal fraction increasing. The moisture injection decreases with the syngas flow rate decreases since the syngas have the same moisture fraction. The energy deduction due to moisture injection decreases. It leads to the steam turbine power outputs increasing from case 2 to case 4. The power output of combined cycle still decrease due to the power output decrease of gas turbine. That also leads to the efficiency of combined cycle decrease a little bit with the CO_2 removal fraction increasing.

6.7 Sensitivity Analysis of Inputs

The sensitivity analysis is implemented to evaluate the effects of the change in inputs on the main outputs of the gas turbine model. The objective of this section is to provide information about the questions: (1) what kinds of change will be caused by the change of an input?; (2) what is the most sensitive, moderate sensitive, or little sensitive inputs of this model?. The answers of these questions are helpful to evaluate the accuracy of the estimates based on the change of the sensitive inputs values.

The effects of inputs on three outputs are evaluated, including gas turbine (GT) power output, simple cycle efficiency, and combined cycle efficiency. The same syngas composition of the calibration case is selected. There are eight inputs that are evaluated based on the outputs of gas turbine (GT) power output and simple cycle efficiency, including adiabatic turbine efficiency, adiabatic compressor efficiency, air cooing fraction, ambient temperature, ambient pressure, compressor pressure drop, turbine back pressure, generator efficiency. The values of inputs are changed and the relative differences in the inputs compared to the corresponding values of the calibration case are computed. Only one input value is changed at one time and others keep constant. The relative changes in the outputs are computed based on the corresponding data in the calibration case. For the combined cycle efficiency, two more inputs besides the above inputs are studied, which are the steam cycle heat rate and HRSG outlet temperature. The effects of the inputs variation on the three outputs are characterized by the following diagrams in Figure 6-4 to 6-6.

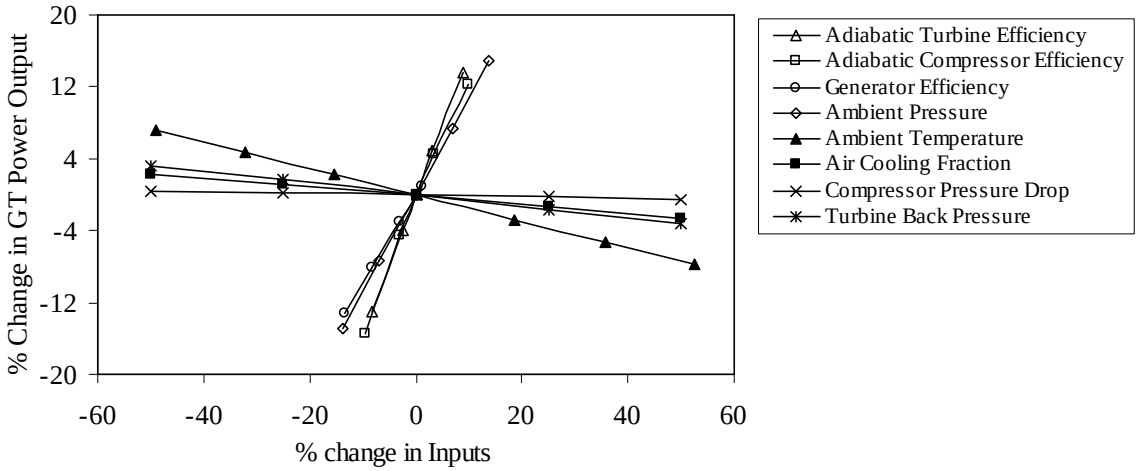

Figure 6-4 Changes in Inputs versus Changes in Gas Turbine (GT) Power Output

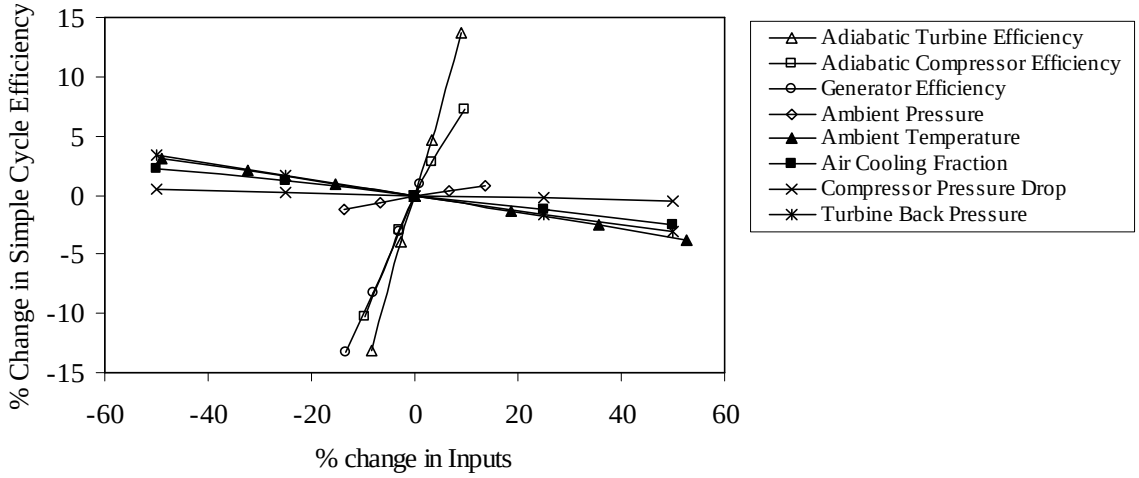

Figure 6-5 Changes in Inputs versus Changes in Simple Cycle Efficiency

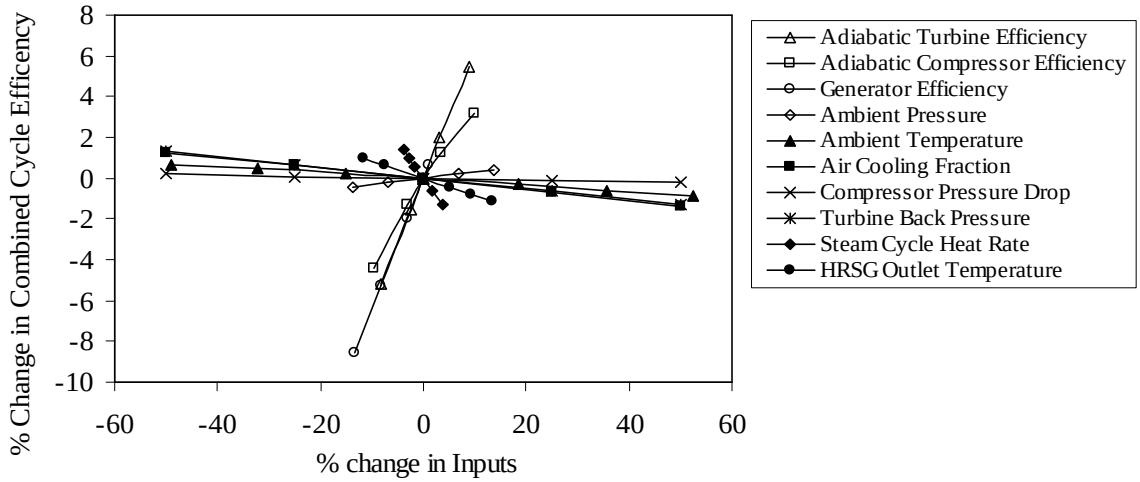

Figure 6-6 Changes in Inputs versus Changes in Combined Cycle Efficiency

Table 6-7 Slopes of Each Line for Effects of Inputs Changes on Outputs

Inputs	Gas Turbine Power	Simple Cycle Efficiency	Combined Cycle Efficiency
Adiabatic Turbine Efficiency	1.55	1.55	0.62
Adiabatic Compressor Efficiency	1.43	0.90	0.39
Generator Efficiency	1.00	1.00	0.63
Ambient Pressure	1.09	0.08	0.03
Air Cooling Fraction	-0.05	-0.05	-0.03
Ambient Temperature	-0.15	-0.07	-0.02
Compressor Pressure Drop	-0.01	-0.01	-0.004
Turbine Back Pressure	-0.06	-0.06	-0.03
Steam Cycle Heat Rate			-0.36
HRSG Outlet Temperature			-0.08

In order to quantify the effects of inputs change on outputs change, the slopes of each line in Figure 6-4 to 6-6 are listed in Table 6-7. The positive slope value means the change trend of input will cause same change trend in outputs and the negative slopes means opposite change in output. The results shown in Table 6-7 indicate 1% increase of adiabatic turbine efficiency will cause 1.55% increase in the gas turbine, 1.55% increase in the simple cycle efficiency, and 0.62% increase in the combined cycle efficiency. The inputs of adiabatic turbine efficiency, the adiabatic compressor efficiency, and generator efficiency have most important effects on the three outputs. The ambient pressure is also very sensitive for the outputs of gas turbine power output and simple cycle efficiency. For the combined cycle efficiency, the steam cycle heat rate also has important effects besides the adiabatic efficiencies. The above inputs are identified as the most sensitive inputs, which have slopes higher than 0.35. The inputs with absolute values of slope in the range of 0.05 to 0.35 for any one output are considered having moderate sensitivity, which include air cooling fraction, ambient temperature, turbine back pressure, and HRSG outlet temperature. The input of compressor pressure drop with slope less than 0.05 for all three outputs is identifies as the low sensitive input.

7.0 UNCERTAINTY ANALYSIS OF IGCC SYSTEMS BASED ON DIFFERENT GAS TURBINE COMBINED CYCLE

Integrated Gasification Combined Cycle (IGCC) systems are a promising alternative for clean generation of power and coproduction of chemicals from coal and other feedstocks. Although some investigation of the performance, emissions, and cost of 7H-based IGCC system has been reported (Holt, 2003; Falsetti, *et al.*, 2000), advanced concepts for IGCC that incorporate state-of-the-art gas turbine systems are not commercially demonstrated. Therefore, there is uncertainty regarding the future commercial-scale performance, emissions, and cost of such technologies. The objective of this study is to evaluate the effects of advances in gas turbine technology on the performance, emissions, and cost of IGCC systems based on uncertainty analysis of IGCC-7FA and IGCC-7H systems and to determine the key factors causing uncertainties in performance and cost.

7.1 Methodology of Uncertainty Analysis

The concept of uncertainty has been introduced in several publications (Morgan and Henrion, 1990; Cullen and Frey, 1999). The uncertainty associated with the predictions of advanced technology is mainly due to lack of true knowledge of the mechanism or uncertainty in parameters caused by limited experimental data. Uncertainty analysis has been applied to evaluate the risks associated with performance, emissions, and cost of many process technologies, including IGCC technology (Frey and Rubin, 1991a, 1992; Diwekar, *et al.*, 1997; Frey, *et al.*, 1994), combined SO_2/NO_x control technologies (Frey and Rubin, 1991b), coal-fired power systems (Rubin, *et al.*, 1997),

and cost of process technology (Hope, 1996; Frey, *et al.*, 1997). In these reports, quantification of uncertainty by probabilistic analysis has become an integral part for risk assessment of advanced process technologies.

7.1.1 Characterization of Uncertainty

As an innovative technology in early commercial phase, there are many unknown areas in the mechanism and true technical data. For IGCC technology, some parameters, such as the carbon conversion rate, may be empirical quantities. The true values of these parameters are unknown or the experimental data for them are very limited. The uncertainty in the parameters leads to the uncertainty in the predictions of performance and cost of IGCC technology, such as efficiency and cost of electricity (Frey and Akunuri, 2001; Frey and Rubin, 1992). Using point values for these parameters cannot represent the uncertainty of these parameters. In order to evaluate the risks of process technologies, uncertainty analysis is required.

There are three general areas of uncertainty that should be reflected in process engineering models, which are: (1) process performance parameters, e.g. temperature; (2) process area capital cost; and (3) process operating cost (Frey and Rubin, 1991a). In the method of probabilistic analysis of uncertainties, the uncertainties of inputs can be specified by a probability distribution representing the likelihood of different parameters values based on the judgments from technical experts. This method is preferred when sufficient statistics is absent for new advanced technology (Pate´-Cornell, 2002). The process performance uncertainties of gasification area and gas turbine are characterized. The uncertainties of the cost model were mainly from uncertain inputs for direct capital

costs, maintenance costs, and variable costs. The characterization of uncertain inputs of IGCC systems is from technical experts (Frey and Rubin, 1997). The probability distributions can be uniform, triangle, normal, lognormal and other types according to the judgments of experts.

7.1.2 Probabilistic Modeling Environment

After the characterization of uncertain inputs, a probabilistic modeling environment is required to propagate the uncertainties of inputs to outputs. A typical method used in Monte Carlo simulation (Ang and Tang, 1984). In Monte Carlo simulation, a model is executed iteratively using different samples for the uncertain input parameters generated from the corresponding probability distributions. An alternative to the random Monte Carlo sampling method is Latin Hypercube Sample (LHS). LHS has an advantage over conventional Monte Carlo simulation in that each distribution for the random variable is stratified into equal probability intervals and one sample is selected from each of the intervals (Cullen and Frey, 1999). Thus, there is better coverage of the full range of the distribution, particularly for small simulation sample sizes. Helton and Davis (2002) also found that the LHS tend to produce more stable uncertainty analysis results than the random sampling. Therefore, LHS is adopted in this study. The samples of different inputs were input to the process models. For different samples, different outputs results were obtained. The uncertainty in outputs can be quantified in cumulative distribution function (CDF). The probabilistic analysis method is superior to the deterministic analysis method when the risk analysis is needed for a new technology. The point estimate of deterministic analysis cannot provide such information.

7.1.3 Sensitivity Analysis for Identifying Key Uncertain Inputs

Based on the samples of inputs and the results of outputs, a sensitivity analysis can be implemented to assess the relationship between the input variables and outputs. A simple and normal method is to calculate the correlation coefficients between the sampled inputs and the output results. There are several methods for correlation analysis, including partial correlation coefficients (PCC), standard regression coefficients (SRC) (Helton and Davis, 2002). The partial correlation coefficient analysis is used to identify the degree to which correlation between output and input random variables may be linear. The standard regression coefficient of an input variable is used to measure the relative contribution of the uncertainty in the input variables on the uncertainty of the output variables.

In this study, the samples of inputs and the output results are collected. The selected outputs include the performance, emissions, and cost outputs, such as the efficiency, the power output, the capital cost, and the cost of electricity (COE). The partial rank correlation coefficients are calculated for inputs and the selected outputs. This analysis is implemented in SAS (SAS OnlineDoc, 1999). The first step is to identify the important inputs for selected response variables. A response variable is regressed on all the 39 inputs. The inputs variables with significant level of 0.0001 for the regression model are selected. The partial correlation coefficients for the selected inputs variables are calculated [26]. In this method, the most highly correlated input variable is identified first by comparing the correlation coefficients of all the selected inputs with output. This input variable is entered into the regression model. The partial correlation method then find out the second variable which is most correlated with the residuals of the regression

model containing the first input variable. The process is repeated until all the key uncertainty variables are included in the regression model. Thus, the PCC for all the key uncertain inputs are obtained.

7.2 Stochastic Simulation in ASPEN Plus

The stochastic modeling capability has been implemented in ASPEN by Diwekar and Rubin (1991). Based on the study of them, four blocks were integrated with IGCC process model to realize the uncertainty analysis of IGCC system. The conceptual diagram for the implementation of probability analysis in ASPEN Plus is listed in Figure 5. In USRSTC block, the number of sampling, number of uncertain input variable, sampling method, the distributions for each variable, and end values for each variable distribution are specified. The STCBEG block is used to assign probabilistic distributions to the input variables. The STCREC block is used for accessing the outputs. In this block, uses can specify the variables as uncertain outputs.

Using Latin Hypercube Sampling (LHS), random samples from the distributions are simulated and assigned to the inputs. The simulation model in ASPEN Plus is executed for each iteration of random input values, and sample values for the outputs are collected. Thus, the output uncertainties caused by the simultaneous input uncertainties are quantified. A sample size of 100 is selected in order to guarantee an acceptably precise estimate of uncertainties in outputs subject to a constraint on run time. The run time is approximately 20 minutes.

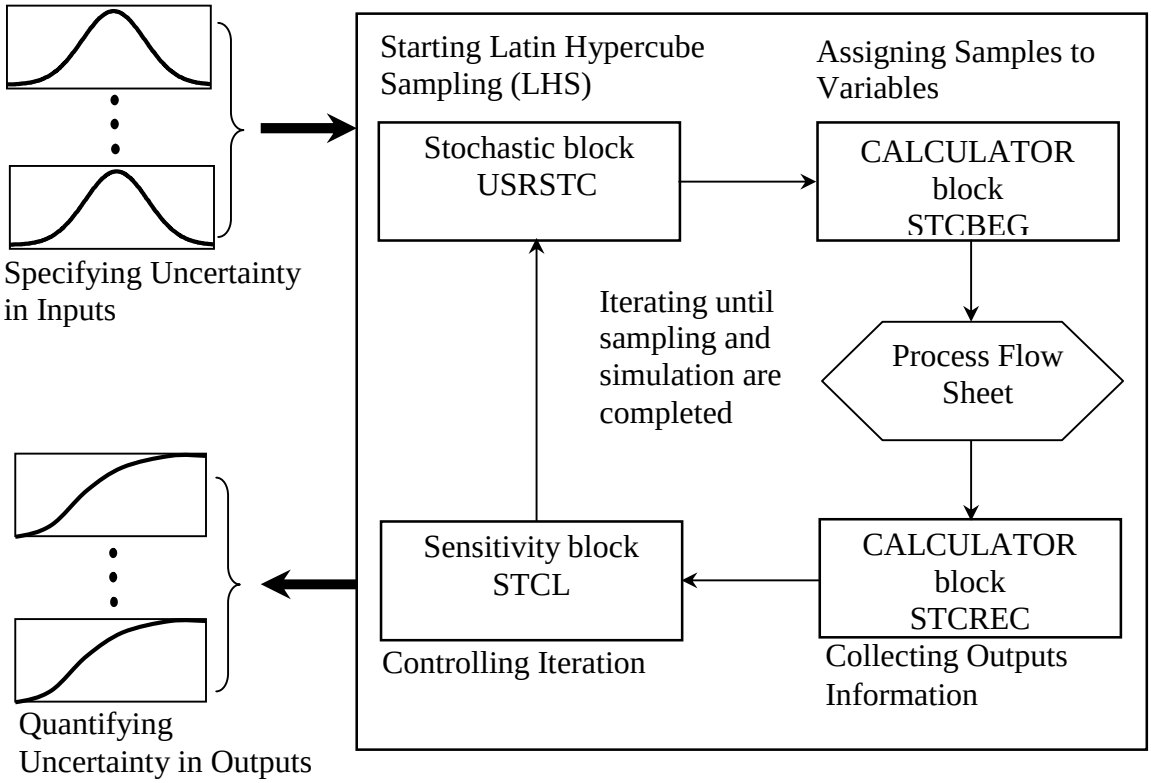

Figure 7-1 Conceptual Diagram of Probabilistic Analysis in ASPEN Plus

7.3 Input Assumptions

A total of 39 inputs are specified as uncertain. The uncertain performance and cost inputs are listed in Table 7-1. The basis for uncertainties used in this study is described in Frey and Akunuri (2001). The uncertain inputs in performance model mainly from gasifier and gas turbine processes. The uncertain inputs in costs model include the cost factors, direct costs fractions of each main process, maintenance costs fractions, and other operating costs. The deterministic values, distributions types, and the 99.8% probability range of the possible values for inputs are given. For example, the deterministic value for carbon conversion in gasifier is assumed to be 0.99. From the judgments of experts, some carbon may be not converted and just pass the gasifier. A

Triangular direction is used to characterize the probability of carbon conversion, which put more “weight” on the published value than the extreme high or low values (Frey and Akunuri, 2001).

The main differences between the IGCC-7FA and IGCC-7H models are the different gas turbine combined cycles, including gas turbine and steam cycle conditions. Therefore, five variables that are unique to each gas turbine design, including thermal NO_x, unconverted CO, the directed cost of gas turbine, direct cost of HRSG, and maintenance cost of gas turbine, are treated as statistically independent variables between the two models. In contrast, the same sample values for the other 34 variables are used in both models. In this manner, correlation in uncertainty between the two systems is properly accounted for.

Table 7-1 Summary of Uncertainties for the Texaco Gasifier-based IGCC Systems with Frame 7F and 7H Gas Turbine [a, b]

No.	Variable ID	Description	Deterministic Value	Distribution and Parameters [c]
1	GASPRE	Gasifier Pressure, psia	615	N; 567.5 to 662.51
2	GASTEM	Gasifier Temperature, ^{o}F	2400	T; 2400 to 2600
3	FRAC	Water/Coal Ratio, lb H_2O/lb Coal	0.504	N; 0.465 to 0.543
4	CONV	Carbon Conversion, fraction	0.99	T; 0.96 to 1.00
5	TAPP1	Approach Temperature 1, ^{o}F	-300	T; -350 to -250
6	TAPP2	Approach Temperature 2, ^{o}F	-500	T; -550 to -450
7	TAPP3	Approach Temperature 3, ^{o}F	-500	T; -550 to -450
8	TAPP4	Approach Temperature 4, ^{o}F	-490	T; -550 to -450
9	TAPP5	Approach Temperature 5, ^{o}F	-500	T; -550 to -450
10	TAPP6	Approach Temperature 6, ^{o}F	-500	T; -550 to -450
11	TAPP7	Approach Temperature 7, ^{o}F	-500	T; -550 to -450
12	TNXCR (*)	Thermal NOx, fraction	$4.5x10^{-5}$	U; $2.5x10^{-5}$ to $7.5x10^{-5}$
13	TCOCR (*)	Unconverted CO, wt-% of CO in fuel gas	0.99985	U; 0.9998 to 0.9999
	CAPITAL COST PARAMETERS, Fractions			
14	FEHO	Engineering and Home Office Fee	0.1	T; 0.07 to 0.13 (0.10)
15	FICC	Indirect Construction Cost Factor	0.2	T; 0.15 to 0.25 (0.20)
16	FPJ	Project Uncertainty	0.175	U; 0.10 to 0.25
	DIRECT COSTS, % of Estimated Direct Cost [d]			
17	FPCCH	Coal Handling	5	U; 0 to 10
18	FPCOF	Oxidant Feed	5	U; 0 to 10
19	FPCG	Gasification	15	T; 0 to 40 (15)
20	FPCS	Selexol	10	T; 0 to 20 (10)
21	FPCLT	Low Temp. Gas Cooling	0	T; -5 to 5 (0)
22	FPCC	Claus Plant	5	T; 0 to 10 (5)
23	FPCBS	Beavon-Stratford	10	T; 0 to 20 (10)
24	FPCPC	Process Condensate Treatment	30	T; 0 to 30 (10)
25	FPCGT (*)	Gas Turbine	12.5	T; 0 to 25 (12.5)
26	FPCHR (*)	HRSG	2.5	T; 0 to 5 (2.5)
27	FPCST	Steam Turbine	2.5	T; 0 to 5 (2.5)
28	FPCGF	General Facilities	5	T; 0 to 10 (5)
	MAINTENANCE COSTS , % of Total Cost [e]			
29	FMCG	Gasification	4.5	T; 3 to 6 (4.5)
30	FMCS	Selexol	2	T; 1.5 to 4 (2)
31	FMCLT	Low Temperature Gas Cooling	3	T; 2 to 4 (3)
32	FMCC	Claus plant	2	T; 1.5 to 2.5 (2)
33	FMCPC	Process Condensate Treatment	2	T; 1.5 to 4 (2)
34	FMCGT (*)	Gas Turbine	1.5	T; 1.5 to 2.5 (1.5)
	OTHER FIXED OPERATING COST PARAMETERS			
35	ALABOR	Labor Rate, $/hr	19.7	N; 17.70 to 21.70
	VARIABLE OPERATING COST PARAMETERS			
36	BCASHD	Ash Disposal, $/tonne	11	T; 11 to 28 (11)
37	BPSULF	Sulfur Byproduct, $/tonne	138	T; 66 to 138 (138)
38	FBM	Byproduct Marketing, fraction	0.10	T; 0.05 to 0.15 (0.10)
39	UCCOAL	Fuel Cost, $/GJ	1.21	T; 1.09 to 1.34 (1.21)

[a] For simulation of 7FA-IGCC system, the 1-39 inputs are used. For simulations of 7H-IGCC system, the variables with (*) are used as independent variables.

[b] N = normal distribution; T = triangular distribution; U = uniform distribution. For uniform distributions, the lower and upper bounds are given. For the triangular distribution, the mode is given in parentheses. For normal and lognormal distribution, the 99.8% probability range is given.

[c] For direct costs, the deterministic values represent "contingency factors" as defined by EPRI (1986) and others. For probabilistic studies, uncertainty in capital cost is represented by an uncertainty factor, which is described by a probability distribution.
[d] Includes indirect capital costs and contingency costs prorated to each process area.

7.4 Probabilistic Analysis Results

The probabilistic analysis of IGCC systems with two different gas turbines are both based upon a Texaco gasifier with radiant and convective cooling. The fuel is Illinois No. 6 coal. The running time for 100 iteration is about 20 minutes for two systems.

The results of probabilistic modeling for IGCC-7H and IGCC-7FA systems are listed in Table 7-2. The deterministic "best guess" point estimate, mean, standard deviation, and 95% probability range for the main outputs of two IGCC systems are given. The results include main outputs of performance, emissions, and costs.

The values for uncertain outputs and uncertain inputs were collected for identifying the key source of uncertainty among the 39 uncertain inputs. The Spearman partial rank-order correlation coefficients between outputs and inputs were computed in SAS. The selected outputs for evaluation include efficiency, power output, emissions, and costs. For each output, the key uncertain inputs are identified and ranked according to the correlation coefficients. A total of 13 key uncertain inputs were found to have significant correlation with the outputs. The correlations coefficients results are listed in Table 7-3. For the power output of IGCC-7FA system, the carbon conversion (CONV) is identified as the most important input with correlation coefficient of -0.758. Developing the regression model of the response variable "power output" based on the predicator

Table 7-2 Summary of Results from Deterministic and Probabilistic Simulations of Coal fueled IGCC System with Frame 7F and 7H Gas Turbines [a]

Parameter	units [b]	"best guess" [c]	$f_{0.50}$	m	s	$f_{0.025} - f_{0.975}$
	IGCC-7FA					
Plant Performance						
Net Efficiency	%, HHV	39.53	38.96	38.88	0.63	37.58 – 39.79
Net Plant Output	MW	284.6	286.0	286.1	1.4	283.7 – 289.0
Plant Emissions						
SO_2 Emissions	lb/Btu	0.223	0.217	0.217	0.018	0.183 – 0.248
NO_x Emissions	lb/Btu	0.127	0.139	0.138	0.040	0.071 – 0.203
CO_2 Emissions	lb/kWh	1.693	1.691	1.691	0.005	1.679 – 1.699
Plant Costs						
Total Capital Cost	$/kW	1882	1881	1882	76	1743 – 2023
Cost of Electricity [d]	mills/kWh	56.11	56.55	56.65	1.81	53.03 – 60.06
	IGCC-7H					
Plant Performance						
Net Efficiency	%, HHV	43.71	43.28	43.23	0.45	42.31 – 43.88
Net Plant Output	MW	414.6	416.2	416.1	1.5	413.6 – 419.3
Plant Emissions						
SO_2 Emissions	lb/Btu	0.218	0.214	0.214	0.015	0.186 – 0.238
NO_x Emissions	lb/Btu	0.132	0.145	0.145	0.042	0.075 – 0.213
CO_2 Emissions	lb/kWh	1.527	1.527	1.526	0.003	1.519 – 1.532
Plant Costs						
Total Capital Cost	$/kW	1708	1701	1706	69	1598 – 1840
Cost of Electricity [d]	mills/kWh	49.98	50.27	50.36	1.62	46.90 – 53.60

[a] The notation in the table heading is defined as followings: f_n = nth fractile ($f_{0.50}$ = median), m = mean, and s = standard deviation of the probability distribution. The range enclosed by $f_{0.025} - f_{0.975}$ is the 95% probability range. All costs are 2000 dollars.

[b] HHV = higher heating value.

[c] Based on a deterministic simulation in which median or modal values of uncertain variables are assumed as "best guess" inputs to the model.

[d] Levelized, constant dollar basis.

variable "CONV", the partial correlation coefficients of the left inputs variables are calculated. The input "FRAC"(water/coal ratio) is found to be the second important variable with biggest correlation coefficients of 0.686 among the left variables for the response variable of efficiency. Thus, adding "FRAC" into the regression model, the partial correlation coefficient for the third important variable can be calculated. This process is repeated until all the key inputs are

Table 7-3 Key Uncertainty Source for Selected Outputs of IGCC based on Frame 7F and 7H Gas Turbines [a]

7FA	Performance		Emissions			Costs	
Rank	Power Output	Efficiency	SO_2 Emissions	NO_x Emissions	CO_2 Emissions	Total Capital Cost	Cost of Electricity
1	CONV (-0.758)	CONV (0.995)	TAPP4 (0.806)	TNXCR (0.999)	CONV (0.868)	FPJ (0.860)	FPJ (0.801)
2	FRAC (0.686)	TAPP4 (-0.609)	TAPP3 (-0.908)		TAPP4 (-0.616)	FICC (0.574)	FPCG (0.529)
3	TAPP4 (-0.796)		CONV (0.759)		FRAC (0.769)	FPCG (0.622)	FICC (0.450)
4	TAPP3 (0.887)		FRAC (-0.617)		TAPP3 (0.834)	FEHO (0.547)	FEHO (0.521)
5	GASTE M (0.928)				GASTEM (0.879)	FPCGT (0.548)	UCCOAL (0.562)
6							FMCG (0.467)
7H	Performance		Emissions			Cost	
Rank	Power Output	Efficiency	SO_2 Emissions	NOx Emissions	CO_2 Emissions	Total Capital Cost	Cost of Electricity
1	FRAC (0.698)	CONV (0.995)	TAPP4 (0.806)	TNXCR (0.999)	CONV (0.841)	FPJ (0.862)	FPJ (0.804)
2	CONV (-0.782)	FRAC (-0.652)	TAPP3 (-0.912)		FRAC (0.643)	FICC (0.595)	FPCG (0.527)
3	TAPP4 (-0.689)		FRAC (-0.583)		TAPP4 (-0.750)	FPCG (0.617)	FICC (0.475)
4	TAPP3 (0.834)		CONV (0.746)		TAPP3 (0.729)	FEHO (0.773)	FEHO (0.551)
5	GASTE M (0.952)				GASTEM (0.877)	FPCGT (0.704)	UCCOAL (0.519)
6							FMCG (0.587)

[a] The key uncertainty sources of inputs are figured out by using partial correlation coefficients based on the sequential regression method with sample size = 100 and significance level α=0.0001.

included into the model and the partial correlation coefficients for all the key inputs are calculated.

The two systems have the same key uncertain inputs for selected outputs despite the difference design of the gas turbine combined cycle. There are six key uncertain inputs for the performance and emissions of two systems, including Carbon Conversion (CONV), water/coal Ratio (FRAC), Approach Temperature 3 (TAPP3), Approach Temperature 4 (TAPP4), thermal NOx conversion (TNXCR), and gasifier temperature (GASTE). For the cost outputs, there are seven key uncertain inputs, including Project

Uncertainty (FPJ), Indirect Construction Cost Factor (FICC), Engineering and Home Office Fee (FEHO), Direct Cost Fraction of Gasification (FPCG), Direct Cost of Gas Turbine (FPCGT), Maintenance Cost Fraction of Gasification (FMCG), and Fuel Cost (UCCOAL).

The carbon conversion (CONV) is the most important uncertainty source for performance, and the project uncertainty (FPJ) is the most important uncertainty source for cost.

7.5 Results and Discussion

In this section, the probabilistic analysis results for selected outputs of IGCC-7FA and IGCC-7H systems are collected and analyzed. The effects of the total 39 uncertain inputs and the key uncertain inputs on the main outputs of the IGCC-7H system are compare and evaluated. For the key uncertain inputs, other inputs were assigned point estimates as the deterministic modeling except the 13 key inputs. The cumulative probability functions for the overall uncertain inputs and key uncertain inputs are put in same diagram for comparison. The results of uncertainty analysis also are compared to the deterministic analysis results for each system. In addition, the uncertainty analysis results of IGCC-7FA and IGCC-7H are compared to each other.

7.5.1 Net Efficiency

For performance of IGCC system, the net efficiency is an important evaluation standard. The uncertain outputs for net efficiency for IGCC-7FA and IGCC-7H were evaluated respectively based on the results given in Section 7.4. The uncertain results of net efficiencies for two systems are compared to each other.

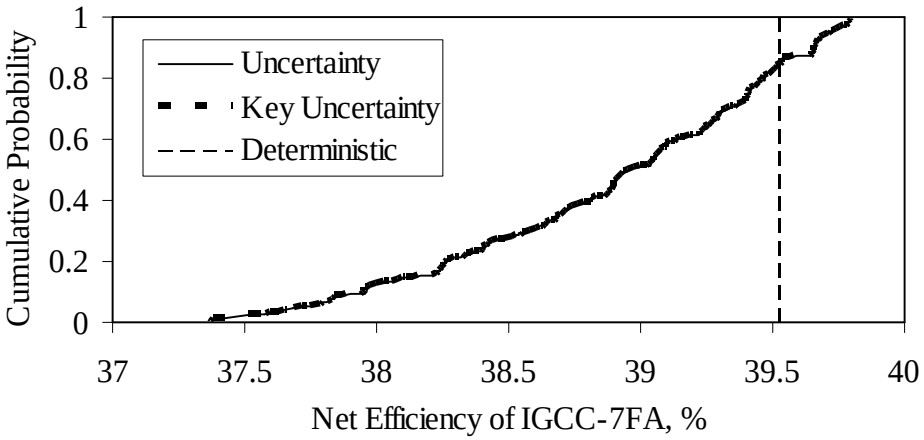

Figure 7-2 Probabilistic Results of Net Efficiency of IGCC-7FA

7.5.1.1 Net Efficiency of IGCC-7FA System

In Table 7-3, the median value and average value of net efficiency for IGCC-7FA system are both less than the deterministic result, "best guess". It means that there is more than 50% chance that the net efficiency of IGCC-7FA is less than the deterministic results. The 95% range of efficiency for IGCC-7FA is 37.6% to 39.8%. The uncertainty range of the efficiency based on the mean is -3% to +2%.

The results of uncertainty analysis based on overall uncertain inputs and key uncertain inputs for net efficiency of IGCC-7FA system are quantified using CDF, which is shown in Figure 7-2. In Figure 7-2, the uncertain results based on key uncertain input are very close to the results from overall uncertain inputs. It indicates the key uncertain inputs identified in sensitivity analysis are the key uncertain sources for the uncertainty in net efficiency. The deterministic result of net efficiency is also given for comparison to uncertainty results. The results in Figure 7-2 indicate that there is about 80% probability that the uncertain results of IGCC-7FA efficiency are lower than that of deterministic result.

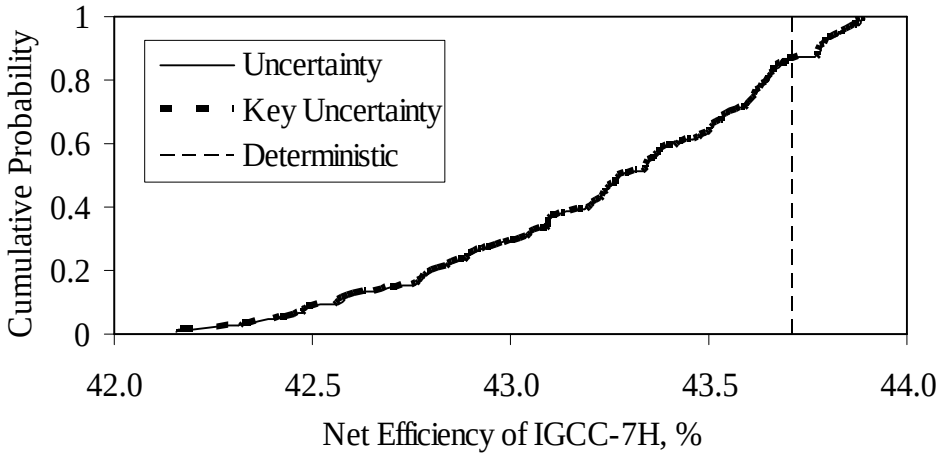

Figure 7-3 Probabilistic Results of Net Efficiency of IGCC-7H System

7.5.1.2 Net Efficiency of IGCC-7H System

For IGCC-7H system, the average value and median value are both less than the deterministic result of net efficiency. The deterministic estimation is about 1% higher than the mean value. The uncertainty range of the efficiency of IGCC-7H system is ~ ± 2%, which is almost same as the uncertainty range of IGCC-7FA system.

In Figure 7-3, the results of the net efficiency of IGCC-7H system are quantified by CDF based on the overall uncertainty and key uncertainty. The deterministic result is represented by a vertical dotted line. The two curves representing the outputs from overall uncertain inputs and key uncertain inputs are very close. It indicates that the key uncertainties can represent the main uncertainty in this technology and other uncertain inputs can be treated as deterministic inputs. Comparing to the deterministic results and probabilistic results, there are about 80% chance that the efficiency of IGCC-7H system is lower than the deterministic result, 43.71%.

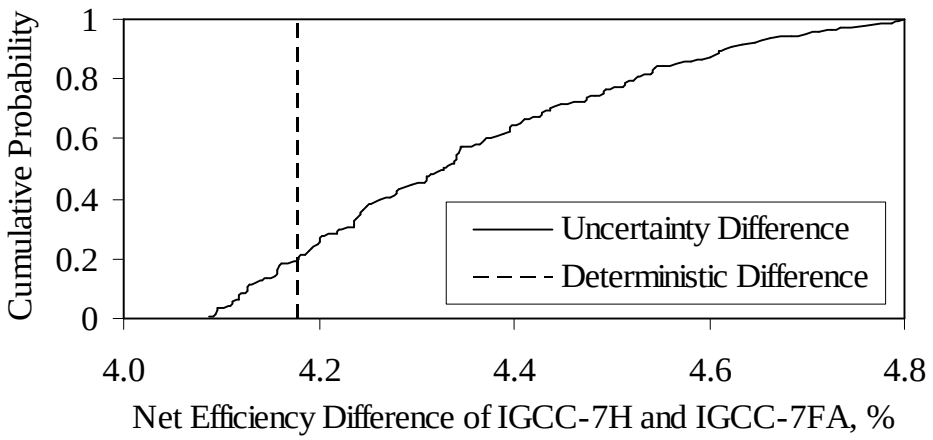

Figure 7-4 Uncertainty in the Difference of Net Efficiency between IGCC-7H and IGCC-7FA Systems

7.5.1.3 Uncertainty in Net Efficiency Difference of Two Systems

The efficiencies of the two systems are compared to each otherand the uncertainties in outputs are considered. The net efficiency differences of two systems are computed by using the 100 observed values of IGCC-7H net efficiency minus the 100 observes of IGCC-7FA system efficiency. As shown in Figure 7-4, the 95% probability range of the net efficiency difference is 4.10% to 4.73%. This result represented the efficiency of IGCC-7H system are always higher than that of IGCC-7FA system despite the uncertainty in inputs. Compared to the difference in efficiency based on deterministic results, the difference based on uncertainty analysis is about 80% higher than the difference based on deterministic analysis. Thus, the results of deterministic analysis possibly underestimate the difference in the efficiencies of two systems.

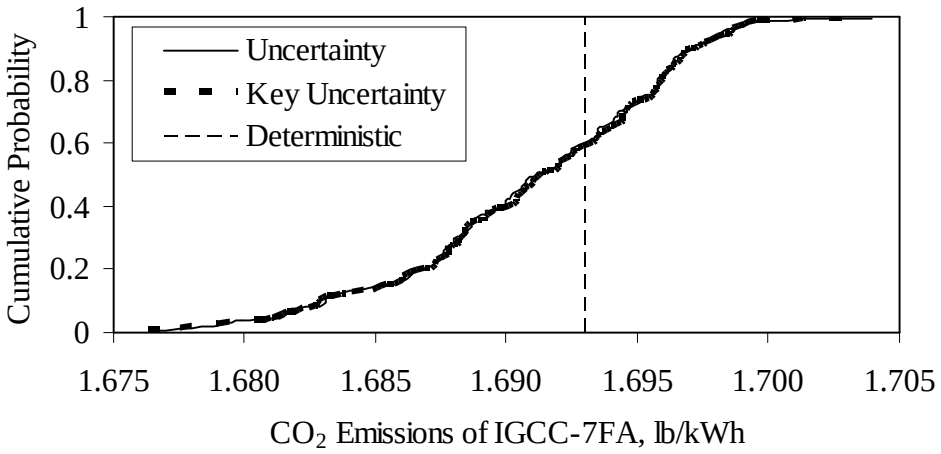

Figure 7-5 Probabilistic Results of CO_2 Emissions of IGCC-7FA System

7.5.2 Emissions

The results of emissions of SO_2, NO_x, and CO_2 for two systems were analyzed.

7.5.2.1 Emissions of IGCC-7FA System

In Table 7-3, the deterministic result of SO_2 emissions is higher than the median value and average value of IGCC-7FA system. It means the deterministic result overestimate the SO_2 emissions. The uncertainty range of SO_2 emissions of IGCC-7FA system is -16% to +14%. It is smaller than the uncertainty range of NO_x emission, -49% to +47%. For NO_x emissions, the deterministic result is lower than the median and mean values. It indicates there is more than 50% chance that NOx emissions are higher than deterministic result. The uncertainty range of CO_2 emissions range is very small, less than ± 1%. Thus, the uncertainty range of NO_x emissions is the biggest one in three. The possible reason is that the NO_x formation in gas turbine combustion process is a complicated process and further information is needed to decrease the uncertainty range of it.

To compare the effects of overall uncertain inputs and key uncertain inputs on the emission results of IGCC-7FA system, the emissions of the CO_2, are selected for evaluation. The deterministic results, uncertain results based on overall uncertainties and key uncertain results are shown in Figure 7-5. The outputs of CO_2 emissions based on key uncertain inputs are very close to the results based on overall uncertain inputs. The comparison of uncertain results to deterministic results indicates that there is about 40% chance that the CO_2 emissions are higher than the deterministic analysis results. It means that there are risks of high emissions for IGCC-7FA system.

7.5.2.2 Emissions of IGCC-7H System

For IGCC-7H system, there are very close results of deterministic and uncertain results for SO_2 emissions and NO_x emissions compared to IGCC-7FA system. The SO_2 emissions of IGCC systems mainly based on the removal fraction of the selexol process and the same removal fractions are same for the two system. The NO_x emissions mainly depend on the combustion temperature of the gas turbine. Although the two gas turbines have difference firing temperature, the H gas turbine has almost same combustion temperature as the Frame F gas turbine due to steam cooling design. Thus, the two systems have similar SO_2 emissions and NO_x emissions.

For CO_2 emission, the uncertainty range is also less than ± 1% for IGCC-7H system. However, the deterministic results indicates that the CO_2 emission of IGCC-7H system is 10% less than that of IGCC-7FA system and the difference between SO_2 and NO_x emissions of two systems are very small. The uncertain results of CO_2 emissions of IGCC-7H system are selected for analysis, which are shown in Figure 7-6. There is little

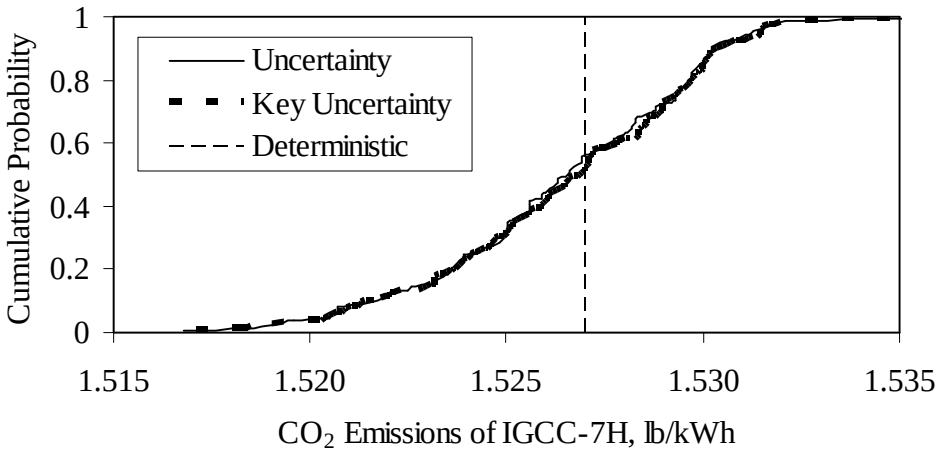

Figure 7-6 Probabilistic Results of CO_2 Emissions of IGCC-7H System

difference between the results of key uncertainties and overall uncertainties. Compared to the deterministic results, there is about 45% probability that the CO_2 emissions based on uncertainty analysis are higher than the deterministic result.

7.5.2.3 Uncertainty in CO_2 Emissions Difference of Two Systems

For the two systems, the uncertainty results of CO_2 emissions are compared to each other. The uncertainty range in CO_2 emissions difference between IGCC-7H and IGCC-7FA is the -0.167 lb/kWh to -0.160 lb/kWh, which is shown in Figure 7-7. The result represented the CO_2 emissions of IGCC-7H are always lower than that of IGCC-7FA system despite the uncertainty in the results. The difference of CO_2 emissions of two systems is -0.166 lb/kWh. With the negative results increasing from -0.167 lb/kWh to -0.160 lb/kWh, the differences in CO_2 emissions decrease. Thus, the difference of CO_2 emissions based on uncertainty analysis is approximately 70% lower than the difference based on deterministic analysis. Therefore, there is 70% probability that the deterministic analysis overestimates the CO_2 emissions of two systems.

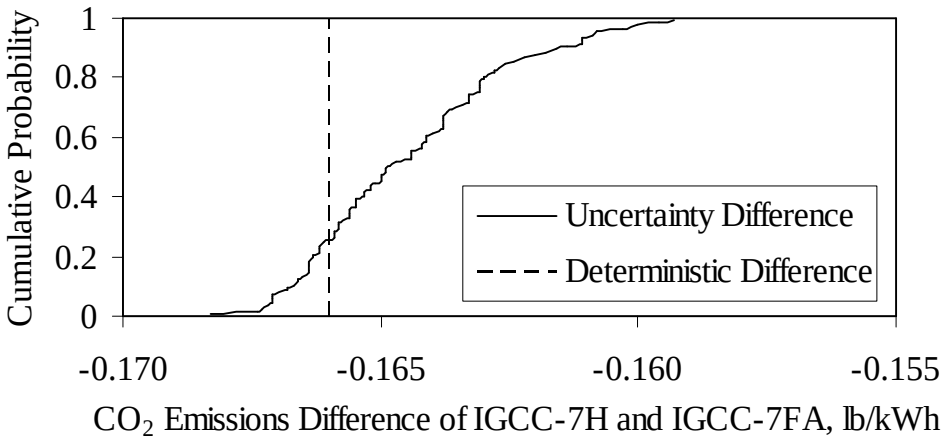

Figure 7-7 Uncertainty in the Difference of CO_2 Emissions of IGCC-7H and IGCC-7FA Systems

7.5.3 Cost of Electricity (COE)

The cost of electricity is a very important parameter for the evaluation of cost feasibility of power production. The results of COE for two systems are collected and analyzed.

7.5.3.1 COE of IGCC-7FA System

As shown in Table 7-3, the median and average values for COE for IGCC-7FA system are higher than corresponding deterministic values. That means the deterministic analysis may overestimate the COE. The uncertainty analysis results of COE of 7FA are quantified by CDF and shown in Figure 7-8. The uncertain results of COE based on key uncertain inputs are close to the results based on overall uncertain inputs. There is about 60% probability that the COE of IGCC-7FA is higher than that of deterministic result.

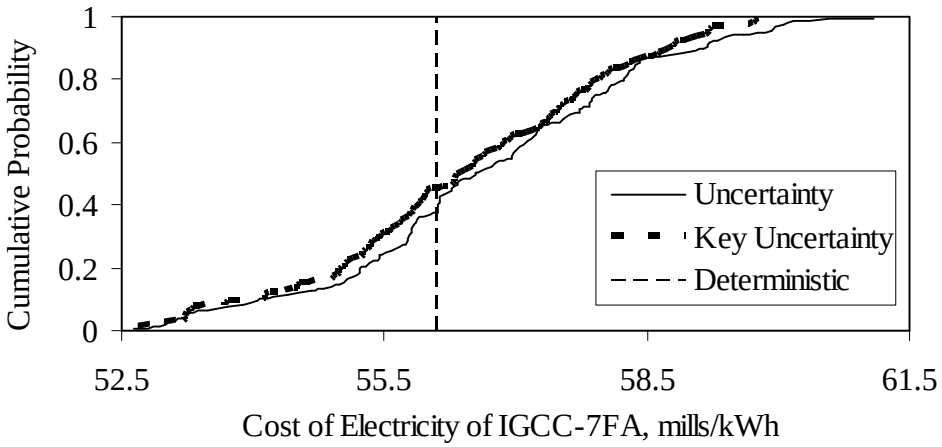

Figure 7-8 Probabilistic Results of COE of IGCC-7FA System

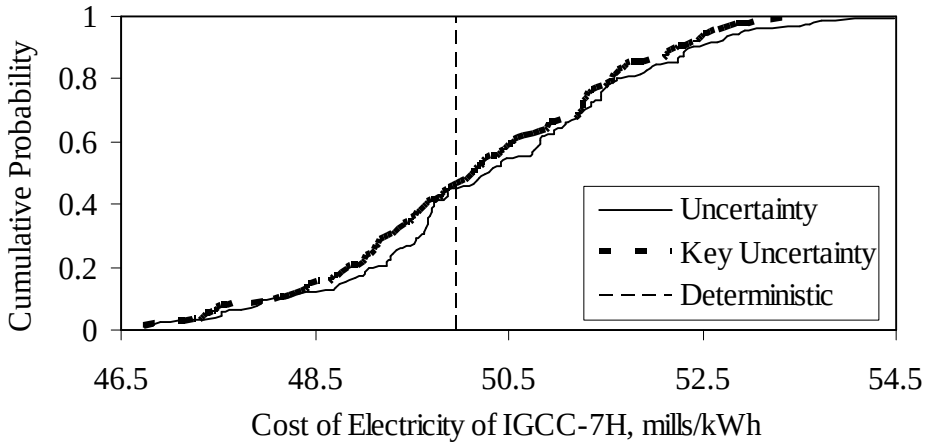

Figure 7-9 Probabilistic Results of COE of IGCC-7H System

7.5.3.2 COE of IGCC-7H System

The median and average values for COE for IGCC-7H system are also higher than corresponding deterministic values. Comparing the means of COE of two systems, the difference is -10% of two systems. The uncertainty range for IGCC-7H system is -7% to +6%. In Figure 7-9, the results of COE based on overall uncertainty and key uncertainty analysis are compared. The two results are very close. Compared to the

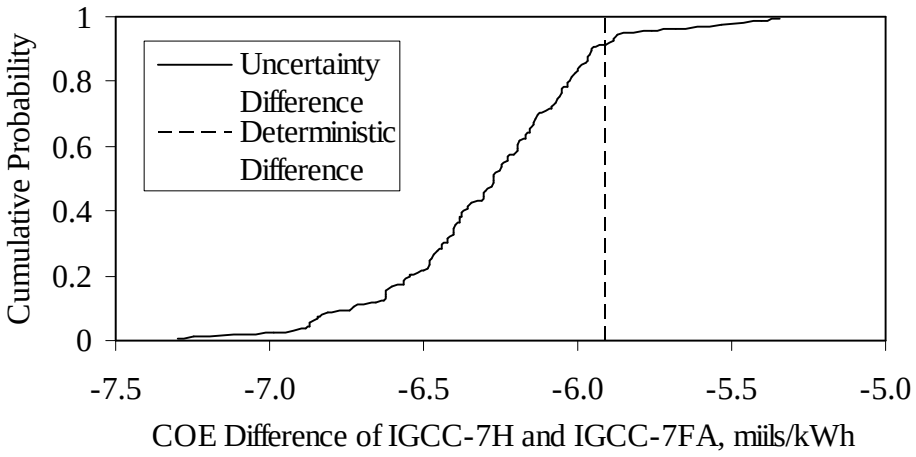

Figure 7-10 Uncertainty in the Difference of COE between IGCC-7H and IGCC-7FA Systems

deterministic results, there is about 55% probability that the COE of IGCC-7H system is higher than the deterministic analysis result.

7.5.3.3 Uncertainty in COEs Difference of Two Systems

The differences in COE results of two systems are computed based on the uncertainty analysis results, which is shown in Figure 7-10. The uncertainty range in the COE difference of two systems is -7.0 to -5.5 mills/kWh. It indicates that the COE of IGCC-7H are always lower than that of IGCC-7FA system. The difference of COE of two systems based on deterministic analysis is -6.1 mills/kWh. All the results of difference in COE are negative values and thus the bigger absolute values of the results means bigger difference. Thus, there is approximately 90% probability that the difference in COEs based on uncertainty analysis is bigger than that based on the deterministic values. Therefore, the deterministic analysis probably underestimated the difference of COE of two systems.

8.0 EVALUATION OF INTEGRATOIN OF AIR SEPARATION UNIT (ASU) WITH IGCC SYSTEM

Different integration designs of the air separation unit (ASU) with Integrated Gasification Combined Cycle (IGCC) system were investigated in this chapter. The models for conventional ASU plant with “low pressure” (LP-ASU) design and an ASU with “elevated pressure” (EP-ASU) design were developed and the ASU process blocks were integrated with IGCC model. Different integration designs based on both LP-ASU and EP-ASU were investigated, including only nitrogen injection, only air extraction, and nitrogen injection and air extraction together. The performance and emissions of IGCC systems based on different pressure level ASU and different integration designs were estimated and compared. The cost of integrated and nonintegrated IGCC designs was studied.

8.1 Introduction

At present, integration of ASU and gas turbine has been applied to some IGCC projects, such as Tampa project (Holt, 2003). The main function of the ASU in an IGCC system is to supply high purity oxygen for the gasifier. Although there are many benefits associated with application of IGCC technology, the commercialization of IGCC is still in early phase and the actual technical data and experiences are limited. Therefore, meaningful R&D work is required to provide guidelines for improvements in IGCC systems over next decades. One example of an opportunity for improved system design and integration pertains to the ASU (Smith, *et al.*, 1997). A conventional stand-alone

ASU designs compress ambient air and produce a pressurized oxidant stream (Thomas, 2001). Nitrogen separated from the air is typically vented to the atmosphere. The ASU can be integrated with the gas turbine by extracting air from the gas turbine compressor. This type of integration has the potential benefit of reducing the auxiliary power consumption for compression in the ASU (Holt, 1998). A portion of the nitrogen stream produced by the ASU can be additionally pressurized and mixed with the syngas to make up for the loss of mass flow to the gas turbine combustor of some of the extracted air.

Typically, study designs that consider integration of the ASU via air extraction also consider the simultaneous use of nitrogen injection (Holt, 1998; Buchanan, *et al*., 1998; White, 1998; Eurling, 1997). The potential advantage of the combination of air extraction and nitrogen injection is an improvement in system efficiency and a corresponding reduction in emission rates on a per fuel usage basis. Some potential disadvantages include increased operational complexity and control challenges, particularly during startup, for a system with a high degree of coupling between the gas turbine and ASU (Holt, 2003). However, there seems to be little assessment of whether the apparent advantages of extraction and injection can be attributed primarily to either extraction or injection alone. Furthermore, the effect of air extraction and nitrogen injection may depend upon the type of ASU design, such as low pressure (LP) versus elevated pressure (EP) designs. For example, if most of the benefits of the combination of both extraction and injection can be obtained based only on nitrogen injection, then a much simpler and easier to control system design could be developed. Thus, this study focuses on answering the following key questions:

(1) what is the effect on IGCC system performance and emissions of different levels of nitrogen injection?:

(2) what is the effect on IGCC system performance and emissions of different percentages of compressor air extraction from the gas turbine to the ASU?:

(3) What is the effect of combinations of both air extraction and nitrogen injection?;

(4) What is the effect of differences in ASU design (e.g., LP vs. EP) on IGCC system performance and emissions for a given level of air extraction, nitrogen injection, or both?

(5) Based upon the answers to the previous four questions, what general guidance can be provided regarding recommended approaches for air extraction, nitrogen injection, or both for a typical IGCC system?

In order to answer the key questions, a process simulation model of a typical IGCC system was developed and implemented in ASPEN Plus. This model is based upon and IGCC system featuring: either LP or EP ASU designs; an entrained flow gasifier; high temperature gas cooling; low temperature acid gas separation; syngas reheating and combinations of either moisturization, nitrogen injection, or both; and a “Frame 7F” gas turbine considering various degrees of air extraction. Thus, the model includes all of the technologies and integration options required to answer the key questions.

In the following sections, the background of ASU integration with gas turbine combined cycle in IGCC systems is introduced. The development of ASU model is described. Case studies based on different integration options are simulated to evaluate the effects on IGCC performance and emissions. The integration options investigated in three groups of case studies are only nitrogen injection, only air extraction, and

combination of both. LP ASU and EP ASU based on three integration options are evaluated. The effects of integration on costs of IGCC are evaluated based on comparison of integrated and nonintegrated designs.

8.2 Current Status of Integration of ASU and Gas Turbine

Integration of ASU and gas turbine has been applied to some IGCC projects and it can increase the overall efficiency, and decrease the cost of power generation (Holt, 2003; Ratafia-Brown, *et al*., 2002a). The three IGCC projects using different integration method are listed in Table 8-1. Depending on difference in nitrogen injection and air extraction, there are three integration options available:

- Nonintegrated ASU – No nitrogen injection and no air extraction. The air required by the ASU is completely from the atmosphere. Oxygen is sent to gasifier and nitrogen is vented to the atmosphere;
- Partially integrated ASU – Nitrogen injection. The nitrogen produced from ASU is partly or totally compressed and sent back to the gas turbine;
- Totally integrated ASU – Combination of nitrogen injection and air extraction. Part or all of the air required by ASU is supplied by the air from the discharge of gas turbine and nitrogen is injected back to gas turbine and mix with syngas to reduce NOx formation during combustion.

The above three kinds of integration mainly include two aspects: nitrogen injection and air extraction. The functions of the two aspects were introduced in the following:

Nitrogen injection Nitrogen produced from the nonintegrated ASU is generally vented into the atmosphere as a waste. In partially and totally integrated designs, this waste gas is injected into gas turbine for dilution of syngas. The nitrogen injection is expected to

Table 8-1 Examples of IGCC Projects with Different Air Extraction and Nitrogen Injection Approaches (Holt, 2003; Ratafia-Brown, *et al.*, 2002a)

Integration Type	Nonintegrated	Partly-Integrated	Totally-Integrated
Project Name	Wabash River	Tampa	ELCOGAS
Location	Indiana, USA	Florida, USA	Puertollano, Spain
Net Power Output (MW)	262	250	298
Fuel Feed	High Sulfur Bituminous	High Sulfur Bituminous	Bituminous Coal and Petroleum Coke
Gasification Technology	E-Gas (Destec)	Texaco	Prenflo
Gas Turbine	GE 7FA	GE 7F	Siemens V94.3
Combustor	Multiple Cans	Multiple Cans	Twin Horizontal Silos
Firing Temperature, ^{o}F	2350	2350	2300
Pressure Ratio	15.5	15.5	16.1
Gas Cleanup System	Low-temperature	Low-temperature	Low-temperature
Sulfur Control	MDEA [a] scrubber and Claus plant	MDEA [a] scrubber and H_2SO_4 plant	MDEA [a] scrubber and Claus plant
Particulate Control	Water scrubber and candle filter	Water scrubber	Candle filter
Air Separation Unit	LP ASU	EP ASU	EP ASU
Pressure (bar)	5	10	10
Air supply	No air extraction	No air extraction	100% air extracted from gas turbine
Nitrogen use	Mostly vented	Gas turbine NO_x Control	Gas turbine NO_x Control

[a] MDEA: Methyl Diethanol Amine;

decrease the combustor zone flame temperature and NOx formation is strongly dependent on the high temperatures. Thus nitrogen injection can reduce NOx emissions from gas turbine. In Tampa project, nitrogen injection is used for NOx emissions (Hornick and McDaniel, 2002). Another diluent for controlling NOx emission is steam or water. The advantage of nitrogen injection compared to the steam injection is that nitrogen can provide additional net power output and reduce the water consumption (Amick, *et al.*, 2002).

Air Extraction The compressed air from gas turbine is sent to ASU, which can reduce the power consumption of the air compressor. For ELCOGAS project, however, not only

nitrogen injection is used, but also water injection is used for nitrogen control (Coca, *et al.*, 1998). The combination of nitrogen and water injections can make up the mass flow deficit caused by 100% air extraction of gas turbine in ELCOGAS project. For 100% air extraction, the benefits are that the air compressor is eliminated and both the power consumption and the cost of ASU were reduced. However, such a high integration degree between the gas turbine and ASU in European IGCC projects is not recommended for new IGCC plant design because it has longer star up times and less operation flexibility, which is caused by a long process of sequential starting up (Coca, *et al.*, 1998). As a result, future IGCC designs based on V94.3 gas turbine are expected to have partial airside integration (Parkinson, 2004). Holt (1998&2003) have pointed out that an air extraction in the 25%~50% range of the total air requirement for ASU is a suitable choice in the integration design with both air extraction and nitrogen injection. In addition, he also points that the optimum choice of integration degree depends on gas turbine and ambient conditions.

Although the integration of ASU with gas turbine combined cycle in IGCC system has great potential to increase the efficiency and decrease the cost of power generation, the commercial experience for integration designs are still very limited. Limited design studies based on certain integration design is not enough to evaluate the performance of different integration design or different ASU configuration. Therefore, the integration of ASU and IGCC system was simulated in ASPEN Plus in this study and case studies based on different ASU designs and integration methods are evaluated.

8.3 Modeling of Air Separation Unit

A performance model for a cryogenic ASU was developed in ASPEN Plus. The flowsheet is shown in Figure 8-1. The air flow from the atmosphere is sent to a multiple-stage compressor, simulated by a compressor unit block, AIRCOMP. The compressed air is cooled in the main heat exchangers by the cold liquid product streams, simulated by a heater block HEATEX. In the integration design, another stream of air is extracted from the compressor of gas turbine, which is also sent to the main heat exchanger, which is simulated by stream ATOASU. The heat from the main exchanger is used to heat of the product streams from the cryogenic separation unit. The cold air is fed into the cryogenic separation unit, simulated by a separator block AIRSEP. The air stream is separated into three streams, including nitrogen, 95% oxygen, and process water. The separation process is simulated by specifying the split fractions based on the compositions of oxygen and nitrogen streams. The gaseous pure nitrogen and liquid pure oxygen are produced. The cold product nitrogen and oxygen are heated by the incoming air to become gaseous streams. The outlet conditions for oxygen flow and nitrogen flow are specified. Part of nitrogen is split from the nitrogen product stream, simulated by a split block, N2SPLIT, and then is vented to the atmosphere or used for other process in plant. The left nitrogen is compressed in the nitrogen compressor, which is simulated by a multistage inter-cooling compressor block, N2COMP. The compressed nitrogen is injected to gas turbine. The 95 % oxidant is further compressed, simulated by O2COMP, and sent to the gasifier.

The main specifications for the blocks in ASU model are listed in Table 8-2. There are some differences in the main specifications for EP ASU and LP ASU, which are described in the following.

The specifications of air compressor used in LP ASU are different from that used in EP ASU. The design basis of air compressor used in LP ASU is a two-stage intercooler compressor, which is a typical design for the air compressor used in LP ASU (Flour, 1984). The outlet pressure of air compressor is typical 80 psia (Amick, *et al.*, 2002; Thomas, 2001). For the air compressor in EP ASU, the design basis is the air compressor used in Tampa project (Hornick and McDaniel, 2002). It is a four-stage intercooler compressor. The outlet condition is not provided in this report. Therefore, the reference data from another study of IGCC plant with EP ASU is used here. In this air separation process, air is compressed to 211 psia (Buchanan, *et al.*, 1998).

For cryogenic separation unit, the components fraction is same for LP ASU and EP ASU, which are specified based on the compositions of air, oxygen, nitrogen streams. The compositions of air, oxygen, and nitrogen are shown in Appendix E. The outlet conditions of cryogenic separation unit are different for LP ASU and EP ASU. For LP ASU, the 95% oxygen is discharged from the air separation unit at 16.5 psia (Flour, 1984). The outlet pressure for EP ASU is 58 psia (Foster Wheeler, 1999).

For LP ASU and EP ASU, the same structure of oxygen compressor is used since it is an independent operation unit from the air compressor. Oxygen compressor is a six-stage intercooled stage compressor (Hornick and McDaniel, 2002). The outlet pressure is

decided by the gasifier operation pressure. In this study, a Texaco gasifier is used. According the Flour report, the outlet pressure for oxygen is 734 psia (Flour, 1984).

The nitrogen compressor design is same for the LP ASU and EP ASU. A four-stage compressor is adopted (Hornick and McDaniel, 2002). The outlet pressure of nitrogen compressor is decided by the outlet pressure of the gas turbine compressor. In this study, the Frame 7F gas turbine is adopted. The outlet pressure for nitrogen compressor is 240 psia (Buchanan, *et al.*, 1998). For different designs, such as different gasifier and gas turbine, the outlet conditions of oxygen compressor and oxygen compressor can be modified to the known specifications.

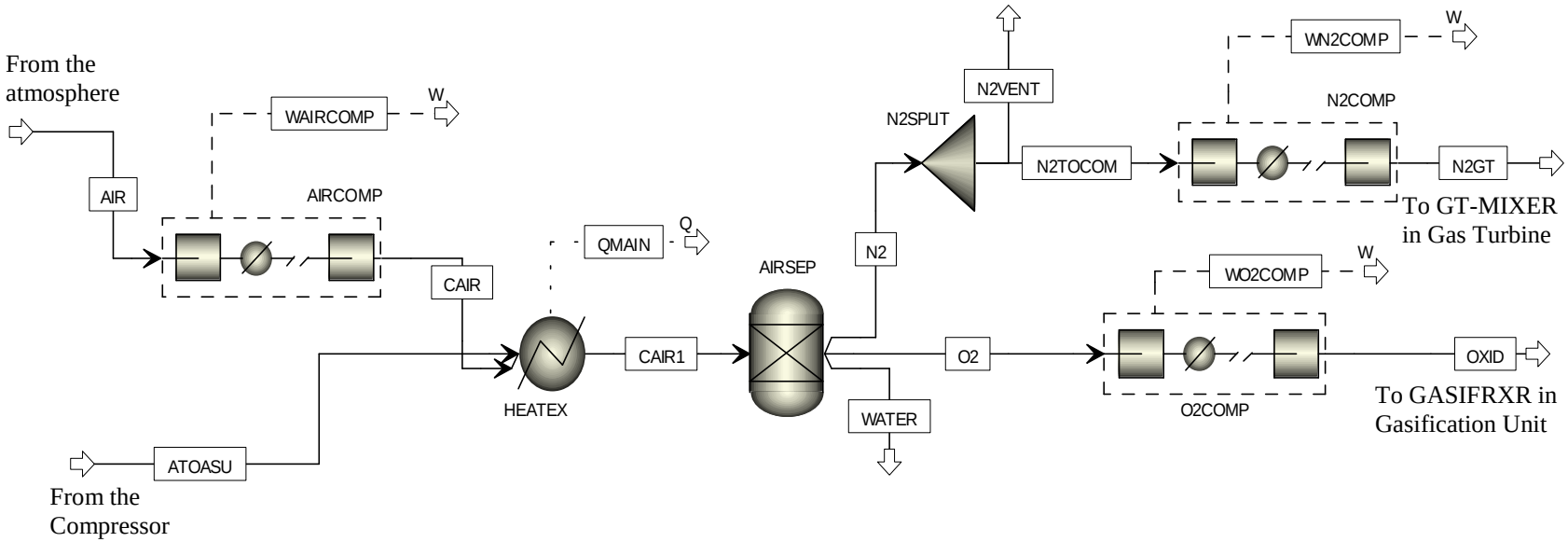

Figure 8-1 Flowsheet of Air Separation Unit Model used in IGCC Systems for Integrated Design

Table 8-2 Unit Blocks Description of Air Separation Unit

No	BLOCK ID	BLOCK PARAMETERS	DESCRIPTION
1	AIRCOMP (COMPR)	LP: Pressure = 80 psia EP: Pressure = 211 psia Isentropic Efficiency = 0.83	Simulates the compression of air to 86 psia
2	HEATEX (HEATER)	LP: Temperature = 90 ^{o}F EP: Temperature = 125 ^{o}F Pressure drop = -10 psia	Simulates the main heat exchanger in ASU.
3	AIRSEP (SEP)	Frac: Stream = OXID N2 = 0.0036 O2 = 0.95 H2O = 0 Ar = 0.78 Stream = WATER N2 = 0 O2 = 0 H2O = 1 Ar = 0 Outlet Condition: LP: P=16.5 psia EP: P= 58 psia	Simulates a crogenic air separation unit to produce 95 mol% oxygen.
4	N2SPLIT (FSPLIT)		Controls the nitrogen injection amount to gas turbine.
5	N2COMP (COMPR)	Isentropic Efficiency = 0.72	Simulates nitrogen is compressed before being sent to gas turbine
6	OXYCOMP (COMPR)	Isentropic Efficiency = 0.74	Simulation a centrifugal compressor to compress high purity oxygen before sent to gasifer

8.3.1 Calibration and Verification of LP ASU Model

The purpose for calibration is to find out the efficiencies for air compressor and oxygen compressor to match the reported LP ASU power consumption. Based on the ASU model, the power consumption of air compressor and oxygen compressor can be estimated by the compressor blocks in ASPEN Plus. For LP ASU, no nitrogen injection is used in present reference reports. Therefore, the isentropic efficiencies of air compressor and oxygen compressor were varied to match the reference values.

8.3.1.1 Calibration of LP ASU Model

The calibration basis for this model is an ASU used in a nonintegrated Texaco gasifier based-IGCC system (Frey and Akunuri, 2001). The 95% oxidant flow rate is

539,297 lb/hr for this IGCC system with three 7FA gas turbines. The reference values for air compressor and oxygen compressor power consumptions are estimated based on the results of Thomas (2001). In the report, a performance model for conventional LP ASU is developed based on the oxygen purity and flow rate. In this study, a typical 95% purity is assumed for used in IGCC systems. Based on this study, for a production of 95% purity oxygen at 539,297 lb/hr, the power consumption of air compressor is 57.5 MW. The oxygen compressor power consumption is 29.5 MW. These two values become the calibration basis for the air compressor and oxygen compressor blocks in LP ASU model.

After specifying the inlet, outlet conditions of compressors, the isentropic efficiencies for the air and oxygen compressors were varied to get the same power consumption as the reference values. For the air compressor block in ASEPN Plus, the inlet and outlet conditions has been specified, the isentropic efficiency for each stage is varied between 0.7 ~ 0.9. Each value of compressor efficiency corresponds to a value of power consumption for the compressor. In Figure 4-2, when the isentropic efficiency of air compressor is 0.83, the power consumption of air compressor is 57.4 MW. This result is consistent with Andersson, *et al.* (2002), which mentioned the air compressor isentropic efficiency is 0.83. For oxygen compressor, the isentropic efficiency of 0.74 is selected and the power consumption is 29.5 MW. The 0.74 is very close to the default value for compressor isentropic efficiency, 0.72, in ASPEN Plus.

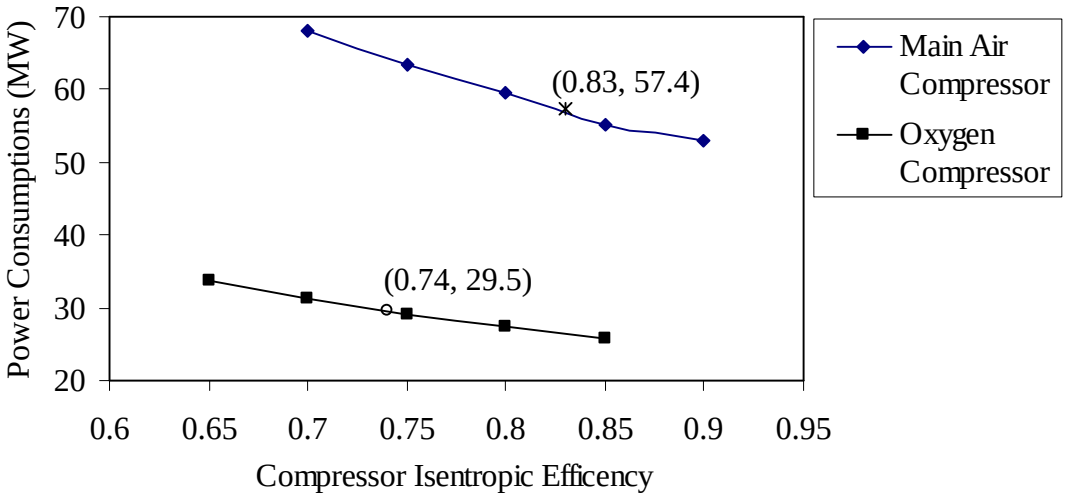

Figure 8-2 Isentropic Efficiency of Air Compressor and Oxygen Compressor in LP-ASU Model

8.3.1.2 Verification of LP ASU Model

A design study using LP ASU is adopted for verification (Condorelli, ***et. al.***, 1991). The reference plant in this project is a Texaco quench IGCC plants. The air at atmosphere conditions is sent to ASU. It is first compressed to 67 psia. It is sent to cryogenic distillation unit for separation. Oxygen exits the separation unit and is compressed to 925 psia and 222 ^{o}F. The total oxygen flow rate is 306,864 lb/hr. All the specifications for LP ASU model keep same as the above case except the outlet conditions the report gives out. The results are listed in Table 8-3. The results showed that the power consumption for LP ASU is close to the reference data.

Table 8-3 Results Comparison of LP ASU Model and Reference Data

	Modeling Results	Reference Data [a]	Relative Difference, %
95% Oxygen Flow Rate, lb/hr	306,864	306,864	
Air Compressor Power Consumption, MW	28.8		
Oxygen Compressor Power Consumption, MW	18.0		
Total Power Consumption, MW	46.8	48.6	0.0

[a] Condorelli, *et al.*(1991), "Engineering and Economic Evaluation of CO_2 Removal From Fossil-Fuel-Fired Power Plants."

8.3.2 Calibration and Verification of EP ASU Model

The EP ASU model is calibrated and compared to related reference data. The modeling process of EPASU is same as LP ASU model. The difference of EP ASU model to LP ASU model is the specifications for air compressor, oxygen compressor, and nitrogen compressor. From present references, nitrogen compressor only is used in the case of EP ASU plant. The calibration purpose for EP ASU is to find out appropriate isentropic efficiencies of the three compressors. The isentropic efficiencies of the compressor blocks in EP ASU model are varied to match the reference values of power consumption for the three compressors. The calibration process is introduced in the following.

8.3.2.1 Calibration of EP ASU Model

For this model, the main conditions and flow rates data for EP ASU are adopted from the ASU in a Destec based oxygen-blown IGCC plant with Frame 7F gas turbine (Buchanan, *et al.*, 1998). The air flow rate is 1,424,775 lb/hr. The elevated pressure air separation unit is designed to produce an output of 329,903 lb/h of 95% purity oxygen. Nitrogen is produced and most of it is injected to gas turbine for fuel gas dilution to

control the NO_x emissions. In this air separation process, air is compressed to 211 psia and cooled. The outlet conditions for oxygen compressor is 635 psia and 310 ^oF. The nitrogen of 989,280 lb/hr is produced and compressed. The outlet conditions for nitrogen compressor are 240 psia and 396 ^oF. The design of nitrogen compressor, such as the stage number, is not given in Buchanan, *et al.*(1998). The nitrogen compressor design of Hornick and McDaniel (2002) is adopted, which is a four-stage intercooled compressor.

For simplifying the calibration, the isentropic efficiencies of air compressor and oxygen compressor are assumed to be the same as the calibrated values of the compressors of LP ASU. That means that for air compressor and oxygen compressor, the power consumptions differences are caused by the different outlet conditions in the design basis for LP ASU and EP ASU. Thus, the isentropic efficiency for air compressor is set as 0.83 and that of oxygen compressor is 0.74. The isentropic efficiency of nitrogen compressor is varied to match the reference value for nitrogen injection, 22.9 MW (Buchanan, *et al.*, 1998). The calibration process is same as that of calibration of LP-ASU. The curve of sensitivity of the nitrogen compressor power consumption based on different isentropic efficiencies is shown in Figure 8-3. The isentropic efficiency of 0.72 is selected for nitrogen compressor and its power consumption is 22.9 MW, which is same as the reference value.

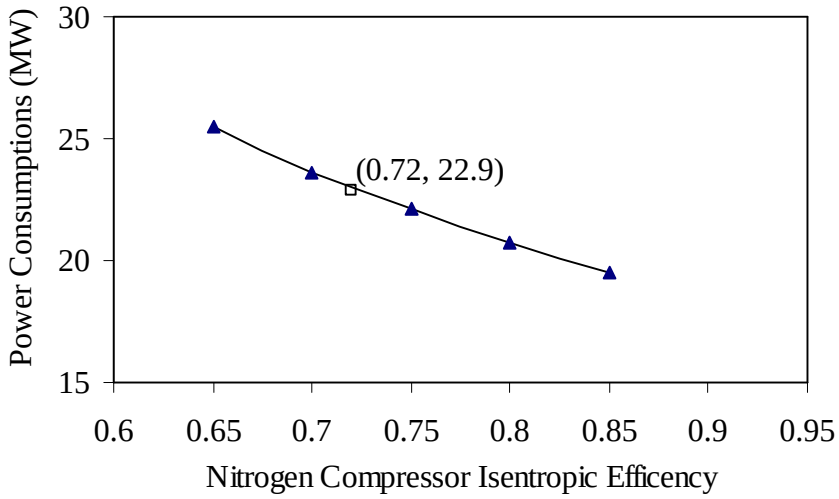

Figure 8-3 Isentropic Efficiency of Nitrogen Compressor in EP-ASU Model

8.3.2.2 Verification of EP ASU Model

The power consumptions results of three compressors from the results of ASPEN Plus model are compared to the reference values of the design study used as calibration basis. The comparison is listed in Table 8-4. Although the isentropic efficiencies for air compressor and oxygen compressor are not calibrated based on this design basis, the power consumptions for the two compressors are close to the reference values. It indicates that it is reasonable to assume that the isentropic efficiencies of air compressor and oxygen compressor are 0.83 and 0.74 respectively.

For power consumption of nitrogen compressor, the reference data of Tampa project are selected (Hornick and McDaniel, 2002). In Tampa project, the air is totally from the atmosphere and large part of product nitrogen is injected in to the Frame 7F gas turbine. A small part of nitrogen is vented for process control and stability of column pressure. The nitrogen, 6000 ton/d (500,000 lb/hr) is compressed to 295 psia and 375 ^{o}F. The power consumption is 14 MW. The nitrogen compressor power consumption result

Table 8-4 Results Comparison of EP-ASU Model to Reference Data

	Modeling Results	Reference Data [a]	Relative Difference, %
Oxygen Flow Rate, lb/hr	329,903	329,903	
Nitrogen Flow Rate, lb/hr	989,280	989,280	
Air Compressor Power Consumption, MW	56.5	55.9	1.1
Oxygen Compressor Power Consumption, MW	10.9	10.7	1.9
Nitrogen Compressor Power Consumption, MW	22.9	22.9	0
Total Power Consumption, MW	90.3	89.5	0.9

[a] Buchanan, *et al*. (1998).

of the model in ASEPN Plus is 13.4 MW. Compared to the reference value, the difference is only about 4%, which is not a big difference. The 96% oxidant stream is compressed and sent to the gasifier. Since the EP ASU model in this study is designed for production of 95% purity oxygen, it will consume more power than the 95% oxygen air plant, specially in the main air comrpressor power consumption part. Therefore, the air compressor and oxygen compressor are not compared to the reference values.

Therefore, the EP ASU model can estimate the actual power consumptions of EP ASU plant well based on the calibration process and verification result.

8.4 Performance Model of IGCC based on Different ASU Integration Design

In order to investigate the effects of different ASU designs and integration methods on IGCC performance, the developed ASU models were combined with the IGCC model without ASU blocks to form a complete performance model. The IGCC model without ASU block was developed in ASPEN Plus, which has been described in

Chapter 3.0. In the following, the combination of two models was introduced. A difference of the integrated IGCC system from the base design is the NO_x emission control methods. The nitrogen injection is adopted for the integration design and the moisture dilution for base nonintegrated design. The requirement for moisture dilution under certain nitrogen injection to keep same NO_x emissions level with only moisture dilution is studied. The integration model was verified by comparison to reference data from similar IGCC design.

8.4.1 Modeling of Integration of ASU and Gas Turbine

After the ASU model is developed, it is combined with the gas turbine section in the earlier IGCC model to form a complete model to simulate the integration of ASU and gas turbine. The previous IGCC model is a Texaco gasifier-based IGCC plant with radiant and convective cooling design based on a Frame 7F gas turbine combined cycle. The details of gas turbine model were described in Chapter 3.0. The integration of ASU and gas turbine is realized mainly through air extraction and nitrogen injection. The conceptual diagram of ASU integration with gas turbine is shown in Figure 8-4. Part of the air from the compressor is sent to the ASU and the nitrogen from ASU is injected into the combustor and mixed with the syngas. In Figure 8-4, the air extraction and nitrogen injection were represented by difference lines and symbols. The flow rate of each stream is represented by $m_{i,j}$. For example, the flow rate of air extraction is represented as $m_{air,EX}$.

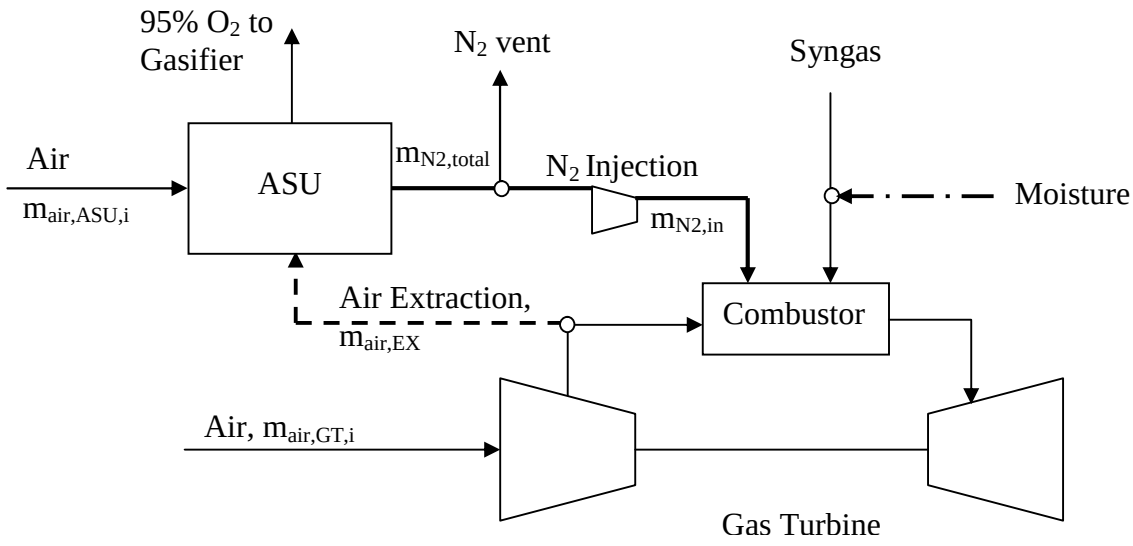

Figure 8-4 Conceptual Diagram of Integration of ASU and Gas Turbine

The two terms, which will be used in this study, were termed by the flowrates of related stream:

$$\text{Air Extraction (Integration Degree)} = \frac{m_{air,EX} \times 100\%}{m_{air,EX} + m_{air,ASU,i}}$$

$$\text{Nitrogen Injection Fraction} = \frac{m_{N2,in}}{m_{N2,total}} \times 100\%;$$

The integration degrees refer to the fraction of air extraction in the total air requirement by ASU. According to different values of these two variables, different integration designs can be categorized into three types. When the integration degree and nitrogen injection fraction are both zero, it is a non-integration design. When either of two is not zero, it is a partially integration designs. When both of them are not zero, it is a totally integrated design.

The overall mass flow in a gas turbine is limited by the turbine nozzle constraints. This choked flow conditions are modeled for the turbine first nozzle inlet (Frey and Akunuri, 2001). Therefore, this feature enables to evaluate the effects of nitrogen injection and air extraction on gas turbine performance. For example, when part of the air from the compressor is extracted to ASU and no nitrogen injection into gas turbine, the air flow to the compressor will increase to make up the deficit of first nozzle caused by air extraction. The power consumption of the compressor will increase. In the totally design, with constant air flow rate to gas turbine, the additional nitrogen injection is required when there is air extraction.

8.4.2 Criteria of Nitrogen Injection and Moisture Dilution

The nitrogen injection and moisture injection both can be used to control NO_x formation from a gas turbine (Hornick and McDaniel, 2001; Hasegawa, et al., 2003). In the earlier model, the moisture injection is used. The syngas is mixed with steam and its moisture content is 28.2 wt% (31.0 mol%). In this study, different nitrogen amount will be injected into the syngas. For the purpose of comparison of IGCC performance with and without nitrogen injection, the preference is to compare cases based upon constant NOx emissions but if necessary (e.g., because of high level of nitrogen injection) the NOx emissions may decrease versus the baseline. The amount of moisture need for a given nitrogen injection to keep constant NO_x emissions is estimated. With nitrogen injection increasing to certain degree, the moisture requirement would be zero. With nitrogen injection further increasing, the NOx emissions will decrease. The following chemical model is used to estimate the NO_x formation in the primary combustion zone in a combustor. The syngas, air, nitrogen, and moisture were included in the model.

Through comparing the characteristic time and residence time of NO_x formation in the primary zone, the NO_x formation can be estimated. Based on the constant, different moisture requirement can be calculated.

Since all of the coal's bound nitrogen is converted to ammonia which is mostly removed from syngas before sent to combustor, most of the NO_x emissions are from thermal NO_x formation (Hornick and McDaniel, 2002). The mechanism used to estiamte the thermal NO_x formation was developed by Flagan and Seinfield (1998). In this mechanism, the adiabatic flame temperature of the prime zone of the combustor is calculated by the combustion heat and the inlet temperatures of air, saturated syngas, and nitrogen. Thus the equilibrium constants for the above reactions and the equilibrium mole fractions of NO, O, N, and OH can be calculated. The characteristic time for NO formation can be calculated as the following:

$$\tau_{NO} = \frac{[NO]_e}{4R_1} \tag{7-1}$$

$$R_1 = k_{+1}[NO]_e[O]_e \tag{7-2}$$

where,

$[NO]_e$ is the equilibrium concentration of NO in unit of gmol/m^3;

$[O]_e$ is the equilibrium concentration of O in unit of gmol/m^3;

R_1 is one-way rate of reaction.

The following chemical kinetic model is used here:

$$f(a) = (1-\kappa)\ln(1+\alpha) - (1+\kappa)\ln(1-\alpha) - \frac{t}{\tau_{NO}} = 0 \qquad (7\text{-}3)$$

where,

$$\alpha = \frac{[NO]}{[NO]_e} \qquad \kappa = \frac{R_1}{R_2 + R_3} \qquad R_2 = k_{+2}[N]_e[O_2]_e \qquad R_3 = k_{+3}[N]_e[OH]_e$$

The above equation is solved to get a value for α. In addition, for a given residence time and flame temperature, the equilibrium NO_x mol fraction is obtained. Under given nitrogen injection, the requirement of moisture is simulated such that

$$y_{NO,e} \times \alpha = \text{constant} \qquad (7\text{-}4)$$

where $y_{NO,e}$ is the equilibrium mol fraction of NO.

Using the above model, the constant of the product at the primary zone is 0.0005 for the syngas with moisture content of 28.2 wt%. With the molar ratio of nitrogen/syngas increasing, the moisture dilution is varied to keep the constant product of NO fraction and ratio α. With nitrogen injection increasing, the moisture dilution decreases. When the nitrogen/syngas molar ratio is 0.604, the moisture requirement is zero to keep the same constant. With nitrogen/syngas ratio continue increasing, the conditions of Eq. (7-4) can no longer be satisfied and the estimated NO_x levels decrease compared to the baseline.

Table 8-5 Comparison of Results of ASU integration Model to Reference Data

Descriptions	Texaco – R&C Model Results	Texaco – HR [a] Reports Results	Relative Difference, %
Integration, %	25	25	
Coal Flow Rate, lb/hr (dry basis)	374,130		
Nitrogen Injection Fraction, %	83.9%		
Gas Turbine, MW	385	384	0.3%
Steam Turbine, MW	284	292	-2.7%
Auxiliary Power, MW	102	109	-6.4%
Net Power, MW	567	567	0
Heat Rate, Btu/kWh (HHV)	40.51	40.93	-1.0%
Efficiency, % (HHV)	25	25	

[a] Texaco Gasifier-based IGCC with totally Radiant Cooling Design, Holt, N. (1998).

8.4.3 Verification of Integrated IGCC Model

In order to verify the ASU integration IGCC model, the study of Holt for the Texaco-base full heat recovery IGCC with integration degree of 25% was selected for comparison (Holt, 1998). In the report, the basic configurations include Illinois No.6 coal, two Frame 7F gas turbines, single reheat steam turbine, and EP ASU. In this study, both nitrogen injection and air extraction are used. The detailed specifications of ASU are not given in the report by Holt (1998). Therefore, the typical input assumptions for EP ASU model in Table 8-2 are used. The nitrogen injection amount is varied to satisfy the first nozzle requirement. The moisture injection is not provided in the report and it is assumed to be zero in this study. The results and the reference data were listed in Table 8-5. The modeling results are close to the report data. That verified that that the model is reasonable for modeling the integrated of ASU and IGCC system.

8.5 Case Studies

To answer the key questions in the introduction, three case studies are investigated in this study. The base design of IGCC plant is a Texaco gasifier-based IGCC with radiant and convective cooling design with no nitrogen injection and no air extraction. A single Frame 7F gas turbine and a reheated steam turbine are used. The fuel is Illinois No. 6 coal. The syngas saturation degree is 28.2wt% moisture. The main input assumptions of three cases were listed in Table 8-6. Difference integration designs selected for case studies include:

Case A – no air extraction from gas turbine and various nitrogen injections to gas turbine. The air extraction is zero and the nitrogen injection is varied as the nitrogen/syngas molar ratio to be 0, 0.15, 0.3, 0.45, 0.604, 0.75, 0.9, and 1.15. The moisture fraction required under certain nitrogen/syngas molar ratio is input to the model. Among those points, the point of 0.604 representing the moisture requirement for keep almost same NOx emissions is zero. Under this point, the nitrogen injection percentage is 51.5%. The increase of nitrogen/syngas molar ratio from 0.604 to 1.15 is to find out the further changing trend of LP ASU and EP ASU under high nitrogen injection. When the nitrogen/syngas molar ratio is 1.15, the nitrogen injection is 98 percent, which is the total available nitrogen for injection (Buchanan, ***et al***., 1998).

Case B – no nitrogen injection to gas turbine but various air extractions from gas turbine to ASU. The air extraction of 0%, 12.5%, 25%, 37.5%, and 50% are selected. In this case, the moisture fraction is 28.2% and the nitrogen injection is zero. Some reference

Table 8-6 Summary of Key Input Assumptions for Case Studies

Description	Value
Air Separation Process Area	
Air Compressor Outlet Condition, psia/ ^{o}F	80/145 (LP-ASU); 211/350 (EP-ASU)
ASU Delivery Pressure, psia/ ^{o}F	16.5/84 (LP-ASU); 58/84 (EP-ASU)
Oxygen Compressor Outlet Pressure, psia/ ^{o}F	734/ 270
Nitrogen Compressor Outlet Pressure, psia/ ^{o}F	240/396
Gasification process Area	
Coal Feed Rate, lb/hr, dry basis (Initial)	585,000
Slurry Water/Coal Ratio, lb H_2O/lb Coal	0.504
Oxygen/Coal Ratio, lb 100%O_2/lb Coal (Initial)	0.915
Gasifier Pressure, psia	615
Gasifier Outlet Temperature, ^{o}F	2,400
Radiant Cooler Outlet Temperature, ^{o}F	1,500
Convective Cooler Outlet Temperature, ^{o}F	650
Gas Turbine Process Area	
Inlet Syngas Temperature, ^{o}F	570
Moisture in Fuel Gas, wt-% [a]	Varied depending on Case Study
Pressure Ratio [b]	15.5
Turbine Inlet Temperature, ^{o}F [b]	2,350
Compressor Isentropic Efficiency, %	79.9
Expander Isentropic Efficiency, %	92.4
Generator Efficiency, %	98.5
HRSG and Steam Cycle Area	
Steam Condition, psia/^{o}F/^{o}F	1450/997/997
HRSG Stack Temperature, ^{o}F	271

[a] In case A, the moisture fraction are varied with nitrogen injection. In case B, the moisture injection keeps same as 28.2%. In case C, the moisture fraction is set to be zero. Other inputs keep same in four cases.
[b] Specifications of GE-7FA gas turbine (Eric, 2000).

reports have reported that the typical optimal air extraction is less than 50% for Frame 7F gas turbine (Holt, 1998; Smith, *et al*., 1997). Thus, the upper limit of 50% is selected.

Case C – both nitrogen injection and air extraction are used, in which the different integration degrees were selected and nitrogen injection was varied. The air extractions of 0%, 12.5%, 25%, 27.5%, and 50% are selected with the moisture injection is zero. Different nitrogen injection is used.

For each case, the IGCC systems based on LP ASU and EP ASU are evaluated individually. The Case A with nitrogen injection being zero is same as the Case B with zero integration degree, which is a nonintegrated deign. The nonintegrated design is treated as the comparison basis for other cases. In Case C with air extraction of zero, the base design is the nitrogen/syngas molar ratio to be 0.604. The values of the air feed flow rate to ASU, the air flow rate to gas turbine, and fuel feed flow rate are set to be constants in this case. The data for the three feed flow are from the corresponding stream results of Case A with 0.604 N_2/syngas molar ratio. The total available nitrogen for injection is assumed to be 98% of the total product nitrogen.

8.6 Results and Discussion

In this section, the results of performance and emissions of different integration methods based on LP ASU and EP ASU are discussed.

8.6.1 Case A – ASU with Only Nitrogen Injection

In this case, the nitrogen injection degree to gas turbine is varied. It is controlled by varying the molar ratio of nitrogen to dry cleaned syngas. With different nitrogen/syngas ratio, the required moisture fraction is obtained. Under each combination of nitrogen injection and steam injection, the results were listed in Table 8-7.

In this case, the nitrogen injection is varied and the related moisture dilution is adjusted to keep constant NO_x emissions level. When N_2/syngas molar ratio is 0.604, the requirement for moisture dilution is zero. The results showed that the moisture consumption in Case A0, 138,610 lb/hr, is only about half of the nitrogen injection, 287,570 lb/hr, to keep same NO_x emissions. With the nitrogen injection increasing, the

Table 8-7 Case Study Results for Nitrogen Injection without Air Extraction (Case A) based on LP-ASU and EP-ASU

Description	A0	A1	A2	A3	A4	A5	A6	A7
Air Extraction, %	0	0	0	0	0	0	0	0
N_2/Syngas(dry) molar ratio	0	0.15	0.30	0.45	0.604	0.75	0.9	1.15
Nitrogen injection, %	0	12.8	25.6	38.4	51.5	63.9	76.7	98.0
H_2O wt% in saturated syngas	28.2	22.9	16.6	9.2	0	0	0	0
Coal Feed Rate, 10^3lb/hr,	192.3	191.0	189.6	188.2	186.7	187.5	188.6	190.6
Moisture Feed Rate, 10^3lb/hr	138.6	104.1	69.2	35.0	0	0	0	0
Nitrogen Feed Rate, 10^3lb/hr	0	73.1	145.1	216.1	287.6	358.7	433.0	559.0
Saturated Syngas, LHV, Btu/scf	181.4	192.6	213.6	234.6	259.1	259.0	258.9	258.8
Air to GT, 10^3 lb/hr	3,420	3,390	3,360	3,330	3,310	3,220	3,130	2,990
Combustor exhaust flow rate, 10^3lbmole/hr	114.9	114.7	114.5	114.2	114.0	114.2	114.4	114.7
	Case A – LP-ASU							
Gas Turbine Net Power, MW	192.1	192.2	192.3	192.3	192.3	196.7	201.3	209.2
Steam Turbine Net Power, MW	132.1	135.0	137.9	140.7	143.5	143.7	144.2	144.8
Total Auxiliary Load, MW	40.0	43.5	46.8	50.1	53.4	57.1	61.1	678
Oxidant Feed, MW	28.2	28.0	27.8	27.6	27.4	27.5	27.6	27.9
Nitrogen Compressor, MW	0	3.4	6.7	9.9	13.2	16.5	20.0	25.6
Net Plant Power Output, MW	284.1	283.7	283.3	283.0	282.4	283.3	284.4	286.1
Plant Efficiency, %, HHV	39.47	39.69	39.93	40.16	40.42	40.37	40.28	40.15
SO_2 Emissions, lb/MWh	1.90	1.91	1.90	1.89	1.88	1.88	1.89	1.89
CO_2 Emissions, lb/MWh	1,700	1,690	1,680	1,670	1,660	1,660	1,660	1,670
Relative NO_x Emissions per Unit Output	1	1.00	1.00	1.00	1.00	0.50	0.24	0.08
	Case A – EP-ASU							
Gas Turbine Net Power, MW	192.1	192.2	192.3	192.3	192.3	196.7	201.3	209.2
Steam Turbine Net Power, MW	132.2	135.0	137.9	140.8	143.6	143.8	144.3	144.9
Total Auxiliary Load, MW	48.9	50.4	51.8	53.3	54.7	56.7	58.9	62.6
Oxidant Feed, MW	36.2	35.9	35.6	35.4	35.1	35.3	35.5	35.8
Nitrogen Compressor, MW	0	1.7	3.4	5.0	6.7	8.3	10.1	13.0
Net Plant Power Output, MW	275.4	276.9	278.3	279.8	281.1	283.7	286.7	291.6
Plant Efficiency, %, HHV	38.26	38.74	39.23	39.71	40.24	40.43	40.58	40.87
SO_2 Emissions, lb/MWh	1.98	1.96	1.94	1.91	1.89	1.88	1.87	1.86
CO_2 Emissions, lb/MWh	1,750	1,730	1,710	1,690	1,660	1,660	1,650	1,640
Relative NO_x Emissions per Unit Output	1.03	1.02	1.02	1.01	1.00	0.50	0.24	0.08

air flow to gas turbine decreases because the gas turbine has limited capacity. For the only nitrogen injection design, it is necessary to throttle the gas turbine compressor inlet air flow to give space to injected nitrogen for dilution. The flow rate of fuel decreases with the increase in the nitrogen injection.

With the increase in nitrogen injection, the moisture dilution decrease. The LHV of syngas sent to the gas turbine increases with moisture fraction decreasing. Therefore, the requirement of coal flow decreases since the LHV of syngas increases and less syngas is needed to reach the firing temperature of gas turbine. After that point, the LHV of syngas has a little bit decrease, the coal flow rate has a little increase due to the nitrogen further dilution and thus more coal is needed to satisfy the energy input requirement of gas turbine.

For IGCC based on LP ASU, the plant efficiency increases with the nitrogen injection increasing until no moisture dilution is required. The reason for increase of the plant efficiency is due to the decrease of coal flow rate and the increase of steam turbine power output. Less moisture fraction leads more steam used to produce power in the steam cycle. Therefore, the power output of the steam cycle increase with the moisture dilution decreasing and the plant efficiency increases. After the nitrogen/syngas molar ratio reach 0.604, the efficiency decreases with the increase in nitrogen injection because the increase in nitrogen compressor consumption in LP ASU is higher than the increase in the gas turbine power output. Comparing Case A0 with nonintegrated design to the case of A4 with LP ASU, the efficiency increases about 1%. For the emissions of IGCC with LP ASU, the lowest SO_2 and CO_2 emissions take place when the nitrogen/syngas

molar ratio is 0.604 of Case A4. The reason is that before the point of 0.604, the efficiency of IGCC plant increase with nitrogen injection. Thus the emissions based on power output decrease. After the point of 0.604, the plant efficiency decreases and thus the emissions o SO_2 and CO_2 increase.

The efficiency of EP-ASU increases with the increase of nitrogen injection. The efficiency of Case A7-EP ASU is about 1.5% higher than that of the base design of Case A0-LP ASU. The reason is that the increase of the nitrogen compressor power consumption for EP-ASU is lower than the increase of gas turbine power output. Although the power consumption for air compressor in EP-ASU is much higher than that of LP-ASU, the power consumption for nitrogen compressor in EP-ASU is lower than that of LP-ASU because the nitrogen compressor inlet pressure is higher in EP ASU than in LP ASU. For IGCC with EP ASU, the SO_2 and CO_2 emissions decrease from case A0 to Case A7 due to the increase in efficiency.

For NO_x emissions, the emission of case A0 with LP ASU is treated as a basis for all other cases with LP ASU or EP ASU. Since the mole fractions of NO_x in the combustion zone have been estimated based on the model of Flagan and Seinfield (1998), the NO_x emissions rate per unit power is based on the combustor exhaust molat flow rate and the plant power output. Thus, the relative NO_x emissions of other cases can be estimated based on that of base design of Case A0 with LP ASU. The combustor exhaust mole flow rates and the power outputs have been listed in Table 8-7. The combustor exhaust flow rate is almost a constant. Thus the NO_x emissions mainly depend on the nitrogen injection and power output. The relative lowest NO_x emission appears in Case

A7 due to high nitrogen injection and high power output. The best environmental performance is case A7 with EP ASU, which has lowest SO_2, CO_2, and NO_x emissions.

Comparing the results of LP-ASU and EP-ASU, the plant efficiency increment of IGCC based on EP ASU is greater than IGCC based on LP-ASU with nitrogen injection percentage increasing. When the nitrogen injection is more than 60%, the efficiency for IGCC based on EP-ASU begins to be higher than that of IGCC with LP-ASU. Therefore, the optimal choice for ASU design is choosing EP-ASU when nitrogen injection requirement is over 60%, otherwise choosing LP-ASU. For this partially integrated case with only nitrogen injection or steam injection and without air extraction from gas turbine, the steam injection is preferred since the steam requirement is only half of the nitrogen requirement for same NO_x emission and the gas turbine compressor inlet has to be throttled if large amount of nitrogen is injected.

Therefore, based on the consideration of emissions and efficiency, case A7 with EP ASU is the best choice based on this study for only nitrogen injection design.

8.6.2 Case B – ASU with Only Air Extraction from GT

In order to investigate the effects of air extraction on IGCC system performance, the air extraction is adopted in this case. The results of Case B are listed in Table 8-8. The results of Case B0 are same as the Case A0 since both have same nonintegrated design.

With the air extraction increasing from 0% to 50%, the power consumption for ASU decreases because more compressed air from the gas turbine is injected to ASU, which saved the power of the air compressor. For the overall IGCC plant, there is a trade-off between the power saving of ASU due to air extraction and the power consumption of

Table 8-8 Case Study Results for Air Extraction without Nitrogen Injection (Case B) based on LP ASU and EP-ASU

Description	B0	B1	B2	B3	B4
Air Extraction, %	0	12.5	25	37.5	50
Nitrogen injection, %	0	0	0	0	0
H_2O wt% in saturated syngas	28.2	28.2	28.2	28.2	28.2
Coal Feed Rate, 10^3lb/hr	192.3	192.5	192.5	192.5	192.6
Moisture Feed Rate, 10^3lb/hr	138.6	138.7	138.7	138.7	138.8
Nitrogen Feed Rate, lb/hr	0	0	0	0	0
Air to GT, 10^6 lb/hr	3.42	3.53	3.64	3.74	3.85
Combustor exhaust flow rate, 10^3lbmole/hr	114.9	114.8	114.5	114.3	114.1
	Case B – LP-ASU				
Gas Turbine Net Power, MW	192.1	186.6	181.0	175.4	169.9
Steam Turbine Net Power, MW	132.1	132.8	132.4	132.1	131.7
Total Auxiliary Load, MW	40.0	37.6	35.0	32.5	29.9
Oxidant Feed, MW	28.2	25.9	23.6	21.2	18.9
Net Plant Power Output, MW	284.1	281.8	278.4	275.0	271.7
Plant Efficiency, %, HHV	39.47	39.11	38.64	38.17	37.69
SO_2 Emissions, lb/MWh	1.90	1.94	1.97	1.99	2.02
CO_2 Emissions, lb/MWh	1,700	1,710	1,730	1,750	1,780
Relative NO_x Emissions per Unit Output	1	1.01	1.02	1.03	1.04
	Case B – EP-ASU				
Gas Turbine Net Power, MW	192.1	186.6	181.0	175.4	169.9
Steam Turbine Net Power, MW	132.2	132.0	131.5	131.2	130.9
Total Auxiliary Load, MW	48.9	44.8	40.7	36.5	32.4
Oxidant Feed, MW	36.2	32.5	28.7	24.9	21.2
Net Plant Power Output, MW	275.4	273.8	271.9	270.1	268.3
Plant Efficiency, %, HHV	38.26	37.98	37.73	37.48	37.22
SO_2 Emissions, lb/Btu	1.98	2.00	2.01	2.03	2.04
CO_2 Emissions, lb/kWh	1,750	1,760	1,770	1,790	1800
Relative NO_x Emissions per Unit Output	1.03	1.04	1.04	1.05	1.05

the compressor due to increase in compressed air. With the increase of air extraction, the power consumption of ASU decreases, while in another hand, the power production of

gas turbine decreases. In order to make up the mass flow deficit at the turbine inlet nozzle caused by the air extracted to ASU, the air flow to the compressor increase with the increase of extracted air flow. However, the air flow to the turbine still keeps constant due to the constraint of turbine first nozzle. Thus the power produced by the expander keeps same and the power consumption of compressor increases. Therefore, the total power output of gas turbine decreases.

The power saving for ASU through air extraction from gas turbine is always lower than the compressor power consumption for compressing of this part of air. It leads to the IGCC power output and the efficiency decrease. For example, comparing the nonintegrated case B0 and case B1 of 12.5% air extraction based on LP ASU, the decrease of gas turbine power output is 5.5 MW, while the decrease in power consumption of ASU is only 2.3 MW. It leads the total power output of Case B1 with LP ASU is lower than that of Case B0 with LP ASU. The reason is that the compressors of ASU are the inter-cooling compressor, which have higher efficiency than the compressors without inter-cooling, i.e. the compressor in the gas turbine. The same results were obtained from the cases of EP-ASU. Therefore, the plant power output and efficiency decrease with the air extraction increase if there is no nitrogen injection to make up the mass deficit caused by the air extraction.

For the emissions of SO_2, CO_2, and NO_x, all of them increase from case B0 to case B4. That indicate the air extraction case has worse environmental performance compared to the only nitrogen injection design, since case B0 is same as case A0. The main reason is that the plant efficiency decreases and then the emissions based on unit

power output increase. Combined the air extraction effects on plant efficiency, the case of only air injection is not an optimal design for IGCC system, whatever the LP ASU or EP ASU is used.

8.6.3 Case C – ASU with Air Extraction and Nitrogen Injection

In Case C, the air extraction is varied from 0% to 50%. The results of Case C are listed in Table 8-9. The purpose of Case C is to investigate the effects of combination of air extraction and nitrogen injection. With the increasing of integration degree, more air is extracted from the air out of the compressor and less air is sent to the combustor when constant air flow rate to the compressor is specified. The nitrogen injection increases to makeup the mass flow deficit caused by the air extraction.

For Case C based on LP-ASU, the plant efficiency is always decreasing with the increase in the air extaction. The reason is that the power consumption by nitrogen compressor is more than the power saving of air compressor of less air feed caused by air extraction.

For the IGCC based on EP-ASU, the efficiency of IGCC increase until the nitrogen injection reaches 98%. The 98% is assumed to be the highest percentage of produced nitrogen that can be used to nitrogen injection (Buchanan, *et al.*, 1998). When the air extraction is 35.9%, the nitrogen injection is just 98.0%. The efficiency of IGCC with EP ASU at this point is 40.59%. With further increase in air extraction, the efficiency of IGCC plant decreases because no more nitrogen can be used to make up the deficit of air extraction. Therefore, based on the design in this study, the optimum air extraction is 35.9%. In another word, the optimum integration degree for IGCC based on

Table 8-9 Case Study Results for Different Integration Degree with Nitrogen Injection (Case C) based on LP-ASU and EP-ASU

Description	C0	C1	C2	C3	C4
Air Extraction, %	0	12.5	25	35.9	37.5
N_2 Injection, %	51.5	67.7	83.9	98.0	98.0
N_2/Syngas(dry) molar ratio	0.604	0.794	0.984	1.150	1.150
H_2O wt% in saturated syngas	0	0	0	0	0
Coal Feed Rate,10^3 lb/hr	186.7	186.7	186.7	186.7	186.7
Nitrogen Feed Rate, 10^3lb/hr	287.7	378.1	468.6	547.4	547.4
Air to GT, 10^3 lb/hr	3,310	3,310	3.31	3.31	3.31
Combustor exhaust flow rate, 10^3lbmole/hr	114.0	114.0	114.0	114.1	113.7
	Case C – LP-ASU				
Gas Turbine Net Power, MW	192.3	192.4	192.5	192.5	191.3
Steam Turbine Net Power, MW	143.5	142.6	141.6	140.8	140.8
Total Auxiliary Load, MW	53.4	55.4	57.5	59.3	59.0
Oxidant Feed, MW	27.4	25.1	22.8	20.9	20.6
Nitrogen Compressor, MW	13.2	17.4	21.5	25.1	25.1
Net Plant Power Output, MW	282.4	279.5	276.6	274.0	273.1
Plant Efficiency, %, HHV	40.42	40.00	39.59	39.22	39.09
SO_2 Emissions, lb/MWh	1.88	1.90	1.92	1.94	1.94
CO_2 Emissions, lb/MWh	1,660	1,670	1,690	1,710	1,710
Relative NO_x Emissions per Unit Output	1.00	0.40	0.17	0.08	0.08
	Case C – EP-ASU				
Gas Turbine Net Power, MW	192.3	192.4	192.5	192.5	191.3
Steam Turbine Net Power, MW	143.6	142.6	141.7	140.9	140.8
Total Auxiliary Load, MW	54.7	53.0	51.3	49.8	49.3
Oxidant Feed, MW	35.1	31.5	27.8	24.7	24.2
Nitrogen Compressor, MW	6.7	8.8	10.9	12.7	12.7
Net Plant Power Output, MW	281.1	282.0	282.8	283.6	282.8
Plant Efficiency, %, HHV	40.24	40.36	40.48	40.59	40.48
SO_2 Emissions, lb/MWh	1.89	1.88	1.88	1.87	1.88
CO_2 Emissions, lb/MWh	1,660	1,660	1,650	1,650	1,650
Relative NO_x Emissions per Unit Output	1.00	0.40	0.16	0.07	0.07

EP-ASU is between 25% ~ 37.5%. This result is consistent with the study result of Holt about the integration of ASU and F class gas turbine in IGCC system (Foster Wheeler, 1999; Holt, 1998). The highest efficiency is about 0.3 percent higher than that of Case C0 with EP ASU and it is about 1% higher than that of nonintegrated design IGCC with LP ASU, 39.41%. The power saving of air compressor caused by air extraction is more than the power consumption of nitrogen compressor. The reason is that in EP ASU, the delivery pressure to nitrogen compressor is higher than that of LP ASU. Thus the power consumption of nitrogen compressor is lower than that in LP ASU. For the integration design with both nitrogen injection and air extraction, EP ASU should be selected to obtain optimal performance.

Considering the emissions, the case C3 with EP ASU have the lowest emissions of SO_2, CO_2, and NO_x than all the other cases from C0 to C4 with LP ASU or EP ASU. The reason is that Case C3 with EP ASU has highest efficiency and high nitrogen injection.

Comparison Case A7-EP ASU and case C3 EP ASU, the efficiency of case A7 is a little higher than that of case C3. In addition, the CO_2 emission of case A7 is lower than that of case C3. Although the NO_x emissions of case C3 is a little lower than that of case A7 due to higher nitrogen injection, the NOx emissions levels of both cases are much lower than the NOx emission level of nonintegrated case. Thus, the Case A7 is a better choice compared to Case C3.

8.6.4 Cost Evaluation

To compare the cost of integrated IGCC base EP ASU and the nonintegrated IGCC system, two cases were selected for comparison that represents a baseline design with no extraction or injection and an alternative design that represents one of the preferred case study results. For the nonintegrated design, Case A0 based on LP ASU was selected since LP ASU is selected. For the latter, Case A7 based on EP ASU was selected because it produced the highest efficiency in the case studies. It also has lowest SO_2 emissions, CO_2 emissions, and low NOx emissions. For nonintegrated IGCC with LP ASU system, a cost model has been developed by Frey and Akunuri (2001). For integrated IGCC with EP ASU design, the cost information is very limited. Thus, an approximate cost estimated is finished in this study. The comparison for case A7-EP ASU and the nonintegrated design IGCC of case A0-LP ASU is listed in Table 8-10.

An important evaluation for cost standard is cost of electricity (COE). To calculate COE, the total capital cost (TCC), fixed operation cost (FOC), and variable operation cost (VOC) should be computed. The capital cost of LP ASU can be calculated by the model of Frey and Akunuri (2001). Based on the report of Amick, *et al.* (2002), the capital cost increase of EP ASU with nitrogen compressor compared to LP ASU without nitrogen compressor is about $9.43 per lb/hr of nitrogen injection. Since the nitrogen injection of case A7-EP ASU is 558,990 lb/hr, the capital cost increase of EP ASU compared to the LP ASU is $5{,}271\times10^3$ $. The integrated IGCC design with EP ASU has no fuel gas saturator since the moisture content in syngas is zero. In this study, the reduction in capital cost if the saturator is not needed was not considered in the analysis,

Table 8-10 Comparison of Costs in for a Base Case and an Alternative Design with Nitrogen Injection [a]

Description, Units	Case A7-EP ASU	Case A0-LP ASU	Relative Difference, %
Nitrogen injection, %	98.0	0	
Moisture Fraction in Syngas, wt %	0	28.2	
Plant Efficiency, %, HHV	40.87	39.47	
Direct Cost, 10^6			
ASU	47.5	42.2	12.6
Steam Turbine	25.6	23.3	
Total Capital Requirement, $/kW [b]	1,880	1,880	
Fixed operation Cost, $/(kW-yr)	64.7	65.7	
Variable operating Cost, mills/kWh	10.0	10.4	
Cost of Electricity, mills/kWh [c]	55.6	56.2	-1.1

[a] Cost is Year 2000 dollars;
[b] Total Capital Requirement includes Total Plant Investments, Startup costs and Land, Inventory Capital, Initial Catalysts and Chemicals;
[c] Fuel Cost = 1.25 $/MMBtu (Jan 2000 Dollars) (Buchanan, *et al*., 1998), Capacity Factor = 0.65.

and thus the TCC for Case A7 may be slightly overestimated. The capital cost of steam turbine in integrated IGCC is higher than that of nonintegrated IGCC plant. The reason is that the steam turbine has larger size in the integrated IGCC plant than that of nonintegrated IGCC plant because more steam is used for power generation due to no steam injection in integrated IGCC of Case A7. For FOC and VOC, it is assumed that there is no obvious difference between two cases with or without nitrogen injection.

The results indicate that the COE of case A7-EP ASU is 1.1% lower than that of case A0-LP ASU though the direct capital cost for the EP ASU with a nitrogen compressor is 12.6% higher than that of LP ASU without a nitrogen compressor. The actual difference in TCC between Case A7 and A0 may be larger than shown here because the cost of saturator is not fully removed in the cost estimate of Case A7. Thus, the cost advantage of Case A7 may be slightly higher than implied by these results.

9.0 SUMMARY, CONCLUSIONS, AND RECOMMENDATIONS

The objective of this study is to evaluate the effects of alternative designs on IGCC performance, emission, and costs. The effects of different fuels, different gas turbine combined cycles, and different integration methods were evaluated. A simplified method for estimating energy and mass balance of gas turbine combined cycle was developed. In order to evaluate the risks of IGCC system associated with advances in gas turbine technology, uncertainty analysis is implemented and key uncertain sources are identified. The work in this study is to provide implications for research direction in future and provide guidelines for potential improvements of IGCC technology.

In this chapter, the summary, conclusions, and recommendation based on this study are introduced.

9.1 Summary

In this section, the objectives, technology options, and methodology of this study are summarized.

9.1.1 Objectives

As a technology in early commercial phase, a lot of research work need to be implemented to provide evaluations of alternative technologies and investigate potential improvements and risks associated with IGCC technology. The evaluation of alternative technologies and potential improvements helps to provide information of development of IGCC technology in future, which may improve the performance of IGCC system and

thus improve the cost competitiveness of this technology. It can also provide guidelines for research direction, plant operation, and decision making. Therefore, the objective of this study is to evaluate the effects on the performance, emissions, and costs of IGCC systems with alternative designs, including different fuels, advances in gas turbine technologies, different integration methods of ASU and gas turbine; to find out a simplified method for estimation and evaluation of process technology; and to quantify the risks associated with IGCC technology.

9.1.2 Technology Options

In this study, the effects of fuel composition on IGCC system is implemented based on three coals, Illinois No. 6 coal, Pittsburgh No.8 coal, and West Kentucky coal. The selection of the three coals is based on the fuels used in the actual projects and design studies of IGCC systems.

The different gas turbine combined cycles selected for evaluation in this study are GE 7F and 7H gas turbine technologies. The 7F gas turbine is used in current IGCC systems and the 7H is the most advanced gas turbine technology at present. The difference of two technologies mainly includes the innovative steam cooling technology used in 7H gas turbine while the conventional air cooling technology used in 7F gas turbine. The comparison of IGCC systems based on these two technology provide implications of the benefits associated with the advanced in gas turbine processes. As an advanced technology, the 7H gas turbine has not been commercially used in IGCC system. Thus, the uncertainty analysis is implemented to evaluate the risks associated with technology advances.

The evaluation of integration of ASU with gas turbine is based on three kinds of integration methods and two kinds of ASU designs. The integration methods selected for evaluation include nitrogen injection, air extraction, and combination of nitrogen injection and air extraction. Different ASU designs include the conventional LP ASU and EP ASU used in current integrated IGCC plant. Integration of ASU and gas turbine has been used in some IGCC projects. However, there is a lack of a systematic evaluation of effects of different integration methods.

9.1.3 Methodology

In this study, the models for Texaco gasifier-based IGCC systems based on different gas turbine combined cycle systems, Frame 7F and 7H, were developed in ASPEN Plus. A spreadsheet model of gas turbine combined cycle was also developed. Uncertainty analysis is applied to the two IGCC systems based on different gas turbines to evaluate and compare the risks associated with the technology advances. The model for ASU is developed and added to the previous IGCC model to simulate different integration methods of ASU and gas turbines.

The performance and cost models incorporates details for evaluation of alternative technologies. The uncertainty analysis is implemented in a probabilistic simulation environment in ASPEN Plus. The rank-order correlation coefficients are used to identify the key uncertain inputs of IGCC system.

9.2 Key Findings

The key findings based on simulation and case studies are summarized as follows:

- A process simulation model of a Texaco gasifier-based IGCC system with radiant and convective design with Frame 7F gas turbine combined cycle was developed, calibrated, and verified both via comparison to published data and via sensitivity analysis. Confidence in the ability of the model to make reasonable predictions was established.
- IGCC system performance, particularly thermal efficiency and emissions of SO_2, are sensitive to fuel properties, such as ash content and sulfur content. The efficiency of IGCC system fueled with West Kentucky coal is 1.7 percents lower than that of the Illinois No.6 coal fueled IGCC system due to highest ash content. The SO_2 emission of IGCC fired with West Kentucky coal is highest one due to highest sulfur content. The capital cost of Illinois No.6 coal based system has lowest capital cost due to lowest carbon feed rate.
- The comparison of IGCC-7FA and IGCC-7H systems based on deterministic modeling indicates that the efficiency of IGCC-7H system is relatively 10% higher than that of IGCC-7FA system and the CO_2 emissions of IGCC-7H system is 10% lower than that of IGCC-7FA system. The COE of IGCC-7H system is approximately 11% relatively lower than that of IGCC-7FA system. Therefore, 7H gas turbine is a promising technology compared to the current used 7FA gas turbine.
- A simplified performance and cost model for a gas turbine combined cycle system implemented in a spreadsheet was verified to respond appropriately to variation in key design and operational factors. For example, the difference

between the model result and the published value of the exhaust flow rate of the syngas fueled gas turbine is only 0.8%.

- The uncertainty analysis provides information about the risks associated with the performance, emissions, and costs of IGCC systems based on 7FA and 7H gas turbine systems. The results indicate the efficiency of 7H based system was higher by an average of 4.2 percentage points than the 7FA based system and with a 95 percent range of 4.1 to 4.7 percentage points of the uncertainty in the difference in efficiency. The SO_2 emissions of IGCC-7FA system have similar uncertainty range compared to IGCC-7FA system. The total capital cost (TCC) of IGCC-7H system is lower than that of IGCC-7FA system and the 95% uncertainty range of TCC of 7H based system is 1598 to 1840 $/kW. The COE of IGCC-7H system is lower by an average 6.1$/kWh than that of the 7FA based system and with a 95 percent range of –7.0 to –5.5$/kWh of the uncertainty in the difference of COE of two systems.
- The findings of ASU integration indicates that with nitrogen injection increasing, the efficiency of IGCC based on EP ASU is approximately 2 percents higher than nonintegrated design while it is 1 percent increase of IGCC based on LP ASU with same nitrogen injection. The emissions based on power output of IGCC with EP ASU are lower than that of IGCC with LP ASU when the injection is more than 60%.
- The design of air extraction design is not preferred due to low efficiency compared to other integration methods.

- For combination of air extraction and nitrogen injection, optimal design is 25% to 50% integration degree with an EP ASU, under which the IGCC has highest efficiency and lowest emissions. The results provide the integration principle to obtain optimal performance.

The conclusions based on finding of simulation and case study of different fuels, gas turbine combined cycles, and different integration methods of ASU and gas turbine is summarized. In addition, the conclusion of uncertainty analysis is introduced.

9.2.1 Coal Properties

The performance and cost of IGCC system based on three coals, Illinois No.6 coal, Pittsburgh No. 8 coal, and West Kentucky coal, are compared to each other. The results of case study of three different coals indicate the syngas produced from Illinois No. 6 coal has highest heating value, while the syngas produced by West Kentucky coal has lowest efficiency. The efficiency of IGCC fueled with West Kentucky coal is 1.7 percents lower than that of IGCC fueled with Illinois No. 6 coal because the West Kentucky coal has higher ash content compared to Illinois No. 6 coal. The efficiency of Pittsburgh based system is 0.6 percent lower than that of Illinois No.6 coal due to the same reason. Therefore, the efficiency of IGCC plant is related with the syngas heating value of coals. Different coals compositions have different heating value syngas. For same IGCC design, the high plant efficiency is related with high heating value syngas.

The sulfur content of fuel is an important source of SO_2 emissions. The IGCC system based on Pittsburgh No.8 coal has lowest SO_2 emissions due to the lowest sulfur content of the coal.

The capital cost of IGCC system fired with West Kentucky coal has highest value than IGCC system fired with other two coals. The reason is that the West Kentucky coal has the highest coal flow rate and the highest oxygen consumption, which lead to higher capital cost of coal treatment, oxidant feed, and gasification. The capital cost of IGCC system fired with West Kentucky coal is 6% higher than that of Illinois No.6 coal fueled system.

The coal parameters have important effects on performance, emission, and costs of IGCC systems. For the wide variety in coals or other fuels compositions, the design of IGCC systems should be considered based on certain fuels parameters, such as an acid gas removal unit with high efficiency is required for high sulfur content fuel.

9.2.2 Advanced Gas Turbine Designs

The deterministic modeling results of IGCC systems based on 7FA and 7H system are compared to each other for the main outputs. The comparison indicates the advance in gas turbine technology has large benefits for the performance, emissions, and costs of IGCC. For example, the efficiency of IGCC-7H is relatively 10% higher than that of IGCC-7FA system. The COE of IGCC-7H is approximately 11% lower than that of IGCC-7FA system. Although the direct cost of 7H gas turbine is much higher than that of 7FA gas turbine, the COE of IGCC-7H system is lower than that of IGCC-7FA system due to improvements in plant efficiency. The two systems have similar SO_2 and NO_x emissions on energy input basis, while the CO_2 emissions of IGCC-7H system is about 10% lower that of IGCC-7FA system due to more efficient utilization of coal.

9.2.3 Simplified Modeling Approaches

The above two gas turbine models are both developed in ASPEN Plus. In this study, another performance model for simple and combined cycle gas turbine systems was developed using an EXCEL spreadsheet. The mass and energy balance of a simple cycle and combined cycle gas turbine model was implemented and the multiple stages of the compressor and turbine and cooling air splits were simulated. The use of the combined cycle model was demonstrated considering two cases of natural gas and syngas. In the combined cycle case study based on sygnas, the heat from gas cooling recovered in the steam cycle and the heat deduction due to steam or water injection to the syngas were estimated. The gas turbine model was calibrated based on natural gas and syngas for a typical “Frame 7F” heavy duty gas turbine. The calibration results indicated that the gas turbine model can predict the performance of the gas turbine well for model outputs that were not used as a design basis for the calibration. The difference between the estimated result and published value for the exhaust flow rate of gas turbine based on syngas is only 0.8%. The estimate of steam turbine power output based on syngas is only 0.1% different from the reference value. For natural gas fueled gas turbine model, the difference between the estimates and the reference values are only 1% or 2%.

Based on the process of simulation and calibration and the sensitivity analysis, the important sensitive inputs for the gas turbine model are (1) gas turbine specifications, including compressor pressure ratio, turbine inlet temperature, and turbine inlet reference mass flow, and exhaust temperature; (2) syngas characteristics, including heating value, moisture fraction, and compositions; (3) turbine adiabatic efficiency and compressor adiabatic efficiency; (4) generator efficiency; (5) ambient pressure; (6) steam cycle heat

rate. It is important to have correct values for the sensitive inputs to obtain accurate estimate of gas turbine performance. The inputs of moderate sensitivity include the ambient temperature, combustor pressure drop, turbine back pressure, air cooling fractions, and HRSG outlet temperature. The input of compressor pressure ratio is identified as low sensitive input in gas turbine model. Therefore, users should focus on the key sensitive inputs first when the estimates values are abnormal.

The results indicate this model can be used to estimate the performance of gas turbine fired with different syngas compositions. The sensitivity analysis of the inputs gives the insights of the important effective factors for estimating the gas turbine performance. This work provides guidelines to judge the accuracy of estimates from the gas turbine model by considering the expected change in outputs caused by the relative change of the inputs. It demonstrated that an accurate and sensitive model can be implement in a spreadsheet, which makes the model much easier to be used and more accessible than model in ASPEN Plus since one does not have to be trained in the use of ASPEN. This study implicated the ability to do desktop simulations to support policy analysis.

9.2.4 Probabilistic Analysis of Process Technologies

In this study, a stochastic process simulation model was developed to evaluate the performance, emissions, and cost of two IGCC systems based on 7FA (IGCC-7FA) and 7H gas turbines (IGCC-7H). The probabilistic analysis provides information about the uncertainty of the main outputs, which are the interaction results of the uncertainties in inputs. The comparison of uncertainty range associated with the performance and costs of

a technology provide another principle for technology selection. Key uncertain inputs were identified for two systems. The gasifier carbon conversion is the most important uncertain input for performance and emissions and the project uncertainty is the most important uncertain input for the cost of electricity.

The comparison of deterministic results and probabilistic results provides information of the potential downside risks of advanced process technology. For example, there are about 80% chance that the efficiency of IGCC-7H system is lower than deterministic result. That means the deterministic result may overestimate the efficiency. The reason is that the deterministic results are based on the optimal inputs values. The deterministic values of inputs may be different from the mean of the possible values of inputs, while it represents the optimal condition of the uncertain inputs. Thus, the optimal inputs lead to the "best guess" of outputs. For example, the most important input for plant efficiency is the carbon conversion. Its deterministic value is 0.99 and its distribution is from 0.96 to 1.00 of a triangle distribution. The mean is 0.98 and it is about 1% lower than the mode of 0.99. The mean of the uncertainty range of efficiency for the IGCC-7H system is also about 1% lower than the "best guess" result. This indicates that the deterministic analysis provide the estimates of a technology based on conservative conditions and cannot provide the information associated with the risks of the technology, such as low efficiency, high emissions, and high costs. In addition, the probabilistic analysis provides a method to estimate the outputs based on simultaneous variations in several parameter, which cannot be realized by sensitivity analysis.

The uncertainty in the difference of efficiency, emissions, and cost of electricity of IGCC-7FA and IGCC-7H system are characterized by CDF. The results indicate that the IGCC-7H system always has higher efficiency, lower CO_2 emissions, and lower cost of electricity compared to IGCC-7FA systems despite the uncertainties of inputs. The IGCC-7H system was clearly superior to the IGCC-7F systems. This indicates that as an advanced gas turbine technology, the 7H gas turbine is a promising technology for improving the performance and lowering the cost of IGCC system though there is still lack of complete knowledge regarding this technology.

In order to find out the key sources for uncertainty in outputs, Spearman rank-order correlation coefficient is used. Total 13 uncertain inputs are identified as key uncertain inputs. The results based upon of key uncertain inputs are compared to overall uncertain inputs and the results are very close to each other. Therefore, the key uncertain inputs are the main factor driving the uncertainty of the outputs. In addition, the identification of key uncertain inputs provides guidelines for operation of IGCC plant. In order to reduce the risks in performance, emissions, and costs, the attention should focus on the key input parameters. For example, the uncertainty of carbon conversion can be reduced by carefully controlling the gasification temperature and pressure. The uncertainty in the input of project uncertainty can be reduced by developing a more detailed cost model. Therefore, the identification of key inputs uncertainties can provide guidelines of potential research direction in future and the operation of IGCC plant.

This study illustrated that the probabilistic analysis can be used to identify the key uncertainties in process design, to improve the designs of IGCC systems, to compare the

trade-offs between different configurations. This method provides a systematic framework for technology evaluation and risk assessment of new process technologies, such as advanced gas turbine combined cycle. Identification of key uncertain inputs provides principle for research direction and decision making of development, and operation of IGCC plants.

9.2.5 Integration of ASU and Gas Turbine

In this study, another potential improvement of IGCC technology, the integration of ASU and gas turbine, is investigated. A process model for ASU is developed in ASPEN Plus to simulate LP ASU and EP ASU. A complete IGCC model containing ASU blocks was developed to simulate different integration methods of ASU and gas turbines. The performance of IGCC system under different integration methods were estimated and evaluated. The development of ASU models and the combination of ASU models with other parts of the IGCC model enables evaluation of the effect of the changes in the design parameters and connection methods of multiple blocks according to different design requirements of the integration ASU systems. Therefore, this study provided insights of the benefits of process simulation for evaluating complicated system designs.

For nitrogen injection design, the efficiency of IGCC system has 1 to 2 percents increase. The emissions of SO_2, NO_x, and CO_2 decreases with nitrogen injection increasing with EP ASU design. For only air extraction design, the efficiency of IGCC system decreases with the integrated degree increasing. The “integration degree” is defined as the fraction of air extraction in the total air requirement of ASU. Thus, the

only air extraction design is not preferred. For the combined nitrogen injection and air extraction, optimal integration for highest efficiency is found between 25% to 50%. The results provide the integration principle to obtain optimal performance.

The selection of LP ASU and EP ASU should consider the nitrogen injection fraction and integration degrees. The LP ASU is preferred for nonintegrated system because it has less power consumption than EP ASU and thus leads to higher efficiency. The EP ASU is preferred when the nitrogen injection is higher than 60% and the design of combination of nitrogen injection and air extraction.

The cost comparison indicated the integrated EP ASU design has higher direct cost than the nonintegrated LP ASU design due to the additional cost of nitrogen compressor in integrated system. However, the integrated IGCC has lower COE than the nonintegrated IGCC with LP ASU due to higher efficiency.

This study provides guidance for integration design of IGCC system through comparing nitrogen injection and air extraction, and EP ASU and LP ASU. Nitrogen injection with the EP ASU design is a preferred choice considering the efficiency, emissions, and cost of IGCC technology.

9.2.6 Key Conclusions

The key conclusions of this study are:

- Fro the same IGCC design, the performance, emissions, and costs of IGCC system are significantly influenced by coal properties, including ash content and sulfur content. The design of IGCC system should consider the fuel parameters.

- Advances in gas turbine design will significantly improve the performance, emissions, and cost of IGCC systems. The IGCC system based on the Frame 7H gas turbine is preferred to the Frame 7F based IGCC system and indicates the benefits of gas turbine technology advances for IGCC system.
- Uncertainty analysis provided insight regarding risks associated with IGCC systems, including risks of low efficiencies, high emissions, and high costs. The identification of key uncertain inputs helps prioritize research direction and strategies for improving plant operation.
- The integrated IGCC system based on only nitrogen injection has substantial benefits in increasing efficiency and lowering emissions compared to nonintegrated design. The only air extraction design has no benefits for improving IGCC performance and is not preferred. The optimal integration degree of combination nitrogen injection and air extraction is between 25% to 50% for EP ASU. The design of integration with nitrogen injection has cost advantage compared to the nonintegrated design.
- The EP ASU is preferred to LP ASU as nitrogen injection fraction is higher than 60%. For combination of nitrogen injection and air extraction, EP ASU should be used.

9.3 Recommendations

Based upon the conclusions, the recommendations for development of IGCC technology is:

- The Frame 7H gas turbine combined cycle is a promising technology for improving IGCC performance and lowering cost of electricity. The advances in

gas turbine enable the IGCC to be a cost-competitive technology compared to traditional PC technology. Therefore, the Frame 7H gas turbine should be used in IGCC system in future and further advances in gas turbine technology should be made to improve performance and thus lower the cost of IGCC system.

- Uncertainty analysis should be applied to evaluation of alternative process technologies, which provides a more objective comparison of alternative technologies than the deterministic comparison based on optimal conditions. Future research priorities for improvement in plant operation should focus on the key uncertain or variable inputs. Reducing the uncertainty in key uncertain inputs helps to reduce the downside risks associated with outputs, such as the risk of lower than anticipated system efficiency.
- Among ASU integration strategies, nitrogen injection alone was found to provide substantial benefits and was more important than air extraction alone. Furthermore, nitrogen injection alone provides benefits comparable to the combination of air extraction and nitrogen injection together. Because air extraction requires very close process integration and control between the gas turbine and ASU, it can be difficult to implement. In contrast, nitrogen injection can be supplemented with water injection to achieve NOx control and power augmentation in the gas turbine, and thus there is flexibility to achieve system performance even if there is fluctuation or loss of the nitrogen steam during a process update. Thus, ASU integration based only on nitrogen injection is recommended as a practical approach for improving system performance.

- For the nitrogen injection design, the choice of EP ASU or LP ASU depends on the nitrogen injection fraction. For the integration design of combination air extraction and nitrogen injection, EP AUS should be selected.

Recommendations for future studies:

- For the uncertainty analysis, the uncertain inputs are treated as independent variables. However, some inputs may be correlated with other inputs. For example, the carbon conversion may be affected by the gasifier temperature and pressure. Future work should consider the effects of the correlation between inputs on the outputs. In another hand, the uncertainty of carbon conversion can be reduced by strictly controlling of gasification temperature and pressure during plant operation process. Thus the uncertainty in outputs is reduced.
- The effects of new air separation technology on IGCC performance should be investigated in future. The technology of OTM has not yet been commercially demonstrated, but has potential benefits in lowering cost and improving efficiency of IGCC system. Estimation and evaluation of the effects of these new technologies may provide guidance of future research direction in the area of application of ASU.
- A new cost model for EP ASU should be developed in future as more cost data become available. In general, key components of the IGCC process simulation models for both performance and cost should be updated as new data become available.

- One or more standard IGCC systems should be developed to provide a consistent basis for benchmarking, verification, and comparison. A difficulty in modeling IGCC systems is that it is difficult to find a consistent basis for verification. In order to arrive at an objective and nonproprietary standard benchmark for which detailed process data (i.e. temperature, pressure, flowrate, and composition of major streams, etc.) can be publicly reported, the needed information should be collected from multiple groups, including the key technology vendors (e.g., gasification, gas turbine, ASU, others), and the process technology modelers who are independent of the vendors (e.g., universities). This work should be sponsored by related departments, e.g., DOE, to involve the information from different groups. For the work in this area, a performance test code (ASME PTC 47) has been developed for IGCC system (Anand, *et al.*, 2003). The purpose of the code is to provide testing procedures to determine performance of IGCC system and the steams flows and properties. The results of the code can be used to compare performance against plant design rating, while does not provide a basis for comparing performance against different plant designs. In addition, the code does not provide information of the costs of IGCC system. Therefore, there is still a lot of work need to be done in this area.

REFERENCES

Allam, R.J., Foster, E.P. and Stein, V.E. (2002), "Improving Gasification Economics through ITM Oxygen Integration," the 5th (IChemE) European Gasification Conference, Noordwijk, The Netherlands, April 8-10, 2002

Akunuri, N. V. (1999), "Modeling the Performance, Emissions, and Costs of Texaco Gasifier-Based Integrated Gasification Combined Cycle Systems," Master's Thesis, Department of Civil Engineering, North Carolina State University, Raleigh, North Carolina, 1999.

Amick, P., Herbanek, R., Jones, R.M. (2002), "NOx Control for IGCC Facilities Steam vs. Nitrogen," The 2002 *Gasification Technologies Conference*, San Francisco, California, October 28-30, 2002.

Ang, A.H.-S, and Tang, W.H. (1984), "Probability Concepts in Engineering Planning and Design," Decision, Risk and Reliability. Volume 2. John Wiley and Sons: New York

Anderson, F.E. (1993), "Generator Cooling, Air or Hydrogen?" GER-3738B, the 37th GE Turbine State-of-the-Art Technology Seminar, GE Power Generation, Schenectady, NY, July 1993.

Andersson, K., Birkestad, H., Maksinen, P., Johnsson, F., Stromberg, L., Lyngfelt, A. (2002), "An 865 MW Lignite Fired CO_2 Green Power Plant-A Technical Feasibility Study," The Sixth International Conference on Greenhouse Gas Control Technologies, Kyoto, Japan, October.

Anand, A.K., Cook, C.S., Corman, J.C., and Smith, A.R. (1996), "New Technology Trends for Improved IGCC System Performance,' *Journal of Engineering for Gas Turbines and Power*, vol. 118(4): 732-736.

Anand, A., Horazak, D., Doering, E., and Le, P. (2003), "ASME PTC 47: Performance Test Codes for IGCC Plants," The 2003 Gasification Technologies Conference, San Francisco, California, October 12-15, 2003.

Aspen Technology, Inc. (1994), ASPEN PLUS Manual, Cambridge, MA.

Bechtel Corp., Global Energy Inc., and Nexant Inc. (2002), "Gasification Plant Cost and Performance Optimization: Task 1 Topical Report, IGCC Plant Cost Optimization," Contract No. DE-AC26-99FT40342, Prepared by Bechtel Corp., Global Energy Inc., and Nexant Inc. for the U. S. Department of Energy, National Energy Technology Laboratory (NETL), Morgantown, West Virginia, May.

Bolland, O. and Mathieu, P. (1998), "Comparison of Two CO_2 Removal Options in Combined Cycle power Plants," *Energy Conversion and Management*, 39(16-18): 1653-1663.

Brdar, R.D. and Jones, R.M. (2000), "GE IGCC Technology and Experience with Advanced Gas Turbines," GE Power Systems, Schenectady, NY.

Brooks, F. J. (2000), "GE Gas Turbine Performance Characteristics," GER-3567H, GE Power Systems, Schenectady, Now York, October 2000.

Brun, K. and Jones, R. M. (2001), "Economic Viability and Outlook of IGCC form a Gas Turbine Manufacturer Perspective," The 2001 *Gasification Technologies Conference*, San Francisco, California, October 2001.

Buchanan T.L., DeLallo M.R., Goldstein H.N., Grubbs G.W., Whites J.S. (1998), "Market-based Advanced Coal Power Systems," Contract No. DE-AC01-94FE62747, prepared by Parsons Infrastructure and Technology for the U.S. Department of Energy, Office of Fossil Energy, Washington DC, December 1998.

Berkenpas, M.B., H.C. Frey, J.J. Fry, J. Kalagnanam, and E.S. Rubin (1999), "Integrated Environmental Control Model: Technical Documentation," Prepared by Carnegie Mellon University for U.S. Department of Energy, Pittsburgh, PA. May 1999.

Burns and Roe-Humphreys and Glasgow Synthetic Fuels, Inc. and General Electric Company (1984), "Coproduction of Methanol and Electricity," EPRI AP-3749, Projects 2029-1, 2029-2, Final Report, Prepared for Electric Power Research Institute, Palo Alto, California.

Cargill, P., DeJonghe, G., Howsley, T., Lawson, B., Leighton, L., and Woodward, M. (2001), "Pinon Pine IGCC Project," DE-FC21-92MC29309, Prepared by Sierra Pacific Resources for the Department of Energy, Morgantown, West Virginia, January 2001.

Caputo, C., Wallace, P., and Bazzoon, L. (2000), "Repowering Conventional Coal plants with Texaco Gasification: The Environmental and Economic Solution," the 2000 *Gasification Technologies Conference*, San Francisco, CA, October, 2000

Carcasci, C. and Facchini, B. (2000), "Comparison between two Gas Turbine Solutions to increase combined power plant efficiency," *Energy Conversion & Management*, 41(2000): 757-773.

Chambers, A. (2000), "Creative Adaptation of Daily Business Key to Success in Evolving Industry," *Power Engineering*, 104(1): 36.

Chemical Engineering Editorial Staff (1984-2003), Chemical Engineering Plant Cost Index (CEPCI). *Chemical Engineering*, 1984-2003.

Coca, M.T., Méndez-Vigo, I., Elias, F.A. (1998), "Coal Gasification. Conception, Implementation and Operation of the ELCOGAS IGCC Power Plant," ELCOGAS, S.A.,

The 17th World Energy Congress, Houston, Texas, September 1998.

Collodi, G. (2000), "Operation of ISAB Energy and Sarlux IGCC Projects," the 2000 *Gasification Technologies Conference*, San Francisco, California, October 8-11, 2000.

Condorelli, P., Smelser, S.C., and McCleary, G. J. (1991), "Engineering and Economic Evaluation of CO_2 Removal From Fossil-Fuel-Fired Power Plants, Volume 2: Coal Gasification-Combined-Cycle Power Plant," prepared by FLUOR DANIEL, Inc. for Internal Energy Agency, Paris, France, and EPRI, Palo Alto, California, June.

Cullen A.C. and Frey H.C. (1999). Probabilistic Techniques in Exposure Assessment: a Handbook for Dealing with Variability and Uncertainty in Models and Inputs. Plenum: New York.

delaMora, J.A., Grisso, J.R., Klumpe, H.W., Musso, A., Roszkowski, T.R., Thompson, B.H., Lienhard, H., and Beyer, T. (1985), "Evaluation of the British Gas Corporation /Lurgi Slagging Gasifier in Gasification-Combined-Cycle Power Generation," EPRI AP-3980, Prepared by Ralph M. .Parsons Company, British Gas Corporation, and Lurgi, GMBH for Electric Power Research Institute, Palo Alto, California.

Diwekar, U.M. and Rubin, E.S.(1991), "Stochastic Modeling of Chemical Processes," *Computers and Chemical Engineering*, 15(2): 105-l 14.

Diwekar, U.M., Rubin, E.A. and Frey, H.C.(1997), "Optimal Design of Advanced Power Systems under Uncertainty," *Energy Conversion & Management*, 38(15-17):1725-1735.

DOE (2003), "The turbine of Tomorrow," Office of Fossil Energy, the U.S. Department of Energy, Washington, DC. January 2004.
(URL: http://www.fe.doe.gov/programs/powersystems/turbines/)

DOE (2004), "Clean Coal Power Initiative," Office of Fossil Energy, the U.S. Department of Energy, Washington, DC. January 2004.
(URL: http://www.fe.doe.gov/programs/powersystems/cleancoal/)

EIA (2004), "United States Country Analysis Brief," Energy Information Administration, Washington, DC. April 2004. (URL: http://www.eia.doe.gov/emeu/cabs/usa.html)

Eldrid, R., Kaufman, L., and Marks, P. (2001), "The 7FB: The Next Evolution of the F Gas Turbine," GER-4194, GE Power Systems, Schenectady, Now York, April 2001.

EPA (1995), "Texaco Gasification Process," EPA 540/R-94/514a, United States Environmental Protection Agency, Center for Environmental Research Information Cincinnati, Ohio, April 1995.

EPRI (1986), "TAG(tm) – Technical Assessment Guide, Volume 1: Electricity Supply-1986," EPRI P-4463-SR. Electric Power Research Institute, Inc. December 1986.

Eric, G. (2000), "The F Technology Experience Story," GE Power Systems, Atlanta, GA, GER-3950C, October 2000.

Eric, G.(1986), "The F Technology Experience Story," GE Power Systems, Atlanta, GA, GER-3950C, October 2000.

Falsetti, J.S., De Puy, R.A., Brdar, D., Anand, A., and Paolino, J. (2000), "From Coal or Oil to 550 MWe via 9H IGCC," the 2000 *Gasification Technologies Conference*, October 19.

Fluor Engineers, Inc. (1984), "Cost and Performance for Commercial Applications of Texaco gasifier-based Gasification-combined-Cycle Plants, Volume 2: Design Details," EPRI AP-3486, Prepared for Electric Power Research Institute, Palo Alto, California.

Foster Wheeler (1999), "Optimizing IGCC Design," *Foster Wheeler Review*, Autumn 1999, pp. 17-21.

Frey, H.C. and Akunuri, N.V. (2001), "Probabilistic Modeling and Evaluation of the Performance, Emissions, and Cost of Texaco Gasifier-based Integrated Gasification Combined Cycle Systems using ASPEN," Prepared by North Carolina State University for Carnegie Mellon University and U.S. Department of Energy, Pittsburgh, PA. January 2001.

Frey, H.C. and Rubin, E.S. (1990), "Stochastic Modeling of Coal Gasification Combined Cycle Systems: Cost Models for Selected Integrated Gasification Combined Cycle (IGCC) Systems," DOE/MC/24248-2901, Prepared by Carnegie-Mellon University for U.S. Department of Energy, Morgantown, West Virginia, June 1990.

Frey, H.C. and Rubin, E.S. (1991a) "Development and Application of a Probabilistic Evaluation for Advanced Process Technologies," DOE/MC/24248-3015, Prepared by Carnegie Mellon University for U.S. Department of Energy, Morgantown, West Virginia, April, 1991.

Frey, H.C. and Rubin, E.S.(1991b), "Probabilistic Evaluation of Advanced SO_2/NO_X Control Technology," *J. Air. Waste Manage. Assoc.*, 41(12):1585-1593.

Frey, H.C., and E.S. Rubin (1992), "Integration of Coal Utilization and Environmental Control in Integrated Gasification Combined Cycle Systems," *Environmental Science and Technology*, 26(10):1982-1990.

Frey, H.C., Rubin, E.D. and Diwekar, U.M. (1994), "Modeling Uncertainties in Advanced Technologies: Application to a Coal Gasification System with Hot-gas Cleanup," *Energy*, 19 (4): 449-463.

Frey, H.C. and Rubin, E.S. (1997), "Uncertainty Evaluation in Capital Cost Projection," Encyclopedia of Chemical Processing and Design 1997; Vol. 59, J.J. McKetta, ed., Marcel Dekker: New York, pp. 480-494.

Gebhardt E. (2000), "The F Technology Experience Story," GER-3950C 2000. GE Power Systems, Atlanta, GA.

Hasegawa, T.; Hisamatsu, T.; Katsuki, Y.; Sato, M.; Kopizumi, H.; Hayashi, A.; Kobayashi, N. (2003), "Development of Low NO_x Combustion Technology in Medium-Btu Fueled 1300 ^oC-Class Gas Turbine Combustor in an Integrated Coal Gasification Combined Cycle," ASME *Journal of Engineering for Gas Turbines and Power*. 125(1): 1-10.

Helton, J.C. and Davis, F.J.(2002), "Illustration of Sampling-Based Methods for Uncertainty and Sensitivity Analysis," *Risk Analysis*, 22(3):591-622.

Holt N. (1998), "IGCC Power Plants – EPRI Design & Cost Studies," 1998 *Gasification Technologies Conference*, San Francisco, CA, October 6, 1998.

Holt, N. (2003), "Operation experience and improvement opportunities for coal-based IGCC plants. *Materials at High Temperatures*, 20(1): 1-6.

Hope, C. (1996), "Uncertainty in full fuel cycle costs," *Energy Conversion and Management*, 37(6-8): 825-830.

Hornick, M. J. and McDaniel, J. E. (2002), "Tampa Electric Polk Power Station Integrated Gasification Combined Cycle Project," Final Technical Report, DE-FC-21-91MC27363, prepared for the U. S. Department of Energy, Office of Fossil Energy, National Energy Technology Laboratory (NETL): Morgantown, West Virginia, August 2002.

Jacob, J. T. and Chu, L.A. (1988), "Evaluation of a Texaco Gasification-Combined-Cycle Plant with Kraftwerk Union Gas Turbines," prepared by FLUOR DANIEL, Inc. for EPRI, Palo Alto, California, December.

Jones, R.M., Wolff, J., and GmbH U., (2002), "Reducing CO_2 Emission by Hydrogen IGCC Power Plants," The 2002 *Gasification Technologies Conference*, San Francisco, California, October 28-30, 2002.

Matta, R.K., Mercer, G.D., and Tuthill R.S. (2000), "Power System for the 21st Century-'H' Gas Turbine Combined-Cycles," GER-3935B, GE Power Systems, Schenectady, NY, October 2000.

McDaniel J.E. and Shelnut, C.A. (1999), "Tempa Electric Company Polk Power Station IGCC Project Status," The 1999 Gasification Technologies Conference, San Francisco, California, October 17-20.

McDougald, N. K. (2003), "Demonstration of the Surface Stabilized Combustor for Advanced Industrial Gas Turbines," Distributed Energy Resources Peer Review, December 2-4, 2003, Washington, DC.

MIT(1987). ASPEN User Manual, Volumes 1 and 2. Prepared by Massachusetts Institute of Technology for U.S. Department of Energy, Morgantown Energy Technology Center: Morgantown, West Virginia. May 1982, Revised 1987.

Moliere, M. (2002), "Benefiting from the Wide Fuel Capability of Gas Turbines: a Review od Application Opportunities," GT-2002-30017, Proceedings of ASME TURBO EXPO 2002, June 3-6, 2002, Amsterdam, The Netherland.

Morgan, M. and Henrion, M. (1990), Uncertainty: a Guide Dealing with Uncertainty in Quantitative Risk and Policy Analysis. Cambridge University Press: New York.

Mudd, M.J. (2003), "IGCC's Chasm-What Drives Technology Choices?" The 2003 *Gasification Technologies Conference*, San Francisco, California, October 12-15, 2003.

O'Keefe, L.F. and Sturm, K.V., (2002), "Clean Coal Technology Options – A Comparison of IGCC vs. Pulverized Coal Boilers," The 2002 *Gasification Technologies Conference*, San Francisco, California, October 28-30, 2002.

Parkinson, G. (2004), "OEMs getting ready for coal gasification," *Turbomachinery International*, 45(6): 6-8.

Pate´-Cornell E.(2002), "Risk and Uncertainty Analysis in Government Safety Decisions," *Risk Analysis*, 22(3): 633-646.

Pechtl, P.A. *et al.* (1992) "Evaluation of 450-Mwe BGL GCC Power Plants Fueled with Pittsburgh #8 Coal," Prepared by Bechtel Group, Inc.; British Gas plc.; Lurgi Gmbh.; GE Power Generation and Lotepro Corp. for Electric Power Research Institute: Palo Alto, CA.

Prasad, R., Chen, J., Hassel, B.V., Sirman, J., White, J., Apte, P., Aaron, T., Shreiber, E. (2002), "Advances in OTM Technology in IGCC," Nineteenth Annual International Pittsburgh Coal Conference, September 23–27, 2002, Pittsburgh, PA

Preston, W.E. (2001), "Texaco Gasification 2001 Status and Path Forward," The 2001 *Gasification Technologies Conference*, San Francisco, California, October 2001.

Ratafia-Brown, J.A., Manfredo, L.M., Hoffmann, J.W., and Ramezan, M. (2002a), "Major Environmental Aspects of Gasification-based Power Generation Technologies," Final Report, Prepared by Science Applications International Corporation for Gasification Technologies Program, U.S. Department of Energy, Washington DC, December 2002.

Ratafia-Brown, J.A., Manfredo, L.M., Hoffmann, J.W., Ramezan, M., and Stiegel, G.J. (2002b), "An Environmental Assessment of IGCC Power Systems," the Nineteenth Annual Pittsburgh Coal Conference, Pittsburgh, PA, September 23-27, 2002.

Rhodes, A. K. (1996), "Kansas Refinery Starts up Coke Gasification Unit," *Oil & Gas Journal*, 94(32):43.

Richter, N. (2002), "Introduction to Gasification," Presented at the gasification technologies public policy workshop, Washington, DC, October 1, 2002.

Rubin, E.S., J.S. Salmento, J.G. Barrett, C.N. Bloyd, and H.C. Frey (1986), "Modeling and Assessment of Advanced Processes for Integrated Environmental Control of Coal-Fired Power Plants," NTIS DE86014713, Prepared by Carnegie-Mellon University for the U.S. Department of Energy, Pittsburgh, Pennsylvania, July 1986.

Rubin, E.S., J.S. Salmento, and H.C. Frey (1988), "Cost-Effective Emission Controls for Coal-Fired Power Plants," *Chemical Engineering Communications*, 74:155-167 (1988).

Rubin, E.S., J.S. Salmento, H.C. Frey, A. Abu-Baker, and M. Berkenpas (1991), "Modeling of Integrated Environmental Control Systems for Coal-Fired Power Plants," Final Report, DOE Contract No. DE-AC22-87PC79864, Prepared by Carnegie-Mellon University for the U.S. Department of Energy, Pittsburgh, Pennsylvania, April 1991.

Rubin, E.S., Kalagnanam, J.R., Frey, H.C. and Berkenpas, M.B. (1997), "Integrated Environmental Control Modeling of Coal-Fired Power Systems," *J. Air & Waste Manage. Assoc.*, 47(11): 1180-1188.

SAS OnlineDoc 1999. SAS Institute Inc., Cary, NC, USA.

Schwager, J. and Whiting, K. (2003), "Progress Towards Commercialization Waste Gasification," 2003 Gasification Technologies Conference, San Francisco, CA, October 14, 2003.

Schimmoller, B.K.(1998), "Technology pushes gas turbines higher," *Power Engineering*, 102(4):1, April 1998.

Smelser, S.C., Stock, R.M., and McCleary, G.J.(1991), "Engineering and Economic Evaluation of CO_2 Removal from Fossil-Fuel-Fired Power Plants, Volume 1: Pulverized-Coal-Fired Power Plants," EPRI IE-7365, Prepared by FLOUR DANIEL, Inc. for EPRI, Palo Alto, California, June 1991.

Simbeck, D.R., Dickenson, R.L., and Oliver, E.D. (1983), "Coal Gasification Systems: A Guide to Status, Applications and Economics," AP-3109, Prepared by Synthetic Fuel Associates, Inc. for Electric Power Research Institute: Palo Alto, California.

Simbeck, D. and Johnson, H. (2001), "World Gasification Survey: Industry Trends & Developments," 2001 *Gasification Technologies Conference*, San Francisco, California, October 2001.

Smith, A.R.; Klosek, J.; Woodward, D.W. (1997), "Next-generation Integration Concepts fro Air Separation Units and Gas Turbines," *Journal of Engineering for Gas Turbines and Power*, 119(2), pp. 298-304.

Smith, D. (1999), "First H System Gas Turbine Planned for Baglan (advanced steam-cooled gas turbine to be developed in South Wales)," *Modern Power System*, 19(5):37, May 1999.

Smith, R.W., Polukort, P., Maslak, C.E., et al (2001), "Advanced Technology Combined Cycle," GER-3936A, GE power System, Schenectady, NY, 2001.

Sturm, K.V., Liaw, V., and Thacker, P.S. (2003), "Beyond the 2002 ChevronTexaco coal IGCC Reference Plant," 2003 Gasification Technologies Conference, San Francisco, California, October 2003.

Supp, E. (1990), How to Produce Methanol from Coal. New York: Springer-Verlag.

Texaco Power Services (2001), "CITGO Lake Charles IGCC Project Update", 2001 *Gasification Technologies Conference*, San Francisco, California, October 2001.

Thomas, M., (2001), "Performance and Cost Models of Oxygen Generation Plants for the IECM," Master Thesis, Department of Engineering and Public Policy, Carnegie Mellon University, Pittsburgh, PA, December 20, 2001.

Trapp, B., Moock, N., and Denton, D. (2004), "Coal gasification: Ready for prime time," *Power*, 148(2): 42.

User's Guide of ASPEN Plus Version 10.1(1988), Aspen Technology, Inc., Cambridge, Massachusetts, August, 1988.

Vatavuk, W. M. (2002), "Updating the *CE* Plant Cost Index", *Chemical Engineering*, 109 (1): 62-63, January 2002.

Wark, K. (1983). *Thermodynamics*, Fourth Edition. McGraw-Hill Book Company: New York.

Wabash River Energy Ltd. (2000), "Wabash River Coal Gasification Repowering Project," Final Technical Report, prepared for the U. S. Department of Energy, Office of Fossil Energy, National Energy Technology Laboratory (NETL), Morgantown, West Virginia, August.

Wilkinson, M.B., Boden, J.C., Panesar, R.S., Allam, R.J. (2001), "CO_2 Capture via Oxyfuel Firing: Optimization of a Retrofit Design Concept for a Refinery Power Station Boiler," First National Conference on Carbon Sequestration, May 15-17 2001, Washington DC.

Wilkinson, M.B., Boden, J.C., Gilmartin, T., Ward, C., Cross, D.A., allam, R.J. and Ivens, N.W.(2002), "CO_2 Capture from oil Refinery Process Heaters Through Oxyfuel Combustion," The Sixth International Conference on Greenhouse Gas Control Technologies, Kyoto, Japan, October.

Zeldovich, J. The Oxidation of Nitrogen in Combustion and Explosions. *Acta Physicochimica*, 1946, 21, pp. 577-628.

APPENDIX A: COAL ENTHALPY COMPUTATION

Coal, as a non-conventional component, is defined in ASPEN Plus through component attributes. Non-conventional components are defined in ASPENPLUS based on component attributes. In this study, the component attributes of coal are defined through ultimate analysis, proximate analysis, and sulfur analysis. The ultimate analysis characterized the component in terms of carbon, hydrogen, sulfur, oxygen, nitrogen, and ash on a moisture-free weight percent basis. A proximate analysis characterizes the component by the fixed carbon, volatile matter, ash, and moisture weight percents. The sulfur analysis characterizes the sulfur in terms of sulfur, pyretic, and organic.

Coal Enthalpy Model

The enthalpy is calculates as:

$$H = \Delta h_f^{Tref} + \int_{Tref}^{T} C_p dT \qquad \text{(A-1)}$$

Where,

Δh_f^{Tref} is the heat of formation of the component at a reference temperature (T_{ref}) and C_p is its specific heat capacity.

Frequently the heat of formation Δh_f^{Tref} is unknown and cannot be obtained directly because the molecular structure of the component is unknown. In ASPEN Plus, the heat of formation can be calculated from the heat of combustion Δh_c^{Tref} when the combustion products and elemental composition of the components are known:

$$\Delta_f h^{Tref} = \Delta_c h^{Tref} + \sum \Delta_f h_p^{Tref} \qquad \text{(A-2)}$$

where $\Delta_c h^{Tref}$ is the heat of combustion of the non-conventional component and the summation is the heat of formation of the combustion products at a reference temperature.

This is the approach used in the coal enthalpy model HCOALGEN. This model includes a number a different correlations for the following: Heat of combustion; Heat of formation; Heat capacity.

1. Heat of Combustion Correlation

For the heat of combustion of coal in the HCOALGEN model, there are six methods to calculate it: the Boie, Mott and Spooner, Grummel and Davis, IGT, and Dulong correlations of user can input the value of the heat of combustion. In this study, the method of user specified heat value of combustion is adopted.

$$\Delta_c h^{Tref} = HHV_{dry\ basis} \qquad \text{(A-3)}$$

Where, HHV is specified by the user.

2. Standard Heat of Formation Correlations

There are two standard formation heat correlations for the HCOALGEN model: Heat of combustion-based and Direct correlations. In this study, the heat of combustion-based correlation is used to calculate the heat of formation of coal:

$$\Delta_f h^{Tref} = \Delta_c h^{Tref} - (1.418\text{x}10^6 w_H{}^d + 3.278\text{x}10^6 w_C{}^d + 9.264\text{x}10^4 w_S{}^d - 2.418\text{x}10^6 w_N{}^d - 1.426\text{x}10^4 w_{Cl}{}^d)\ 10^2 \qquad \text{(A-4)}$$

where *w* is the weight percent, the superscript *d* specifies dry basis, subscripts *H*, *C*, *S*, *N* and *Cl* note hydrogen, carbon, sulfur, nitrogen and chlorine, respectively (ASPEN PLUS Manual, 1996).

3. Heat Capacity Kirov Correlation

The Kirov correlation considered coal to be a mixture of moisture, ash, fixed carbon, and primary and secondary volatile matter. The correlation treats the heat capacity as weighted sums of these constituents. The Kirov correlation is shown in the following:

$$C_p^{\,d} = \Sigma w_j(a_{j1} + a_{j2}T + a_{j3}T^2 + a_{j4}T^3) \qquad \text{(A-5)}$$

where $C_p^{\,d}$ is the heat capacity on a dry basis, a are coefficients for the constituents, subscript j is the constituent index, *w* is the mass fraction of the constituent on a dry basis, and T is the temperature in Kelvin.

Through the above three correlations, the enthalpy of coal can be calculated.

Flow Sheet

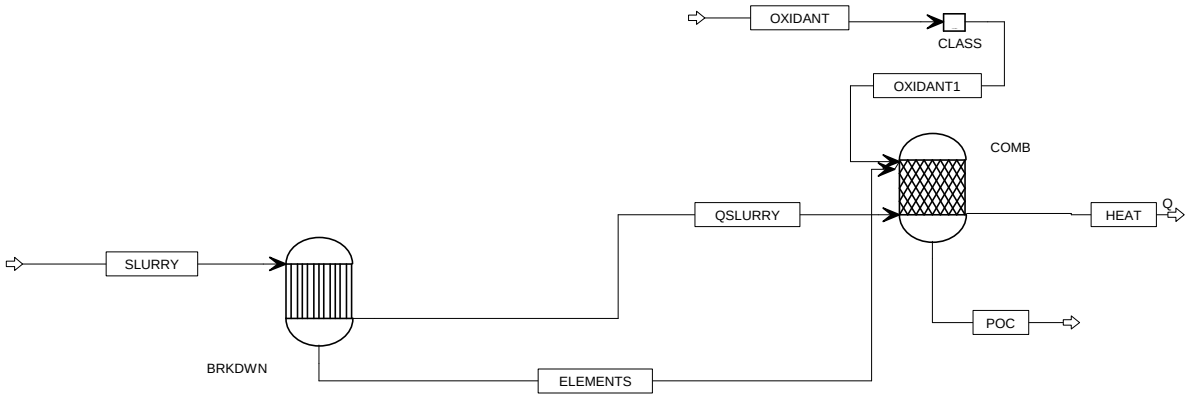

Figure A-1 Flow Sheet for Enthalpy Verification of Non-Conventional Components in ASPEN Plus

The flow sheet developed for enthalpy calculation is shown in Figure 1. The model consists of two reactors, an RYIELD and RSTOIC reactors. The RYIELD is used to break the fuel to conventional elements and the RSTOIC is used as a combustor.

The CALCULATOR block MASSFLOW uses the input of the ultimate analysis and proximate analysis of determine the mass flow rates of the elemental compounds, carbon, hydrogen, sulfur, oxygen, nitrogen, and ash. The enthalpy of the elements stream is calculated based on the data in the thermal dynamic database in ASPEN Plus. The enthalpy of the elemental stream is not same as the enthalpy of the non-conventional coal stream. SO the CALCULATOR block NRGFLOW is used to calculate the energy difference and maintain the energy balance. Another CALCULATOR block SETO2 is used to determine the stoichiometric amount of oxygen that is supplied to COMB reactor for complete combustion of the fuel.

The RIELD reactor is specified at a temperature of 25 ^{o}C and a pressure of 1 atm. The RSTOIC reactor is also specified at the same standard condition. The reactions designated in the RSTOIC reactor are the following:

$$C + O_2 \rightarrow CO_2 \quad (1)$$

$$2\,H_2 + O_2 \rightarrow 2\,H_2O \quad (2)$$

$$S + O_2 \rightarrow SO_2 \quad (3)$$

$$N_2 + .5\,O_2 \rightarrow NO_2 \quad (4)$$

Table A-1 Estimation of Heating Values of Different Coals

	Illinois No. 6	Pittsburgh No. 8	West Kentucky
Mass Flow (lb/hr)[a]	560,780	560,780	560,780
Heat from Reactor (BTU/hr)[b]	6.4580×10^9	6.9520×10^9	6.1060×10^9
Heating Value (BTU/lb)[c]	11,516	12,397	10,888
Moisture Content (%)	10.0	6.0	9.45

[a] Input Assumptions
[b] ASPEN Plus Results
[c] Heating value basis: as received, with moisture and ash.

Case Study

The case studies were done using the model with three kinds of coals as fuels, Illinois No. 6, Pittsburgh No. 8 and West Kentucky coals. The proximate analysis and ultimate analysis for three coals have been listed in Table 5-1.

For Illinois No. 6 Coal,

$$12774 \text{ BTU/lb} * (1-0.10) = 11497 \cong 11516 \text{ BTU/lb}$$

The 12,774 BTU/lb is the HHV of the Illinois No. 6 coal on a dry basis given in Table 5-1. The 0.10 is weight fraction of moisture in the fuel. Thus the 11,497 Btu/lb represents the reference value of HHV containing moisture. The 11,516 BTU/lb is calculated by using the heat from the reactor divided by the fuel mass flow to the reactor on a moisture-containing basis. The relative difference between the reference value and the ASPEN Plus result is 0.17%. It indicates that the estimate of coal HHV from model in ASPEN Plus matches the reference value well.

For Pittsburgh No. 8 coal,

$$13138 \text{ BTU/lb} * (1-0.06) = 12350 \cong 12397 \text{ BTU/lb}$$

For West Kentucky coal,

$$11969 \text{ BTU/lb} * (1-0.0945) = 10838 \cong 10888 \text{ BTU/lb}$$

The relative differences of reference values and ASPEN Plus results of HHV are 0.38% for Pittsburgh No. 8 coal and 0.46% for West Kentucky coal. The above comparison indicates that the estimate of fuel HHV in ASPEN Plus is accurate. The small difference may be due to the difference between the ASPEN Plus database and the actual data.

APPENDIX B: CALIBRATION OF APPROACH TEMPERATURES OF REACTIONS IN GASIFIER

The approach temperature is a design parameter for a RGIBBS reactor, simulating gasifer reactor. It represents the difference between the equilibrium temperature of a specific reaction and the outlet temperature of the reactor. Adjusting the approach temperatures make each reaction happening at a specific temperature and thus control the syngas composition. The reactions happened in the gasifier reactor are listed in following. The approach temperatures of them are specified based on the original ASPEN model of Stone (1985).

(1)	$C + 2\ H_2 \leftrightarrow\ CH_4$	-300	(B-9)
(2)	$C + H_2O \leftrightarrow\ CO + H_2$	-500	(B-10)
(3)	$CH_4 + 2O_2 \leftrightarrow\ CO_2 + 2H_2O$	-500	(B-11)
(4)	$CO + O_2 \leftrightarrow\ 2CO_2$	-500	(B-12)
(5)	$S + H_2 \leftrightarrow\ H_2S$	-500	(B-13)
(6)	$0.5\ N_2 + 1.5\ H_2 \leftrightarrow\ NH_3$	-500	(B-14)
(7)	$CO + H_2S \leftrightarrow\ COS + H_2$	-500	(B-15)

There are difference in the physical database used in ASPEN Plus and ASPEN, which has been found by Picket (2001). Therefore, the approach temperatures should be recalibrated. The calibration basis is the reference data of Condrelli, *et al.* (1991). The coal used in that report is West Kentucky coal, whose compositions analysis ahs been given in Appendix A. The cooled syngas compositions data were selected as calibration basis since the raw gas compositions were not available in that report.

Since there are 7 reactions and about 13 components in syngas, it is very difficult for calibration to match the reference compositions of all components. The most important components in syngas are hydrogen and carbon monoxide. Therefore, to simplify the calibration process, the sensitivity analysis is completed to find out the most sensitive reaction approach temperature for compositions of H_2 and CO. The relative changes in H_2 and CO caused by the change in approach temperatures of reaction (1) to (4) are shown in Figure B-1 and B-2, respectively. For reaction (5) to (7), the changes caused by their approach temperature changes were almost zero and thus they are not shown in the figures. The reason for less sensitivity of reaction (5) to (7) is that the amounts of their reactant, S, N_2, and H_2S, are very small compared to other reactants. From Figure B-1 and B-2, it is obvious that the most sensitive approach temperature is the one of reaction (4). The calibration focuses on the approach temperature of Reaction (4).

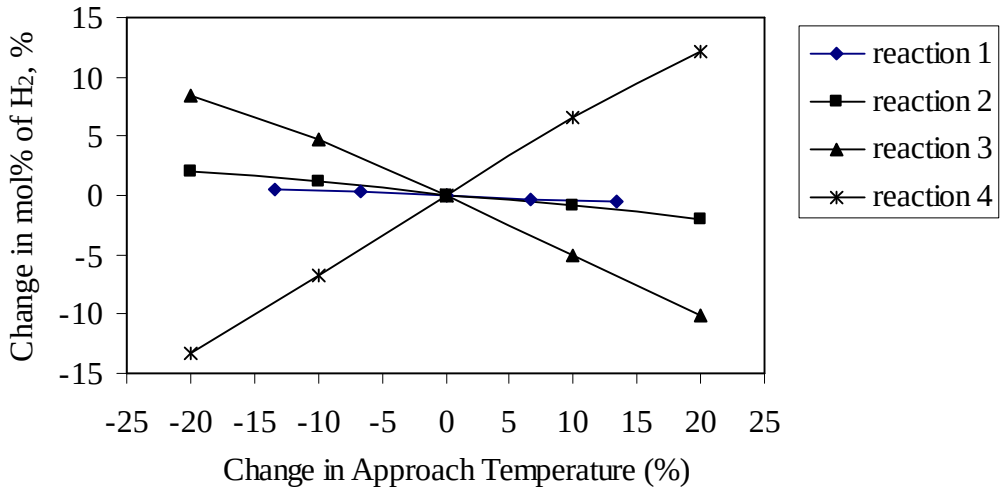

Figure B-1 Effects of Changes in Approach Temperatures on H_2 mol%

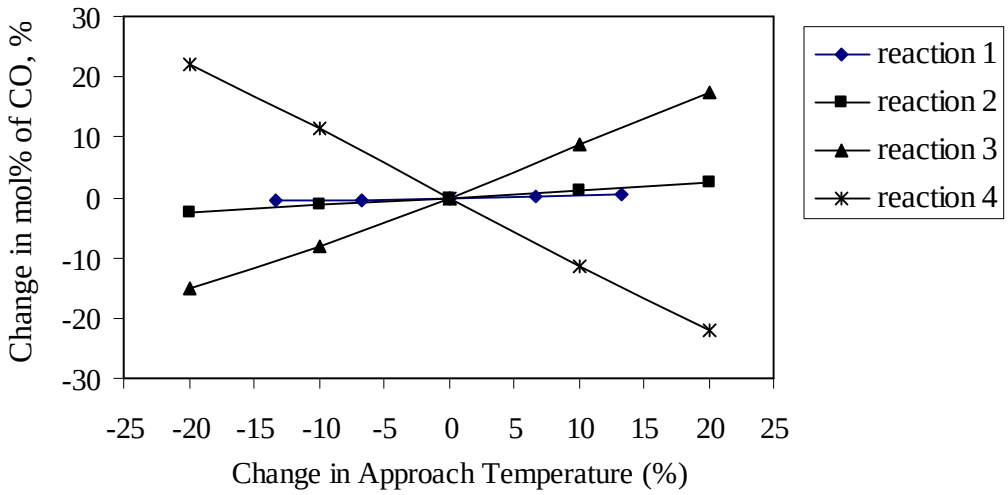

Figure B-2 Effects of Changes in Approach Temperatures on CO mol%

For reaction (4), the sensitivity analysis of approach temperature vs. mole fraction of H_2, CO, and CO_2 in the raw syngas out of a Texaco gasifier is made. The sensitivity analysis results are given out in Table B-1 and Figure B-3. The results indicate that when the approach temperature of reaction (4) is -490 ^oF, the compositions of CO, H_2 and CO_2 are most close to the reference values.

Table B-1 Sensitivity Analysis of Approach Temperature of Equation

Approach Temperature of Reaction (4), ^oF	Mole Fractions of Main Products in Cooled Syngas		
	CO	H_2	CO_2
-510	45.3%	35.9%	14.6%
-500	46.4%	35.4%	14.0%
-490	47.5%	35.0%	13.4%
-480	48.5%	34.4%	12.8%
-470	49.6%	33.9%	12.2%

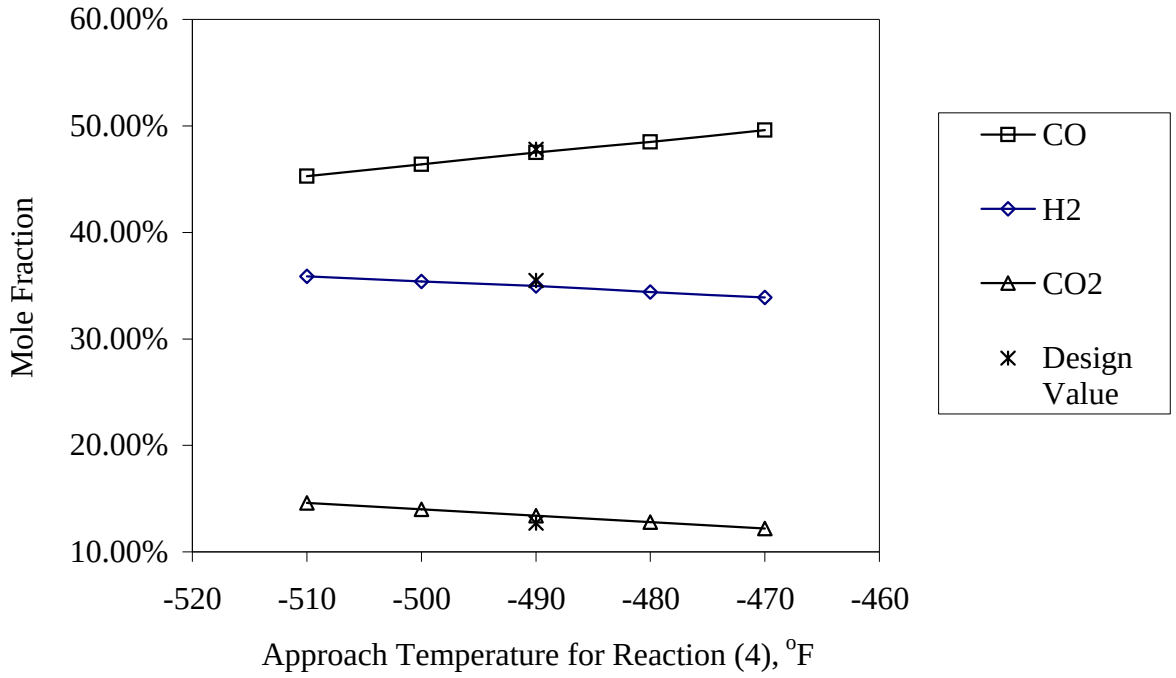

Figure B-3 The variance of Mole Fraction of H_2, CO, and CO_2 in Cooled Gas vs. Approach Temperature of Reaction (4)

APPENDIX C: DIRECT COSTS COMPARISON OF IGCC SYSTEM

The cost information about the IGCC systems based on Texaco gasifier and different combined cycle are collected and compared to verify the cost model used in the IGCC model in ASPEN Plus.

Direct Cost of Units in IGCC Projects with Texaco Gasifier or 7FA Combined Cycle

The direct cost information about Texaco gasification and Frame 7F gas turbine are collected and described in the following:

Case 1. ASEPN Plus Model – Texaco gasifier-based with 7FA Combined Cycle;

Case 2. Tampa Elec. Polk Project – Texaco gasifier-based with 7FA Combined Cycle;

Case 3. Texaco gasifier-based Total Quench with 9FA Combined Cycle;

Case 4. Texaco gasifier-based with 7F Combined Cycle with total quench cooling design;

Case 5. Texaco gasifier-based with 7F Combined Cycle with radiant cooling design;

Case 6. Destec gasifier-based with 7FA Combined Cycle;

Case 7. Wabash River Project – Destec gasifier-based with 7FA Combined Cycle;

Case 8. E-Gas gasifier-based IGCC system with 7FA Combined Cycle.

From the above cost comparison of each main unit in IGCC, the following results can be found:

(1) For the cost of coal handling, the range in this paper is 50.4 ~ 63.9 $/kW. Four reference data are available and three of them are around 50 $/kW. The result from ASPEN Plus is close to this number.

(2) For Air Separation Unit (ASU), the cost range is 122.5 ~ 162.2 $/kW. The results are basically consistent.

(3) For the cost of Texaco gasification, the range is about 113 ~ 487 $/kW. For case 2 – Tampa Elec. Project, the cost for Texaco gasification is much higher than others because it is a first-of-a-land demonstration project and not a fully commercial plant. The cost for it is much higher than the results of other design studies. The result of ASPEN Plus model is a little lower compared to others. For case 3, the reason for the cost is a little higher than others is perhaps that the cost for gasification includes the cost for cold gas clean-up in this case. The total cost for gasification and cold-gas clean-up in case 1 is 282.3 $/kW and it is 201$/kW in case 4, and 257.4$/kW in case 5. For case 3, it is $247x10^3$$/kW. For case 3 used the total quench cooling method and case 1 used the radiant and convective cooling, the results for case 1 is reasonable.

(4) For cold gas clean up, the data are very close. The range is 82.6 ~ 88.4 $/kW. For case 2, a different cold gas clean-up method, MDEA (Methyl Diethanol Amine) process, is adopted compared to the selexol process in case 1, 4, and 5.

(5) For power block, the costs basically are 251 ~ 464 $/kW. There is big difference for the total cost for power block of each case. The costs for Tampa project and Wabash River are much higher than other two projects. The possible reason is Tampa project is a first-of-a-land demonstration project and not a fully commercial plant. For Wabash River project, the cost for the actual Wabash project is much higher than the modeling results. The reason is that there are some problems, including weather delays, equipment problems, mechanical contracting,

and other problems, in the actual project. If there is no above problems, the power block cost is 407$/kW based on 2000$ (Wabash River Energy Ltd., 2000). The sum of power block and general facility for case 1 is 385 $/kW. For case 3, it is 460 $/kW. The result for the model in ASEPN Plus is a little lower. For the cost of HRSG, the values in ASPEN Plus model are little lower than that of other cases. The cost of steam turbine in ASPEN Plus is a little higher than other values. For 7FA gas turbine, only one design result is found. The two values are close.

Based on the above comparison of modeling results and reference data, the conclusion is that the cost model developed by Frey and Rubin (1991) and refinements by Frey and Akunuri (2001) is suitable for estimating the Texaco gasifier-based IGCC system with F gas turbine.

Table C-1 Direct Cost Information of IGCC Projects with Texaco Gasification and 7FA Combined Cycle

	Case 1	Case 2	Case 3	Case 4	Case 5	Case 6	Case 7	Case 8
Description	ASPEN Plus [a]	Tampa Elec. [b]	Texaco-9F[c]	Texaco-7F[d]	Texaco-7F [e]	Destec-7FA[f]	Wabash River [g]	E-Gas – 7FA [h]
Gasification	Texaco	Texaco	Texaco	Texaco	Texaco	Destec	E-Gas	E-Gas
Plant Size	284.7	252.5	449.2	431.6	633.3	543.2	262	269.3
Gas Turbine	7FA	7F	9FA	7F	7F	7FA	7FA	7FA
Gas Cooling	Radiant and Convective	Radiant and Convective	Quench	Quench	Radiant	Radiant	Radiant	Radiant
Gas Cleaning-up	Selexol & Claus Plant	MDEA [i] & Claus Plant	Cold Gas	Selexol & Claus Plant	Selexol & Claus Plant	Hot Gas	MDEA & Claus plant	MDEA & Claus plant
Cost Base	Jan. 1998	Mid-2001	2000	Jan. 1991	Jan. 1988	Jan. 1998	1994	2000
Case Type	Model	Actual	Design	Design	Design	Design	Actual	Design
Unit	Direct Cost (Equipment, Material, and Labor), $/kW (January 1998 Dollar)							
Coal Handling	48.9	--	--	52.8	63.9	50.4	--	52.4
Air Separation Unit	147.1	150	154	146.1	148.8	122.5	134.4	162.2
Texaco Gasification	198.3	487	247	112.7	174.8	--	--	--
Cold Gas Clean-up [j]	84.7	148	--	88.4	82.6	--	--	--
Power Block	249.2	449	398	297.2	365.4	251	558	462
Gas Turbine	124.1	--	--	--	--	122.5	--	--
HRSG	43.8	--	--	64.1	--	62.4	--	--
Steam Turbine	81.3	--	--	57.2	--	66.1	--	--
General Facility	127.7	412	61.7	297.4	203.1	--	--	--
Total Installed Cost	879	1,647	860	1079	1076	--	--	--

[a] The results of case 1 are from the modeling results of Texaco based IGCC with 7FA combined cycle model in ASPEN Plus.
[b] Hornick and McDaniel (2002);
[c] Falsetti, *et al*. (1999);
[d] Condorelli, *et al.*, (1991). The original costs are converted to the cost base of Jan. 1998.
[e] Jacob and Chu, (1988). The original costs are converted to the cost base of Jan. 1998.
[f] Buchanan, *et al*., (1998);
[g] Wabash River Energy Ltd. (2000). The original cost basis is 1994 average, which is converted to the cost base of Jan. 1998.
[h] Bechtel, *et al*. (2002);
[i] MDEA: Methyl Diethanol Amine;
[j] Cold Gas Clean-up includes the low-temperature cooling, acid gas removal, acid gas recovery processes.

Direct Cost of Units in IGCC Projects with Texaco Gasifier and 7H Combined Cycle

The following is the cost information for 7H combined cycle in IGCC system

Table C-2 Direct Cost Information for IGCC Projects with Texaco Gasifier or 7H Combined Cycle

	Case 9	Case 10	Case 11	Case 12
Description	ASPEN Plus [a]	Destec-H [b]	9H-HEQ_C[c]	9H_RO_C[d]
Gasification	Texaco	Destec	Texaco	Texaco
Plant Size	284.7	427.7	520.9	527.0
Gas Turbine	7H	7H	9H	9H
Gas Cooling	Radiant and Convective	Radiant	Quench	Radiant
Gas Cleaning-up	Selexol & Claus Plant	Hot-Gas	Cold Gas (No details)	Cold Gas (No details)
Cost Base	Jan. 1998	Jan. 1998	2000	2000
Case Type	ASPEN Plus Model	Conceptual	Design	Design
Unit	Direct Cost (Equipment, Material, and Labor), $/kW			
Coal Handling	44.3	38.9	--	--
ASU	116.1	134.0	132.8	126.0
Texaco Gasification	176.2	--	227.5	317.6
Cold Gas Clean-up	75.6	--	--	--
Power Block	251.5	230.2	434.6	433.4
Gas Turbine	114.1	110.6	--	--
HRSG	64.2	54.7	--	--
Steam Turbine	73.3	64.9	--	--
General Facility	116.1	--	56.8	59.0
Total Installed Cost	800	849.2	852	935

[a] The results of case 1 are from the modeling results of Texaco based IGCC with 7H combined cycle model in ASPEN Plus.
[b] Buchanan, *et al*., (1998);
[c, d] Falsetti, *et al*. (1999).

The cases selected are described as following:

Case 9: Original Cost Model for Texao-based IGCC with 7H Combined Cycle;

Case 10: Destec-based Radiant with 7H Combined Cycle;

Case 11: Texaco gasifier-based High Efficiency Quench with 9H Combined Cycle;

Case 12: Texaco gasifier-based Radiant Only with 9H Combined Cycle;

The cost for Texaco gasification is lower in case 1 than that in other case 11 and case 12. The possible reason is that the gasification costs in case 11 and 12 has included the cost for gas cleaning while the cost of gasification of model results does not include this cost. The total cost for gasification and gas cleaning is 251.8 $/kW for the modeling results. It is between 227.5 and 317.6 $/kW. It indicates that the modeling result of the cost of the gasification including the gas cleaning is reasonable. The direct cost of power block is close to the reference data of case 10. Specially, for the 7H gas turbine directs cost, the modeling results is very close to the reference data.

Therefore the model in ASPEN Plus has reasonable estimates for the direct costs of IGCC plant based on 7H gas turbine.

APPENDIX D: SPREADSHEET MODEL OF GAS TURBINE COMBINED CYCLE

In this section, the detailed spreadsheet model for gas turbine simple and combined cycles are described.

1. Compressor

For each stage, the outlet temperature is estimated via a multi-step procedure. The first step is to estimate the entropy of the inlet air based upon a regression relationship of thermodynamic data shown in Figure D-1:

$$s_{C,i,in} = 1.0327 \ln(T) - 4.1905 \quad \text{(D-1)}$$

Based upon the estimated entropy of the inlet air and the pressure ratio, the entropy of the compressor outlet air is estimated:

$$s_{C,i,out} = s_{C,i,in} + \left(\frac{R}{MW_{air}}\right) \ln(r_{P,i}) \quad \text{(D-2)}$$

Using the estimate of the entropy of the outlet air, a regression expression shown in Figure D-2 is used to estimate the temperature of the outlet air.

$$T_{C,i,out} = 217.73 s_{C,i,out}^{\ 2} - 463.29 s_{C,i,out} + 455.77 \quad \text{(D-3)}$$

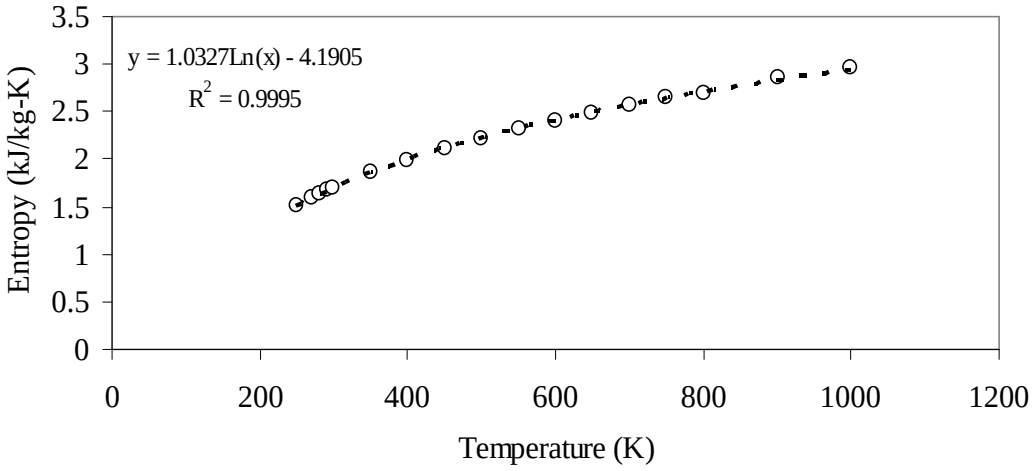

Figure D-1 Regression Results for Entropy as a Function of Temperature for Air

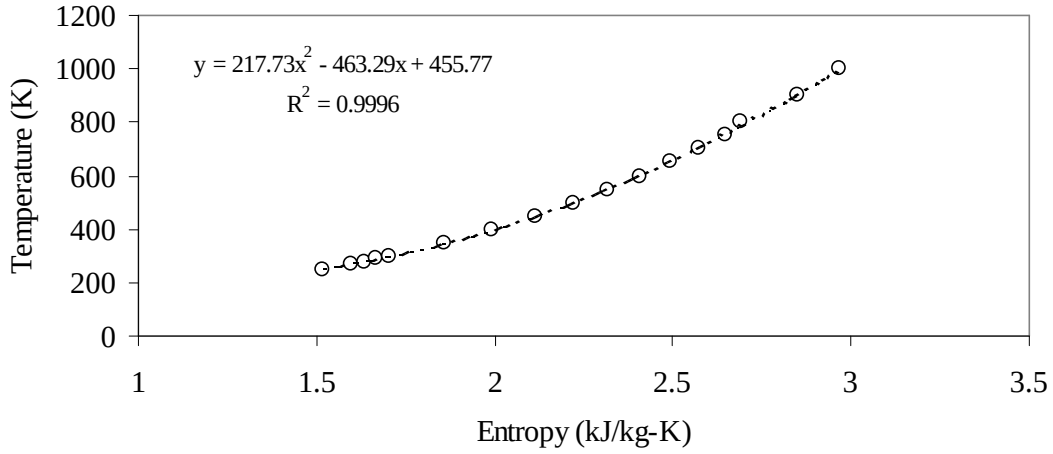

Figure D-2 Regression Results for Temperature as a Function of Entropy for Air

With knowledge of the temperature of the outlet air, the enthalpy of the outlet air is estimated based upon the regression expression shown in Figure D-3.

$$h_{C,i,out,isentropic} = 0.0001T^2 + 0.9302T + 11.687 \qquad \text{(D-4)}$$

The estimated enthalpy is 489.9 kJ/kg, versus a reported value of 492.7 kJ/kg. This procedure is based upon an isentropic compressor.

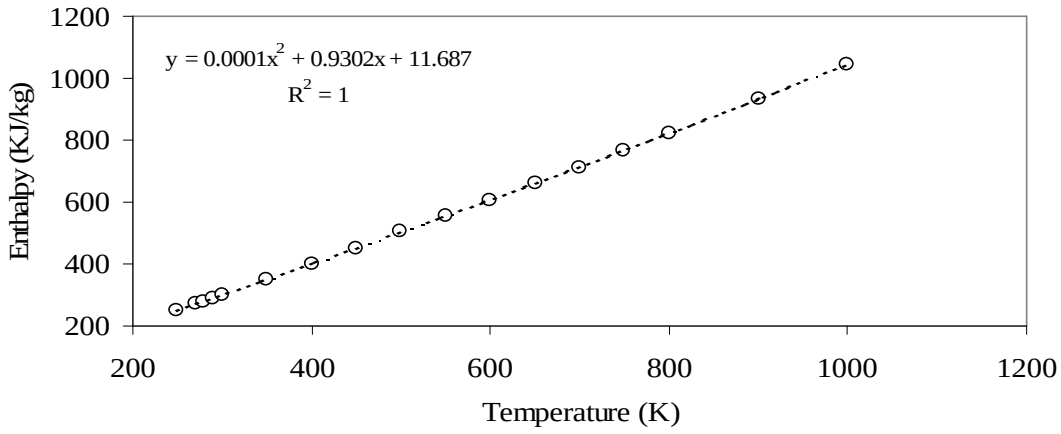

Figure D-3 Regression Results for Enthalpy as a Function of Temperature for Air

To take into account the irreversibilities in an actual compressor, the actual enthalpy of the outlet air is estimated based upon the following relationship:

$$h_{C,i,out} = h_{C,i,in} + \frac{h_{C,i,out,isentropic} - h_{C,i,in}}{h_{C,i}} \qquad \text{(D-5)}$$

Based upon the estimated enthalpy for the actual compressor outlet air, the actual outlet temperature is estimated based upon the regression equation shown in Figure D-4:

$$T_{C,i,out} = -9\times10^{-5}h_{C,i,out} + 1.0563h_{C,i,out} - 9.0996 \qquad \text{(D-6)}$$

The outlet temperature of stage *i* is treated as the inlet temperature of the next stage. The above computation is repeated and the outlet temperature for the last stage can be obtained.

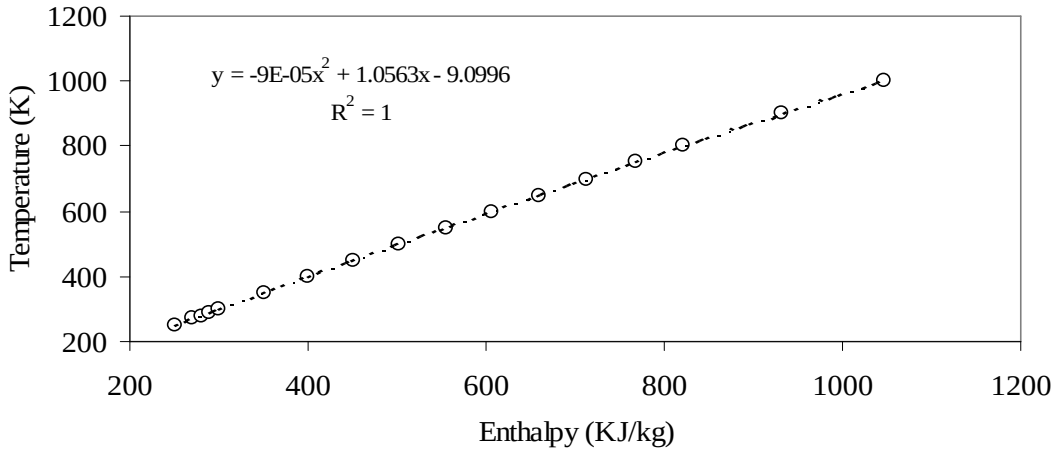

Figure D-4 Regression Results for Temperature as a Function of Enthalpy for Air

2. Combustor

In general, the fuel to a combustor contains the six major components, including carbon monoxide (CO), hydrogen (H_2), methane (CH_4), carbon dioxide (CO_2), nitrogen (N_2), and water vapor (H_2O). The volume percent (or, equivalently, mole fraction) of each of the six major components will be known. Therefore, a heating value can be estimated for the fuel. Based upon data reported by Flagan and Seinfeld (1988), the enthalpy of reaction of CO is estimated as 283,400 J/gmole, the enthalpy of reaction of H_2 is estimated as 242,200 J/gmole, and the enthalpy of reaction of CH_4 is estimated as 803,500 J/gmole. These are estimated on a lower heating value basis, assuming that H_2O produced is in the form of vapor. The other three major components are assumed to be non-reactive. The heating value of the fuel gas, on a J/gmole basis, is given by:

$$\Delta h_{r,fuel} = y_{CO}\Delta h_{r,CO} + y_{H_2}\Delta h_{r,H_2} + y_{CH_4}\Delta h_{r,CH_4} \qquad \text{(D-8)}$$

Air is a mixture primarily of oxygen and nitrogen. For every mole of oxygen in the air, there are approximately 3.76 moles of nitrogen. The major products of combustion are carbon dioxide, water vapor, nitrogen, and excess oxygen. The gas turbine combustors operate with a significant amount of excess air. The mass balance for the case with excess air can be developed based upon the stoichiometric mass balance by introducing a new variable for the fraction of excess air, e_a. The fraction of excess air is given by:

$$e_a = \frac{\textit{(Total air - stoichiometric air)}}{\textit{(Stoichiometric air)}} \qquad \text{(D-9)}$$

The mass balance for excess air is:

$$[y_{CO}CO + y_{H_2}H_2 + y_{CH_4}CH_4 + y_{CO_2}CO_2 + y_{N_2}N_2 + y_{H_2O}H_2O] + a(1+e_a)O_2 + 3.76a(1+e_a)N_2 \rightarrow b\,CO_2 + cH_2O + d'N_2 + (a)(e_a)O_2 \qquad \text{(D-10)}$$

The mass balance is given on the basis of one mole of syngas mixture. Thus, the units of each stoichiometric coefficient are moles of the respective compound per mole of syngas mixture. The mole fractions of each component in the syngas are known. Therefore, the unknowns are the stoichiometric coefficients a, b, c, and d. These can be solved based upon elemental balances:

Carbon: $y_{CO} + y_{CH_4} + y_{CO_2} = b$

Hydrogen: $2y_{H_2} + 4y_{CH_4} + 2y_{H_2O} = 2c$

Oxygen: $y_{CO} + 2y_{CO_2} + y_{H_2O} + 2a = 2b + c$

Nitrogen $2y_{N_2} + 2(3.76)a = 2d$

Based upon these four Equations, the solutions for a, b, c, and d are:

$$a = \frac{1}{2} y_{H_2} + 2y_{CH_4} + \frac{1}{2} y_{CO} \tag{D-11}$$

$$b = y_{CO} + y_{CH_4} + y_{CO_2} \tag{D-12}$$

$$c = y_{H_2} + 2y_{CH_4} + y_{H_2O} \tag{D-13}$$

$$d' = y_{N_2} + 3.76\, a(1 + e_a) \tag{D-14}$$

For example, suppose that a fuel contains, on a mole or volume percentage basis, 24.8% hydrogen, 39.5 % carbon dioxide, 1.5 % methane, 9.3 % carbon dioxide, 2.3 % nitrogen, and 22.7 % water vapor. Stoichiometric combustion of this fuel would require 0.3515 moles of oxygen per mole of syngas mixture, and 1.32 moles of nitrogen in the inlet air. The exhaust gas would contain 0.50 moles of carbon dioxide, 0.50 moles of water vapor, and 1.34 moles of nitrogen, all based upon one mole of syngas combusted. If the fuel were burned with 100 percent excess air, then the exhaust gas would contain 0.50 moles of carbon dioxide, 0.50 moles of water vapor, and 2.67 moles of nitrogen, and 0.35 moles of oxygen, all based upon one mole of syngas combusted.

The actual amount of air that is needed to combust the fuel depends upon the desired turbine inlet temperature. Therefore, it is necessary to solve an energy balance in order to estimate the fuel to air ratio. The turbine inlet temperature, $T_{T,in}$, is a known design parameter. The temperature of the air from the compressor is known based upon the compressor pressure ratio and adiabatic compressor efficiency, as explained in the

previous section. The syngas temperature would also be known. The only unknown is the excess air ratio. Thus, the energy balance is:

$$\begin{gathered} bH_{CO_2}(T_{T,in}) + cH_{H_2O}(T_{T,in}) + d'H_{N_2}(T_{T,in}) + (a)(e_a)H_{O_2}(T_{T,in}) - \\ [y_{CO}H_{CO}(T_{SG}) + y_{H_2}H_{H_2}(T_{SG}) + y_{CH_4}H_{CH_4}(T_{SG}) + \\ y_{CO_2}H_{CO_2}(T_{SG}) + y_{N_2}H_{N_2}(T_{SG}) + y_{H_2O}H_{H_2O}(T_{SG})] - \\ a(1+e_a)H_{O_2}(T_{C,out}) - 3.76a(1+e_a)H_{N_2}(T_{C,out}) = \Delta h_{r,SG} \end{gathered} \tag{D-15}$$

Because all of the terms in this equation are known except for the excess air fraction, the Equation can be rearranged in terms of excess air fraction as follows:

$$\begin{gathered} bH_{CO_2}(T_{T,in}) + cH_{H_2O}(T_{T,in}) + \{y_{N_2} + 3.76a(1+e_a)\}H_{N_2}(T_{T,in}) + (a)(e_a)H_{O_2}(T_{T,in}) - \\ [y_{CO}H_{CO}(T_{SG}) + y_{H_2}H_{H_2}(T_{SG}) + y_{CH_4}H_{CH_4}(T_{SG}) + \\ y_{CO_2}H_{CO_2}(T_{SG}) + y_{N_2}H_{N_2}(T_{SG}) + y_{H_2O}H_{H_2O}(T_{SG})] - \\ a(1+e_a)H_{O_2}(T_{C,out}) - 3.76a(1+e_a)H_{N_2}(T_{C,out}) = \Delta h_{r,SG} \end{gathered} \tag{D-16}$$

For convenience, we create the following groups of terms:

$$\begin{gathered} H_{fuel} = y_{CO}H_{CO}(T_{SG}) + y_{H_2}H_{H_2}(T_{SG}) + y_{CH_4}H_{CH_4}(T_{SG}) + \\ y_{CO_2}H_{CO_2}(T_{SG}) + y_{N_2}H_{N_2}(T_{SG}) + y_{H_2O}H_{H_2O}(T_{SG}) \end{gathered} \tag{D-17}$$

$$H_{air,stoich} = aH_{O_2}(T_{C,out}) + 3.76aH_{N_2}(T_{C,out}) \tag{D-18}$$

$$H_{products,stoich} = b\,H_{CO_2}(T_{T,in}) + c\,H_{H_2O}(T_{T,in}) + \{y_{N_2} + 3.76\,a\}\,H_{N_2}(T_{T,in}) \tag{D-19}$$

The solution for the excess air fraction is given by:

$$e_a = \frac{H_{fuel} + H_{air,stoich} + \Delta h_{r,fuel} - H_{products,stoich}}{a\,[3.76\{H_{N_2}(T_{T,in}) - H_{N_2}(T_{C,out})\} + \{H_{O_2}(T_{T,in}) - H_{O_2}(T_{C,out})\}]} \tag{D-20}$$

After the computation of excess air, the molar fraction per mole fuel gas of exhaust gas of combustor can be estimated.

$$y_{ex,CO_2} = y_{CO} + y_{CH_4} + y_{CO_2} \quad \text{(D-21)}$$

$$y_{ex,H_2O} = y_{H_2} + 2y_{CH_4} + y_{H_2O} \quad \text{(D-22)}$$

$$y_{ex,N_2} = y_{N_2} + 3.76(1+e_a)(\frac{1}{2}y_{H_2} + 2y_{CH_4} + \frac{1}{2}y_{CO}) \quad \text{(D-23)}$$

$$y_{ex,O_2} = e_a(\frac{1}{2}y_{H_2} + 2y_{CH_4} + \frac{1}{2}y_{CO}) \quad \text{(D-24)}$$

From Equation (6-1) in Section 6.1, the mass flow of exhaust gas out of the combustor or at the turbine inlet can be estimated. The actual and reference pressures in the turbine inlet are $P_{ref} = P_{act} = P_{T,in}$. For a specific design basis, the actual and reference temperatures are $T_{act} = T_{ref} = 2{,}880\ ^oR$, which is converted from the firing temperature of $2{,}420\ ^oF$ for a 7FA+e gas turbine (Gebhardt, 2000). According to Equations (D-21) to (D-24), the molecular weight of mixture gas at the inlet of turbine can be estimated as:

$$MW_{act} = y_{ex,CO_2}MW_{CO_2} + y_{ex,H_2O}MW_{H_2O} + y_{ex,N2}MW_{N_2} + y_{ex,O_2}MW_{O_2} \quad \text{(D-25)}$$

The reference molecular weight is assumed to be $MW_{ref} = 28.4$. Therefore, the actual mass flow in the inlet of turbine can be calculated by Equation (1). The reference mass flow is calibrated to make the result of power output match the published value. The total mass flow through the combustor the sum of combustor air mass flow and fuel gas mass flow, which is same as the actual mass flow to the turbine.

$$m_{fuel} + m_{comb,air} = m_{act} \tag{D-26}$$

The mass flow of fuel gas is calculated in the following. The molecular weight of fuel gas can be estimated as follows:

$$\begin{aligned} MW_{fuel} = {} & y_{CO}MW_{CO} + y_{H_2}MW_{H_2} + y_{CH_4}MW_{CH_4} + y_{CO_2}MW_{CO_2} \\ & + y_{N2}MW_{N_2} + y_{H_2O}MW_{H_2O} \end{aligned} \tag{D-27}$$

The ratio of fuel to air required for combustion can be calculated by the following Equation:

$$r_{f,air} = \frac{MW_{fuel}}{a(1+e_a)MW_{O_2} + 3.76\,a(1+e_a)MW_{N_2}} \tag{D-28}$$

Since the actual mass flow to the turbine is the sum of combustor air mass flow and fuel gas mass flow, the mass ratio of fuel and the actual mass flow to the turbine is:

$$r_{f,act} = \frac{r_{f,air}}{1+r_{f,air}} \tag{D-29}$$

Therefore, the mass flow of fuel can be estimated as:

$$m_{fuel} = m_{act} \times r_{f,act} \tag{D-30}$$

The mole flow rate of fuel gas is estimated based on the following Equation:

$$M_{fuel} = \frac{m_{fuel}}{MW_{fuel}} \tag{D-31}$$

The combustor air mass flow is estimated as:

$$m_{comb,air} = m_{act} - m_{fuel} \quad \text{(D-32)}$$

Therefore, the total mass flow of air to the combustor is estimated as:

$$m_{air} = \frac{m_{act} - m_{fuel}}{1 - f_{a,1} - f_{a,2} - f_{a,3}} \quad \text{(D-33)}$$

3. Turbine

For each stage, the turbine outlet temperature is calculated. Because nitrogen comprises approximately 70 percent or more (by volume) of the exhaust gases from the gas turbine, we use nitrogen as the basis for the calculations to determine the turbine exhaust temperature. Figures D-5 and D-6 displayed the regression Equations for entropy as a function of temperature, and for temperature as a function of entropy, respectively. The entropy at the turbine inlet is estimated based upon the regression equation shown in Figure D-5.

$$s_{T,i,in} = 3.0044T^{0.1443} \quad \text{(D-34)}$$

For example, if the turbine inlet temperature is 1,100 K, then the estimated entropy from the Equation in Figure D-5 will be 8.253 kJ/kg-K. The entropy at the stage outlet is estimated as:

$$s_{T,i,out} = s_{T,i,in} + \left(\frac{R}{MW_{N_2}}\right)\ln\left(\frac{1}{r_{P,i,turb}}\right) \quad \text{(D-35)}$$

At this value of entropy, the turbine outlet temperature is calculated, based upon the regression equation given in Figure D-6.

$$T_{T,i,out} = 4.9161\times10^{-4}(s_{T,i,out})^{6.9277} \quad \text{(D-36)}$$

The temperature is estimated to be 694 K. This temperature is exactly the same as that reported by Wark (1983) for a similar calculation based upon air. If the turbine is not isentropic, then the turbine outlet temperature will be higher than that predicted based upon isentropic calculation.

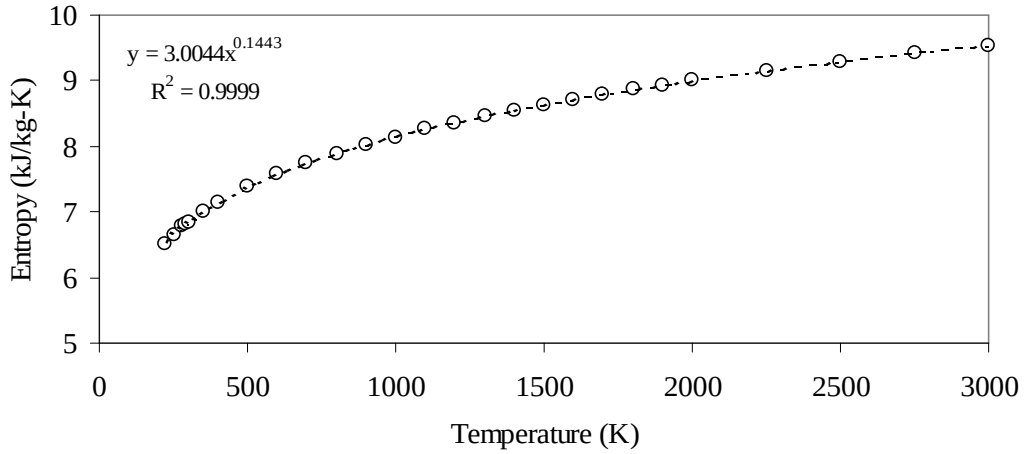

Figure D-5 Regression Results for Entropy as a Function of Temperature for Nitrogen (N_2)

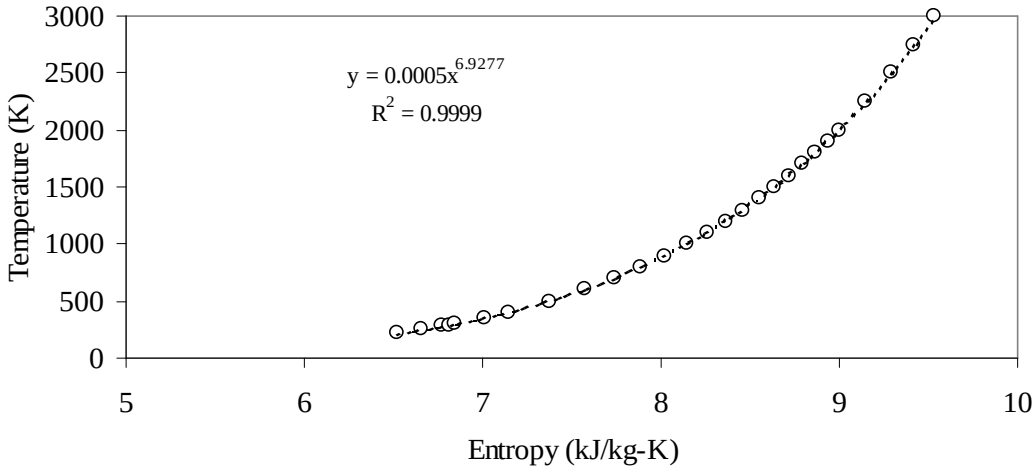

Figure D-6 Regression Results for Temperature as a Function of Entropy for Nitrogen (N_2)

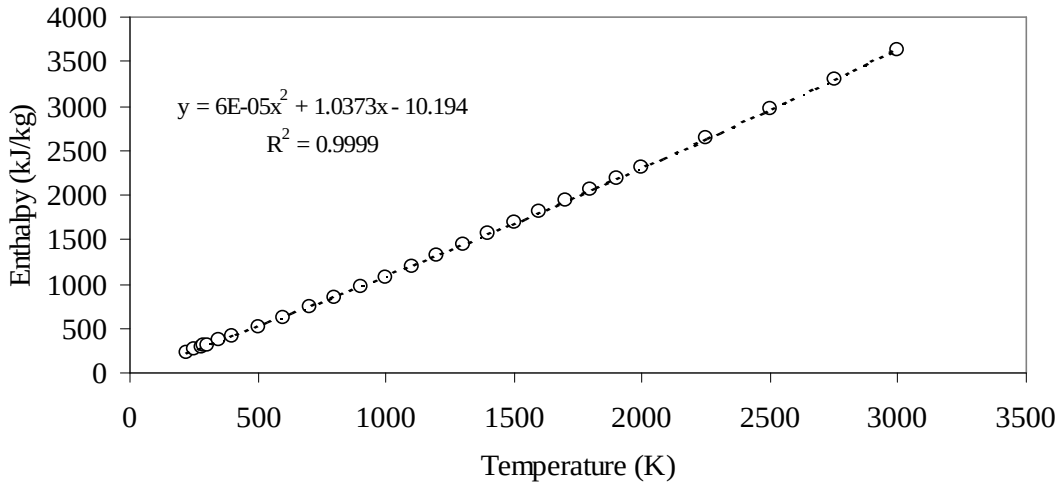

Figure D-7 Regression Results for Enthalpy as a Function of Temperature for Nitrogen

The isentropic turbine work output is given by the difference between the enthalpies of the inlet and outlet under isentropic conditions. The enthalpy of exhaust gas is estimated based on the regression Equation shown in Figure D-7.

$$h_{T,i,\,out,isentropic} = 5.9731\times10^{-5}\,T^2 + 1.0373\,T - 10.1939 \qquad \text{(D-37)}$$

To take into account the efficiency of an actual expander, the actual enthalpy of the outlet gas is estimated based on the following relationship:

$$h_{T,i,out} = h_{T,i,in} + (h_{T,\,i,\,out,\,isentropic} - h_{T,\,i,\,in})\eta_{Ti,} \qquad \text{(D-38)}$$

Then the actual temperature at the stage outlet is estimated based upon the regression expression shown in Figure D-8.

$$T_{T,i,out} = -3.2769\times10^{-5}\,h_{T,i,out}{}^2 + 0.9347\,h_{T,i,out} + 17.3221 \qquad \text{(D-39)}$$

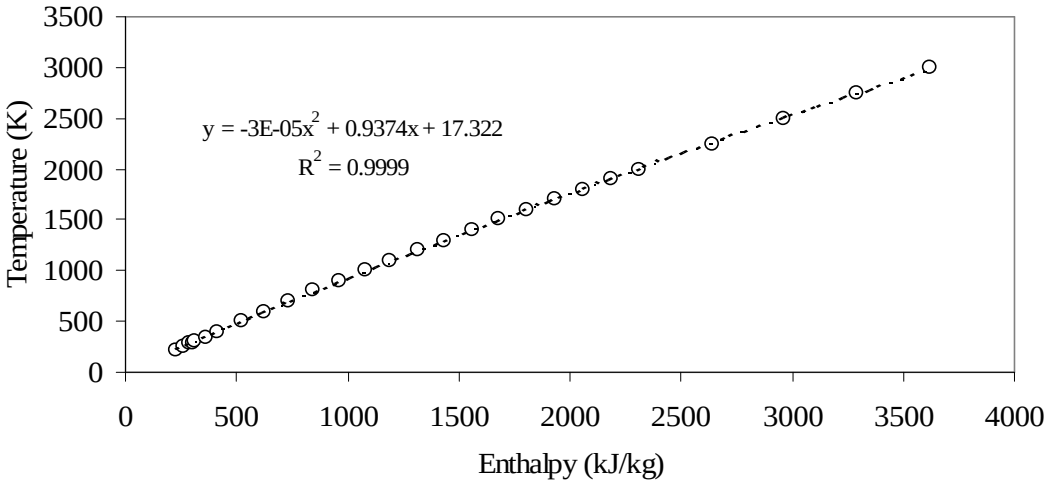

Figure D-8 Regression Results for Temperature as a Function of Enthalpy for Nitrogen

After each stage, the cooling air is mixed with the exhaust flow. The mixture temperature is estimated based on the specific heat and the mass flow of the streams in the mixture:

$$T_{T,i+1,in} = \frac{(m_{air} f_{a,i}) c_{p,air} T_{a,i} + m_{T,i,out} c_{p,i,out} T_{T,i,out}}{(m_{air} f_{a,i}) c_{p,air} + m_{T,i,out} c_{p,i,out}} \quad \text{(D-40)}$$

The mixture temperature is treated as the inlet temperature for next stage. After the third stage of the turbine, the mixture temperature is the exhaust temperature of the gas turbine.

4. Power Output

The compressor work requirement is estimated based on the amount of air needed per mole fuel gas combusted and the enthalpy difference between the outlet and inlet of the compressor. The air mainly consists of nitrogen and oxygen and other minor composition are ignored. Using the IECM enthalpy function, the oxygen and nitrogen enthalpies are estimated as a function of temperature. For each stage of the compressor,

the inlet temperature and the outlet temperature are computed in the section of compressor. The enthalpy difference per mole syngas of the first stage is computed as:

$$\Delta h_{C,i} = y_{c,i,air,N_2}[h_{N_2}(T_{C,i,out}) - h_{N_2}(T_{C,i,in})] + y_{C,i,air,O_2}[h_{O_2}(T_{C,i,out}) - h_{O_2}(T_{C,i,in})] \quad \text{(D-41)}$$

Therefore, the total enthalpy difference for the compressor is:

$$\Delta h_C = \Delta h_{C,1} + \Delta h_{C,2} + \Delta h_{C,3} \quad \text{(D-42)}$$

The turbine work is estimated based on the amount of exhaust gas produced per mole fuel. The exhaust gas mainly consists of carbon dioxide (CO_2), steam (H_2O), nitrogen (N_2), and oxygen (O_2). The enthalpy functions of carbon dioxide and steam are listed as Equation (D-48) to Equation (D-54). The amount of exhaust gas per mole fuel is estimated based on the Equations in the section of combustor. The inlet temperature and the outlet temperature for each stage of the turbine are estimated in the previous section. The enthalpy difference per mole syngas of stage is estimated as:

$$\begin{aligned}\Delta h_{T,i} = {} & y_{T,i,CO_2}[h_{CO_2}(T_{T,i,in}) - h_{CO_2}(T_{T,i,out})] + y_{T,i,H_2O}[h_{H_2O}(T_{T,i,in}) - h_{H_2O}(T_{T,i,out})] \\ & + y_{T,i,N_2}[h_{N_2}(T_{T,i,in}) - h_{N_2}(T_{T,i,out})] + y_{T,i,O_2}[h_{O_2}(T_{T,i,in}) - h_{O_2}(T_{T,i,out})]\end{aligned} \quad \text{(D-43)}$$

Therefore, the total enthalpy difference for the compressor is:

$$\Delta h_T = \Delta h_{T,1} + \Delta h_{T,2} + \Delta h_{T,3} \quad \text{(D-44)}$$

The energy recovered from the exhaust gas into the HRSG is estimated by the difference in inlet and outlet exhaust gas enthalpy. The exhaust gas mainly consists of carbon dioxide (CO_2), steam (H_2O), nitrogen (N_2), and oxygen (O_2). The HRSG inlet temperature is the gas turbine outlet temperature. Thus, the HRSG outlet temperature is known. The equations for enthalpy computation have been introduced in the previous section. The total enthalpy difference associated with heat recovery per mole fuel gas is estimated based on the exhaust from the turbine:

$$\begin{aligned}\Delta h_H &= y_{T,out,CO_2}\Delta h_{CO_2} + y_{T,out,H_2O}\Delta h_{H_2O} + y_{T,out,N_2}\Delta h_{N_2} + y_{T,out,O_2}\Delta h_{O_2} \\ &= y_{T,out,CO_2}[h_{CO_2}(T_{T,out}) - h_{CO_2}(T_{H,out})] + y_{T,out,H_2O}[h_{H_2O}(T_{T,out}) - h_{H_2O}(T_{H,out})] \\ &\quad + y_{T,out,N_2}[h_{N_2}(T_{T,out}) - h_{N_2}(T_{H,out})] + y_{T,out,O_2}[h_{O_2}(T_{T,out}) - h_{O_2}(T_{H,out})]\end{aligned} \quad \text{(D-45)}$$

The heat from gas cooling is computed based on the clean dry syngas composition and the temperature drop during cooling. Assuming that the syngas at the exit temperature of a gasifier is cooled down to the inlet temperature of the combustor and that the cleaned syngas composition is known, the sensible heat is estimated as:

$$\begin{aligned}\Delta h_{cooling} &= y_{CH_4}\Delta h_{CH_4} + y_{CO_2}\Delta h_{CO_2} + y_{CO}\Delta h_{CO} + y_{H_2}\Delta h_{H_2} + y_{N_2}\Delta h_{N_2} \\ &= y_{CH_4}[h_{CH_4}(T_{G,out}) - h_{CH_4}(T_{fuel,in})] + y_{CO_2}[h_{CO_2}(T_{G,out}) - h_{CO_2}(T_{fuel,in})] \\ &\quad + y_{CO}[h_{CO}(T_{G,out}) - h_{CO}(T_{fuel,in})] + y_{H_2}[h_{H_2}(T_{G,out}) - h_{H_2}(T_{fuel,in})] \\ &\quad + y_{N_2}[h_{N_2}(T_{G,out}) - h_{N_2}(T_{fuel,in})]\end{aligned} \quad \text{(D-46)}$$

The sensible heat of injected steam or water is estimated based on the enthalpy of saturated water and the enthalpy of vaporization. When the water injection is selected, the heat of water is deducted from total heat input to the steam cycle. The water in the syngas is heated to steam. The heat for vaporization is from the gas cooling. Therefore, the total

heat deduction due to the water injection is the heat of water and the heat of the vaporization. When the steam injection is selected, the heat of saturated steam is same as the sum of the saturated water and the vaporization. Therefore, the heat deduction of water injection or steam injection is estimated as the following:

$$\begin{aligned} h_{moisture} &= m_{moisture} h_f(T_{moisture}) + m_{moisture} h_{fg}(T_{moisture}) \\ &= M_{fuel} \times y_{H_2O} \times MW_{H_2O} \times h_g(T_{moisture}) \end{aligned} \quad \text{(D-47)}$$

Other equations for estimating the power output and efficiency for simple cycle and combined cycle have been described in Chapter 6.

Enthalpy Functions

$$h_{N_2}(T) = 6.66T + 2.8333\times10^{-4}\,T^2 - 3655.83 \quad \text{(D-48)}$$

$$h_{O_2}(T) = 7.16T + 2.7778\times10^{-4}\,T^2 + 129600\,T^{-1} - 4164.05 \quad \text{(D-49)}$$

$$h_{CO_2}(T) = 10.55T + 6\times10^{-4}\,T^2 + 660960\,T^{-1} - 7066.27 \quad \text{(D-50)}$$

$$h_{H_2O}(T) = 7.17T + 7.1111\times10^{-4}\,T^2 - 25920\,T^{-1} - 4004.44 \quad \text{(D-51)}$$

$$h_{CH_4}(T) = 2.975T + 5.0914\times10^{-3}\,T^2 + 4.427\times10^{-7}\,T^3 - 112100\,T^{-1} - 2785.67 \quad \text{(D-52)}$$

$$h_{CO}(T) = 6.79T + 2.7222\times10^{-4}\,T^2 + 35640\,T^{-1} - 3788.8 \quad \text{(D-53)}$$

$$h_{H_2}(T) = 6.52T + 2.1667\times10^{-4}\,T^2 - 38880\,T^{-1} - 3489.04 \quad \text{(D-54)}$$

where the enthalpy is in units of BTU/lbmole and the temperature is in units of degrees Rankine.

Notation

The following symbols are used in this chapter:

e_a = The fraction of excess air

$f_{cooling}$ = Fraction of heat recovered from syngas cooling

$f_{a,i}$ = Extraction fraction of cooling air of stage i of teh compressor, i = 1, 2, and 3

GT = Gas Turbine

$h_{i,j,k}$ = Enthalpy of stream at the stage j of device i inlet or outlet k, where k = *in* is inlet and k = *out* is outlet, Btu/lbmole

$H_i(T)$ = Enthalpy of species i at temperature T (Rankin), Btu/lbmole syngas

$H_{air,stoic}$ = Enthalpy of air needed in a stoichiometric reaction with fuel, J/gmole

H_{fuel} = Fuel Enthalpy, J/gmole

$H_{product,stoic}$ = Enthalpy of stoichiometric reaction product, J/gmole

HR = Heat rate of the steam cycle, Btu/kWh

LHV = Lower heating value of fuel, Btu/lb

$m_{C,i,air}$ = Air flow rate to the stage i of compressor, lb/hr, i = 1, 2, or 3

$m_{Comb,air}$ = Air flow rate to the combustor, lb/hr

m_{fuel} = Fuel mass flow rate, lb/hr

$m_{T,i,out}$ = Stream flow rate at outlet of stage i of the outlet of turbine, lb/hr

M_{fuel} = Fuel molar flow rate, lbmole/hr

MW_i = Molecular weigh of stream at the turbine inlet, i = act or ref.

P_i = Pressure of stream at the turbine inlet, psia, where i = act or ref

P_a = Ambient pressure of inlet air, psia

$P_{i,j}$ = Pressure at device i, psia, where j = in or out

Q_{fuel} = Total energy input of the system, Btu/hr

Q_H = Energy input of HRSG, Btu/hr

Qs = Shaft work, Btu/hr

r_p = Pressure ratio of compressor outlet pressure to compressor inlet pressure

$r_{p,i}$ = Pressure ratio of a single stage i of compressor

$r_{p,turb}$ = Pressure ratio of turbine inlet pressure to turbine outlet pressure

$r_{p,turb,i}$ = Pressure ratio of a single stage i of turbine

T_i = Temperature of steam at the turbine inlet, K, where i = act or ref

$T_{i,j,k}$ = Temperature of stream at the device i stage j inlet or outlet k, where k = *in* is inlet and k = *out* is outlet, K

W_{CC} = Net power output of the combined cycle, MW

W_{SC} = Net power output the simple cycle, MW

W_{ST} = Net electricity produced by the steam turbine, MW

y_i = Mole fraction of compound i

Δh_i = Total enthalpy difference between the inlet and outlet of device i, j/gmole

$\Delta h_{cooling}$ = Sensible heat from syngas cooling, j/gmole

$\Delta h_{r,i}$ = Enthalpy of reaction for compound i, j/gmole

Δp_{back} = turbine back pressure, psia

h_S = Shaft work efficiency

h_{CC} = Combined cycle efficiency

h_{SC} = Simple cycle efficiency

Subscripts

act = Actual

C = Compressor

CC = Combined Cycle

Comb = Combustor

H = Heat Recovery Steam Generator

In = Inlet

NGCC = Natural Gas Combined Cycle

IGCC = Integrated Gasification Combined Cycle

Out = Outlet

ref = Reference

SC = Simple Cycle

SG = Syngas

ST = Steam Turbine

T = Turbine